Communications of BAO, Vol. 73, Issue 1, 2026, pp. 1-7

The time characteristics of spectral line quanta diffusion in scattering and absorbing media

A. Nikoghossian*

NAS RA V.Ambartsumian Byurakan Astrophysical Observatory, Byurakan 0213, Aragatsotn Province, Armenia

Abstract

The paper presents new results on the patterns of evolution of spectral lines formed in absorbing and scattering media under the influence of non-stationary energy sources. When describing the time evolution of radiation diffusion, both possible causes of time consumption are taken into account: the time spent in the absorbed state and the time taken to travel the path between two successive scattering events. Mathematically, this is expressed as a convolution of the probability distributions of these two quantities. Proof is provided of the existence of a relationship between two time averages characterising the process of spectral lines radiation diffusion. It follows that the description of the evolution of a spectral line becomes a mathematically single-parameter problem, with the ratio of the mentioned two temporal values as a parameter. The value of the ratio for a given spectral line is determined by the number-density of emitting or absorbing atoms/ions (dependent on spectrum) and their thermal velocity. The fact that the dependence on the number-density far exceeds that on thermal velocity significantly simplifies the determination of the chemical composition of the object under study.

1. Introduction

The previous work (Nikoghossian, 2025) considered the temporal changes in spectral line profiles formed in an atmosphere of finite optical thickness in the presence of non-stationary primary energy sources. To provide a comprehensive picture of the evolution of the spectral lines under study, data were presented on changes in certain average statistical characteristics of the line radiation transfer in the medium, such as the average number of photon scattering acts and the average time taken during the diffusion process.

The observed evolution of the line spectrum depends, obviously, both on the nature of internal or external primary sources and on the response of the optically active medium, which is generally determined by the process of multiple scattering within it. The latter is characterised by the time photons spend in the medium, which, in turn, consists of the time spent by them in the absorbed state and the transit time between two successive scattering events. In cases where radiative equilibrium is established in the medium, only the second of these characteristic values is usually taken into account when solving time-dependent transfer problems (see e.g. Sobolev, 1950, 1956). It is assumed that the problem of determining the time the photon spends in an absorbed state is reduced to finding the average number of scattering events in the medium. This approach can be applied if the medium is in a state of equilibrium. However, in the non-stationary regime, one should take into account possible changes in the characteristic time taken by photons to travel after each scattering event due to possible changes in the physical conditions in the medium. Moreover, we shall see that there is some relationship between the two considered quantities that plays an important role in the observed changes in the line spectrum.

Thus, for an adequate description of the observed changes in the line spectra, there is a need to develop a proper theory of the evolution of spectral lines that takes into account the combined participation of the two characteristics considered in the photon scattering process.

*nikoghoss@yahoo.com

doi: https://doi.org/10.52526/25792776-26.73.1-1

2. Basic equations

As we know (Nikoghossian, 2022, 2023, 2025), the probability density distribution of the time spent by a photon during a certain number of scattering acts is given by the so-called Erlang distribution, which is the sum of exponentially distributed random variables and is a particular case of two-parameter Gamma distribution. In our problem, the distributions of each of these two possible processes of time loss can be represented as

$$F_1(t,n,\lambda_1) = \frac{\Lambda_1^n t^{n-1}}{(n-1)!}\mathrm{e}^{-\Lambda_1 t}, \qquad F_2(t,n,\Lambda_2) = \frac{\Lambda_2^{n+1} t^n}{n!}\mathrm{e}^{-\Lambda_2 t}, \tag{1}$$

where n is the number of scattering events in the medium, the so-called 'rates' of distributions $\Lambda_1 = 1/t_1, \Lambda_2 = 1/t_2$ and t_1, t_2 represent the average time spent by a photon in a single scattering event, respectively, in the absorbed state and during the flight between two consecutive scattering events. The first of these is obviously determined by the value of Einstein's spontaneous transition coefficient A_{ji} corresponding to the spectral line under consideration $t_1 = 1/A_{ji}$ (for the sake of simplicity, we do not consider the effects of collision processes here).

The value of t_2 can be chosen (see Nikoghossian, 2025) the overflight time of the distance of unit optical thickness for a given spectral line. The latter can be presented in the form $t_2 = 1/n_a k_0 c$, where the following notations are used: c is the speed of light, n_a is the number density of the atom/ion participating in a given line formation, and k_0 is the coefficient of absorption of the atom/ion in the center of the line. Of importance for us here is the fact that a relationship can be established between the two time characteristics mentioned, provided that the normalization condition for the scattering coefficient in the spectral line is applied (see Sobolev, 1956)

$$\int_{-\infty}^{\infty} k_\nu d\nu = \frac{h\nu_0}{c} B_{ij} \tag{2}$$

where ν_0 is the frequency in the centre of the line. Note that this formula is more accurate the sharper the peak of the absorption coefficient. Using known relationships between Einstein transition coefficients and given that the velocity distribution of absorbing atoms is Maxwellian, we find

$$k_0 = \frac{c^3}{8\pi^{3/2}\nu_0^3 v}\frac{g_j}{g_i}A_{ji}, \tag{3}$$

where $v = \sqrt{2kT/m}$ is the average thermal velocity of atoms/ions, k is the Boltzmann constant, m is the mass of an atom/ion, ν_0 is the central frequency, and g_j, g_i are the statistical weights of the upper and lower levels, respectively, between which transitions form a given spectral line. It follows that

$$\frac{t_1}{t_2} = 0.0224\frac{g_j}{g_i}\frac{n_a \lambda_0^3}{\bar{v}}, \tag{4}$$

where λ_0 is the central wavelength of the line, $\bar{v}$ is the thermal velocity of the medium in units of the speed of light. We see that the ratio between the two average values depends on the spectral range where the line is formed and, as expected, also on the physical characteristics of the medium itself, namely number density and the thermal velocity of the scattering centres. Both of these values must be taken into account jointly with the roles they play in the resulting evolution.

In this case, temporal changes are given by the convolution of the two Erlang distributions (Eq.1) considered above in the form

$$\Phi_n(z) = \int_0^z F_1(x,n,\Lambda_1) F_2(z-x,n,\Lambda_2)\, dx, \tag{5}$$

where the dimensionless temporal variable here is determined as $z = \Lambda_1 t$. With regard of analytic forms of Erlang distributions we obtain

doi: https://doi.org/10.52526/25792776-26.73.1-1

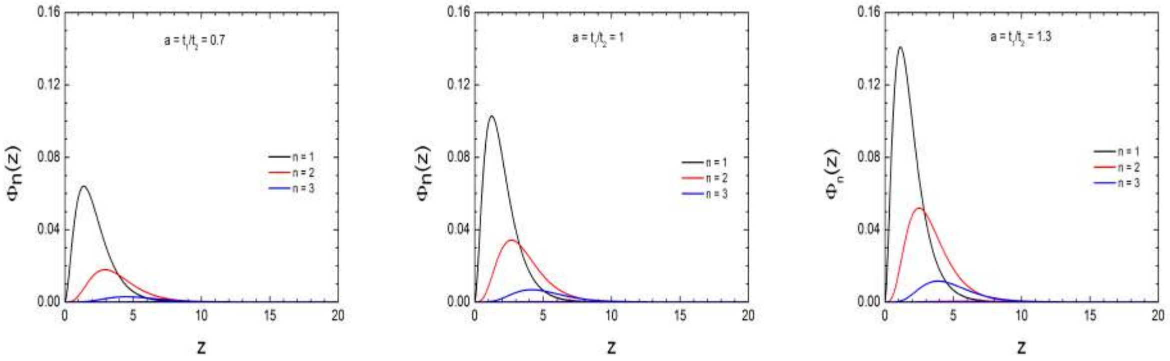

Figure 1. The first three functions Φ_n for different values of the ratio t_1/t_2.

$$\Phi_n(z) = \frac{\Lambda_2 a^n}{n!\,(n-1)!} \mathrm{e}^{-az} \int\limits_0^z \mathrm{e}^{-(1-a)z'} z'^{n-1} \left(z - z'\right)^n dz' \tag{6}$$

where the parameter $a = \Lambda_2/\Lambda_1 = t_1/t_2$.

Thus, in general, the functions $\Phi_n(z)$ have a rather complex form, expressed through hypergeometric functions, and only in the special case of approximate equality of the mean values of time t_1 and t_2, we have $a = 1$ and arrive at the expression used in our previous works.

$$\Phi_n(z) = \frac{\Lambda z^{2n}}{(2n)!} \mathrm{e}^{-z}, \tag{7}$$

where $\Lambda = 1/t_1 = 1/t_2$.

Fig.1 shows graphs of the first few functions of the family functions $\Phi_n(z)$ for three different values of the parameter a chosen arbitrarily in such a way that its effect can be clearly distinguished. We conclude that the dependence is strong enough since even with relatively small changes in its value, the main characteristics of the functions under consideration, such as duration, the maximum value, the time at which this peak is reached, etc., undergo quite noticeable changes. The latter, in turn, obviously affects the behavior of the components of the Neumann series of the observed varying spectral lines over time.

For illustrative purposes, we construct the Neumann series for the reflection and transmission coefficients of a medium of optical thickness $\tau_0 = 3$ at the central frequency of the spectral line. It is assumed that the scattering in the medium occurs with complete redistribution of radiation over frequencies for a given value of the scattering coefficient λ and the value of β, which takes into account absorption in the continuous spectrum. As the nodes used to describe the frequency dependence within the spectral line are the zeros of the 25th-order Hermite polynomials. This model case has been considered in Nikoghossian (2022), where the Neumann series for both reflectance and transmittance of the medium were obtained. In contrast to the mentioned paper, here the evolution of the spectral lines will be determined by functions Eq.(6).

3. Evolution of the line spectra.

One way of describing the evolution of spectral lines is to study the temporal variations in the probability density functions (PDF) of radiation in the lines emerging from the medium. Fig.2 and Fig.3 demonstrate these functions for the above formulated transfer problem for the case of non-stationary energy sources of the Dirac δ-function form. The calculations performed for the lines formed with different values of the above-mentioned parameter a show that the temporal changes in the components of the time-dependent Neumann's series are largely determined by the dominance of the functions $\Phi_n(z)$ discussed above. Despite the relatively small interval covered by its values

doi: https://doi.org/10.52526/25792776-26.73.1-1

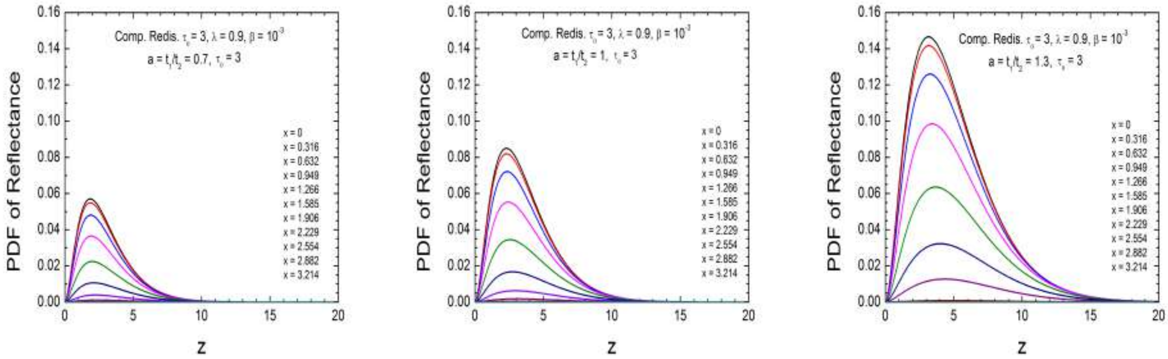

Figure 2. Typical changes in PDF for reflectance of the medium of optical thickness $\tau_0 = 3$ dependent on the value of the parameter a.

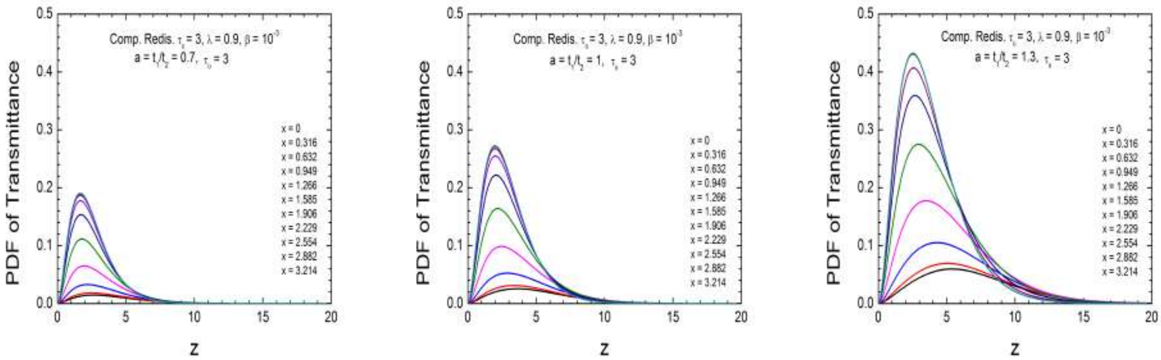

(!)

Figure 3. Typical changes in PDF for transmittance of the medium of optical thickness $\tau_0 = 3$ dependent on the value of of the parameter a.

$0.7 \le a \le 1.3$, one sees significant changes in the form and values of the main characteristics, such as the moment when the distribution reaches its peak and the value of this maximum, as well as the total duration of the evolution.

Additional conclusions can be drawn from the temporal changes in spectral line profiles formed both before and after the peak is reached, which can be directly used for comparison with observational data. To obtain a complete picture of the temporal variations in spectral lines, it is important to reveal their dependence on the optical thickness of the medium and the role of multiple scattering in it.

To this end, we consider separately the emission and absorption spectra that arise as a result of reflection from the medium and transmission through it. As the main characteristics for comparison, we will choose the value of the maximum achieved and the time it takes to reach it.

It is easier to make such a comparison for the absorption spectrum since, as evidenced by calculations, both of the mentioned values depend very weakly on the optical thickness of the medium (right panels in Figs.4,5). Meanwhile, the dependence of these quantities on the scattering coefficient becomes more or less significant only in the case of media opaque enough for the lines (see right panels in Figs.6,7). Therefore, in the case of absorption spectra, the parameters relating to the maximum value of the PDF depend solely on the value of a. Such behavior of the PDF makes it possible to estimate its value, which, in turn, given the known characteristics of the spectral line under consideration, allows one to form an idea of the density of atoms/ions to which it belongs. The case of spectral lines formed by reflection from a medium is somewhat more complex. As might be expected, the dependence of the maximum value of the PDF is particularly pronounced for optically thin media. A similar study can be carried out by examining the evolution of theoretically constructed spectral line profiles before and after they reach their maximum values. Finally, it may be equally interesting to describe the changes in the equivalent widths of lines during their evolution. A typical example illustrating such changes

doi: https://doi.org/10.52526/25792776-26.73.1-1

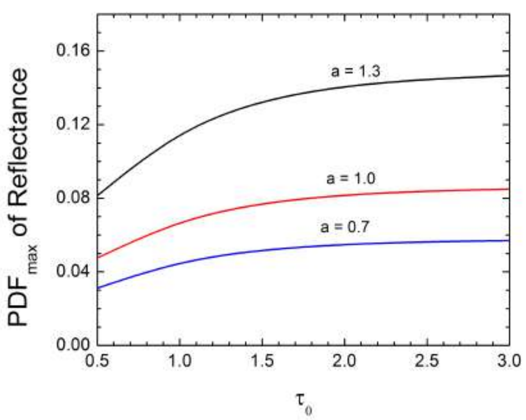

Figure 4. Dependence of Z_{max} (left panel) and maximum value of PDF (right panel) on optical thickness of the medium for different value of the parameter a

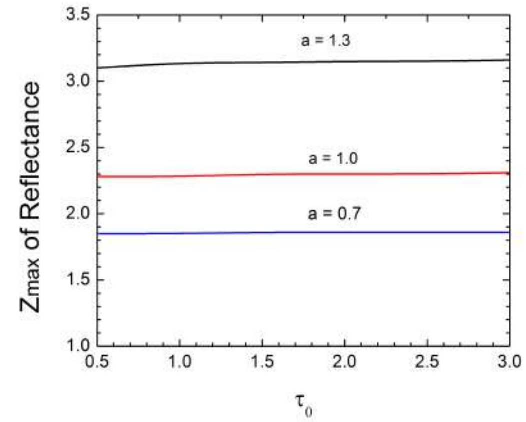

Figure 5. Dependence of Z_{max} (left panel) and maximum value of PDF (right panel) on the value of scattering coefficient λ for the line formed as a result of transmission.

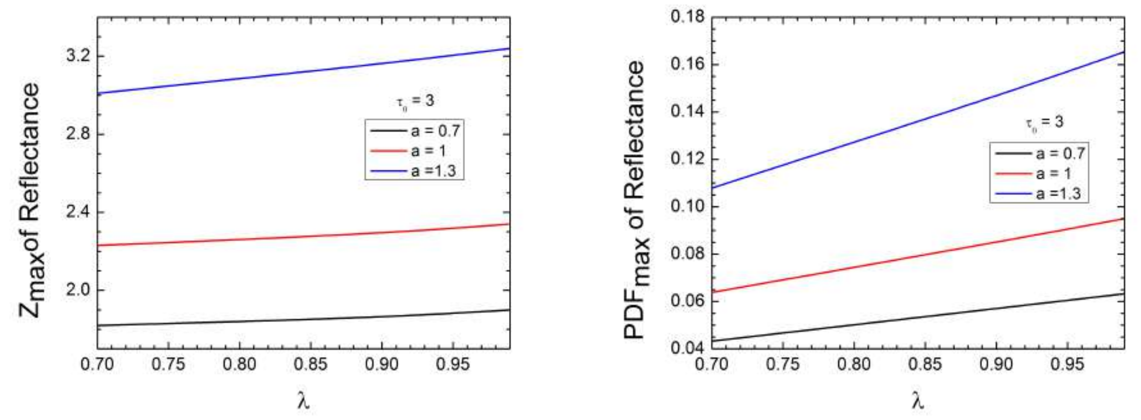

Figure 6. Dependence of Z_{max} (left panel) and maximum value of PDF (right panel) on optical thickness of the medium for different value of the parameter a

doi: https://doi.org/10.52526/25792776-26.73.1-1

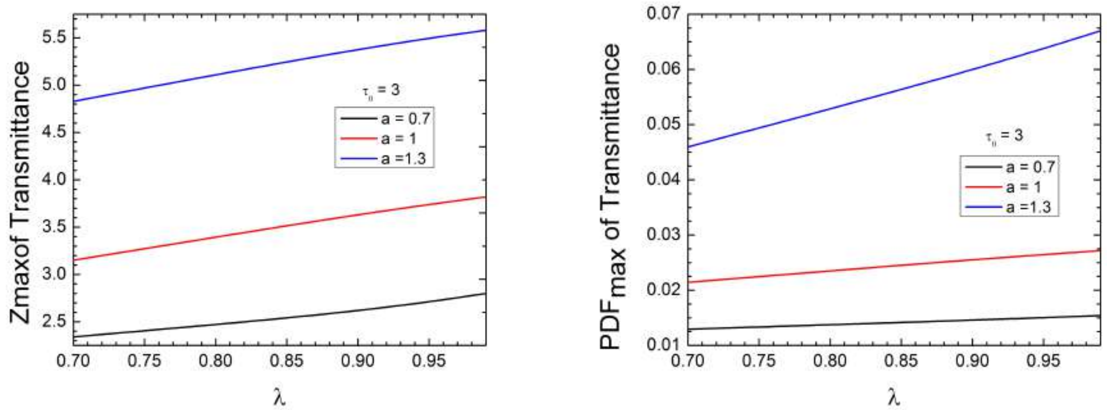

Figure 7. Dependence of Z_{max} (left panel) and maximum value of PDF (right panel) on the value of scattering coefficient λ for the line formed as a result of transmission.

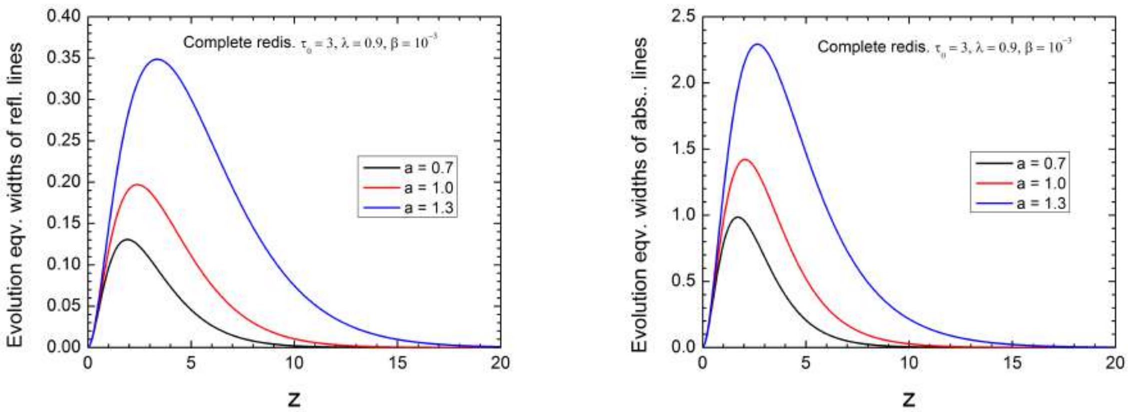

Figure 8. Evolution of equivalent widths of spectral lines for the case of external non-stationary illumination of the Dirac delta-function form.

is shown in Fig.8.

4. Concluding remarks

The relationship we have established between the two characteristic times t_1 and t_2 which describes the diffusion in a medium emitting in spectral line frequencies, now makes it possible to formulate the changes caused by non-stationary energy sources as a single-parameter problem that depends significantly on the value of the parameter a we have introduced. As the key parameters to be determined when monitoring the evolution of spectral lines, we have selected the time at which their peaks occur and the values they attain at that point. Note that a number of other parameters can, of course, be compared with theoretical results, including equivalent widths, rates of increase or decrease in intensity, and so on.

Estimation of the value of the parameter a from observations allows, in principle, to form an idea of the chemical composition of the non-stationary object after estimating the excitation temperature using other methods. It follows from Eq.(4) being written in the form

$$n_a = 44.64 \frac{g_i}{g_j} a \bar{v} \lambda_0^{-3}, \tag{8}$$

or

doi: https://doi.org/10.52526/25792776-26.73.1-1

$$n_a = 44.64 \frac{g_i}{g_j} \frac{a}{c\lambda_0^3} \sqrt{\frac{2kT}{m}} \tag{9}$$

It is also possible to use data from other lines produced by transitions from a given energy level, followed by the application of the Boltzmann formula.

In conclusion, let us consider the relationship between the two average time scales t_1 and t_2 of two phenomena occurring during the diffusion of radiation under different physical conditions, as found in various astrophysical objects frequently encountered in applications. For instance, in stellar photospheres and atmospheres, including those of dwarfs, the number density of hydrogen atoms varies in the interval between $6 \cdot 10^{15} sm^{-3} - 2 \cdot 10^{17} sm^{-3}$ while the dimensionless thermal velocity $\bar{v}$ is of the order $3 \cdot 10^{-4} - 4.3 \cdot 10^{-4}$ which implies that the inequality $a < 1$ becomes valid only in the extreme shortwave regions of wavelengths of the order of some angstroms and less. It follows that the average time spent by hydrogen photons in the optic domain on the flight between two consecutive acts of scattering is less compared to that spent by them in the absorbed state. However, the situation may be the opposite in the case of spectra of other atoms and ions, whose number densities are many orders of magnitude lower than that of hydrogen.

From this viewpoint, objects with lower density, such as the chromosphere and the solar corona, are of particular interest, as both the atomic number density and thermal velocities vary over a fairly wide range in these regions. Indeed, from the lower layers of the chromosphere to the corona, right up to its upper layers, the density of hydrogen atoms/ions decreases by 12 orders of magnitude, whilst the non-dimensional thermal velocity $\bar{v}$ decreases by approximately one order of magnitude (from $7 \cdot 10^{-5}$ to $4 \cdot 10^{-4}$), so that the inequality $t_1 \leq t_2$ depending on the height will hold if $\lambda \leq 70.6\dot{\mathrm{A}}$ for lower optically thick layers of the chromosphere with $n \approx 10^{16} cm^{-3}$ and $\lambda \leq 7600\dot{\mathrm{A}}$ for the upper, respectively thin layers. Finally, in the case of more rarefied media such as nebulae and the interstellar medium, the inequality in question for hydrogen atoms holds for all wavelengths shorter than those in the far-infrared region. As can be seen from the examples given, the value of the parameter a depends primarily on the density of the atoms (or ions) whose spectral lines are being considered.

References

Nikoghossian A., 2022, Communications of the Byurakan Astrophysical Observatory, 69, 140

Nikoghossian A. G., 2023, Communications of the Byurakan Astrophysical Observatory, 70, 131

Nikoghossian A., 2025, Communications of the Byurakan Astrophysical Observatory, 72, 106

Sobolev V. V., 1950, Astron. J. , 27, 81

Sobolev V. V., 1956, Transfer of Radiative Energy in Stellar and Planetary Atmospheres. Gostechizdat, M., (in Russian)

doi: https://doi.org/10.52526/25792776-26.73.1-1

Communications of BAO, Vol. 73, Issue 1, 2026, pp. 8-16

Classical analog of extended phase space SUSY: spectrum generating algebra

G.Ter-Kazarian*

Byurakan Astrophysical Observatory, Byurakan, Aragatsotn Province, Armenia

Abstract

We address the classical analog of the *extended phase space* (EPS) (N=2)-supersymmetric quantum mechanics (SUSY QM). We derive the integrals of motion and calculate the parameters that measure the breaking of EPS-SUSY. We analyze the non-perturbative mechanism for its breaking in the instanton picture, which has resulted from tunneling between the classical vacua of the theory. Particular attention is given to the independent group theoretical method and its connection to the factorization procedure in developing a spectrum generating algebra (SGA) for the EPS-SUSY.

Keywords: *Extended phase space quantum mechanics–Supersymmetric quantum mechanics–Symmetry breaking–Spectrum generating algebra*

1. Introduction

Much use has been made of the technique of EPS QM Nasiri (2006), Sobouti & Nasiri (1993) for keeping the symmetry between coordinates (q) and momenta (p) in the process of quantization. It was observed that the concept of an *extended* Lagrangian, $\mathcal{L}(p,\, q,\, \dot{p},\, \dot{q})$ in phase space allows a subsequent extension of Hamilton's principle to actions minimum along the actual trajectories in $(p,\, q)-$, rather than in $q-$space. This extension, in turn, allows a definition of "second" momenta $\pi_p = \delta\,\mathcal{L}/\delta\,\dot{p}$ and $\pi_q = \delta\,\mathcal{L}/\delta\,\dot{q}$, and a subsequent introduction of an *extended* phase space $(p,\, q,\, \pi_p,\, \pi_q)$ and of an *extended* Hamiltonian, $H_{ext}(p,\, q,\, \pi_p,\, \pi_q)$. In particular, the vanishing of π_q or π_p is the condition for p and q to constitute a canonical pair. In the language of statistical quantum mechanics, this choice picks a pure state (*actual path*). Otherwise, one is dealing with a mixed state (*virtual path*). In Ter-Kazarian & Sobouti (2008) we address the EPS stochastic quantization of Hamiltonian systems with first class holonomic constraints. This, in a natural way, results in the Faddeev-Popov conventional path-integral measure for gage systems. Consequently, in Ter-Kazarian (2009), we construct an (N=2) realization of the EPS-SUSY algebra. A new feature of this formulation over the ordinary SUSY QM formalism E. (1981, 1982), Gamboa & Plyushchay (1998), Inomata (1992), Inomata & Junker (1991), Nicolai (1976), Salomonson & Van Holten (1982), E. (rf:) is, in particular, the fact that even if the SUSY was broken in $q-$ or $p-$ spaces, it can still be good in $(q,p)-$ space, and vise versa. We also explore the shape-invariance Balantekin (1998), Gangopadhyaya (1998), Gendenshtein (1983) of exactly solvable EPS SUSY potentials. These aspects of conventional SUSY QM and its connection to the factorization method have been extensively investigated by several authors. In the present article, we investigate further the above mentioned aspects of EPS-SUSY QM.

We proceed according to the following structure. In section 2 we address the classical analog of the EPS (N=2)-SUSY QM. In section 3 we calculate the parameters that measure the breaking of EPS SUSY. We analyze non-perturbative mechanism for EPS SUSY breaking in the instanton picture. The section 4 deals with the independent group theoretical methods with nonlinear extensions of Lie algebras from the EPS SUSY QM. Unless otherwise stated we take the geometrized units. Also, an implicit summation on repeated indices are assumed throughout this paper.

*gago_50@yahoo.com

doi: https://doi.org/10.52526/25792776-26.73.1-8

2. The integrals of motion

The sufficient details of EPS quantization are given below to make the rest of the paper understandable. The extended Lagrangian can be written as

$$\mathcal{L}_{ext}(p,\,q,\,\dot{p},\,\dot{q}) = -\dot{q}_i\,p_i - q_i\,\dot{p}_i + \mathcal{L}^q + \mathcal{L}^p, \tag{1}$$

where a dynamical system with N degrees of freedom described by the 2N independent coordinates $q = (q_1, \ldots\, q_N)$ and momenta $p = (p_1, \ldots\, p_N)$ which are not, in general, canonical pairs. A Lagrangian $\mathcal{L}^q(q,\,\dot{q})$ is given in $q-$representation and the corresponding $\mathcal{L}^p(p,\,\dot{p})$ in $p-$representation. A dot will indicate differentiation with respect to t. One may now defines an extended Hamiltonian

$$H_{ext}(p,\,q,\,\pi_p,\,\pi_q) = \pi_{q_i}\,\dot{q}_i + \pi_{p_i}\,\dot{p}_i - \mathcal{L}_{ext}(p,\,q,\,\dot{p},\,\dot{q}) = H(p+\pi_q,\,q) - H(p,\,q+\pi_p), \tag{2}$$

where $H(p,\,q) = p_i\dot{q}_i - \mathcal{L}^q = q_i\dot{p}_i - \mathcal{L}^p$ is the conventional Hamiltonian of the system. Here p and q will be considered as independent c-number operators on the integrable complex function $\chi(q,p)$. For π_p and π_q, however, the differential operators and commutation brackets will be borrowed from the conventional quantum mechanics, $\pi_{q_i} = -i\dfrac{\partial}{\partial\,q_i}$, $\quad [\pi_{q_i}, q_j] = -i\delta_{ij}$, and similar relations hold for the pair π_{p_i} and p_i. Note also the following $[p_i, q_j] = [p_i, p_j] = [q_i, q_j] = \left[\pi_{p_i}, \pi_{q_j}\right] = \left[\pi_{p_i}, \pi_{p_j}\right] = \left[\pi_{q_i}, \pi_{q_j}\right] = 0$. The solutions of Schrӧdinger-like equation $i\,\dfrac{\partial}{\partial\,t}\chi = H_{ext}\,\chi$, are

$$\chi(q,p,t) = \overline{\chi}(q,p,t)e^{-ipq} = a_{\alpha\beta}\,\psi_\alpha(q,\,t)\,\phi^*_\beta(p,\,t)\,e^{-i\,pq}, \tag{3}$$

where $a = a^\dagger$ positive definite, ψ_α and ϕ^*_α are solutions of the conventional Schrӧdinger equation in $q-$ and $p-$representations, respectively. The normalizable χ is a physically acceptable solution. The exponential factor is a consequence of the total time derivative, $-d(qp)/dt$, in Eq. (1) which can be eliminated due to $(p+\pi_q)\chi(q,p,t) = (\pi_q\overline{\chi}(q,p,t))\,e^{-ipq}$, and so on. This substitution gives $i\,\dfrac{\partial}{\partial\,t}\,\overline{\chi}(q,p,t) = \overline{H}_{ext}\,\overline{\chi}(q,p,t)$, provided by the reduced Hamiltonian, $\overline{H}_{ext}$ where we put $p+\pi_q \to \pi_q$ and $q+\pi_p \to \pi_p$. So, we may replace H_{ext} by $\overline{H}_{ext}$, and $\chi(q,p,t)$ by $\overline{\chi}(q,p,t)$, respectively, but retain the former notational conventions. The interested reader is referred to Nasiri (2006) for further details.

Following Gamboa & Plyushchay (1998), let us consider a nonrelativistic particle of unit mass with two $(\alpha = 1, 2)$ odd (Grassmann) degrees of freedom. The classical extended Lagrangian Eq. (1) explicitly can be written

$$\mathcal{L}_{ext}(p,\,q,\,\dot{p},\,\dot{q}) = -\dot{q}\,p - q\,\dot{p} + \frac{1}{2}\,\dot{q}^2 - F(q) + \frac{1}{2}\,\dot{p}^2 - G(p) - R(q,\,p)\,N + \frac{1}{2}\,\psi_\alpha\dot{\psi}_\alpha, \tag{4}$$

provided by $N = \psi_1\,\psi_2 = -i\,\psi_+\,\psi_-$, where ψ_α are the two odd (Grassmann) degrees of freedom. Here $F(q) : \mathcal{R} \to \mathcal{R}$, $\quad G(p) : \mathcal{R} \to \mathcal{R}$ and $R(q,\,p) : \mathcal{R} \to \mathcal{R}$ are arbitrary piecewise continuously differentiable functions defined over the 1-dimensional Euclidean space $\mathcal{R}$. The nontrivial Poisson-Dirac brackets of the system Eq. (4) are

$$\begin{aligned} &\{q,\,\pi_q\} = 1, \quad \{p,\,\pi_p\} = 1, \quad \{\psi_\alpha,\,\psi_\beta\} = \delta_{\alpha\beta}, \\ &\{\psi_+,\,\psi_-\} = 1, \quad \psi_\pm^2 = 0, \quad \psi_\pm = \frac{1}{\sqrt{2}}\,(\psi_1 \pm i\psi_2)\,. \end{aligned} \tag{5}$$

The extended Lagrangian Eq. (4) yields the Hamiltonian H_{ext} which, in turn, gives the following equations of motion:

$$\begin{aligned} &\dot{q} = \pi_q, \quad \dot{p} = \pi_p, \quad \dot{\pi}_q = -F'_q(q) - R'_q(q,\,p)\,N, \\ &\dot{\pi}_p = -G'_p(p) + R'_p(q,\,p)\,N, \quad \dot{\psi}_\pm = \pm iR(q,\,p)\,\psi_\pm, \end{aligned} \tag{6}$$

where N is the integral of motion additional to H_{ext}. Along the trajectories $q(t)$ and $p(t)$ in $(p,q)-$ spaces, the solution to the equations of motion for odd variables is

$$\psi_\pm(t) = \psi_\pm(t_0)\,\exp\left[\pm i\int_{t_0}^{t} R(q(\tau),\,p(\tau))\,d\tau\right]. \tag{7}$$

Hence, the odd quantities

$$\theta_\pm = \psi_\pm(t)\,\exp\left[\mp i\int_{t_0}^{t} R(q(\tau),\,p(\tau))\,d\tau\right] \tag{8}$$

doi: https://doi.org/10.52526/25792776-26.73.1-8

are nonlocal in time integrals of motion. In the trivial case $R = 0$, we have $\dot{\psi}_\pm = 0$, and $\theta_\pm = \psi_\pm$. Suppose the system has even complex conjugate quantities $B_{q,p\pm}$, $(B_{q,p+})^* = B_{q,p-}$, whose evolution looks, up to the term proportional to N like the evolution of odd variables in Eq. (6). Then local odd integrals of motion could be constructed in the form $Q_{X\pm} = B_{X\pm}\,\psi_{\pm,}$, where X denotes concisely either $q-$ or $p-$ representations (no summation on X is assumed). Let us introduce the oscillator-like bosonic variables $B_{X\pm}$ as

$$\begin{array}{ll} B_{q\pm} : \mathcal{L}^2(\mathcal{R}) \to \mathcal{L}^2(\mathcal{R}), & B_{q\pm} = [p + \pi_q \pm iW(q)]\,, \\ B_{p\pm} : \mathcal{L}^2(\mathcal{R}) \to \mathcal{L}^2(\mathcal{R}), & B_{p\pm} = [q + \pi_p \pm iV(p)]\,, \end{array} \tag{9}$$

where $W(q) : \mathcal{R} \to \mathcal{R}$ and $V(p) : \mathcal{R} \to \mathcal{R}$ are the piecewise continuously differentiable functions called SUSY potentials. In particular, if $R(q,\,p) = R_q(q) - R_p(p)$, we obtain

$$\begin{array}{l} \dot{Q}_{q\pm} = \pm i\left[\left(W'_q - R'_{q\pm}\right) - \sqrt{i}\left(F'_q - WW'_q\right)\,\psi_\mp\right], \\ \dot{Q}_{p\pm} = \pm i\left[\left(V'_p - R'_{p\pm}\right) - \sqrt{i}\left(G'_p - VV'_p\right)\,\psi_\mp\right]. \end{array} \tag{10}$$

This shows that either $\dot{Q}_{q\pm} = 0$ or $\dot{Q}_{p\pm} = 0$ when $W'_q(q) = R'_{q\pm}(q)$ and $F'_q = \frac{1}{2}(W^2)'_q$ or $V'_p(p) = R'_{p\pm}(p)$ and $G'_p = \frac{1}{2}(V^2)'_p$, respectively. Therefore, when the functions R_X, $F(q)$ and $G(p)$ are related as

$$R'_{q\pm}(q) = W'_q(q), \quad F_q = \tfrac{1}{2}W^2 + C_q, \quad R'_{p\pm}(p) = V'_p(p), \quad G_p = \tfrac{1}{2}V^2 + C_p, \tag{11}$$

where C_X are constants, then odd quantities $Q_{X\pm}$ are integrals of motion in addition to H_{ext} and N. Using the explicit form $H_{ext} = H_q - H_p$:

$$H_q = \frac{1}{2}\,\pi_q^2 + F^2(q) + R_q\,N, \quad H_p = \frac{1}{2}\,\pi_p^2 + G^2(p) + R_p\,N, \tag{12}$$

it can be seen that $Q_{X\pm}$ and N together with the H_q and H_p form the classical analog of the EPS SUSY algebra

$$\begin{array}{l} \{Q_{X+},\,Q_{X-}\} = 2(H_X - C_X), \quad \{H_X,\,Q_{X\pm}\} = \\ \{Q_{X\pm},\,Q_{X\pm}\} = 0, \quad \{N,\,Q_{X\pm}\} = \pm iQ_{X\pm}, \quad \{N,\,H_X\} = 0, \end{array} \tag{13}$$

with constants C_X playing a role of a central charges in $(q,p)-$ spaces, N is classical analog of the grading operator. Putting $C_q = C_p = 0$, we arrive at classical analog of the EPS SUSY QM Ter-Kazarian (2009) given by the extended Lagrangian

$$\mathcal{L}_{ext}(p,\,q,\,\dot{p},\,\dot{q}) = \frac{1}{2}\,\pi_q^2 - \frac{1}{2}\,W^2(q) + \frac{1}{2}\,\pi_p^2 - \frac{1}{2}\,V^2(p) + \psi_1\psi_2(W'_q + V'_p) + \frac{1}{2}\psi_\alpha\dot{\psi}_\alpha. \tag{14}$$

We conclude that the classical system Eq. (4) is characterized by the presence of two additional local in time odd integrals of motion, $Q_{X\pm}$, being supersymmetry generators. Along the actual trajectories in $q-$space, the Eq. (14) reproduces the results obtained in Ter-Kazarian (2009). In the matrix formulation of EPS (N=2)-SUSY QM, the $\hat{\psi}_\pm$ will be two real fermionic creation and annihilation nilpotent operators describing the fermionic variables. The $\hat{\psi}_\pm$, having anticommuting c-number eigenvalues, imply

$$\hat{\psi}_\pm = \sqrt{\frac{1}{2}}\left(\hat{\psi}_1 \pm i\hat{\psi}_2\right), \quad \left\{\hat{\psi}_\alpha,\,\hat{\psi}_\beta\right\} = \delta_{\alpha\beta}, \quad \left\{\hat{\psi}_+,\,\hat{\psi}_-\right\} = 1, \quad \hat{\psi}_\pm^2 = 0. \tag{15}$$

They can be represented by finite dimensional matrices $\hat{\psi}_\pm = \sigma^\pm$,

$$\hat{\psi}_+ = \sigma^+ = \begin{pmatrix} 0 & 1 \\ 0 & 0 \end{pmatrix}, \quad \hat{\psi}_- = \sigma^- = \begin{pmatrix} 0 & 0 \\ 1 & 0 \end{pmatrix}, \quad \hat{f} = \frac{1}{2}\,\sigma_3, \tag{16}$$

where the $\sigma^\pm = \frac{\sigma_1 \pm i\sigma_2}{2}$ denote the usual raising and lowering operators for the eigenvalues of σ_3. The fermionic operator Eq. (46) commutes with the H_{ext} and is diagonal in this representation with conserved eigenvalues $\pm\frac{1}{2}$. Due to it the wave functions become two-component objects:

$$\chi(q,p) = \begin{pmatrix} \chi_{+1/2}(q,p) \\ \chi_{-1/2}(q,p) \end{pmatrix} = \begin{pmatrix} \chi_1(q,p) \\ \chi_2(q,p) \end{pmatrix} = \begin{pmatrix} \psi_1(q)\phi_1(p) \\ \psi_2(q)\phi_2(p) \end{pmatrix}, \tag{17}$$

where the states $\psi_{1,2}(q)$, $\phi_{1,2}(p)$ correspond to fermionic quantum number $f = \pm\dfrac{1}{2}$, respectively, in $q-$ and $p-$ spaces. They belong to Hilbert space $\mathcal{H} = \mathcal{H}_0 \otimes \mathcal{C}^2 = \left[\mathcal{L}^2(\mathcal{R}) \otimes \mathcal{L}^2(\mathcal{R})\right] \otimes \mathcal{C}^2$. Hence the Hamiltonian H_{ext} of EPS (N=2)-SUSY QM system becomes a 2×2 matrix Ter-Kazarian (2009).

doi: https://doi.org/10.52526/25792776-26.73.1-8

3. The EPS SUSY breaking

To calculate the parameters that measure the breaking of EPS SUSY, let us first find the approximate ground state solutions to the extended Schrödinger-like equation

$$H_{ext}\,\chi(q,p) = (H_q - H_p)\,\chi(q,p) = \varepsilon\,\chi(q,p), \tag{18}$$

with the supposedly small groundstate energy ε. As we mentioned above the solutions for non-zero ε come in pairs of the form $\chi_\uparrow(q,p) = \begin{pmatrix} \chi_1(q,p) \\ 0 \end{pmatrix}$ or $\chi_\downarrow(q,p) = \begin{pmatrix} 0 \\ \chi_2(q,p) \end{pmatrix}$, related by supersymmetry, where $\chi_{1,2}(q,p) = \psi_{1,2}(q)\phi_{1,2}(p)$. The state space of the system is defined by all the normalizable solutions of Eq. (18) and the individual states are characterized by the energies ε_q and ε_q and the fermionic quantum number f. One of these solutions is acceptable only if $W(q)$ and $V(p)$ become infinite at both $q \to \pm\infty$ and $p \to \pm\infty$, respectively, with the same sign. If this condition is not satisfied, neither of the solutions is normalizable, and they cannot represent the groundstate of the system. The Eq. (18) yields the following relations between energy eigenstates with fermionic quantum number $\pm\frac{1}{2}$:

$$\left(-\frac{\partial}{\partial q} + W(q)\right)\sqrt{\varepsilon_q}\,\psi_2(q)\phi_1(p) - \left(-\frac{\partial}{\partial p} + V(p)\right)\sqrt{\varepsilon_p}\,\psi_1(q)\phi_2(p) = \sqrt{2}\,\varepsilon\psi_1(q)\phi_1(p), \tag{19}$$

and

$$\left(\frac{\partial}{\partial q} + W(q)\right)\sqrt{\varepsilon_q}\,\psi_1(q)\phi_2(p) - \left(\frac{\partial}{\partial p} + V(p)\right)\sqrt{\varepsilon_p}\,\psi_2(q)\phi_1(p) = \sqrt{2}\,\varepsilon\psi_2(q)\phi_2(p), \tag{20}$$

where $\varepsilon = \varepsilon_q - \varepsilon_p$, ε_q and ε_p are the eigenvalues of H_q and H_p, respectively. The technique now is to devise an iterative approximation scheme, as developed in Salomonson & Van Holten (1982), to solve Eq. (19) and Eq. (20) by taking a trial wave function for $\chi_2(q,p)$, substitute this into the first equation (19) and integrate it to obtain an approximation for $\chi_1(q,p)$. This can be used as an ansatz in the second equation Eq. (20) to find an improved solution for $\chi_2(q,p)$, etc. As it was shown in Salomonson & Van Holten (1982), the procedure converges for well-behaved potentials with a judicious choice of initial trial function. If the W_q and V_p are odd, then $\psi_1(-q) = \psi_2(q)$, $\phi_1(-p) = \phi_2(p)$, since they satisfy the same eigenvalue equation. The independent nature of q and p gives the freedom of taking $q = 0$, $p = 0$ which yield an expression for energies: $\sqrt{2\varepsilon_q} = W(0) + \psi_1'(0)\,/\psi_1(0)$, $\sqrt{2\varepsilon_p} = V(0) + \phi_1'(0)\,/\phi_1(0)$. Suppose the potentials $W_q(q)$ and $V_p(p)$ have a maximum, at q_- and p_-, and minimum, at q_+ and p_+, respectively. For the simplicity sake we choose the trial wave function as $\chi^{(0)}_{1,2}(q) = \delta(q - q_\pm)\delta(p - p_\pm)$. After one iteration, we obtain

$$\begin{aligned}
\chi_1^{(1)}(q,p) &= \frac{1}{N}\theta(q - q_-)\,\theta(p - p_-)\,e^{-\int_0^q dq'\,W(q') - \int_0^p dp'\,V(p')},\\
\chi_2^{(1)}(q,p) &= \frac{1}{N}\theta(q_+ - q)\,\theta(p_+ - p)\,e^{\int_0^q dq'\,W(q') + \int_0^p dp'\,V(p')},
\end{aligned} \tag{21}$$

where N is the normalization factor. The next approximation leads to

$$\begin{aligned}
\chi_1^{(2)}(q,p) &= \frac{1}{N'}\,e^{-\int_0^q dq'\,W(q') + \int_0^p dp'\,V(p'))}\int_{max(-q,q_-)}^{\infty} dq' e^{-2\int_0^{q'} dq''\,W(q'')}\times\\
&\int_{max(-p,p_-)}^{\infty} dp' e^{-2\int_0^{p'} dp''\,V(p'')},\\
\chi_2^{(2)}(q,p) &= \frac{1}{N'}\,e^{\int_0^q dq'\,W(q') - \int_0^p dp'\,V(p'))}\int_{\infty}^{min(-q,q_+)} dq' e^{2\int_0^{q'} dq''\,W(q'')}\times\\
&\int_{\infty}^{min(-p,p_+)} dp' e^{2\int_0^{p'} dp''\,V(p'')}.
\end{aligned} \tag{22}$$

It can be verified that to this level of precision Eq. (21) is self-consistent solution. Actually, for example, for $q' > q_-$ the exponential $e^{-2\int_0^{q'} W(q'')dq''}$ will peak sharply around q_+ and may be approximated by a $\delta-$function $c\delta(q_+ - q')$; similarly $e^{2\int_0^{q'} W(q'')dq''}$ we may replace approximately by $c\delta(q_- - q')$ for $q' < q_+$. The similar arguments hold for the p-space. With these approximations equations (22) reduce to Eq. (21). The normalization constant N' is

$$N' = \left(\int_{q_-}^{\infty} dq\,e^{-2\int_0^q W(q')dq'}\int_{p_-}^{\infty} dp\,e^{-2\int_0^{p'} V(p')dp'}\right)^{3/2}. \tag{23}$$

doi: https://doi.org/10.52526/25792776-26.73.1-8

The energy expectation value $\varepsilon = (\chi_1,\, H_{ext}\,\chi_1)$ gives the same result as that obtained for odd potentials by means of the $\sqrt{2\varepsilon_q}$, $\sqrt{2\varepsilon_p}$, and Eq. (22). Assuming the exponentials $e^{-2\int_{q_-}^{0} W(q)dq}$ and $e^{-2\int_{p_-}^{0} V(p)dp}$ to be small, which is correct to the same approximations underlying the ε, the difference is negligible and the integrals in both cases may be replaced by gaussians around q_+ and p_+, respectively. Hence, it is straightforward to obtain

$$\varepsilon = \frac{\hbar W_q'(q_+)}{2\pi}\, e^{-2\Delta W/\hbar} - \frac{\hbar V_p'(p_+)}{2\pi}\, e^{-2\Delta V/\hbar}, \tag{24}$$

which gives direct evidence for the SUSY breaking in the EPS QM system. Here we have reinstated $\hbar$ to show the order of adopted approximation and its non-perturbative nature, and denoted $\Delta W = \int_{q+}^{q-} W(q)\, dq, \quad \Delta V = \int_{p+}^{p-} V(p)\, dp$. However, a more practical measure for the SUSY breaking, in particular, in field theories is the expectation value of an auxiliary field, which can be replaced by its equation of motion right from the start: $< F >= (\chi_\uparrow,\, i\{Q_+,\, \sigma_-\}\chi_\uparrow)$. Taking into account the relation $Q_+\chi_\uparrow = 0$, with Q_+ commuting with H_{ext}, which means that the intermediate state must have the same energy as χ, the expectation value $< F >$ can be written in terms of a complete set of states as $< F >= i\,(\chi_\uparrow,\, Q_+\,\chi_\downarrow)\,(\chi_\downarrow,\, \sigma_-,\, \chi_\uparrow)$. Note that

$$\begin{aligned}
&\varepsilon =< H_{ext} >= (\chi_\uparrow,\, H_{ext}\,\chi_\uparrow) = \frac{1}{2}\,(\chi_\uparrow,\, Q_+\,\chi_\downarrow)\,(\chi_\downarrow,\, Q_-\,\chi_\uparrow) = \\
&\varepsilon_q - \varepsilon_p =< H_q > - < H_p >= \quad (\psi_\uparrow,\, H_q\,\psi_\uparrow) - (\phi_\uparrow,\, H_p\,\phi_\uparrow) = \\
&\frac{1}{2}\,(\psi_\uparrow,\, Q_{q+}\,\psi_\downarrow)\,(\psi_\downarrow,\, Q_{q-}\,\psi_\uparrow) - \frac{1}{2}\,(\phi_\uparrow,\, Q_{p+}\,\phi_\downarrow)\,(\phi_\downarrow,\, Q_{p-}\,\phi_\uparrow)\,,
\end{aligned} \tag{25}$$

where $\chi_{\uparrow\downarrow} = \psi_{\uparrow\downarrow}\phi_{\uparrow\downarrow}$, and $\psi_\uparrow = \begin{pmatrix} \psi_1 \\ 0 \end{pmatrix}, \quad \psi_\downarrow = \begin{pmatrix} 0 \\ \psi_2 \end{pmatrix}, \quad \phi_\uparrow = \begin{pmatrix} \phi_1 \\ 0 \end{pmatrix}, \quad \phi_\downarrow = \begin{pmatrix} 0 \\ \phi_2 \end{pmatrix}$. By virtue of SUSY algebra, we have $\frac{1}{\sqrt{2\varepsilon}}\, Q_-\,\chi_\uparrow = \chi_\downarrow = \hat\psi_-\,\chi_\uparrow, \quad \frac{1}{\sqrt{2\varepsilon_q}}\, Q_{q-}\,\psi_\uparrow = \psi_\downarrow = \hat\psi_-\,\psi_\uparrow, \quad \frac{1}{\sqrt{2\varepsilon_p}}\, Q_{p-}\,\phi_\uparrow = \phi_\downarrow = \hat\psi_-\,\phi_\uparrow$, and the Eq. (25) reads

$$\begin{aligned}
&\sqrt{\varepsilon}\,\,(\chi_\uparrow,\, Q_+\,\chi_\downarrow)\left(\chi_\downarrow,\, \hat\psi_-\,\chi_\uparrow\right) = \sqrt{\varepsilon_q}\,\,(\psi_\uparrow,\, Q_{q+}\,\psi_\downarrow)\left(\psi_\downarrow,\, \hat\psi_-\,\psi_\uparrow\right) - \\
&\sqrt{\varepsilon_p}\,\,(\phi_\uparrow,\, Q_{p+}\,\phi_\downarrow)\left(\phi_\downarrow,\, \hat\psi_-\,\phi_\uparrow\right),
\end{aligned} \tag{26}$$

Using the matrix representations of Q_{q+}, Q_{p+} and $\hat\psi_-$ and the wave functions Eq. (22), we obtain

$$(\chi_\uparrow,\, Q_+\,\chi_\downarrow)\left(\chi_\downarrow,\, \hat\psi_-\,\chi_\uparrow\right) = i\sqrt{\frac{\varepsilon_q}{\varepsilon}}\,\frac{W_q'(q)}{\pi}\, e^{-2\Delta W}\,\Delta q - i\sqrt{\frac{\varepsilon_p}{\varepsilon}}\,\frac{V_p'(p)}{\pi}\, e^{-2\Delta V}\,\Delta p, \tag{27}$$

where $\Delta q = q_+ - q_-$ and $\Delta p = p_+ - p_-$. Hence

$$< F >= -\sqrt{\frac{\varepsilon_q}{\varepsilon}}\,\frac{W_q'(q)}{\pi}\, e^{-2\Delta W}\,\Delta q + \sqrt{\frac{\varepsilon_p}{\varepsilon}}\,\frac{V_p'(p)}{\pi}\, e^{-2\Delta V}\,\Delta p. \tag{28}$$

It is remarkable that the expressions Eq. (27) and Eq. (28) can be obtained in the path integral formulation of the theory by calculating the matrix elements of tunneling between two classical vacua in an one-instanton background Polyakov (1977). That is, the matrix elements of $\hat\psi_\pm$, $Q_{q\pm}$ and $Q_{p\pm}$ can be calculated in the background of the classical solutions $\dot q_c = -W_c$ and $\dot p_c = -V_c$. In doing this we re-write the matrix element Eq. (26) in terms of eigenstates of the conjugate operator $\hat\psi_\pm$:

$$\begin{aligned}
&\sqrt{\varepsilon}\,\, < +0q_+p_+|Q_+|q_-p_-0- >< -0q_-p_-|\hat\psi_-|q_+p_+0+ >= \\
&\sqrt{\varepsilon_q}\,\, < +0q_+|Q_{q+}|q_-0- >< -0q_-|\hat\psi_-|q_+0+ > - \\
&\sqrt{\varepsilon_p}\,\, < +0p_+|Q_{p+}|p_-0- >< -0p_-|\hat\psi_-|p_+0+ > .
\end{aligned} \tag{29}$$

This, in turn, can be presented by path integrals defined in terms of anticommuting c-number operators ζ and η where $\psi = \sqrt{\frac{1}{2}}\begin{pmatrix} \eta+\zeta \\ i(\eta-\zeta) \end{pmatrix}$, with Euclidean actions of the instantons S_X^E in $q-$ and $p-$ spaces, respectively. Given S_X^E one may calculate the matrix elements of $\hat\psi_\pm$ and $Q_{X\pm}$. The corresponding functional integrals include an integration over *instanton time* τ_0 which is due to the problem of zero modes of the bilinear terms in Euclidean actions Salomonson & Van Holten (1982). The zero mode problem is solved by introducing a collective coordinate τ_0 replacing the bosonic zero mode Balantekin (1998). In the case when

doi: https://doi.org/10.52526/25792776-26.73.1-8

the SUSY potentials in $q-$ and $p-$ spaces have more than two extrema q_ν and p_μ, $\nu, \mu = 1, 2, \ldots, N$, one can put asymptotic conditions on the SUSY potentials Sobouti & Nasiri (1993) as

$$\begin{aligned} &\int_0^\infty W(q')dq' \to \infty \quad \text{at} \quad q \to \pm\infty \quad \text{for} \quad \psi_0^+, \\ &\int_0^\infty W(q')dq' \to -\infty \quad \text{at} \quad q \to \pm\infty \quad \text{for} \quad \psi_0^-, \end{aligned} \tag{30}$$

and similar ones for $V(p)$, that the extrema are well separated: $\int_{q_\nu}^{q_\nu+1} W(q')dq' \gg 1$, and $\int_{p_\mu}^{q_\mu+1} V(p')dp' \gg 1$. Around each of the classical minima q_ν and p_μ of the potentials $W^2(q)$ and $V^2(p)$, respectively, one can approximate the theory by a suppersymmetric harmonic oscillator. Then there are N ground states which have zero energy. These states are described by upper or lower component of the wave function, depending on whether ν and μ are odd or even. With this provision the functional integrals are calculated in Salomonson & Van Holten (1982), hence

$$\begin{aligned} &< +0q_+|Q_{q+}|q_-0- >= i\sqrt{\frac{W_c'(q_+)}{\pi}}\, e^{-\Delta W_c}, \\ &< -0q_-|\hat{\psi}_-|q_+0+ >= \sqrt{\frac{W_c'(q_+)}{\pi}}\, e^{-\Delta W_c}\Delta q_c, \end{aligned} \tag{31}$$

etc. Inserting this in Eq. (29), we arrive at the Eq. (27)

$$\begin{aligned} &< +0q_+p_+|Q_+|q_-p_-0- >< -0q_-p_-|\hat{\psi}_-|q_+p_+0+ >= \\ &i\sqrt{\frac{\varepsilon_q}{\varepsilon}}\,\frac{W_c'(q)}{\pi}\, e^{-2\Delta W_c}\Delta q_c - i\sqrt{\frac{\varepsilon_p}{\varepsilon}}\,\frac{V_c'(p)}{\pi}\, e^{-2\Delta V_c}\Delta p_c, \end{aligned} \tag{32}$$

and, thus, of Eq. (28). This proves that the extended SUSY breaking has resulted from tunneling between the classical vacua of the theory. The corrections to this picture are due to higher order terms and quantum tunneling effects.

4. Spectrum generating algebra

An extended Hamiltonian H_{ext} can be treated as a set of two ordinary two-dimensional partner Hamiltonians Sobouti & Nasiri (1993)

$$H_\pm = \frac{1}{2}\left[\pi_q^2 - \pi_p^2 + U_\pm(q,p)\right], \tag{33}$$

provided by partner potentials

$$\begin{aligned} &U_\pm(q,p) = U_{q\pm}(q) - U_{p\pm}(p), \quad U_{q\pm}(q) = W^2(q,\, a_q) \mp W_q'(q,\, a_q), \\ &U_{p\pm}(p) = V^2(p,\, a_p) \mp V_p'(p,\, a_p). \end{aligned} \tag{34}$$

A subset of the SUSY potentials for which the Schrödinger-like equations are exactly solvable share an integrability conditions of *shape-invariance* Balantekin (1998), Gangopadhyaya (1998), Gendenshtein (1983):

$$U_+(a_0,q,p) = U_-(a_1,q,p) + R(a_0), \quad a_1 = f(a_0), \tag{35}$$

where a_0 and a_1 are a set of parameters that specify phase-space-independent properties of the potentials, and the reminder $R(a_0)$ is independent of (q,p).

Using the standard technique, we may construct a series of Hamiltonians H_N, $\quad N = 0, 1, 2, \ldots,$

$$H_N = \frac{1}{2}\left[\pi_q^2 - \pi_p^2 + U_-(a_N,q,p) + \sum_{k=1}^{N} R(a_k)\right], \tag{36}$$

where $a_N = f^{(N)}(a)$ (N is the number of iterations). From Eqs. (34) and (35) we obtain $N = n+m$ coupled nonlinear differential equations which are the two recurrence relations of Riccati-type differential equations:

$$\begin{aligned} &W_{n+1}^2(q) + W_{q(n+1)}'(q) = W_n^2(q) - W_{qn}'(q) - \mu_n, \\ &V_{m+1}^2(p) + V_{p(m+1)}'(p) = V_m^2(p) - V_{pm}'(p) - \nu_m, \end{aligned} \tag{37}$$

doi: https://doi.org/10.52526/25792776-26.73.1-8

where we denote $W_n(q) \equiv W(q, a_{qn})$, $V_m(p) \equiv V(p, a_{pm})$, $\mu_n \equiv R_q(a_{qn})$ and $\nu_m \equiv R_p(a_{pm})$. Here we admit that for unbroken SUSY, the eigenstates of the potentials $U_{q,p}$, respectively, are

$$E^{(-)}_{q0} = 0, \quad E^{(-)}_{qn} = \sum_{i=0}^{n-1} \mu_i, \quad E^{(-)}_{p0} = 0, \quad E^{(-)}_{pm} = \sum_{j=0}^{m-1} \nu_j, \tag{38}$$

that is, the ground states are at zero energies, characteristic of unbroken supersymmetry. The differential equations (37) can be investigated to find exactly solvable potentials.

The shape invariance condition of Eq. (35) can be expressed in terms of bosonic operators as

$$\begin{aligned} &B_+(x, a_0)B_-(x, a_0) - B_-(x, a_1)B_+(x, a_1) = R(a_0) = \mu_0 - \nu_0, \\ &B_{X+}(X, a_{X0})B_{X-}(X, a_{X0}) - B_{X-}(X, a_{X1})B_{X+}(X, a_{X1}) = (\mu_0 \,\text{or}\, \nu_0), \end{aligned} \tag{39}$$

where $x(q, p)$-is the coordinate in $(q, p)-$ space. To classify algebras associated with the shape invariance, following Gangopadhyaya (1998) we introduce an auxiliary variables $\phi(\phi_q, \phi_p)$ and define the following creation and annihilation operators:

$$J_+ = e^{ik\phi}B_+(x, \chi(i\partial_\phi)), \quad J_- = B_-(x, \chi(i\partial_\phi))e^{-ik\phi}, \tag{40}$$

where $k(k_q, k_p)$ are an arbitrary real constants and $\chi(\chi_q, \chi_p)$ are an arbitrary real functions. Consequently, the creation and annihilation operators in $(q, p)-$spaces can be written as

$$J_{X+} = e^{ik_X\phi_X}B_{X+}(X, \chi_X(i\partial_{\phi_X})), \quad J_{X-} = B_{X-}(X, \chi_X(i\partial_{\phi_X}))e^{-ik_X\phi_X}. \tag{41}$$

The operators $B_\pm(x, \chi(i\partial_\phi))$ and $B_{X\pm}(X, \chi_X(i\partial_{\phi_X}))$ are the generalization of Eqs. (39), where $a_0 \to \chi(i\partial_\phi))$ and $a_{X0} \to \chi_X(i\partial_{\phi_X}))$. If we choose the function $\chi(i\partial_\phi)$ such that $\chi(i\partial_\phi + k) = f[\chi(i\partial_\phi)]$, then we have identified $a_0 \to \chi(i\partial_\phi))$, and $a_1 = f(a_0) \to f[\chi(i\partial_\phi))] = \chi(i\partial_\phi + k)$. From Eq. (39) we obtain

$$\begin{aligned} &B_+(x, \chi(i\partial_\phi))B_-(x, \chi(i\partial_\phi)) - B_-(x, \chi(i\partial_\phi + k))B_+(x, \chi(i\partial_\phi + k)) = R[\chi(i\partial_\phi))], \\ &B_{X+}(X, \chi_X(i\partial_{\phi_X}))B_{X-}(X, \chi(i\partial_{\phi_X}))- \\ &B_{X-}(X, \chi_X(i\partial_{\phi_X} + k_X))B_{X+}(X, \chi_X(i\partial_{\phi_X} + k_X)) = R_X[\chi_X(i\partial_{\phi_X}))]. \end{aligned} \tag{42}$$

Introducing the operators $J_3 = -\dfrac{i}{k}\partial_\phi$ and $J_{X3} = -\dfrac{i}{k_X}\partial_{\phi_X}$, and combining Eqs. (41) and (42), we arrive at a deformed Lie algebras as follows:

$$\begin{aligned} &[J_+, J_-] = [J_{q+}, J_{q-}] - [J_{p+}, J_{p-}] = \xi(J_3) = \xi_q(J_{q3}) - \xi_p(J_{p3}), \\ &[J_3, J_\pm] = \pm J_\pm, \quad [J_{X+}, J_{X-}] = \xi_X(J_{X3}), \quad [J_{X3}, J_{X\pm}] = \pm J_{X\pm}, \end{aligned} \tag{43}$$

where $\xi(J_3) \equiv R[\chi(i\partial_\phi))]$ and $\xi_X(J_{X3}) \equiv R_X[\chi_X(i\partial_{\phi_X}))]$ define the deformations. Different χ functions in Eq. (42) define different reparametrizations corresponding to several models. For example:
1. The translational models ($a_1 = a_0 + k$) correspond to $\chi(z) = z$. If R is a linear function of J_3 the algebra becomes SO(2.1) or SO(3). Similar in many respects prediction is made in somewhat different method by Balantekin Balantekin (1998).
2. The scaling models ($a_1 = e^k a_0$) correspond to $\chi(z) = e^z$, etc.

To find the energy spectrum of the partner SUSY Hamiltonians

$$\begin{aligned} &2H_-(x, \chi(i\partial_\phi)) = B_-(x, \chi(i\partial_\phi + k))B_+(x, \chi(i\partial_\phi + k)), \\ &2H_{X-}(X, \chi_X(i\partial_{\phi_X})) = B_{X-}(X, \chi_X(i\partial_{\phi_X} + k_X))B_{X+}(X, \chi_X(i\partial_{\phi_X} + k_X)), \end{aligned} \tag{44}$$

one must construct the unitary representations of the deformed Lie algebra defined by Eq. (43) Gangopadhyaya (1998), E. (rf:). Using the standard technique, one defines up to additive constants the functions $g(J_3)$ and $g_X(J_{X3})$:

$$\xi(J_3) = g(J_3) - g(J_3 - 1), \quad \xi_X(J_{X3}) = g_X(J_{X3}) - g_X(J_{X3} - 1). \tag{45}$$

The Casimirs of this algebra can be written as $C_2 = J_-J_+ + g(J_3)$ and accordingly $C_{X2} = J_{X-}J_{X+} + g_X(J_{X3})$. In a basis in which J_3 and C_2 are diagonal, J_- and J_+ are lowering and raising operators (the same holds for X-representations). Operating on an arbitrary state $|h>$ they yield

$$J_3|h >= h|h >, \quad J_-|h >= a(h)|h-1 >, \quad J_+|h >= a^*(h+1)|h+1 >, \tag{46}$$

doi: https://doi.org/10.52526/25792776-26.73.1-8

where

$$|a(h)|^2 - |a(h+1)|^2 = g(h) - g(h-1). \tag{47}$$

Similar arguments can be used for the operators $J_{(p,q)3}$, C_{X2} and $J_{X\pm}$, which yield similar relations for the states h_X. The profile of $g(h)$ (and, thus, of $g_X(h_X)$) determines the dimension of the unitary representation. Having the representation of the algebra associated with a characteristic model, consequently we obtain the complete spectrum of the system. Let us obtain, for example, analytic expressions for the entire energy spectrum of extended Hamiltonian with *Self-Similar* potential without ever referring to underlying differential equation. A scaling change of parameters is given as $a_1 = Qa_0, \quad a_{X1} = Q_X a_{X0}$, at the simple choice $R(a_0) = -r_1 a_0$, where r_1 is a constant. That is,

$$\xi(J_3) \equiv -r_1 \exp(-kJ_3) = \xi_q(J_{q3}) - \xi_p(J_{p3}) = -r_{q1}\exp(-k_q J_{q3}) + r_{p1}\exp(-k_p J_{p3}). \tag{48}$$

This yields

$$[J_+,\, J_-] = \xi(J_3) = -r_1 \exp(-kJ_3), \quad [J_3,\, J_\pm] = \pm J_\pm, \tag{49}$$

which is a deformation of the standard $SO(2.1)$ Lie algebra. Therefore, one gets

$$\begin{aligned} g(h) &= \frac{r_1}{e^k - 1} e^{-kh} = -\frac{r_1}{1-Q} Q^{-h}, \quad Q = e^k, \\ g_X(h_X) &= \frac{r_{X1}}{e^{k_X} - 1} e^{-k_X h_X} = -\frac{r_{X1}}{1-Q_X} Q_X^{-h_X}, \quad Q_X = e^{k_X}. \end{aligned} \tag{50}$$

For scaling problems Gangopadhyaya (1998) one has $0 < q < 1$, which leads to $k < 0$. The unitary representation of this algebra for monotonically decreasing profile of the function $g(h)$, are infinite dimensional. Let the lowest weight state of the J_3 be h_{min}, then $a(h_{min}) = 0$. One can choose the coefficients $a(h)$ to be real. From Eq. (47), for an arbitrary $h = h_{min} + n, n = 0, 1, 2, \ldots$, we obtain

$$a(h)^2 = g(h-n-1) - g(h-1) = r_1 \frac{Q^n - 1}{Q-1} Q^{1-h}. \tag{51}$$

The spectrum of the extended Hamiltonian $H_-(x, a_1)$ reads

$$H_-|h>= a(h)^2|h>= r_1 \frac{Q^n - 1}{Q-1} Q^{1-h}|h>, \tag{52}$$

with the eigenenergies

$$E_n(h) = r_1 \alpha(h) \frac{Q^n - 1}{Q-1}, \quad \alpha(h) \equiv Q^{1-h}. \tag{53}$$

Similar expressions can be obtained for the H_{X-} and eigenenergies E_{qn_1} and E_{pn_2} $(n \equiv (n_1, n_2), \quad n_{1,2} = 0, 1, 2, \ldots)$, as

$$\begin{aligned} H_{q-}|h_q>&= a_q(h_q)^2|h_q>= r_{q1} \frac{Q_q^{n_1} - 1}{Q_q - 1} Q_q^{1-h_q}|h_q>, \\ H_{p-}|h_p>&= a_p(h_p)^2|h_p>= r_{p1} \frac{Q_p^{n_2} - 1}{Q_p - 1} Q_p^{1-h_p}|h_p>, \end{aligned} \tag{54}$$

and

$$\begin{aligned} E_{qn_1}(h_q) &= r_{q1}\alpha_q(h_q) \frac{Q_q^{n_1} - 1}{Q_q - 1}, \quad \alpha_q(h_q) \equiv Q_q^{1-h_q}, \\ E_{pn_2}(h_p) &= r_{p1}\alpha_p(h_p) \frac{Q_p^{n_2} - 1}{Q_p - 1}, \quad \alpha_p(h_p) \equiv Q_p^{1-h_p}. \end{aligned} \tag{55}$$

Hence

$$E_n(h) = E_{qn_1}(h_q) - E_{pn_2}(h_p). \tag{56}$$

5. Concluding remarks

A considered classical system is characterized by the presence of two additional local in time odd integrals of motion being (N=2)-supersymmetry generators. We calculate the parameters which measure the breaking of EPS SUSY and analyze non-perturbative mechanism for EPS SUSY breaking in the instanton picture. We show that this has resulted from tunneling between the classical vacua of the theory. Using the factorization procedure we explore the algebraic property of shape invariance and SGA.

doi: https://doi.org/10.52526/25792776-26.73.1-8

References

Balantekin A., 1998, Phys. Rev. A, 57, 4188

E. W., 1981, Nucl. Phys., B 188, 513

E. W., 1982, Nucl. Phys., B 202, 253

Gamboa J., Plyushchay M., 1998, Nucl. Phys., B 512, 485

Gangopadhyaya A. e. a., 1998, UICHEP-TH/98-11, [hep-th/9810074]

Gendenshtein L., 1983, JETP Lett., 38, 356

Inomata A., 1992, in Inomata H et al. *Path Integrals and Coherent States of SU(2) and SU(1,1)*. (World Scientific, Singapore)

Inomata A., Junker G., 1991, Quasi-classical approach to path integrals in supersymmetric quantum mechanics, in Cerdeira H et al. *Lectures on Path Integration*. (World Scientific, Singapore)

Nasiri S. e. a., 2006, J. of Math. Phys., 47, 092106

Nicolai H., 1976, J. Phys., A 9, 1497

Polyakov A., 1977, Nucl. Phys., B 120, 429

Salomonson P., Van Holten J., 1982, Nucl. Phys., B 196, 509

Sobouti Y., Nasiri S., 1993, Int. J. of Mod. Phys., B 7, 3255

Ter-Kazarian G., 2009, J. Phys. A: Math. Theor., 42, 055302

Ter-Kazarian G., Sobouti Y., 2008, J. Phys. A: Math. Theor., 41, 315303

doi: https://doi.org/10.52526/25792776-26.73.1-8

Communications of BAO, Vol. 73, Issue 1, 2026, pp. 17-23

Non-Linear Realizations of 'Distortion' Group

G.Ter-Kazarian*

Byurakan Astrophysical Observatory, Byurakan, Aragatsotn Province, Armenia

Abstract

In the framework of the method of phenomenological Lagrangians, we address the non-linear realizations of the Lie group G concerning the 'distortion' of 12-dimensional space. Treating the 'distortion' group G and its stationary subgroup $H = SO(3)$, respectively, as the dynamical group and its algebraic subgroup, we identify the parameters of the quotient space G/H of adjacent classes by the subgroup H with the Goldstone fields of spontaneous breaking of 'distortion' symmetry. We study the geometrical structure of the space of parameters in terms of Cartan forms introduced through the appropriate Maurer-Cartan's structure equations. This allows us to infer the group invariants and calculate the conserved currents as its inevitable corollaries.

Keywords: *Phenomenological Lagrangians–non-linear realizations of Lie group–Symmetry breaking–Maurer-Cartan's equations–Conserved currents*

1. Introduction

We have gained some insight into the concept of gauge group of gravitation in the proposed 'general gauge principle' (GGP) formalism Ter-Kazarian (1997, 2001). This is an alternative to the conventional gauge principle and accounts for gravity generated by hidden local internal symmetries implemented on 'maximally symmetric' (MS) auxiliary space. This formalism manifests its practical and technical virtue, providing a framework for the unitary mapping of the conventional gauge field dynamics from auxiliary MS-space to curved Riemannian space. In this, we need only to regard the auxiliary MS-space with a whole set of well-defined Killing vectors as a guide in dealing with an intricate 'jungle' of curved Riemannian geometry. On the other hand, this formalism allows for a subsequent extension of the curvature of the space-time continuum to the 'distortion' of 12-dimensional MS-space: $G_{12} = G_6 \oplus \overline{G}_6$, $DimG_{12} = 12$, $DimG_6 = 6$, $Dim\overline{G}_6 = 6$. As that initial phase of the investigation neared completion, however, it also became apparent that the most controversial point of the suggested approach is that 'distortion' transformations are not uniquely specified, leaving open the possibility to assign many physically inequivalent metrics to one and the same distortion gage field. Keeping in mind the aforementioned, our interest in the present article is to complete this formalism; in particular, much more can be done to clarify and rigorously formulate the results and formulations already provided if we uniquely determine the 'distortion' transformations and, thus, the 'distortion' group. This can be achieved by a non-linear realization of the Lie group G of 'distortion' of the G_{12} in the framework of the method of phenomenological Lagrangians Coleman & Zumino (1969)-Isham (1969). Conceptually and technically, this method is versatile and powerful. This allows, for example, to treat chiral dynamics as the theory of spontaneous breaking of chiral symmetry and/or General Relativity as the theory of spontaneous breaking of affine and conformal symmetries Borisov (1974). In what follows, we study the geometrical structure of the space of parameters in terms of Cartan forms , implying the appropriate Maurer-Cartan's structure equations. In its present formulation, we identify the 'distortion' gage fields with the Goldstone fields and calculate the conserved currents. However, the formalism being followed may seem a purely formal exercise. To avoid this unnecessary misimpression, as a tangible example indicating the potential insights this formalism may yield, we refer to Ter-Kazarian (1997, 2001) for further details. The paper consists of four parts. Section 2 deals with the space G_{12} and its distortion, section 3 considers the spontaneous breaking of 'distortion' symmetry. Section 4 deals with the Lagrangian of Goldstone fields and conserved currents. We will be brief and often suppress the indices without notice.

*gago_50@yahoo.com

doi: https://doi.org/10.52526/25792776-26.73.1-17

2. The space G_{12}

2.1. General prescription

Consider the curve $\lambda(t) : R^1 \to G_{12}$ passing through the point $p = \lambda(0) \in G_{12}$ with tangent vector $\mathbf{A}|_{\lambda(t)}$. The $\{\zeta\}$ are local coordinates in an open neighborhood of $p \in \mathcal{U}$. The 12-dimensional smooth vector field $\mathbf{A}_p = \mathbf{A}(\zeta)$ belongs to the section of tangent bundle $\mathbf{T}_p$ at the point $p(\zeta)$. The one parameter group of diffeomorphisms A^t for the curve $\zeta(t)$ passing through the points p and $\zeta(0) = \zeta_p$, $\quad \dot{\zeta}(0) = \mathbf{A}_p$, is written as

$$d\,A^t_p(\mathbf{A}) = \frac{d}{d\,t}\bigg|_{t=0} A^t\,(\zeta(t)) = \mathbf{A}_p(\zeta),$$

such that

$$d\,A^t : \mathbf{T}(G_{12}) \to R\left(\mathbf{T}(G_{12}) = \bigcup_{p(\zeta)} \mathbf{T}_p\right).$$

The $e_{(\lambda,\mu,\alpha)} = O_{\lambda,\mu} \times \sigma_\alpha \qquad (\lambda, \mu = 1, 2; \quad \alpha = 1, 2, 3)$ are linear independent 12 unit basis vectors at the point $p \in G_{12}$ provided by the unit vectors $O_{\lambda,\mu}$ and σ_α implying

$$< O_{\lambda,\mu}, O_{\tau,\nu} >= {}^*\delta_{\lambda\tau}{}^*\delta_{\mu\nu}, \quad < \sigma_\alpha, \sigma_\beta >= \delta_{\alpha\beta}, \tag{1}$$

where $\delta_{\alpha\beta}$ is the Kronecker symbol, but ${}^*\delta_{11} = {}^*\delta_{22} = 0$ and ${}^*\delta_{12} = {}^*\delta_{21} = 1$. The basis vectors σ_α refer to given three dimensional ordinary space $R^3_{\lambda\mu}$. The metric on G_{12} reads

$$\hat{\mathbf{g}} : \mathbf{T}_p \times \mathbf{T}_p \to C^\infty(G_{12}).$$

Let also the massless gauge field $a_A(\zeta)$ associate with the connection in the principal bundle $p : E \to G_{12}$ with a structure group U^{loc}, where the coordinates ζ exist in the whole region $\mathcal{U}$ of space G_{12}.

2.2. Distortion of the G_{12}

Determining the distortion transformations of basis vectors e, given at point $p \in G_{12}$, by matrix $D(a)$ of 'distortion' group G, we assume that the basis vectors O undergo distortion transformations generated by the matrix $\mathcal{Q}(a)$ of the group Q

$$O_A(a) = \mathcal{Q}^{\tau,\nu}_A(a)\, O_{\tau,\nu}, \quad \mathcal{Q}^{\tau,\nu}_A(a) = \delta^\tau_\lambda \delta^\nu_\mu + æ\, a_A{}^*\delta^\tau_\lambda{}^*\delta^\nu_\mu, \tag{2}$$

where summation over repeated indices is implied, æ is the gauge coupling constant. To avoid from the proliferation of indices, hereafter the following convention (A) will be observed in indexing $(\lambda\mu\alpha)$, etc. Note that the distortion transformations Eq. (2) violate the first condition in Eq. (1). The basis vectors σ, in turn, undergo distortion transformations of rotation: $\sigma_A(\theta) = \mathcal{R}^\beta_A(\theta)\,\sigma_\beta$, where $\quad \mathcal{R}(\theta) \in SO(3)$ is the element of group of rotations of planes involving two arbitrary axes around orthogonal third axes in the given three-dimensional ingredient space $R^3_{\lambda\mu} \quad (G_{12} = \sum_{\lambda\mu} \oplus R^3_{\lambda\mu})$. Even though, the rotation $\mathcal{R}(\theta)$ violates the second relation of orthogonality in Eqs. (1) between the basis vectors σ of different ingredient spaces, however, the three-dimensionality of each ingredient space remains intact. The resulting rotation matrix $\mathcal{R}(\theta)$ should be independent of the sequence of rotations carried out. This implies a symmetrization of resulting matrix $\mathcal{R}(\theta) = \frac{1}{6}\sum_{i\neq j\neq k} \mathcal{R}^{(ijk)}(\theta)$, where $\mathcal{R}^{(ijk)}(\theta) \in SO(3)$ is the matrix of rotations carried out in the given sequence $(ijk) \quad (i, j, k = 1, 2, 3)$. The infinitesimal transformations read

$$\delta\,\mathcal{Q}^{\tau,\nu}_A(a) = æ\,\delta\,a_A X^{\tau\nu}_{\lambda\mu} \in Q, \quad \delta\,\mathcal{R}(\theta) = -\tfrac{i}{2} M_{\alpha\beta}\delta\,\omega^{\alpha\beta} \in SO(3), \tag{3}$$

provided by the generators $X^{\tau\nu}_{\lambda\mu} = {}^*\delta^\tau_\lambda{}^*\delta^\nu_\mu$, and $I_i = \frac{\sigma_i}{2}$, where σ_i are the Pauli's matrices, that

$$M_{\alpha\beta} = \varepsilon_{\alpha\beta\gamma} I_\gamma, \quad \left[\tfrac{\sigma_i}{2}, \tfrac{\sigma_k}{2},\right] = i\varepsilon_{ikj}\tfrac{\sigma_j}{2}, \quad \delta\,\omega^{\alpha\beta} = \varepsilon_{\alpha\beta\gamma}\delta\,\theta_\gamma. \tag{4}$$

One may now implement the matrix

$$D(a,\,\theta) = \mathcal{Q}(a) \times \mathcal{R}(\theta) \tag{5}$$

doi: https://doi.org/10.52526/25792776-26.73.1-17

of 'distortion' group $G = Q \times SO(3)$ by which the basis vector e is transformed at point $p \in G_{12}$. The infinitesimal transformations of the group G read

$$\begin{array}{l} D_{(d\,a^A,\,d\,\theta^A)} = I + d\,D_{(a^A,\,\theta^A)}, \\ d\,D_{(a^A,\,\theta^A)} = i\left[d\,a^A X_A + d\,\theta^A I_A\right], \end{array} \tag{6}$$

where $I_A \equiv I_\alpha$ at given λ and μ $(A = (\lambda\mu\alpha))$. We associate with each point $(a,\,\theta)$ of the group space the Cartesian basis vector, in group sense, that corresponds to the basis vector at the point of origin $(0,\,0)$

$$\begin{array}{l} G(g) \equiv G(a + d\,a,\,\theta + d\,\theta)\,G^{-1}(a,\,\theta) = \\ G(d\,a',\,d\,\theta')\,G^{-1}(0,\,0) = G(d\,a',\,d\,\theta'). \end{array} \tag{7}$$

It is introduced to ensure that the vector $(a,\,\theta;\,a + d\,a,\,\theta + d\,\theta)$ has the same analytical expression of the vector $(0,\,0;\,d\,a',\,d\,\theta)'$ (Eq. (6))

$$D_{(a,\,\theta)}\,d\,D^{-1}_{(a,\,\theta)} = i[\omega^A\,X_A + \vartheta^A\,I_A], \tag{8}$$

where we denote $d\,a'^A = \omega^A(a,\,\theta;\,d\,a,\,d\,\theta)$ and $d\,\theta'^A = \vartheta^A(a,\,\theta;\,d\,a,\,d\,\theta)$. In accordance, an infinitesimal action of the group on basis vectors e_A can be written as

$$\begin{array}{l} d\,e_A = e_A\,d\,F_A = O_A(d) \times \sigma_A + O_A \times \sigma_A(d) = \\ i[\omega^A(d)\,X_A + \vartheta^A(d)\,I_A]\,e_A, \end{array} \tag{9}$$

where we denote $e_A \equiv (\exp F_A)$. The functions $\omega^A(d)$ and $\vartheta^A(d)$ will be determined in the next section. One may, however, envisage that the distortion transformations of basis vectors O and σ, in fact, are not independent but rather governed by a spontaneous breaking of 'distortion' symmetry, which yields the uniquely determined matrix Eq. (5).

3. A spontaneous breaking of 'distortion' symmetry

Our major goal is now to proceed to the spontaneous breaking of 'distortion' symmetry. Although the generators X_A (Eq. (3)) of the group Q cannot be considered the generators of the quotient space G/H, because they do not complete the group H to the dynamical group G, and therefore the 'distortion' fields $a_A(\zeta)$ cannot be identified directly with the Goldstone fields of the spontaneous breaking of the 'distortion' symmetry. However, the modified 'distortion' fields can be identified with the Goldstone fields. Actually, let us deal with the non-linear realizations of the 'distortion' group G. Following a general prescription of the method of phenomenological Lagrangians Coleman & Zumino (1969), Curtis G. & Zumino (1969), Isham (1969), Weinberg (1970), in the case at hand we treat the 'distortion' group G and its stationary subgroup $H = SO(3)$, respectively, as the dynamical group and its algebraic subgroup, respectively, and then let the parameters $\overline{a}_A(a)$ of the quotient space G/H of adjacent classes be the Goldstone fields of the spontaneous breaking of the 'distortion' symmetry. In order to obtain a feeling for this point, we re-define, for example, the pair of basis vectors O_{11} and O_{22} in terms of new orthogonal unit vectors n_1 and n_2

$$O_{11} = \tfrac{1}{\sqrt{2}}\,(n_1 + n_2)\,, \quad O_{22} = \tfrac{1}{\sqrt{2}}\,(n_1 - n_2)\,, \tag{10}$$

where $n_1^2 = -n_2^2 = 1, \quad < n_1,\,n_2 >= 0$ (see Eq. (1)). Denoting $\tan\,\overline{\theta}_A = -æ\,a_A$, it is straightforward to show that the distortion transformations Eq. (2) of basis vectors O_{11} and O_{22} are reduced to the transformations of the group $SO(3)$ of modified basis vectors

$$\overline{O}_A = \frac{1}{\sqrt{2}}\left(n_1(\overline{\theta}_A) + \epsilon_A\,n_2(\overline{\theta}_A)\right) = \cos\,\overline{\theta}_A O_A, \tag{11}$$

where $\epsilon_{(11\alpha)} = -\epsilon_{(22\alpha)} = 1$, such that

$$\left(\begin{array}{c} n_1(\overline{\theta}_A) \\ n_2(\overline{\theta}_A) \end{array}\right)\left(\begin{array}{cc} \cos\,\overline{\theta}_A & \sin\,\overline{\theta}_A \\ -\sin\,\overline{\theta}_A & \cos\,\overline{\theta}_A \end{array}\right)\left(\begin{array}{c} n_1 \\ n_2 \end{array}\right). \tag{12}$$

Here the rotation on $\overline{\theta}_{(11\alpha)}$ is in clockwise direction, while it is counterclockwise for $\overline{\theta}_{(22\alpha)}$. The same holds for the pair O_{12} and O_{21}. The 'distortion' group $G = Q \times SO(3)$, therefore, can be mapped onto the

doi: https://doi.org/10.52526/25792776-26.73.1-17

group $G = SO(3) \times SO(3)$ in a one-to-one manner. The latter is isomorphic to the isotopic chiral group $SU(2) \times SU(2)$, for which the method of phenomenological Lagrangians is well known Coleman & Zumino (1969), Curtis G. & Zumino (1969), Isham (1969), Weinberg (1970). For the sake of simplicity, throughout this subsection we leave the Greek indices implicit unless otherwise stated, such that $A = (\lambda\mu i) \to i = 1, 2, 3,$. But it goes without saying that all the results obtained refer to the given three-dimensional ingredient space $R^3_{\lambda\mu}$. Three I_i among the six generators of the group correspond to isotopic transformations, and three K_i correspond to special chiral transformations mixing the states of different parities. They imply the conventional commutation relations

$$[I_i,\, I_j] = i\varepsilon_{ijk} I_k; \quad [I_i,\, K_j] = i\varepsilon_{ijl} K_l; \quad [K_i,\, K_j] = i\varepsilon_{ijk} I_k, \tag{13}$$

of the invariant subgroup $H = SO(3)$, with the generators I_i, and of the quotient space G/H, with the generators K_i, where ε_{ijk} denotes the antisymmetric unit tensor. Three parameters $\overline{a}^i(a)$ of special chiral transformations, with respect to which the Lagrangian of physical fields is not invariant, can be identified as three Goldstone fields. They are introduced to make provisions for Eq. (9), which, when incorporated into Eq. (11), are designed to yield

$$\begin{aligned} &d\,\overline{e}_A(\overline{a}) = \overline{e}_A(a)\, d\,\overline{F}_A(\overline{\theta},\, \theta) = \overline{O}_A(d) \times \sigma_A + \overline{O}_A \times \sigma_A(d) = \\ &i[\omega^i(\overline{a},\, d\,\overline{a})\, K_i + \vartheta^l(\overline{a},\, d\,\overline{a})\, I_l]\, \overline{e}_A(\overline{a}) \end{aligned} \tag{14}$$

in terms of generators of the group $SU(2) \times SU(2)$, where $\overline{e}_A(\overline{a}) = \overline{O}_A(\overline{a}) \times \sigma_A(\overline{a})$. Now we are looking for the function $\overline{\theta}(\theta)$ for which $d\,\overline{F}_A(\overline{\theta},\, \theta)$ constitutes a total differential and, thus, $\omega^i(\overline{a},\, d\,\overline{a})$ and $\vartheta^l(\overline{a},\, d\,\overline{a})$ are the Cartan's forms. Then

$$\frac{\partial^2\, \overline{F}_A}{\partial\,\overline{\theta}\,\partial\,\theta} = \frac{\partial^2\, \overline{F}_A}{\partial\,\theta\,\partial\,\overline{\theta}}, \tag{15}$$

where we suppress the indices without notice ($\overline{\theta} \equiv \overline{\theta}_A$ and $\theta \equiv \theta_A$). Using the explicit form of infinitesimal transformations (Eq. (3))

$$d\,\sigma_{(\lambda\mu l)} = \sigma_{(\lambda\mu l)}(d) = \tfrac{1}{2}\varepsilon_{lkj}\sigma_k d\,\theta_{(\lambda\mu j)}, \tag{16}$$

it is straightforward to calculate the partial derivative

$$\frac{\partial\, F_A}{\partial\,\theta} = \frac{\partial\,\sigma_A}{\sigma_A\,\partial\,\theta} \equiv \frac{\sigma_A(\partial)}{\sigma_A\,\partial\,\theta} = \frac{1}{\sin\,\theta_A}. \tag{17}$$

The similar relation holds for the vectors $d\,n_{1A}(\overline{\theta})$ and $d\,n_{2A}(\overline{\theta})$ (Eq. (12)), and thus $\frac{\partial\,\overline{F}_A}{\partial\,\overline{\theta}} = \frac{1}{\sin\,\overline{\theta}_A}$. Hence , the holonomy condition Eq. (15) is reduced to

$$\frac{\partial}{\partial\,\theta}\left(\frac{1}{\sin\,\overline{\theta}_A}\right) = \frac{\partial}{\partial\,\overline{\theta}}\left(\frac{1}{\sin\,\theta_A}\right), \tag{18}$$

the nontrivial solution of which is $\theta_A = \overline{\theta}_A$, and thus, we arrive at

$$\tan\,\theta_A = -æ\, a_A. \tag{19}$$

This key relation contains no new information, beyond the fact that it uniquely determines the 12 angles θ_A of rotations around each of the 12 axes (A) at a given distortion field a_A. We are now in a position to infer the Maurer-Cartan's structure equations. According to Poincaré's theorem, the external derivative $(')$ of the total differential form is zero, and therefore Eq. (14) gives

$$\begin{aligned} &(\overline{e}_A(a)\, d\,\overline{F}_A)' = \overline{e}_A(a)\, \left([d\,\overline{F}_A, \delta\,\overline{F}_A] + (d\,\overline{F}_A)'\right) = \\ &i\left([\omega^i(\overline{a},\, d\,\overline{a})\, K_i + \vartheta^l(\overline{a},\, d\,\overline{a})\, I_l]\, \overline{e}_A(a)\right)' = 0, \end{aligned} \tag{20}$$

where $[d\,\overline{F}_A, \delta\,\overline{F}_A] = (d\,\overline{F}_A)' = 0$. In the calculation of the external differential and external product of the forms in Eq. (20), the differentials of functions $(K_i\,\overline{e}_A)$ and $(I_l\,\overline{e}_A)$ figured in the bilinear differential

$$\begin{aligned} &\delta\,d\,\overline{e}_A = i[\delta\,\omega^i(d)\, X_i + \delta\,\vartheta^l(d)\, I_l]\,\overline{e}_A + \\ &i[\omega^i(d)\,\delta(K_i\,\overline{e}_A) + \vartheta^l(d)\,\delta(I_l\,\overline{e}_A)], \end{aligned} \tag{21}$$

will be defined according to Eq. (14). Equating the coefficients of the same linearly independent generators of the external differential in Eq. (20) to zero yields the following system of structure equations:

$$\begin{aligned} &(\omega^i)' = [\omega^k,\, \vartheta^\beta]\, \varepsilon_{ik\beta}, \\ &(\vartheta^\gamma)' = [\vartheta^\alpha,\, \vartheta^\beta]\, \varepsilon_{\gamma\alpha\beta}/2 + \varepsilon_{\gamma ki}[\omega^k,\, \omega^i]/2, \end{aligned} \tag{22}$$

doi: https://doi.org/10.52526/25792776-26.73.1-17

provided we have the external differential and external product of the forms written as

$$\begin{aligned}&(\omega^i)' = -\delta\,\omega^i(d) + d\,\omega^i(\delta),\\ &\left[\omega^k,\, \vartheta^\beta\right] = \omega^k(d)\vartheta^\beta(\delta) - \omega^k(\delta)\vartheta^\beta(d).\end{aligned} \tag{23}$$

Defining the new forms $\omega^i_k = \vartheta^\beta \varepsilon_{ik\beta}$ and using the relations $\varepsilon_{k\alpha\beta}\,\varepsilon_{ijk} = (\varepsilon_{i\beta k}\,\varepsilon_{k\alpha j} - \varepsilon_{i\alpha k}\,\varepsilon_{k\beta j})$, which stem from Yacobi's identity.

$$\{[K_i[I_\alpha,\, I_\beta]]\} + \quad \text{permutations} \equiv 0, \tag{24}$$

the Eqs. (22) yield the Maurer-Cartan's structure equations

$$\begin{aligned}&(\omega^i)' = [\omega^k,\, \omega^i_k],\\ &(\omega^i_k)' = -R^l_{jki}[\omega^k,\, \omega^i]/2 + [\omega^k_j,\, \omega^l_k],\end{aligned} \tag{25}$$

where $R^l_{jki} = -\varepsilon_{lj\gamma}\varepsilon_{\gamma ki}$ is the curvature of the group space, These equations describe the motion of the orthogonal reper joint to the given point of the group space. The forms ω^i and ω^i_k are interpreted as the transformations of translation and rotation of the orthogonal reper, such that the rotation $(\vartheta^l I_l)$ belongs to the stationary group H, while the translation reads as $(\omega^i K_i)$. Whereas the invariant constraint Eq. (18) means that there always exists a rotation transformation of the stationary subgroup H annulling the change in the equation of Cartan's forms arising from the translation transformation of the quotien space $\overline{Q} = G/H$. A general transformation of the group G can be written as

$$G = \overline{Q}(\overline{a})H(\theta), \tag{26}$$

where $\overline{Q}(\overline{a})$ is the transformation belonging to the left adjacent class G/H of the group G by subgroup H. Acting from the left by the group element g we define the transformation of parameters $\overline{a}$ and θ:

$$G(g)\overline{Q}(\overline{a})H(\theta) = \overline{Q}(\overline{a}'(\overline{a},\, g))H(\theta'(\theta,\, \overline{a},\, g)). \tag{27}$$

The Cartan's forms allow an exponentiation of the group element $\overline{Q}(a) = \exp(i\overline{a}^i K_i)$, which determines the modified 'distortion' fields $\overline{a}(a)$

$$d\,\overline{e}_A(\overline{a}) = \left[\exp(-i\overline{a}^i K_i)\, d\, \exp(i\overline{a}^i K_i)\right]\, \overline{e}_A(\overline{a}). \tag{28}$$

Exponential parametrization of the finite transformations of the group is equivalent to the choice of normal coordinates in the quotien space G/H. The solution of the structure equations (25) reads

$$\begin{aligned}&\omega^i(\overline{a},\, d\,\overline{a}) = (\sin\sqrt{m}/\sqrt{m})^i_k\; d\,\overline{a}^k, \quad m^i_k = -\varepsilon_{ij\alpha}\varepsilon_{\alpha kl}\,\overline{a}^j\,\overline{a}^k,\\ &\vartheta^\alpha(\overline{a},\, d\,\overline{a}) = [(1-\cos\sqrt{m})\,/m]^i_k\; d\,\overline{a}^k\,\varepsilon_{\alpha il}\,\overline{a}^l,.\end{aligned} \tag{29}$$

Using the relations

$$\left(m^{(n)}\right)^i_j = (\overline{a}^2)^{n-1}\left(m^{(1)}\right)^i_j, \quad m^i_j = \varepsilon_{ilk}\varepsilon_{kjn}\overline{a}^l\overline{a}^n = \overline{a}^2\delta_{ij} - \overline{a}^i\overline{a}^j, \tag{30}$$

the Eq. (29) was reduced as

$$\begin{aligned}&\omega^i_A = \omega^i(\overline{a},\, \partial_A\,\overline{a}) = \partial_A\,\overline{a}^i + (\delta_{ik} - \overline{a}^i\overline{a}^k/\overline{a}^2)\left(\sin\sqrt{\overline{a}^2}/\sqrt{\overline{a}^2} - 1\right)\partial_A\,\overline{a}^k,\\ &\vartheta^i_A = \vartheta^i(\overline{a},\, \partial_A\,\overline{a}) = \left[\left(1-\cos\sqrt{\overline{a}^2}\right)/\overline{a}^2\right]\partial_A\,\overline{a}^l\,\varepsilon_{ilj}\,\overline{a}^j.\end{aligned} \tag{31}$$

4. Conserved currents

The Lagrangian of Goldstone field $(\overline{a})$ can be identified with the square of the interval of the geodesic line, with a minimal number of derivatives, between the infinitely close points $\overline{a}^i$ and $\overline{a}^i + d\,\overline{a}^i$

$$L_{\overline{a}}(\zeta) = \tfrac{1}{2}\,\omega^i(\overline{a},\, \partial_A\,\overline{a})\omega^i(\overline{a},\, \partial_A\,\overline{a}), \tag{32}$$

where $\varepsilon_{\alpha il}\varepsilon_{l\alpha j} = -\delta_{ij}$ is the metric tensor of the group space. In normal coordinates, it takes the form

$$\begin{aligned}&L_{\overline{a}}(\zeta) = (\partial_A\,\overline{a})^2/2+\\ &(\delta_{ik} - \overline{a}^i\overline{a}^k/\overline{a}^2)\left(\sin^2\sqrt{\overline{a}^2}/\sqrt{\overline{a}^2} - 1\right)\partial_A\,\overline{a}^i\,\partial_A\,\overline{a}^k/2.\end{aligned} \tag{33}$$

doi: https://doi.org/10.52526/25792776-26.73.1-17

Since the massless gauge field (a) is associated with the gauge group U^{loc}, the Lagrangian Eq. (34) should be equated to undegenerated Killing form defined on the Lie algebra of the group U^{loc} in adjoint representation

$$L_{\overline{a}}(\zeta) = L_a(\zeta) = -\tfrac{1}{4} < F_{AB}(a),\, F^{AB}(a) >_K, \tag{34}$$

where $F_{AB}(a)$ is the antisymmetric tensor of the gauge field (a). The Goldstone field $(\overline{a})$ as a function of the gauge field (a) can be determined from Eq. (34). Suppose Ψ is a collection of matter fields of arbitrary spin , which are sections of the vector bundles associated with U^{loc} by mapping $\Psi : G_{12} \to E$ that $p\,\Psi(\zeta) = \zeta$. The various suffixes of Ψ are left implicit. They take values in the standard fiber $\mathcal{F}_\zeta$ upon $\zeta : p^{-1}(\mathcal{U}) = \mathcal{U} \times \mathcal{F}_\zeta$, where an expansion into the direct product $p^{-1}(\mathcal{U}) = \mathcal{U} \times G_{12}$ is defined upon $\mathcal{U}$. The fiber is the Hilbert vector space on which the linear representation $U(\zeta)$ of the group U^{loc} is given. This space can be regarded as the Lie algebra of the group U^{loc} upon which the Lie algebra acts according to the law of the adjoint representation: $a \leftrightarrow ad\,a\;\Psi \to [a\,,\Psi]$. The covariant derivatives of the matter fields Ψ interacting with the Goldstone fields $\overline{a}$ are determined by means of the form ϑ^α

$$L = L_0\,(\Psi,\, \partial_A \Psi + \vartheta^\alpha(\overline{a},\, \partial_A\,\overline{a}) T_\alpha\,\Psi)\,, \tag{35}$$

where $L_0\,(\Psi,\, \partial_A\Psi)$ is the Lagrangian of interacting matter fields classified by the linear representations T_α of the subgroup H. The Lagrangians Eq. (33) and Eq. (35) are invariant with respect to 'distortion' translations and rotations. These also should be completed by the transformations

$$\Psi' = \left(\exp\,[i\eta'^\alpha(\overline{a},\, g) T_\alpha]\right)\,\Psi, \tag{36}$$

where the parameters $\eta'^\alpha(\overline{a},\, g)$ can be determined from Eq. (27). In exponential parametrization this gives

$$G(g)\exp(i\overline{a}^i K_i)\exp(i\eta^\alpha I_\alpha) = \exp\left[i\overline{a}^i(\overline{a},\, g) K_i\right]\exp\left[i\eta'^\alpha(\overline{a},\, g) I_\alpha\right]. \tag{37}$$

According to the Eq. (37), the transformation of parameters $\overline{a}$ and θ at the infinitesimal translation $G(g) = (1 + i\varepsilon^i\,K_i) + O(\varepsilon^2)$ can be written

$$(1 + i\varepsilon^i\,K_i)\exp(iK_i\overline{a}^i) = \exp\left[iK_i(\overline{a}^i + \delta\,\overline{a}^i(\overline{a},\,\varepsilon))\right]\exp\left[i\delta\,\theta^\alpha(\overline{a},\,\varepsilon)) I_\alpha\right]. \tag{38}$$

Employing the Feynman's method of ordering by means of auxiliary parameter t Gell-Mann (1960) which implies $\int_x^y\, A(t)d\,t = A(y-x)$, in standard manner we expand

$$\begin{array}{l} \exp\left[iK_i(\overline{a}^i + \delta\,\overline{a}^i)\right] = \exp(iK_i\overline{a}^i) + i\exp(iK_i\overline{a}^i)\times \\ \times \int_0^1\, d\,t\,\exp(-iK_i\overline{a}^i\,t)\,(\delta\,\overline{a}^i\,K_i)\,\exp(iK_i\overline{a}^i\,t) + \cdots . \end{array} \tag{39}$$

Then the Eq. (38) gives

$$i\varepsilon^i\,K_i(1) = i\int_0^1\, d\,t\delta\,\overline{a}^i K_i(t) + i\delta\,\theta^\alpha(\overline{a},\,\theta) I_\alpha, \tag{40}$$

where

$$K_j(t) = \exp(-iK\overline{a}^i t) K_j \exp(iK_i\overline{a}^i t). \tag{41}$$

In analogy defining the $I_\alpha(t)$, and taking derivatives of the $K_j(t)$ and $I_\alpha(t)$ with respect to parameter t, we get

$$\begin{array}{ll} \frac{\partial}{\partial t}\,K_j(t) = i\varepsilon_{\alpha j i}\overline{a}^i\,I_\alpha(t); & K_j(0) = K_j, \\ \frac{\partial}{\partial t}\,I_\alpha(t) = i\varepsilon_{l\alpha k}\overline{a}^k\,K_l(t); & I_\alpha(0) = 0, \end{array} \tag{42}$$

the solution of which can be written in the form of Eq. (29)

$$K_j(t) = (\cos\,\sqrt{m}\,t)^i_j\;K_j + i\,(\sin\,\sqrt{m}\,t/\sqrt{m})^l_j\;\varepsilon_{\alpha lk}\,\overline{a}^k\,I_\alpha. \tag{43}$$

Inserting this solution into the Eq. (40) and equating the coefficients at the same generators $K_j I_\alpha$, one gets

$$\begin{array}{l} \delta\,\overline{a}^i(\overline{a},\,\theta)) = -(\sqrt{m}\,\coth\,\sqrt{m})^i_k\varepsilon^k + O(\varepsilon^2), \\ \delta\,\theta^\alpha(\overline{a},\,\theta)) = \{[\sin\,\sqrt{m} - \coth\,\sqrt{m}(1-\cos\,\sqrt{m})]/\sqrt{m}\}^l_i\,\varepsilon^i\,\varepsilon_{\alpha lk}\overline{a}^k. \end{array} \tag{44}$$

The transformation of parameters in the case of rotation $G(g') = (1 + i\xi^\alpha\,I_\alpha) + O(\xi^2)$ is obtained in the same way

$$\delta\,\overline{a}^i(\xi)) = -\varepsilon_{i\alpha k}\,\xi^\alpha\,\overline{a}^k + O(\xi^2), \quad \delta\,\theta^\alpha(\overline{a},\,\xi)) = \xi^\alpha. \tag{45}$$

doi: https://doi.org/10.52526/25792776-26.73.1-17

Let the fields undergo the infinitesimal transformations

$$\Phi^j(\zeta) \rightarrow \Phi^j(\zeta) + \varepsilon(\zeta)^k \prod\nolimits_k^j(\Phi), \tag{46}$$

where $\prod_k^j(\Phi)$ is the non-linear function of the fields. The current related to transformation Eq. (46)

$$J_k^A = -\delta L(\Phi, \partial \Phi)/\delta (\partial_A \varepsilon^k) = -\prod\nolimits_k^j(\Phi)\, \delta L(\Phi, \partial \Phi)/\delta (\partial_A \Phi^j), \tag{47}$$

can be written

$$\partial_A J_k^A = -\delta L(\Phi, \partial \Phi)/\delta \varepsilon^k. \tag{48}$$

Thus, if the Lagrangian is invariant with respect to constant transformations Eq. (46), then the corresponding current is conserved. Leaving the 12-dimensional indices A implicit, the conserved currents corresponding to Eq. (29), Eq. (44) and Eq. (45) can be calculated in normal coordinates as

$$\begin{aligned} J^k(\overline{a}, \partial \overline{a}) &\equiv \omega^k(2\overline{a}, \partial \overline{a}) = (\sin 2\sqrt{m}/2\sqrt{m})_i^k \partial \overline{a}^i, \\ J^\alpha(\overline{a}, \partial \overline{a}) &\equiv \vartheta^\alpha(2\overline{a}, \partial \overline{a}) = -\left[(1 - \cos 2\sqrt{m})/2m\right]_k^i \partial \overline{a}^k \varepsilon_{\alpha i l}\, \overline{a}^l. \end{aligned} \tag{49}$$

5. Concluding remarks

It is worth reflecting briefly on the results obtained so far. Based on the powerful method of phenomenological Lagrangians, the new conceptual element in non-linear realizations of the Lie group G of 'distortion' of the space G_{12}, is noteworthy. This restores the most important unifying feature of the theory and completes the GGP formalism; in particular, it clarifies and rigorously establishes the results and formulations already given in Ter-Kazarian (1997, 2001). We have identified the parameters of quotien space G/H of adjacent classes by the subgroup H with the Goldstone fields of spontaneous breaking of 'distortion' symmetry. The inferred key relation Eq. (19) uniquely determines the 12 angles θ_A of rotations around each of the 12 axes at a given distortion field a_A, due to which the distortion transformations and, thus, the distortion group G become uniquely determined. We have studied the geometrical structure of the space of parameters in terms of Cartan forms, implying the appropriate Maurer-Cartan's structure equations, which allow us to infer the group invariants and calculate the conserved currents.

References

Borisov A.B. O. V., 1974, Theor. and Math. Phys., 21, 329

Coleman S. W. J., Zumino B., 1969, Phys.Rev., 177, 2239

Curtis G. Callan J. C. S. W. J., Zumino B., 1969, Phys.Rev., 177, 2247

Gell-Mann M. Levi M., 1960, Nuovo Cimento, 16, 705

Isham C., 1969, Nuovo Cimento, Sec. A 59, 356

Ter-Kazarian G., 1997, Nuovo Cimento, Sec. B 112

Ter-Kazarian G., 2001, J. Phys. Soc. Japan, Suppl. B 70, 84

Weinberg S., 1970, Lectures on elementary particles and quantum field theory. Cambridge

doi: https://doi.org/10.52526/25792776-26.73.1-17

Rearrangement of Vacuum State in Gravitation

G.Ter-Kazarian*

Byurakan Astrophysical Observatory, Byurakan, Aragatsotn Province, Armenia

Abstract

We address the processes of rearrangement of vacuum state and spontaneous gauge symmetry breaking in gravity. This is achieved by an extension of 'standard gauge principle' to 'general gauge principle' (GGP). The GGP accounts for the gravity generated by hidden local internal symmetries implemented on 'maximally symmetric' (MS) auxiliary space. In doing this, we extend the curvature to a general 'distortion' of the space-time continuum as the theory of spontaneous breaking of 'distortion' symmetry. We have to implement the hidden gauge symmetry of two-parameter abelian group $U^{loc} = U(1)_Y \times \overline{U}(1)$ on the extended 12-dimensional MS-space, with the group elements of $exp\,[i\frac{Y}{2}\,\theta_Y(\zeta)]$ of $U(1)_Y$ and $exp\,[iT^3\,\theta_3(\zeta)]$ of $\overline{U}(1)$, respectively. This group has two generators, the hypercharge Y and the third component T^3 of isospin. The neutral complex Higgs scalar breaks the vacuum symmetry, leaving the 'gravitation' subgroup intact. The massive field component of the so-called 'inner distortion' (ID) causes the shift of zero point energy and, thus, simultaneously with the strong gravity, a significant change in the properties of the space-time continuum has occurred at huge energies. This leads to the 'matter-to-proto-matter' phase transition of second kind.

Keywords: *Gravity–General gauge principle–Spontaneous breaking of gauge symmetry–Inner distortion of spacetime*

1. Introduction

Although the geometrical interpretation of gravitation has advantages in solving the problems of cosmology, nevertheless such a distinction of the gravitational field among the fields gives rise to difficulties in the unified theories of all interactions of elementary particles and in the quantization of gravitation. Even though it being among the most significant advances in physics, in particular, General Relativity (GR) as a geometrized theory of gravitation clashes from the outset with the basic principles of field theory. It is rather not conducive to resolving the controversial problems of energy-momentum conservation laws, localization of energy of gravitational waves, etc. These stem from the fact that Riemannian geometry, in general, does not admit a group of isometries; i.e., Poincaré transformations no longer act as isometries, and, in particular, it is impossible to define energy-momentum as Noether local currents related to exact symmetries. This, in turn, posed severe problems in Riemannian space interacting quantum field theory, among which is the non-uniqueness of the 'physical' vacuum and the associated Fock space. It is perhaps worth remarking that one of the underlying principles of Minkowski space interacting quantum field theory is that the vacuum is unique, in particular, $|in>=|out>$ (up to a phase factor). The peculiar shortcoming of the interacting quantum field theory in curved space-time is the following two important questions to be addressed yet: a) an absence of the definitive concept of space-like separated points, particularly in the canonical approach, and the 'light-cone' structure at each space-time point; b) the separation of positive and negative-frequencies for completeness of the Hilbert-space description. Due to it, the definition of positive frequency modes cannot, in general, be unambiguously fixed in the past and future. This leads to $|in>\neq|out>$, because $|in>$ is unstable against decay into many particle $|out>$ states due to interaction processes allowed by lack of Poincaré invariance. Whereas, non-trivial Bogolubov transformation between past and future positive frequency modes implies that particles are created from the vacuum and this is one of the reasons for $|in>\neq|out>$. Riemannian space interacting quantum field theory based on GR, thus, cannot be a satisfactory ground for addressing the processes of rearrangement of vacuum state and spontaneous gauge symmetry breaking in gravity. As a remarkable extension of GR is an analogy revealed

*gago_50@yahoo.com

doi: https://doi.org/10.52526/25792776-26.73.1-24

between the gravitons and $SU(2) \times SU(2)$ chiral dynamics based on non-linear realizations of chiral symmetry Borisov (1974). This based on the main fact that infinite-dimensional algebra of general covariance group is the closure of finite-dimensional algebra of conformal and linear affine groups Borisov (1973).

Our interest in Ter-Kazarian (2026) was to discuss the most controversial point that 'distortion' transformations are not uniquely specified, leaving the possibility to assign many physically inequivalent metrics to one and the same distortion gauge field. We therefore uniquely determined the 'distortion' transformations and, thus, the 'distortion' group. This was achieved by the non-linear realization of the Lie group G of 'distortion' of the G_{12} by employing the exponential parametrization of the metric tensor in the framework of the method of phenomenological Lagrangians Coleman & Zumino (1969), Curtis G. & Zumino (1969), Isham (1969), Weinberg (1970). Treating the 'distortion' group G and its stationary subgroup $H = SO(3)$, respectively, as the dynamical group and its algebraic subgroup, we identify the parameters of quotien space G/H of adjacent classes by the subgroup H with the Goldstone fields of spontaneous breaking of 'distortion' symmetry. We study the geometrical structure of the space of parameters in terms of Cartan forms introduced through the appropriate Maurer-Cartan's structure equations. This allows us to infer the group invariants and calculate the conserved currents as its inevitable corollaries. Conceptually and technique-wise this method is versatile and powerful. Continuing along this line, in the present article we have gained some insight into the proposed GGP formalism to clarify and rigorously present the results and formulations already given. We show that the theory of the gravitational field is, in fact, the theory of spontaneous breaking of the affine and conformal symmetries just as chiral dynamics is the theory of spontaneous breaking of chiral symmetry. In this manner, non-linear realizations of the group of general covariance, linearized on the Poincaré group, are constructed. Although such an unexpected treatment entails a significant extension beyond the geometrical interpretation of gravity, no single theory has been invented yet that successfully addresses the solution to the problems involved.

1.1. Rationale

We develop on the extension of standard gauge principle to the framework of GGP Ter-Kazarian (1997, 2001) (see Appendix), wherein general covariance and gauge invariance are maintained. In this, we discuss the gauge group of gravitation generated by hidden local internal symmetries implemented on the auxiliary MS-space. Involving the auxiliary MS-space, with the whole set of well-defined Killing's vectors, has a single aim as a guiding tool in dealing with an intricate'jungle' of curved geometry. We extend the curvature of the space-time continuum to general 'distortion' as the theory of spontaneous breaking of 'distortion' symmetry. This can be achieved by non-linear realizations of the 'distortion' group. In terms of Cartan's forms, implying the Maurer-Cartan's structure equations, we treat the modified 'distortion' fields as the Goldstone fields and calculate the conserved currents. The framework of GGP allows to address the processes of rearrangement of vacuum state and spontaneous gauge symmetry breaking in gravity. We have to implement the simplest hidden gauge symmetry of the abelian group $U^{loc} = U(1)_Y \times \overline{U}(1)$ on the extended 12-dimensional MS-space (sect.III). The introduced group entails two neutral gauge vector bosons of $\overline{U}(1) \equiv diag[SU(2)]$ or that coupled of third component T^3 of isospin $\vec{T}$, and of $U(1)_Y$, or hypercharge Y. Since in the MS-space interacting quantum field theory the vacuum is well-determined and unique, spontaneous symmetry breaking is achieved in the standard manner by introducing the neutral complex Higgs scalar. A Non-vanishing vacuum expectation value (VEV) leaves one Goldstone boson, which is gaged away from the scalar sector. However, it essentially reappears in the gage sector, providing the longitudinally polarized spin state of one of the gage bosons that acquires mass through its coupling to the Higgs scalar. Two neutral gauge bosons were mixed to form two physical orthogonal states: one is the massless component of the 'distortion' field responsible for gravitational interactions, and the other is its massive component responsible for the ID-regime. At this level, the theory is renormalizable, and thus one has a self-contained theory because gauge invariance ensures conservation of charge and the cancelation of quantum corrections that would otherwise result in infinitely large amplitudes. Without careful thought, we expect that in the framework of GGP the renormalizability of the theory will not be spoiled in curved space-time too because the infinities arise from the ultra-violet properties of Feynman integrals in momentum space which, in coordinate space, are short distance properties, and locally (over short distances) all curved space-time looks like MS-space. A more detailed analysis and calculations on this will be presented in another paper to follow at a later date. In the resulting theory, simultaneously with the strong gravity, the massive ID-field component causes the shift of zero point energy and, thus, a significant change in the properties of the space-time continuum occurs. This leads to the 'matter-to-proto-matter' phase transition occurring at huge energies.

doi: https://doi.org/10.52526/25792776-26.73.1-24

1.2. Result

The paper is organized as follows: In the sect.II we briefly outline the framework of GGP and relate it to non-linear realization of the group of general covariance. We will refrain from providing lengthy details of the formalism of GGP and unitary mapping. For this, the reader is referred to the Appendix. In the sect.III we extend the space-time continuum to the extra-dimensions, and show that the curvature is a particular regime of general 'distortion' of the space-time continuum. The latter is due to spontaneous breaking of 'distortion' symmetry. We supplement this by addressing the processes of rearrangement of vacuum state and spontaneous gauge symmetry breaking in gravity (sect.IV), and, further, study the resulting process of 'matter-to-proto-matter' phase transition (sect.V). In the Appendix, we complete the formalism of GGP; in particular, much more can be done to clarify and rigorize the results and formulations already given in Ter-Kazarian (1997, 2001). We will be brief and often suppress the indices without notice; also, unless otherwise stated, we take geometrized units throughout this paper.

2. GGP and Non-Linear Realization of The Group of General Covariance in R_4

In the framework of GGP Ter-Kazarian (1997, 2001) the most general trend emerges as the formalism of unitary mapping of the standard gauge field dynamics from auxiliary MS-space M_4 to curved Riemannian R_4 space. The quantities denoted by wiggles hereafter refer to 'distorted' space; in particular, in this section, they refer to curved space, while the quantities referring to MS- space are left without wiggles.

2.1. General prescription

• Let $a(x)\,(\equiv a_\mu(x))$ be the massless gauge field, taking values in the Lie algebra $\hat{g}$ of abelian group U^{loc}. It is a local form of expression of connection in the principal bundle $p: E \rightarrow M_4$ with a structure group U^{loc}. The coordinates (x) exist in the whole region $\mathcal{U}$ of M_4, where the metric $(\hat{\eta})$ is $S^2\tau^*$: $\hat{\eta}: \tau\times\tau \rightarrow C^\infty(M_4)$, with symmetric components (η_{lk}) in the basis e_l. A collection Φ of matter fields of arbitrary spin are the sections of vector bundles associated with U^{loc} by mapping $\Phi: M_4 \rightarrow E$ such that $p\,\Phi(x) = x$. The various suffixes of Φ are left implicit. They take values in the standard fiber $\mathcal{F}_x$ upon $x: p^{-1}(\mathcal{U}) = \mathcal{U}\times\mathcal{F}_x$, where an expansion into a direct product $p^{-1}(\mathcal{U}) = \mathcal{U}\times M_4$ is defined upon $\mathcal{U}$. The fiber is a Hilbert vector space on which a linear representation $U(x)$ of the group U^{loc} is given. This space can be regarded as the Lie algebra of the group U^{loc} upon which the Lie algebra acts according to the law of adjoint representation: $a \leftrightarrow ad\,a\;\Phi \rightarrow [a\,,\Phi]$.
• Furthermore, let $(\widetilde{x})$ be the coordinates existing in the whole region $\widetilde{\mathcal{U}}$ of curved Riemannian space R_4, where the metric is the section of conjugate vector bundle $S^2\widetilde{\tau}^*$ (symmetric part of tensor degree): $\hat{g}: \widetilde{\tau}\times\widetilde{\tau} \rightarrow C^\infty(R_4)$, with symmetric components given in the basis $\widetilde{e}_\mu$. That $\widetilde{e}_\mu = g_{\mu\nu}\,\widetilde{e}^\nu$. In holonomic basis, one has $\hat{g} = g_{\mu\nu}\,d\widetilde{x}^\mu \times d\widetilde{x}^\nu$. The general coordinate transformations $\delta\widetilde{x}_\mu = f_\mu(\widetilde{x})$, where $f_\mu(\widetilde{x})$ is an arbitrary function of coordinates $\widetilde{x}_\mu$, give rise to the infinite-parameter group of general covariance in R_4 if only the functions $f_\mu(\widetilde{x})$ can be expanded in power series of $\widetilde{x}_\mu$. While the expansion coefficients can be considered as the group-parameters, and the group-algebra includes an infinite number of generators $L_\mu^{n_1\,n_2\,n_3\,n_4} = -i\widetilde{x}_1^{n_1}\,\widetilde{x}_2^{n_2}\,\widetilde{x}_3^{n_3}\,\widetilde{x}_4^{n_4}\,\widetilde{\partial}_\mu \qquad (\widetilde{\partial}_\mu = \partial/\partial\widetilde{x}^\mu)$.

Remark: The invariance of Lagrangian of the given field $\widetilde{\Phi}(\widetilde{x})$ of arbitrary spin under the infinite-parameter group of general covariance in R_4 entails the invariance of Lagrangian under the finite local gauge transformations $U_R\,(\widetilde{x})$ of the unitary Lie group of 'gravitation' G_R and vice versa, if only the local gauge transformations of the field $\widetilde{\Phi}(\widetilde{x})$ and covariant derivative $\nabla_\mu\widetilde{\Phi}(\widetilde{x})$ hold as

$$
\begin{aligned}
&\widetilde{\Phi}'(\widetilde{x}) = U_R\,(\widetilde{x})\,\widetilde{\Phi}(\widetilde{x}),\\
&\left[g^\mu(\widetilde{x})\,\nabla_\mu\widetilde{\Phi}(\widetilde{x})\right]' = U_R\,(\widetilde{x})\left[g^\mu(\widetilde{x})\,\nabla_\mu\widetilde{\Phi}(\widetilde{x})\right].
\end{aligned}
\tag{1}
$$

The ∇_μ is the covariant derivative agreed with the metric: $\nabla_\mu = \partial_\mu + \Gamma_\mu$, where $\Gamma_\mu(\widetilde{x}) = \frac{1}{2}\,\Sigma^{\alpha\beta}\,V^\nu_\alpha(\widetilde{x})\widetilde{\partial}_\mu\,V_{\beta\nu}(\widetilde{x})$ is the connection Birrell & Davies (1982), $\Sigma_{\alpha\beta}$ are the generators of Lorentz group Λ. The components $V^\mu_\alpha(\widetilde{x}) =< \widetilde{e}^\mu, \widetilde{e}_\alpha > (\quad V_{\beta\nu} = g_{\mu\nu}V^\mu_\beta)$ of affine tetrad vectors $\widetilde{e}^\alpha$ in used coordinate net $\widetilde{x}^\mu$ associate with the chosen representation $D(\Lambda)$ by which the many-component filed $\Phi(x)$ is transformed as $[D(\Lambda)]^{l'\cdots k'}_{l\cdots k}\Phi(x), \quad D(\Lambda) = I + \frac{1}{2}\omega^{\alpha\beta}\Sigma_{\alpha\beta}$, where $\omega_{\alpha\beta} = -\omega_{\beta\alpha}$ are the parameters of the Lorentz group.

doi: https://doi.org/10.52526/25792776-26.73.1-24

One has, for example, to set $g^{\mu}(\widetilde{x}) \to \widetilde{e}^{\mu}(\widetilde{x})$ and $\gamma^{l} \to e^{l}$ for the fields of spin ($j = 0, 1$); for vector field $[\Sigma_{\alpha\beta}]^{l}_{k} = \delta^{l}_{\alpha}\eta_{\beta k} - \delta^{l}_{\beta}\eta_{\alpha k}$; but $g^{\mu}(\widetilde{x}) = V^{\mu}_{\alpha}(\widetilde{x})\,\gamma^{\alpha}$ and $\Sigma_{\alpha\beta} = -(1/4)[\gamma_{\alpha}, \gamma_{\beta}]$ for the spinor field ($j = \frac{1}{2}$), where γ^{α} are Dirac's matrices. We shall for the moment write the unitary matrix $U_R\,(\widetilde{x})$ in symbolic form which will be determined below as a function of U^{loc}. We can state:

Theorem 1: There always exists the gauge field dynamics defined on M_4 underlying the given gauge dynamics of Eqs. (1) defined on R_4.

Proof: One has to construct the diffeomorphism $\widetilde{x}^{\mu}(x^{l}) : M_4 \to R_4$ (App.1) and then show that the following smooth unitary mapping of the fields and their covariant derivatives holds:

$$\begin{aligned} &R(a) : \Phi \to \widetilde{\Phi}(\Phi), \quad (\mathcal{F}_x \to \widetilde{\mathcal{F}}_{\widetilde{x}}), \\ &S(a)\,R(a) : \left(\gamma^{k} D_k \Phi\right) \to \left(g^{\nu}(x)\nabla_{\nu}\widetilde{\Phi}\right), \end{aligned} \tag{2}$$

where $\Phi \subset \mathcal{F}_x$, $\widetilde{\Phi} \subset \widetilde{\mathcal{F}}_{\widetilde{x}}$, $\widetilde{\mathcal{F}}_{\widetilde{x}}$ is the fiber upon $\widetilde{x} : p^{-1}(\widetilde{\mathcal{U}}) = \widetilde{\mathcal{U}} \times \widetilde{\mathcal{F}}_{\widetilde{x}}$, $\widetilde{\mathcal{U}}$ is the region of base R_4, $R(a)$ denotes the unitary mapping matrix, $D_k = \partial_k - i æ\, a_k(x)$, æ is the gauge coupling constant which relates to the Newton gravitational constant as in Eq. (51), $S(a)$ is the gauge invariant scalar function given on M_4 (see Eq. (44)). We use the following notational conventions throughout this section: Greek indices stand for variables in R_4, but Latin indices refer to M_4, also $\psi^{\mu}_{l} \equiv \partial_l\, \widetilde{x}^{\mu}$ where $\partial_l = \frac{\partial}{\partial x^{l}}$. Putting forth the tensor suffixes in illustration of the point at issue, the Eqs. (2) explicitly read

$$\widetilde{\Phi}^{\mu\cdots\delta}(\widetilde{x}) = \psi^{\mu}_{l}\cdots\psi^{\delta}_{m}\, R(a)\, \Phi^{l\cdots m}(x) \equiv (R_{\psi})^{\mu\cdots\delta}_{l\cdots m}\, \Phi^{l\cdots m}(x), \tag{3}$$

and

$$g^{\nu}(x)\nabla_{\nu}\widetilde{\Phi}^{\mu\cdots\delta}(\widetilde{x}) = S(a)\, \psi^{\mu}_{l}\cdots\psi^{\delta}_{m}\, R(a)\, \gamma^{k} D_k\, \Phi^{l\cdots m}(x). \tag{4}$$

It is a straightforward to determine the transformation matrix $U_R\,(\widetilde{x})$ from the Eq. (3) or Eq. (4) and gauge transformations on M_4, such that

$$\widetilde{\Phi}'(\widetilde{x}) = U_R\,(\widetilde{x})\,\widetilde{\Phi}(\widetilde{x}) = U_R\, R_{\psi}(a)\,\Phi = R'_{\psi}\,\Phi' = R'_{\psi}\,U\,\Phi,$$

or

$$\begin{aligned} &\left(g^{\nu}(x)\nabla_{\nu}\widetilde{\Phi}(\widetilde{x})\right)' = U_R\,(\widetilde{x})\ \left(g^{\nu}(x)\nabla_{\nu}\widetilde{\Phi}(\widetilde{x})\right) = U_R\, S(a)\, R_{\psi}(a)\ \left(\gamma^{k} D_k \Phi\right) = \\ &S(a')\, R'_{\psi}\ \left(\gamma^{k} D_k\, \Phi\right)' = S(a')\, R'_{\psi}\, U\ \left(\gamma^{k} D_k\, \Phi\right). \end{aligned}$$

Hence $U_R = R'_{\psi}\, U\, R^{-1}_{\psi}$, where $R'_{\psi} \equiv R_{\psi}(a')$ and a' is the gauge field transformed under the gauge group U^{loc}. The Theorem 1 leads to the extension of standard gauge scheme to GGP, the principle idea of which is framed into requirement of *invariance of physical system of fields $\widetilde{\Phi}(\widetilde{x})$ under the finite local gauge transformations Eq. (1) of the Lie group of gravitation U_R. The latter is generated by hidden local internal symmetry U^{loc} implemented on the MS-space*:

$$\begin{array}{ccc} \widetilde{\Phi}'(\widetilde{x}) = U_R\,\widetilde{\Phi}(\widetilde{x}) & \xleftarrow{\;U_R = R'_{\psi}\, U\, R^{-1}_{\psi}\;} & \widetilde{\Phi}(\widetilde{x}) \\ R'_{\psi}(\widetilde{x},\, x)\ \Big\uparrow & & \Big\uparrow\ R_{\psi}(\widetilde{x},\, x) \\ \Phi'(x) = U\,\Phi(x) & \xleftarrow{\quad\mathrm{U}\quad} & \Phi(x) \end{array}$$

A scheme of GGP.

In this paper we employ a simplest abelian symmetry U^{loc} as the hidden symmetry, but this can be easily generalized to non-abelian symmetries.

• Following Ter-Kazarian (2026), the infinite-parameter group of general covariance can be substituted by the joint invariance with respect to affine and conformal groups simultaneously. Therefore, the GR is the theory of spontaneous breaking of the affine and conformal symmetries, just as chiral dynamics is the theory of spontaneous breaking of the chiral symmetry. This is achieved in the framework of the method of phenomenological Lagrangians Coleman & Zumino (1969), Curtis G. & Zumino (1969), Isham (1969), Weinberg (1970). The key idea of this powerful approach based on the identification of Goldstone fields with those parameters of the dynamical group corresponding to the generators which do not relate to the conservation laws. A study of geometrical structure of the space of these parameters allows to infer the

doi: https://doi.org/10.52526/25792776-26.73.1-24

explicit form of the group invariants and calculate the conserved currents. The affine group $A(4)$ is the group of all the linear transformations in the 4-dimensional space-time, having Poincaré group as subgroup. The algebra of $A(4)$ consists of 4-generators of translations P_μ, 6-generators of Lorentz subgroup $L_{\mu\nu}$, and 10-generators of special linear (affine) transformations $R_{\mu\nu}$ containing the strains. The Poincaré subgroup relates to conservation of total energy-momentum and angular momentum. But a non-linear realization of the affine group, linearized on the Poincaré group, leads to 10-component symmetric tensor of Goldstone fields $h_{\mu\nu}$. The $h_{\mu\nu}$ correspond to the rest of 10-parameters of special affine transformations of the quotien space of adjacent classes by the Lorentz stationary subgroup. The abelian group of translations has an essential role because of the coordinates, now being the parameters of the group they are figured as Goldstone fields. In the framework of GGP formalism, it is straightforward to re-write the $h_{\mu\nu}$ in terms of 'distortion' transformations matrix $D(a)$: $\quad h_{\mu\nu} = (\ln D(a))_{\mu\nu}$, where the basis vectors e at point $P \in M_4$ transformed into the basis vectors $\widetilde{e}(a)$ (Eq. (41)) at point $\widetilde{P} \in R_4$ under the action of the gauge field (a). The action of element of the group $A(4)$ in exponential parametrization is given as

$$\begin{array}{l} g\,\exp(i\widetilde{x}_\mu P_\mu)\exp(ih_{\mu\nu}R_{\mu\nu}/2) = \\ \exp(i\widetilde{x}'_\mu P_\mu)\,\exp[ih'_{\mu\nu}(\widetilde{x}')R_{\mu\nu}/2]\exp[iU_{\mu\nu}L_{\mu\nu}/2], \end{array} \tag{5}$$

where the $\widetilde{x}'_\mu$, $h'_{\mu\nu}(\widetilde{x}')$ and $U_{\mu\nu}$ are dependent of the parameters of the transformation g and the field $h_{\mu\nu}$. The Cartan's forms are determined from the equation

$$\begin{array}{l} \exp(-\frac{i}{2}h_{\alpha\beta}R_{\alpha\beta})\exp(-i\widetilde{x}_\mu P_\mu)d\,\exp(i\widetilde{x}_\mu P_\mu)\,\exp(\frac{i}{2}h_{\alpha\beta}R_{\alpha\beta}) = \\ i[\omega^p_\mu(d)P_\mu + \omega^R_{\mu\nu}(d)R_{\mu\nu}/2 + \omega^L_{\mu\nu}(d)L_{\mu\nu}/2]. \end{array} \tag{6}$$

The latter allows to rewrite explicitly the Cartan's forms in terms of distortion matrix $D(a)$ (see Eq. (41)-Eq. (42)):

$$\begin{array}{l} \omega^p_\mu(d) = D_{\mu\nu}(a)d\,\widetilde{x}^\nu = (\delta_{\mu l} + < e_\mu \chi_l >)d\,x^l = \\ d\,x_\mu - \frac{1}{2}D_{\mu\nu}\int_0^x(\partial_k D^\nu_l - \partial_l D^\nu_k)d\,x^k d\,x^l, \\ \omega^R_{\mu\nu}(d) = \left(D^{-1}_{\mu\sigma}(a)d\,D_{\sigma\nu}(a) + D^{-1}_{\nu\sigma}(a)d\,D_{\sigma\mu}(a)\right)/2, \\ \omega^L_{\mu\nu}(d) = \left(D^{-1}_{\mu\sigma}(a)d\,D_{\sigma\nu}(a) - D^{-1}_{\nu\sigma}(a)d\,D_{\sigma\mu}(a)\right)/2, \end{array} \tag{7}$$

where the invariant bilinear form reads

$$\begin{array}{l} (ds^2) = \omega^p_\mu(d)\,\omega^p_\mu(d) = g_{\mu\nu}\,d\,\widetilde{x}^\mu\,d\,\widetilde{x}^\nu = \\ r_{\mu\sigma}(\widetilde{x})\,r_{\sigma\nu}(\widetilde{x}) = D^\sigma_\mu(a)\,D^\nu_\sigma(a), \quad D^{-1}_{\mu\nu}(a) = (\exp^{-h})_{\mu\nu}. \end{array} \tag{8}$$

The forms ω^p and ω^R determine the covariant differentials of coordinate and Goldstone field h, but the form ω^L determines the covariant differential of the matter field $\widetilde{\Phi}(\widetilde{x})$. However, in general, the theory cannot be unambiguously fixed just by requirement of introducing the minimal number derivatives. As it is shown in Borisov (1974), the requirement that the theory will correspond at the same time to the realization of the conformal group, uniquely leads to the Einstein 's Lagrangian of gravitational field. Algebra of the conformal group contains the generators of the Poincaré group $L_{\mu\nu}$ and P_μ, and the generators of scaling and special conformal transformations. A determination of covariant derivative of the spinor field is identical to that as in tetrad formalism Eq. (1). Utilizing then Einstein 's Lagrangian of gravitational field as $\widetilde{L}_a(\widetilde{x}) = R/16\pi G$, where R denotes the scalar curvature on R_4, and we readily get the 10 field equations (see Eq. (50))

$$\left(R^\mu_\lambda - \frac{1}{2}\delta^\mu_\lambda R\right)\,D^l_\mu = -8\pi G\widetilde{T}_{\lambda\nu}D^{\nu l}, \tag{9}$$

obviously leading to Einsten 's 10 equations for 10 metric components of $g_{\mu\nu}(a)$. But the principle difference is now that: one is allowed to determine the energy-momentum tensor of gravitational field Ter-Kazarian (1997) and formulate local energy-momentum conservation laws for the whole gravitational system quite naturally by exploiting the advantages of auxiliary 'shadow' field dynamics on M_4, and transferring it further to R_4 in accordance to unitary mapping laws.

3. Static spherical-symmetric gravitational field

According to general prescription, the field equations are derived from an invariant action $S = S_a + \widetilde{S}_{\widetilde{\Phi}}$, being set up in the similar form of Eq. (48). The action of gauge field of distortion S_a, defined on G_{12}, is invariant under the coordinate Λ and gauge U^{loc} groups, but the action of matter fields $\widetilde{S}_{\widetilde{\Phi}}$, defined on $\widetilde{G}_{12}$,

doi: https://doi.org/10.52526/25792776-26.73.1-24

is invariant under the gauge group of gravitation G_R. Field equations follow in terms of Euler-Lagrange variations respectively on the G_{12} and $\widetilde{G}_{12}$. Using the Lagrangian of undegenerated Killing form on the Lie algebra of the group U^{loc} in adjoint representation

$$L_a(\zeta) = -\tfrac{1}{4} < F_{AB}(\zeta),\, F^{AB}(\zeta) >_K, \tag{10}$$

defined on G_{12}, the equation of distortion field then reads

$$\partial^B \partial_B\, a_A - (1-\zeta_0^{-1})\partial_A \partial^B\, a_B = -\tfrac{1}{2}\sqrt{g}\,\tfrac{\partial g^{BC}}{\partial a_A}\widetilde{T}_{BC}, \tag{11}$$

where $\widetilde{T}_{BC}$ denotes the energy-momentum tensor, ζ_0 is the gauge fixing parameter. The curvature of manifold $G_6 \to \widetilde{G_6}$, which leads to Riemannian space R_4 (Eq. (69)), is the particular distortion at

$$a_{(1,1,\alpha)} = a_{(2,1,\alpha)} \equiv \tfrac{1}{\sqrt{2}}\, a_{(+\alpha)}, \quad a_{(1,2,\alpha)} = a_{(2,2,\alpha)} \equiv \tfrac{1}{\sqrt{2}} a_{(-\alpha)}. \tag{12}$$

We determine, for example, the line element in case of static spherical-symmetric gravitational field $a_0(r)$ in outside of the configuration with mass M. Passing back $\widetilde{G}_6 \to R_4$, there is the group of motions $SO(3)$ with two-dimensional space-like orbits S^2 where the standard coordinates are $\widetilde{\theta}$ and $\widetilde{\varphi}$. The stationary subgroup of $SO(3)$ acts isotropically upon the tangent space at the point of sphere S^2 of radius $\widetilde{r}$. So, the bundle $p: R_4 \to \widetilde{R}^2$ has the fiber $S^2 = p^{-1}(\widetilde{x})$, $\quad \widetilde{x} \in R_4$ with a trivial connection on it, where $\widetilde{R}^2$ is the quotient-space $R_4/SO(3)$. The coordinates $\widetilde{x}^\mu(\widetilde{t}, \widetilde{r}, \widetilde{\theta}, \widetilde{\varphi})$ implying the diffeomorphism $\widetilde{x}^\mu(x)^l : M_4 \to R_4$ exist in the whole region $p^{-1}(\widetilde{\mathcal{U}}) \in R_4$, where $\widetilde{x}^{0r} \equiv \widetilde{t}$, $\quad \widetilde{x}^{0\theta} = \widetilde{x}^{0\varphi} = 0$. The field equation Eq. (11) given in Feynman gauge is reduced to $\nabla^2 a_0 = 0$, which has the solution $x_0 \equiv æ\, a_0 = -\frac{r_g}{2r}$, where the diffeomorphism $\widetilde{r}(r) : M_4 \to R_4$ is given $r = \widetilde{r} - \frac{r_g}{4}$, $\quad r_g$ is the gravitational radius. A straightforward calculations show that the relations $\frac{\partial \psi^l_\mu}{\partial \widetilde{x}^\nu} \neq \Gamma^\lambda_{\mu\nu}\, \psi^l_\lambda$ hold for the non-vanishing Christoffel symbols, where

$$\frac{\partial \widetilde{x}^\mu}{\partial x^l} \equiv \psi^\mu_l = \frac{1}{2}\left(D^\mu_l + \omega^m_l D^\mu_m\right), \tag{13}$$

provided by $D^0_0 = 1 + x_0$, $\quad D^r_r = 1 - x_0$, $\quad \omega^1_1 = \omega^2_2 = \omega^3_3 = 1$, $\quad \omega^0_1 = t\,\partial_r D^0_0$. Hence, the curvature is not zero. The line element can be written as

$$d\,s^2 = (1-x_0)^2\, d\widetilde{t}^2 - (1+x_0)^2\, d\widetilde{r}^2 - \widetilde{r}^2(\sin^2\widetilde{\theta}\, d\,\widetilde{\varphi}^2 + d\,\widetilde{\theta}^2), \tag{14}$$

where $x_0 = \frac{r_g}{2\,r}$. At $\frac{r_g}{r} << 1$, one has $x_0 \simeq \frac{r_g}{2\,\widetilde{r}}\left(1 + \frac{r_g}{4\,\widetilde{r}}\right)$, such that

$$\begin{aligned} &g_{00} = 1 - \tfrac{r_g}{\widetilde{r}}, \quad g_{11} = -\left(1 + \tfrac{r_g}{\widetilde{r}} + \tfrac{r_g^2}{2\,\widetilde{r}^2}\right), \\ &g_{22} = -\widetilde{r}^2, \quad g_{33} = -\widetilde{r}^2\, \sin^2\widetilde{\theta}, \end{aligned} \tag{15}$$

while all the other components are zero. Therefore, from the view point of post-Newton experiments, the discussed gravitational theory is indiscernible from the general relativity . But, the milestone of difference will be arisen at strong gravity.

4. Rearrangement of Vacuum State

Collecting together the results just established in previous sections we finally arrive at the quite promising discussion of the rearrangement of vacuum state in gravitation, while the renormalizability of the theory remains intact because of spontaneously broken gauge symmetry. Notice that abelian U^{loc}-gauge invariant theory is renormalizable because gauge invariance gives conservation of charge, also ensures the cancelation of quantum corrections that would otherwise result in infinitely large amplitudes. To trace this line we implement the simple abelian gauge group

$$U^{loc} = U(1)_Y \times \overline{U}(1) \equiv U(1)_Y \times diag[SU(2)], \tag{16}$$

on the G_{12}, with the group elements of $exp\,[i\frac{Y}{2}\,\theta_Y(\zeta)]$ of $U(1)_Y$ and $exp\,[iT^3\,\theta_3(\zeta)]$ of $\overline{U}(1)$. The group Eq. (16) leads to the renormalizable theory on G_{12}. This has two generators, the third component T^3 of isospin $\overrightarrow{T}$ related to the Pauli spin matrix $\frac{\overrightarrow{\tau}}{2}$, and hypercharge Y implying $Q^{gr} = T^3 + \frac{Y}{2}$, where Q^{gr} is the "gravitational charge" operator assigning the number -1 to particles, but +1 to anti-particles. The

doi: https://doi.org/10.52526/25792776-26.73.1-24

group Eq. (16) entails two neutral gauge bosons W^3_A of $\overline{U}(1)$ or that coupled of T^3, and B_A of $U(1)_Y$, or hypercharge Y. Gauge invariant Lagrangian of fermion field is given in standard form $\mathcal{L} = \overline{\psi}(\zeta)i\gamma^A D_A\psi(\zeta)$, provided by covariant derivative

$$D_A\,\psi(\zeta) = \left(\partial_A - ig\,T^3\,W^3_A - ig'\,\tfrac{Y}{2}\,B_A\right)\,\psi(\zeta), \tag{17}$$

and g, g' being the $\overline{U}(1)$, $\;U(1)_Y$ coupling strength, respectively. Spontaneous symmetry breaking can be achieved by the introduction of neutral complex scalar Higgs field

$$\phi = \begin{pmatrix} 0 \\ \phi^0 \end{pmatrix}, \quad Y(\phi) = 1, \quad \phi^0 = \tfrac{1}{\sqrt{2}}(\phi_1 + i\phi_2), \tag{18}$$

with the standard potential energy density function $V(\phi) = -\mu^2\phi^+\,\phi + \lambda\,(\phi^+\,\phi)^2$, where $\mu^2 > 0, \quad \lambda > 0$. This is ingredient of the gauge invariant Lagrangian of Higgs field $\mathcal{L}_H = (D_A\,\phi)^+\,\left(D^A\,\phi\right) - V(\phi)$, where

$$D_A\,\phi(\zeta) = \left(\partial_A - ig\,T^3\,W^3_A - ig'\,\tfrac{Y}{2}\,B_A\right)\,\phi(\zeta). \tag{19}$$

Minimization of the vacuum energy fixes non-vanishing VEV:

$$<\phi>_0 \equiv < 0|\phi|0 > = \begin{pmatrix} 0 \\ \frac{v}{\sqrt{2}} \end{pmatrix}, \quad v = \left(\tfrac{\mu^2}{\lambda}\right)^{1/2}, \tag{20}$$

leaving one Goldstone boson. The VEV of Eq. (20) spontaneously breaks the theory, leaving the $U(1)_{gr}$ subgroup intact. The unitary gauge

$$\phi(\zeta) = U^{-1}(\xi_3)\begin{pmatrix} 0 \\ \frac{v+\eta(\zeta)}{\sqrt{2}} \end{pmatrix}, \quad U(\xi_3) = \exp\left[\tfrac{i\xi_3\cdot\tau^3}{v}\right], \tag{21}$$

is parameterized by two real shifted fields ξ_3 and η, such that $< 0|\xi_3|0 > = < 0|\eta|0 > = 0$. The gauge transformation

$$\phi' = U(\xi_3)\,\phi = \tfrac{v+\eta}{\sqrt{2}}\,\chi, \quad \chi = \begin{pmatrix} 0 \\ 1 \end{pmatrix}, \tag{22}$$

then leads to $V(\phi') = \mu^2\eta^2 + \lambda v\eta^3 + \frac{\lambda}{4}\,\eta^4$, which gives the mass of Higgs boson $M_H = \sqrt{2}\,\mu$. An examination of the v^2-terms in the kinetic piece of the Lagrangian $\mathcal{L}_H = (D_A\,\phi')^+\,\left(D^A\,\phi'\right) - V(\phi')$, reveals the mass terms for the physical gauge bosons:

$$\begin{gathered} \tfrac{v^2}{2}\,\left|\left(i\tfrac{g}{2}\,\tau^3\,W'^3_A + ig'\,\tfrac{Y}{2}\,B'_A\right)\,\chi\right|^2 = \\ \tfrac{1}{2}\,(Z_A,\,A_A)\begin{pmatrix} M_Z^2 & 0 \\ 0 & 0 \end{pmatrix}\begin{pmatrix} Z^A \\ A^A \end{pmatrix}. \end{gathered} \tag{23}$$

The mass matrix is diagonalized by the standard orthogonal transformations:

$$\begin{aligned} &Z_A = \cos\theta_W\,W'^3_A + \sin\theta_W\,B'_A, \quad M_Z = \tfrac{v}{2}\sqrt{g^2 + g'^2}, \\ &A_A = \sin\theta_W\,W'^3_A + \cos\theta_W\,B'_A, \quad M_A = 0, \end{aligned} \tag{24}$$

where $\tan\theta_W = g'/g$. Namely, the neutral gauge field W'^3_A mixes with the abelian gauge field B'_A to form the physical states Z_A and A_A, with the masses M_Z and M_A, respectively. For neutral current we get

$$\mathcal{L}_{int} = æ\,\left(\mathcal{J}^{gr}_A\,A^A + \mathcal{J}^{in}_A\,Z^A\right) \equiv æ\,\left(\mathcal{J}^{dis}_A\,a^A\right), \tag{25}$$

where $æ = g\,\sin\theta$, and

$$\begin{aligned} &\mathcal{J}^{gr}_A = \overline{\psi}(\zeta)i\gamma_A\,Q^{gr}\,\psi(\zeta), \quad \mathcal{J}^{in}_A = \overline{\psi}(\zeta)i\gamma_A\,Q^{in}\,\psi(\zeta), \\ &\mathcal{J}^{dis}_A = \overline{\psi}(\zeta)i\gamma_A\,\psi(\zeta), \quad Q^{in} = \tfrac{T^3 - \sin^2\theta_W,\,Q^{gr}}{\sin\theta_W\,\cos\theta_W},. \end{aligned} \tag{26}$$

To obtain some feeling for the distortion field $a_A(\zeta)$ defined on G_{12}, the massless field $Q^{gr}\cdot A_A$ will be identified with the gravitational field component $a_a \quad (a \equiv (\lambda\alpha),\ \lambda = \pm)$ of $a_A \equiv (a_a,\,\overline{a}_a)$, but the massive field $Q^{in}\cdot Z_A$ will be identified with the ID-component $\overline{a}_a$, that

$$Q^{gr}\cdot A_A(\zeta) \equiv (a_a(\zeta),\,0)\,, \quad Q^{in}\cdot Z_A(\zeta) \equiv (0,\,\overline{a}_a(\zeta))\,. \tag{27}$$

doi: https://doi.org/10.52526/25792776-26.73.1-24

Hence

$$\begin{aligned} A_a &= \frac{a_a}{Q^{gr}} = \frac{1}{\cos\theta_W} B'_a = \frac{1}{\sin\theta_W} W'^3_a, \\ Z_a &= \frac{\overline{a}_a}{Q^{in}} = -\frac{1}{\sin\theta_W} \overline{B}'_a = \frac{1}{\cos\theta_W} \overline{W}'^3_a, \end{aligned} \tag{28}$$

where $B'_A \equiv \left(B'_a,\, \overline{B'}_a\right)$, $W^{3\prime}_A \equiv \left(W^{3\prime}_a,\, \overline{W^{3\prime}}_a\right)$. Therefore,

$$\begin{aligned} & M_{B'} = M_{W'} = M_a = 0, \quad M_Z = \sin\theta_W\, M_{\overline{B}'} = \cos\theta_W\, M_{\overline{W}'}, \\ & M_{\overline{a}} = M_Z/Q^{in} = \tan\theta_W\, M_Z, \end{aligned} \tag{29}$$

where we have taken into account that $Y(a) = Q(a) = T^3(a) = 0$. Corresponding coupling constants are: $æ_A = æ\, Q^{gr}$ and $æ_Z = æ\, Q^{in} = æ\cot\theta_W$, respectively for the components A_a and Z_a. The Compton wave-length of the massless gravitational component A_a is infinite $\lambda_A = \infty$, but the Compton wave-length of the massive ID-component Z_a is finite due to spontaneous symmetry breaking. This may be of vital interest for the physics of superdense matter in very compact astrophysical sources if (Ter-Kazarian (2001))

$$\lambda_Z = \frac{2\hbar}{cv\sqrt{g^2 + g'^2}} \leq 0.4\, fm, \tag{30}$$

where $\simeq 0.4\, fm$ is the distance between the particles at nuclear density (we re-instate c).

Remark: The principle assumption went into the building of the suggested approach that the Higgs boson is coupled only with the distortion field $a_A(A_a,\, Z_a)$, but not with other auxiliary fields defined on G_{12}. This means that all the coupling constants of Yukawa's interaction of Higgs particle with auxiliary "shadow" fields are zero. Therefore, the Higgs boson interacts with the real matter fields defined on the distorted space $\widetilde{G}_{12}$ only via the metric tensor.

5. The 'matter-to-proto-matter' phase transition

For the reminder of this article, we discuss the 'matter $\rightarrow$ proto-matter' phase transition processes occurred in the ID-regime at

$$a_{(1,1,\alpha)} = -a_{(2,1,\alpha)} \equiv \frac{1}{\sqrt{2}}\, \overline{a}_{(+\alpha)}, \quad a_{(1,2,\alpha)} = -a_{(2,2,\alpha)} \equiv \frac{1}{\sqrt{2}}\, \overline{a}_{(-\alpha)}. \tag{31}$$

This yields the 12 distorted basis vectors $(\widetilde{e}^\mu,\, \widetilde{\overline{e}}^\mu)$ transformed by the matrices $(D^\mu_\nu(æ_Z\, Z),\, \overline{D}^\mu_\nu(æ_Z\, Z))$, where $\widetilde{e}^\mu$ and $\widetilde{\overline{e}}^\mu$ are the basis vectors given in distorted spaces $\widetilde{G}_6 = \widetilde{R}^3 \oplus \widetilde{T}^3$ and $\widetilde{\overline{G}}_6 = \widetilde{\overline{R}}^3 \oplus \widetilde{\overline{T}}^3$, respectively. The transformation matrices read

$$D^\mu_\nu(æ_Z\, Z) = \delta^\mu_\nu + d^\mu_\nu(æ_Z\, Z), \quad \overline{D}^\mu_\nu(æ_Z\, Z) = \delta^\mu_\nu + \overline{d}^\mu_\nu(æ_Z\, Z), \tag{32}$$

where we leave the matrices $d^\mu_\nu(æ_Z\, Z)$ and $\overline{d}^\mu_\nu(æ_Z\, Z)$ implicit, and $\tan\theta_a = -æ_Z\, Z_a$. Given the distorted basis vectors, it is straightforward to derive the laws of phase transition of individual particle found in the ID-region. Actually, the 12-momentum $\widetilde{P}_A$ of the particle, as the Poincaré generator of translation in the $\widetilde{G}_{12}$, can be written

$$\widetilde{\overline{P}} = \widetilde{e}^A\, \widetilde{P}_A = \widetilde{e}^\mu\, p_\mu - \widetilde{\overline{e}}^\mu\, \overline{p}_\mu \equiv e^\mu\, p^f_\mu - \overline{e}^\mu\, \overline{p}^f_\mu. \tag{33}$$

Accordingly,

$$p^f_\mu \equiv p_\mu - \overline{d}^\nu_\mu\, \overline{p}_\nu, \quad \overline{p}^f_\mu \equiv \overline{p}_\mu - d^\nu_\mu\, p_\nu. \tag{34}$$

Due to condition $\widetilde{P}^2 = P^2 = 0$ held for any field defined on $\widetilde{G}_{12}$ or G_{12}, one has

$$p^{f\,2}_\mu = \overline{p}^{f\,2}_\mu \equiv m^2_f, \quad p^2_\mu = \overline{p}_\mu{}^2 \equiv m^2, \tag{35}$$

where m and m_f are taken to denote the ordinary and distorted masses at rest of a particle, respectively. According to the laws described in section III of the passage, we may then proceed to the 4-dimensional space-time continuum. Thus, the matter found in the ID-region of the 4-dimensional space-time continuum undergoes a phase transition of the second kind, i.e., the new phase of 'proto-matter' comes into being, and the particles of which are released from the mass shell as the shift of mass $(m \rightarrow m_f)$ and energy-momentum $(p_\mu \rightarrow p^f_\mu)$ occurs upwards along the energy scale.

In the particular case, for example, of a static spherically symmetric distortion field a_A, with two components

doi: https://doi.org/10.52526/25792776-26.73.1-24

of a one-dimensional massless gravitational field $a(r) \equiv a_{0\,3}(r)$ and a one-dimensional space-like massive ID-field $\overline{a}(r) \equiv \overline{a}_3(r)$, we have

$$\begin{array}{l} a_{(1,1,3)} = a_{(2,2,3)} = \frac{1}{2}\left(-a + \overline{a}\right), \quad a_{(1,2,3)} = a_{(2,1,3)} = \frac{1}{2}\left(-a - \overline{a}\right), \\ a_{(\lambda,\mu,1)} = a_{(\lambda,\mu,2)} = 0, \quad (\lambda, \mu = 1, 2). \end{array} \tag{36}$$

In this case, the metric Eq. (14), given in a holonomic coordinate basis, is generalized as

$$\begin{array}{l} g_{00} = (1 - x_0)^2 + \overline{x}^2, \quad g_{11} = -\widetilde{r}^2, \quad g_{22} = -\widetilde{r}^2 \sin^2 \widetilde{\theta}, \\ g_{33} = -\left[(1 + x_0)^2 + \overline{x}^2\right], \quad g_{\mu\nu} = 0 \quad (\mu \neq \nu), \end{array} \tag{37}$$

where $x_0 \equiv æ_A\, a$ and $\overline{x} \equiv æ_Z\, \overline{a}$.

6. Concluding remarks

The missing ingredient of our approach is the Higgs boson. The four parameters g, g', μ, λ are inserted by hand, which, in turn, determine the coupling constants $æ_A$ and $æ_Z$ of the massless gravitational (A) field and the massive (Z) ID-component, respectively. Two relations can be imposed upon these parameters:

$$2\sqrt{\pi\, G_N} = \frac{g\, g'}{\sqrt{g^2 + g'^2}}, \quad \frac{2\hbar}{cv\,\sqrt{g^2 + g'^2}} \leq 0.4\, fm.$$

It is worth to note that the quanta of the gravitational gauge field (a) possess one unit of spin, and the gauge coupling constant ($æ_A$) has dimension -1. Though the properties of suggested theory are far better: some divergences are got rid off. One could hope that the problems above will disappear and the quantizing gravity will be straightforward if one proceeds heuristically, from the stand point of particle physicist. That is, one may start with building the quantized theory of interacting distortion gauge field a on the MS-space, at which the theory is renormalizable. Then, in the framework of GGP, to transform this, further, into the theory of quantum gravity defined on R_4. Given a particular choice of a regularization scheme, a theory of interest is said to be renormalizable if only a finite number of constants require normalization. Without careful thought, we expect that the renormalizability of the theory will not be spoiled in curved space-time too, because, the infinities arise from ultra-violet properties of Feynman integrals in momentum space which, in coordinate space, are short distance properties, and locally (over short distances) all curved space-time look like MS-space. A more detailed analysis and calculations on this will be presented in another paper to follow at a later date. The advantages of suggested approach may summary as:

- Unitary.
- Renormalizability at least on the MS-space.
- The phase transition of "matter $\to$ proto-matter" in ID-regime ($Z \neq 0$) simultaneously with strong gravity($A \neq 0$) at density range above nuclear density.
- The prospect for the future theory of quantum gravity.

Despite these success, a number of important questions, which may have rather interesting implications for the physics of superdense astrophysical sources, should be addressed yet.

Appendices

Appendix A The GGP

The following steps went into the building of the framework of GGP:

A.1 Diffeomorphism $\widetilde{x}^{\mu}(x^l) : M_4 \to R_4$

The basis vectors e at point $P \in M_4$ transformed into the basis vectors $\widetilde{e}(a)$ at point $\widetilde{P} \in R_4$ under the action of the gauge field a:

$$\widetilde{e}^{\mu}(a) = D^{\mu}_{l}(a)\, e^{l}. \tag{38}$$

doi: https://doi.org/10.52526/25792776-26.73.1-24

The explicit form of transformation matrix $D(a)$ is uniquely specified in the sect. III. Constructing the diffeomorphism $\widetilde{x}^{\mu}(x^l) : M_4 \to R_4$, the holonomic functions $\widetilde{x}^{\mu}(x^l)$ are the solution of following equation:

$$\widetilde{e}_{\mu}(a)\, \psi^{\mu}_{l} = e_l + \chi_l(a), \tag{39}$$

where

$$\chi_l(a) = \widetilde{e}_{\mu}\, \chi^{\mu}_{l} = -\frac{1}{2}\, \widetilde{e}_{\mu} \int_0^x (\partial_k\, D^{\mu}_{l} - \partial_l\, D^{\mu}_{k})\, dx^k. \tag{40}$$

Proposition: The covector $\chi_l(a)$ realizes coordinates $\widetilde{x}^{\mu}$ by providing the conditions of integrability

$$\partial_k\, \psi^{\mu}_{l} = \partial_l\, \psi^{\mu}_{k} \tag{41}$$

and undegeneration $\|\psi\| \neq 0$ Dubrovin & et al. (1986), Pontryagin (1984).

Proof: It is straightforward to show that $\psi^{\mu}_{l} = D^{\mu}_{l} + \chi^{\mu}_{l}$, where

$$\chi^{\mu}_{l} = \frac{1}{2} \int_0^x \chi^{\mu}_{kl}\, dx^k, \quad \chi^{\mu}_{kl} \equiv -(\partial_k\, D^{\mu}_{l} - \partial_l\, D^{\mu}_{k}).$$

Therefore $\partial_k\, \chi^{\mu}_{l} - \partial_l\, \chi^{\mu}_{k} = \chi^{\mu}_{kl}$, and Eq. (42) holds.

Remark: Out of all the arbitrary coordinates in R_4 the *real -curvilinear* coordinates $\widetilde{x}$ can be distinguished, which are inferred from Eq. (39) under all possible coordinate (Λ) and gauge (U^{loc}) transformations. Therefore, there exist preferred systems and group of transformations of real -curvilinear coordinates. The wider group of arbitrary coordinate transformations in R_4 no longer is of importance for field dynamics. If an inverse function ψ^{l}_{μ} meets condition

$$\tfrac{\partial \psi^{l}_{\mu}}{d\widetilde{x}^{\nu}} \neq \Gamma^{\lambda}_{\mu\nu}\, \psi^{l}_{\lambda}, \tag{42}$$

where $\Gamma^{\lambda}_{\mu\nu}$ denotes the usual Christoffel symbols agreed with the metric $g_{\mu\nu}$, then the curvature on R_4 is not zero Weinberg (1972). The equation (39) yields an invariant bilinear form $d\, s^2$ on R_4, as well as the gauge invariant scalar functions χ and S as follows:

$$\begin{array}{l} d\, s^2 = g_{\mu\nu}\, d\,\widetilde{x}^{\mu} d\,\widetilde{x}^{\nu} = \left[(e_l + \chi_l)\ d\, x^l\right]^2 = inv, \\ \chi = < e^l,\, \chi_l > = \frac{\omega}{2} - 2, \quad S = \frac{1}{4}\, \psi^{l}_{\mu}\, D^{\mu}_{l} = \frac{1}{2}(1 + \frac{\omega}{4}), \end{array} \tag{43}$$

where the tensor ω implies

$$\partial_l D^{\mu}_{k}(a) = \partial_k \left[\omega^{m}_{l}(x)\, D^{\mu}_{m}(a)\right]. \tag{44}$$

The trace $\omega = tr\, \omega^{m}_{l}$ should be invariant under U^{loc}-gauge group. This can be satisfied if ω is a function of the trace of curvature form Ω of connection $\mathbf{a}$ with the values in Lie algebra of group U^{loc}: $\omega = \omega(tr\, \Omega) = \omega(d\, tr\, \mathbf{a})$, provided by

$$\Omega = \sum_{l<k} F_{lk}\, dx^l \wedge dx^k, \quad \mathbf{a} = a_l\, dx^l,$$

where $F_{lk} = \partial_l\, a_k - \partial_k\, a_l$. Hence, a functional ω has a null variational derivative $\frac{\delta\omega(tr\, \Omega)}{\delta a_l} = 0$ at local variations of connection $a_l \to a_l + \delta a_l$. Thus, the ω is an invariant with respect to coordinate ($\Lambda^{l'}_{k} = \partial_k\, x'^{l}$) and U^{loc}-gauge transformations: $\omega = inv(\Lambda, U^{loc})$.

There is a conformity between corresponding tensors with various suffixes on R_4 and M_4. While, each co- or contra -variant index transformed incorporating the functions ψ^{μ}_{l} or ψ^{l}_{μ}, respectively. Then, some coordinate or gauge transformations underly the given transformation of real -curvilinear coordinates $\widetilde{x} \to \widetilde{x}'$: $\frac{\partial\, \widetilde{x}'^{\mu'}}{\partial\, \widetilde{x}^{\mu}} = \psi^{\mu'}_{l'}(a')\psi^{l}_{\mu}(a)\Lambda^{l'}_{l}$. As we are presumably living in curved Riemannian geometry, therefore, the fields $\Phi(x)$ no longer hold and $\widetilde{\Phi}(\widetilde{x})$ should be regarded as the real physical fields. But a conformity mentioned above enables the $\Phi(x)$ to serve as an auxiliary 'shadow' fields, given on the MS-space M_4, as a guiding tool in dealing with an intricate curved geometry. These notions arise basically from the most important fact that the Lagrangian $\widetilde{L}(\widetilde{x})$ of the fields $\widetilde{\Phi}(\widetilde{x})$ can be obtained under the unitary mapping from the Lagrangian $L(x)$ of corresponding $\Phi(x)$ fields and vice versa:

$$J_{\psi} \widetilde{L}(\widetilde{x})\Big|_{inv(G_R;\, \widetilde{x} \to \widetilde{x}')} = L(x)|_{inv(\Lambda;\, U^{loc})}\,, \tag{45}$$

where $J_{\psi} \equiv \|\psi\|\, \sqrt{-g}$, $\quad g$ denotes the determinant of metric tensor. The resulting Lagrangian $\widetilde{L}(\widetilde{x})$ is also an invariant under the wider group of arbitrary curvilinear transformations. The local internal gauge

doi: https://doi.org/10.52526/25792776-26.73.1-24

symmetry U^{loc} is now hidden, as it was replaced by gauge group of gravitation G_R. The tetrad $\widetilde{e}^{\alpha} \in R_4$ and basis $e^l \in M_4$ vectors meet the condition

$$< \widetilde{e}^{\alpha}, e_l >= V^{\alpha}_{\mu}(\widetilde{x})\, D^{\mu}_l(a), \quad < e^{\alpha}, e_{\beta} >=< \widetilde{e}^{\alpha}, \widetilde{e}_{\beta} >= \delta^{\alpha}_{\beta}, \tag{46}$$

while the Minkowski metric reads $< \widetilde{e}^{\alpha}, \widetilde{e}^{\beta} >= diag(1,-1,-1,-1)$. In case of zero curvature $R^{\lambda}_{\mu\nu\tau} = 0$, the Eq. (39) can be satisfied globally in M_4 by setting

$$\psi^{\mu}_l = D^{\mu}_l = V^{\mu}_l = \frac{\partial x^{\mu}}{\partial \xi^l}, \quad \|D\| \neq 0, \quad \chi_l = 0, \tag{47}$$

where ξ^l are inertial coordinates. Namely in this case $S = J_{\psi} = 1$, we have gauge theory given on the M_4 in both the curvilinear and inertial coordinates.

A.2 Field equations

Field equations can be inferred from an invariant action as

$$\begin{aligned} S = S_a + \widetilde{S}_{\widetilde{\Phi}} = \int \sqrt{-\eta}\, L_a(x)\, d^4x + \int \sqrt{-g}\, \widetilde{L}_{\widetilde{\Phi}}(\widetilde{x})\, d^4\widetilde{x} = \\ \widetilde{S}_{\widetilde{a}} + \widetilde{S}_{\widetilde{\Phi}} = \int \sqrt{-g}\, \left(\widetilde{L}_a(\widetilde{x}) + \widetilde{L}_{\widetilde{\Phi}}(\widetilde{x})\right)\, d^4\widetilde{x}, \end{aligned} \tag{48}$$

where L_a and $\widetilde{L}_{\widetilde{a}}$ denote the Lagarangians of the gauge field (a) given on the M_4 and R_4, respectively. The Lagrangian $L_a(x)$ is invariant under Λ-coordinate and U^{loc}-gauge groups. But the Lagrangians $\widetilde{L}_{\widetilde{\Phi}}(\widetilde{x})$ and $\widetilde{L}_{\widetilde{a}}(\widetilde{x})$ of matter fields $\widetilde{\Phi}(\widetilde{x})$ and gauge field $\widetilde{a}$, respectively, given on the R_4, are invariant under the gauge group of gravitation G_R. In terms of Euler-Lagrange variations in M_4 and R_4, we readily obtain

$$\begin{aligned} &\frac{\delta(\sqrt{-\eta}\, L_a)}{\delta\, a_l} = J^l = -\frac{\delta(\sqrt{-\eta}\, L_{\Phi})}{\delta\, a_l} = -\frac{\partial\, g^{\mu\nu}}{\partial\, a_l}\frac{\delta(\sqrt{-g}\, \widetilde{L}_{\widetilde{\Phi}})}{\delta\, g^{\mu\nu}} = - \\ &\frac{1}{2}\frac{\partial\, g^{\mu\nu}}{\partial\, a_l}\frac{\sqrt{-g}}{\|D\|}\frac{D_{k\mu}\, \delta(\sqrt{-g}\widetilde{L}_{\widetilde{\Phi}})}{\delta\, D^{\nu}_k} = -\frac{\sqrt{-g}}{2}\frac{\partial\, g^{\mu\nu}}{\partial\, a_l}\widetilde{T}_{\mu\nu}, \\ &\frac{\delta\widetilde{L}_{\widetilde{\Phi}}}{\delta\, \widetilde{\Phi}} = 0, \quad \frac{\delta\, \widetilde{L}_{\widetilde{\Phi}}}{\delta\overline{\widetilde{\Phi}}} = 0, \end{aligned} \tag{49}$$

where $\widetilde{T}_{\mu\nu}$ is the energy-momentum tensor of the matter fields $\widetilde{\Phi}(\widetilde{x})$. It is straightforward to choose the 10 components of symmetric tensor $D^{\mu\nu}(a)$ as the characteristic of gravitational field defined on M_4 without invoking the gauge field a. Actually, from Eq. (49) we get

$$\frac{D_{k\mu}\, \delta\, L_a}{\|D\|\, \delta\, D^{\nu}_k} = \frac{2}{\sqrt{-g}}\frac{\delta(\sqrt{-g}\, \widetilde{L}_a)}{\delta\, g^{\mu\nu}} = -\widetilde{T}_{\mu\nu}. \tag{50}$$

Therefore, we must fix either the Lagrangians L_a or $\widetilde{L}_a$. In section III we would uniquely determine the transformation matrix $D(a)$ and Lagrangian L_a.

Remark: To re-define the gauge coupling constant æ in terms of Newton gravitational constant G_N, we ought to consider the theory at the limit of Newton's non-relativistic law of weak gravitation for the static weak gravitational field given by Poisson equation $\nabla^2 g_{00} = -8\,\pi\, G_N\, T_{00}$. First equation in (49), for the static field $x_0 = æ\, a_0$, gives: $\nabla^2\, x_0 = \frac{æ^2}{2}\frac{\partial\, g_{00}}{\partial\, x_0}T_{00}$, where in linear approximation fitting our interest $g_{00} \approx (1 - 2x_0)$. Hence $\nabla^2\, g_{00} = -2\, \nabla^2\, x_0 = -2æ^2\, T_{00}$ and

$$G_N = æ^2/4\pi, \tag{51}$$

which shown that only the gravitational attraction exists.

A.3 Unitary mapping matrix for the fields of spin $j = 0, 1\,\frac{1}{2}$

In this section we determine the unitary mapping matrix $R(a)$ and gauge invariant scalar function $S(a)$ in case of the most simple fields of spin 0, 1, and $\frac{1}{2}$. But, this can be readily extended to any spin (see next section).

Remark: A general recipe for determination of the functions $R(a)$ and $S(a)$ for given field is to insert Eq. (3) into Eq. (4) to obtain the identity, in which then one may equate the coefficients in front of either functions $\partial\,\Phi$ and Φ to zero. In this manner one obtains two equations from which one determines the functions $R(a)$ and $S(a)$:

doi: https://doi.org/10.52526/25792776-26.73.1-24

1) A straightforward calculation for the fields of spin $j = 0, 1$ gives the unitary matrix

$$R(\widetilde{x}, x) = R(x)\, R_g(\widetilde{x}) = \exp\left(-i\Theta(x) - \Theta_g(\widetilde{x})\right), \tag{52}$$

provided by

$$\Theta(x) = æ \int_0^x a_l(x)\, d\, x^l, \quad \Theta_g(\widetilde{x}) = \int_0^x \left[R^+\, \Gamma_\mu\, R + \psi^{-1} \widetilde{\partial}_\mu\, \psi\right]\, d\, \widetilde{x}^\mu, \tag{53}$$

where $\psi \equiv \left(\psi_l^\mu\right)$, $\Theta_g = 0$ for scalar field and $\Theta_g + \Theta_g^+ = 0$ for vector field, because of $\Gamma_\mu + \Gamma_\mu^+ = 0$. The scalar function $S(a)$ has the form of Eq. (44) : $S(B_f) = \frac{1}{4}\, R^+ (\psi_\mu^l\, D_l^\mu)\, R = \frac{1}{4}\, \psi_\mu^l\, D_l^\mu$.

2) Unitary mapping of spinor field $\Psi(x)$ $\quad (j = \frac{1}{2})$ can be written:

$$\begin{array}{l} \widetilde{\Psi}(\widetilde{x}) = R(a)\, \Psi(x), \quad \widetilde{\overline{\Psi}}(\widetilde{x}) = \overline{\Psi}(x)\, \widetilde{R}^+(a), \\ g^\mu(\widetilde{x}) \nabla_\mu\, \widetilde{\Psi}(\widetilde{x}) = S(a)\, R(a)\, \gamma^l D_l\, \Psi(x), \\ \left(\nabla_\mu\, \widetilde{\overline{\Psi}}(\widetilde{x})\right)\, g^\mu(\widetilde{x}) = S(a)\, \left(D_l\, \overline{\Psi}(x)\right)\, \gamma^l\, \widetilde{R}^+(a), \end{array} \tag{54}$$

where

$$\widetilde{R} = \gamma^0 R \gamma^0, \quad \Sigma^{\alpha\beta} = \frac{1}{4}[\gamma^\alpha, \gamma^\beta], \quad \Gamma_\mu(x) = \frac{1}{4}\Delta_{\mu,\alpha\beta}(x) \gamma^\alpha \gamma^\beta, \tag{55}$$

$\Delta_{\mu,\alpha\beta}(x)$ denote the Ricci rotation coefficients. The unitary mapping matrix $R(a)$ is in the form of Eq. (52), provided we make single change

$$\Theta_g(x) = \frac{1}{2} \int_0^x R^+ \left\{g^\mu \Gamma_\mu R,\, g_\nu\, d\, x^\nu\right\}. \tag{56}$$

A calculation now gives

$$S(a) = \frac{1}{8K} \psi_\mu^l \left\{\widetilde{R}^+ g^\mu R,\, \gamma_l\right\} = inv, \tag{57}$$

where $K = \widetilde{R}^+\, R = \widetilde{R}_g^+\, R_g$, and

$$\begin{array}{l} K = \exp\left(-\frac{1}{2} \int_0^x \left(\left\{R^+ \widetilde{\Gamma}_\mu^+ g^\mu,\, g_\nu dx^\nu\ \right\}R +\ R^+ \left\{g^\mu \Gamma_\mu R,\, g_\nu dx^\nu\right\}\right)\right), \\ \widetilde{\Gamma}_\mu^+ = \gamma^0 \Gamma_\mu^+ \gamma^0. \end{array} \tag{58}$$

Taking into account a commutation relation $[R, g_\nu] = 0$, and substituting (Weinberg (rf1)):

$$\widetilde{\Gamma}_\mu^+ g^\nu + g^\nu \Gamma_\mu = -\nabla_\mu g^\nu = 0, \tag{59}$$

we get $K = 1$. Note that $\widetilde{U}_R^+ U_R = \widetilde{R} U^+ \widetilde{R'}^+ R' U R^+ = \widetilde{R} U^+ \widetilde{R}^+ R U R^+$, and $\widetilde{R'}^+ R' = \widetilde{R}^+ R = 1$, therefore

$$\widetilde{U}_R^+ U_R = \gamma^0 U_R^+ \gamma^0 U_R = 1. \tag{60}$$

A.4 The GGP for any spin

The higher-spin equations in given curved space were studied earlier by many authors Belifante (1940), Buchdhal (1958, 1962), Christensen & Duff (1978), M.M. (1954), Penrose (1962), which have led to a number of insights, but also obvious limitations. For instance, it is well known inconsistencies emerged in the standard approach Buchdhal (1958, 1962), Dowker (1972) to derive these equations, except for spins half and one, by the formal prescription of replacing ordinary derivatives by covariant ones. It is necessary to introduce modifications which would provide compatibility condition in curved space Buchdhal (1962), but it is open question how this can be achieved without the rather artificial implication of auxiliary fields. Some authors prefer to describe a spin-j particle by a $(2j + 1)$-component field ϕ_m^j Cap (1953), Dowker (1972), Weinberg (1964) in order to avoid this inconsistency problem. A new framework that we shall implement here has the following features. We employ an unitary mapping formalism developed in section II incorporated with the most convenient Bargman-Wigner's wave functions for higher-spin in flat space Bargman & Wigner (1948). The formalism of GGP will then hold for the field of arbitrary spin j, because the latter is treated as a system of $2j$ fermions of half-integer spin. This approach is obviously free of inconsistency problem mentioned above. Actually, note that the latter emerges under unwanted subsidiary conditions occurring only if the original spin-j field and the pure spin-2 object Ω formed from the Weyl conformal tensor can combine to produce a nonzero spin-$(j - 1)$ object, which becomes meaningless for $j = 1/2$ Ter-Kazarian (2026).

doi: https://doi.org/10.52526/25792776-26.73.1-24

The wave function of spin-$j=\frac{n}{2}$ particle with momentum $\vec{p}$ defined on the M_4 can be obtained by Lorentz transformation from the symmetric Dirac spinor of rank n corresponding to the particle in the rest $U_{\alpha_1\ldots\alpha_n}(0)$ implying $(\gamma_4-1)^{\beta'}_{\beta}U_{\beta'\beta_2\ldots\beta_n}(0)$ for each index

$$U_{\beta_1\ldots\beta_n}(\vec{p})=S^{\beta'_1}_{\beta_1}(\alpha(\vec{p}))\ldots S^{\beta'_n}_{\beta_n}(\alpha(\vec{p}))U_{\beta'_1\ldots\beta'_n}(0), \tag{61}$$

where $\overline{U}'(\vec{p})\,U'(\vec{p})=\overline{U}(\Lambda^{-1}\vec{p})\,U(\Lambda^{-1}\vec{p})$. A spin part is written $\Sigma_{\mu\nu}=\frac{1}{2}\sum_{r=1}^{n}\Sigma^{(r)}_{\mu\nu}$, where a matrix $\Sigma^{(r)}_{\mu\nu}$ acts only on the r-th index

$$\left(\Sigma^{(r)}_{\mu\nu}\right)^{\beta_1\ldots\beta_n}_{\alpha_1\ldots\alpha_n}=\delta^{\beta_1}_{\alpha_1}\cdots\delta^{\beta_{r-1}}_{\alpha_{r-1}}\left(\Sigma^{(r)}_{\mu\nu}\right)^{\beta_r}_{\alpha_r}\delta^{\beta_{r+1}}_{\alpha_{r+1}}\cdots\delta^{\beta_n}_{\alpha_n},$$

that $\Sigma^{(r)}_{\mu\nu}=\frac{1}{4}[\gamma^r_\mu,\,\gamma^r_\nu]$, and

$$\left(\gamma^r_\mu\right)^{\beta_1\ldots\beta_n}_{\alpha_1\ldots\alpha_n}=\delta^{\beta_1}_{\alpha_1}\cdots\delta^{\beta_{r-1}}_{\alpha_{r-1}}\left(\gamma^r_\mu\right)^{\beta_r}_{\alpha_r}\delta^{\beta_{r+1}}_{\alpha_{r+1}}\cdots\delta^{\beta_n}_{\alpha_n}.$$

The spin-j field $\Phi_{\beta_1\ldots\beta_n}(x)$ (Eq. (61)) takes values in standard fiber $\mathcal{F}_x$ upon $x:\ p^{-1}(\mathcal{U})=\mathcal{U}\times\mathcal{F}_x$. In the framework of GGP, the mapped spin-j field $\widetilde{\Phi}^{(r)}_{\beta_1\ldots\beta_n}(\widetilde{x})$, where $\widetilde{\Phi}^{(r)}=R^{(r)}\,\Phi$, takes values in the fiber $\widetilde{F}_{\widetilde{x}}$ $(\widetilde{x}\in\widetilde{\mathcal{U}},\quad\widetilde{\mathcal{U}}$ denotes the region of the base R_4. The unitary mapping matrix $R^{(r)}$ is given in the form of Eq. (52) and Eq. (56), but now refers to the r-th index. The Lagrangian of this field will be invariant under the local gauge transformations

$$\begin{aligned}&\widetilde{\Phi}'(\widetilde{x})=U^{(r)}_R\,\widetilde{\Phi}(\widetilde{x}),\\&\left(g^\mu_{(r)}(\widetilde{x})\,\nabla^{(r)}_\mu\widetilde{\Phi}(\widetilde{x})\right)'=U^{(r)}_R\left(g^\mu_{(r)}(\widetilde{x})\,\nabla^{(r)}_\mu\widetilde{\Phi}(\widetilde{x})\right),\end{aligned} \tag{62}$$

where $g^\mu_{(r)}(\widetilde{x})=V^\mu_\alpha(\widetilde{x})\gamma^\alpha_{(r)}$, $\nabla^{(r)}_\mu$ denotes the covariant derivative on R_4 defined only for the r-th index by the conventional substitution Bargman & Wigner (1948):

$$\nabla^{(r)}_\mu\widetilde{U}_{\beta_1\ldots\beta_n}\to\Lambda^{\alpha'}_\alpha(\widetilde{x})S^{\beta'_1}_{\beta_1}(\alpha(\Lambda))\ldots S^{\beta'_n}_{\beta_n}(\alpha(\Lambda))\nabla^{(r)}_\mu\widetilde{U}_{\beta_1\ldots\beta_n}. \tag{63}$$

Here, as usual, we denote $\nabla^{(r)}_\alpha=V^\mu_\alpha\,(\partial_\mu+\Gamma^{(r)}_\mu)$ and

$$\Gamma^{(r)}_\mu=\frac{1}{2}\,\Sigma^{\alpha\beta}_{(r)}\,V^\nu_\alpha(\widetilde{x})\,\partial_\mu V_{\beta\nu}(\widetilde{x})=\frac{1}{4}\Delta^{(r)}_{\mu,\alpha\beta}\,\gamma^\alpha_{(r)}\,\gamma^\beta_{(r)}, \tag{64}$$

$\Delta^{(r)}_{\mu,\alpha\beta}(x)$ are the Ricci rotation coefficients. The Eqs. (62) hold if

$$g^\mu_{(r)}\,\nabla^{(r)}_\mu\widetilde{\Phi}^{(r)}=R^{(r)}\,S^{(r)}\,(\gamma^l\,D_l\,\Phi), \tag{65}$$

where $D_l=\partial_l-ig\,a_l(x)$, $S(a)$ is the gauge invariant Lorentz scalar of Eq. (57) but refers to r-th index. According to the results of subsection B, we get $\widetilde{U^{(r)}_R}^{+}\,U^{(r)}_R=\gamma^0\,U^{(r)+}_R\,\gamma^0\,U^{(r)}_R=1$. The Lagrangian of the spin-j field can be set up as

$$\begin{aligned}&L(x)=J_\psi\widetilde{L}(\widetilde{x})=J_\psi\left\{\frac{i}{2}\left[\overline{\widetilde{\Phi}}^{(r)}(\widetilde{x})\,g^\mu_{(r)}(\widetilde{x})\nabla^{(r)}_\mu\widetilde{\Phi}^{(r)}(\widetilde{x})-\right.\right.\\&\left.\left.(\nabla^{(r)}_\mu\overline{\widetilde{\Phi}}^{(r)}(\widetilde{x}))\,g^\mu_{(r)}(\widetilde{x})\widetilde{\Phi}^{(r)}(\widetilde{x})\right]-m\overline{\widetilde{\Phi}}^{(r)}(\widetilde{x})\widetilde{\Phi}^{(r)}(\widetilde{x})\right\}=\\&J_\psi\left\{S^{(r)}(a)\frac{i}{2}\left[\overline{\Phi}\,\gamma^l_{(r)}D_l\,\Phi-(D_l\overline{\Phi})\,\gamma^l_{(r)}\Phi\right]-m\overline{\Phi}\,\Phi\right\}.\end{aligned} \tag{66}$$

Generalized Bargman-Wigner's equation for the spin-$j=\frac{n}{2}$ particle in curved space stems from the Lagrangian eq. (66):

$$\begin{aligned}&\left(g'^\mu\,\nabla'_\mu\widetilde{\Phi}^{(r)}-m\right)^{\beta'}_{\beta}\,\widetilde{\Phi}_{\beta'\beta_2\ldots\beta_n}(\widetilde{\vec{p}})=\\&[R'\,(S'\,D-m)]^{\beta'}_{\beta}\,\Phi_{\beta'\beta_2\ldots\beta_n}(\vec{p})=0,\end{aligned} \tag{67}$$

where $R',S',\ldots$ refer to index β'.

doi: https://doi.org/10.52526/25792776-26.73.1-24

A.5 The manifold G_{12}, and a passage to M_4 or R_4

Consider the curve $\lambda(t) : R^1 \to G_{12}$ passing through the point $p = \lambda(0) \in G_{12}$ with tangent vector $\mathbf{A}|_{\lambda(t)}$. The $\{\zeta\}$ are local coordinates in open neighborhood of $p \in \mathcal{U}$. The 12 dimensional smooth vector field $\mathbf{A}_p = \mathbf{A}(\zeta)$ belongs to the section of tangent bundle $\mathbf{T}_p$ at the point $p(\zeta)$. The one parameter group of diffeomorphisms A^t is given for the curve $\zeta(t)$ passing through point p and $\zeta(0) = \zeta_p, \quad \dot{\zeta}(0) = \mathbf{A}_p$: $d\,A^t_p(\mathbf{A}) = \frac{d}{d\,t}\big|_{t=0} A^t\,(\zeta(t)) = \mathbf{A}_p(\zeta)$, that

$$d\,A^t : \mathbf{T}(G_{12}) \to R\left(\mathbf{T}(G_{12}) = \bigcup_{p(\zeta)} \mathbf{T}_p\right).$$

The $e_{(\lambda,\mu,\alpha)} = O_{\lambda,\mu} \times \sigma_\alpha \quad (\lambda, \mu = 1, 2; \quad \alpha = 1, 2, 3)$ are linear independent 12 unit basis vectors at the point $p = \lambda(0) \in G_{12}$. The basis vectors σ_α refer to three dimensional ordinary space $R^3_{\lambda\mu}$ at given $(\lambda,\, \mu)$. The metric on G_{12} is $\hat{\mathbf{g}} : \mathbf{T}_p \times \mathbf{T}_p \to C^\infty(G_{12})$. The decompositions

$$G_6 = R^3 \oplus T^3, \quad \overline{G}_6 = \overline{R}^3 \oplus \overline{T}^3, \tag{68}$$

hold with $sgn(R^3) = (+{+}+)$, $\quad sgn(T^3) = (-{-}-)$ and inverse signatures for $sgn(\overline{R}^3) = (-{-}-)$, $\quad sgn(\overline{T}^3) = (+\,+\,+)$. Within this scheme, one is presumably allowed to perceive directly the G_6 related to space (R^3) and time (T^3), but not the $\overline{G}_6$ displayed as the space of inner degrees of freedom.

Remark: 1) To describe the dynamics of physical system on 4-dimensional Minkowski space, we use the fact that all directions in flat time space T^3 are equivalent. Therefore, reducing two extra dimensions of time vector and passing from G_6 to $M_4 = R^3 \oplus T^1$, under the notion 'time' one is free to imply its projection on fixed arbitrary universal direction in T^3. By this reduction, which clearly respects the physical ground, the goal pursued should be readily achieved.
2) In similar passage $\widetilde{G}_6 \to R_4$ made in case of curved space, we reduce the 'three time' components $\widetilde{e}_{0\alpha}$ of basis six-vector $\widetilde{\vec{e}}\,(\widetilde{e}_\alpha,\, \widetilde{e}_{0\alpha})$, at given point, to single one $\widetilde{e}_0$ in given universal direction. By this we fixed the 'time' coordinate. Certainly, as far as the Lagrangian of given physical system defined on $\widetilde{G}_6$, is the function of scalars $A_{(\lambda\alpha)}B^{(\lambda\alpha)} = A_\alpha B^\alpha + A_{0\alpha}B^{0\alpha}$, then the following reduction $A_{0\alpha}B^{0\alpha} = A_{0\alpha} < \widetilde{e}^{0\alpha}, \widetilde{e}^{0\beta} > B_{0\beta} = A_0 < \widetilde{e}^0, \widetilde{e}^0 > B_0 = A_0 B^0$ leads to the 4-dimensional Riemannian space:

$$\begin{array}{l} d\,\widetilde{\zeta}^2 = d\,s_6^2 - d\,\overline{s}_6^2 = 0, \\ d\,s_6^2\big|_{6\to 4} = d\,s_4^2 = g_{\mu\nu} d\,\widetilde{x}^\mu d\,\widetilde{x}^\nu = d\,\overline{s}_6^2 = inv. \end{array} \tag{69}$$

References

Bargman V., Wigner E. ., 1948, Proc. Am. Acad. Sci., 34, 211

Belifante F., 1940, Physica (Utrecht), 7, 305

Birrell N., Davies P., 1982, Quantum Fields in Curved Space. Cambridge University Press

Borisov A., 1973, Lett. Nuovo Cimento, 8, 988

Borisov A.B. O. V., 1974, Theor. and Math. Phys., 21, 329

Buchdhal H., 1958, Nuovo Cimento, 10, 96

Buchdhal H., 1962, Nuovo Cimento, 25, 486

Cap F., 1953, Z. Naturforsch., A8, 740

Christensen S., Duff J., 1978, Phys. Lett., 76B, 571

Coleman S. W. J., Zumino B., 1969, Phys.Rev., 177, 2239

Curtis G. Callan J. C. S. W. J., Zumino B., 1969, Phys.Rev., 177, 2247

Dowker J., 1972, Annals of Phys., 71, 577

Dubrovin B., et al. 1986, Contemporary Geometry. Nauka, Moscow

Isham C., 1969, Nuovo Cimento, Sec. A 59, 356

M.M. H., 1954, Phys.Rev., 94, 1472

Penrose R., 1962, Proc.R.Soc. (London), A284, 159

doi: https://doi.org/10.52526/25792776-26.73.1-24

Pontryagin L., 1984, Continous Groups. Nauka, Moscow

Ter-Kazarian G., 1997, Nuovo Cimento, Sec. B 112

Ter-Kazarian G., 2001, J. Phys. Soc. Japan, Suppl. B 70, 84

Ter-Kazarian G., 2026, Communications of BAO, 73, Issue 1,

Weinberg S., 1964, Phys.Rev., B133, 1318

Weinberg S., 1970, Lectures on elementary particles and quantum field theory. (Cambridge)

Weinberg S., 1972, Gravitation and Cosmology. J W and Sons, New York

doi: https://doi.org/10.52526/25792776-26.73.1-24

Communications of BAO, Vol. 73, Issue 1, 2026, pp. 39-58

Recovering Stellar Flare-Rate Distributions: Comparative Study of Methods, Application to Flare Stars in Galactic Field

A. A. Akopian*

NAS RA V.Ambartsumian Byurakan Astrophysical Observatory, Byurakan 0213, Aragatsotn Province, Armenia

Abstract

The revised and substantially extended pipeline/code for recovering the flare-rate distribution $\varphi(\nu)$ of a population of randomly flaring objects is presented. The capabilities of existing methods have been significantly expanded, and new ones have been added. Specifically, the new code allows *(i)* the use of the χ^2 test to significantly improve the estimation of the number of unknown (undiscovered) flare stars n_0, *(ii)* a refinement of the moment fit via a maximum likelihood estimate of a truncated Poisson distribution and a comparison of Pearson's types based on AIC/BIC metrics, *(iii)* an analysis of the temporal evolution of $\varphi(\nu)$ to account for accumulated observations, *(iv)* the application of modern numerical calculation methods, and *(v)* the use of numerical simulation to work with both synthetic and real observational data. Finally, two methods for recovering the flare-rate distribution $\varphi(\nu)$ of a stellar population are considered. The first method is the inverse-Laplace formulation from Ambartsumian (1978), applied to the discovery curve of first-flare events. The second is the method of moments (MoM, Akopian, 2003), improved and extended here to the full Pearson family of probability distributions. A comparative analysis of these methods is also presented.

In the second part of the study, the code was used to determine the distribution of flare rate among flare stars within the Kepler telescope's field of view. Typically, both methods yield identical results for synthetic data. However, when applied to a sample of flare stars from the Kepler field of view, their results diverge. The MoM yields a Pearson Type III distribution, or gamma distribution, with a negative bias in the minimum flare frequency, which is physically impossible. In contrast, Ambartsumian's approach yields a Type III distribution, which is physically plausible, with $\nu_0 > 0$. To identify the cause of the discrepancies, regardless of the specific form of the Pearson distribution, a numerical inverse Laplace transform was applied using modern algorithms. The inverse function $m_1(t)/m_1(0)$, where $m_1(t)$ is the frequency of the first flare, was in this case represented and approximated by its purely observational realization $n_1(t)/n(t)$, where $n_1(t)$ is the number of stars that have survived exactly one flare by time t, and $n(t)$ is the cumulative number of flares. This approach does not require knowledge of N_{tot} and provides the most reliable of the available cross-checks for reconstruction using the inverse Laplace transform. The nature of these discrepancies reveals the structure of the underlying distribution: a smooth density curve with a peak shifted towards values of $\nu \sim 2 \times 10^{-3}\ d^{-1}$, with a long tail in the region of high ν values.

Keywords: *stellar flares, Poisson mixtures, Pearson distributions, Laplace transform, method of moments, rate/frequency distribution function*

*aakopian57@gmail.com

doi: https://doi.org/10.52526/25792776-26.73.1-39

1. Introduction

In the second half of the last century, there was considerable interest in flare stars,and Ambartsumian's final series of scientific papers was devoted to the statistics of these stars. As is often the case, the new methods developed by Ambartsumian have found—and continue to find—applications far beyond the field of astrophysics. In particular, Ambartsumian's estimator of the unknown number of undiscovered flare stars (Ambartsumian, 1969) is now widely used in various fields of statistics, medicine and the social sciences, biology and ecology, linguistics, criminology, epidemiology, cryptography and other disciplines. In these fields, various names are used for this or similar methods: "capture-recapture, mark-recapture, capture-mark-recapture, observation-reobservation and mark-release-recapture, etc...".

Due to the specific characteristics of flaring stars and the relatively limited capabilities for their detection and study, interest in them gradually waned. However, over the past few decades, the Kepler and TESS space observatories have provided new, far more informative data on these objects. Significant advances in statistical and computational methods, combined with the new data, have revived interest in statistical studies of flaring stars. In this article, the statistical research methods developed at the Byurakan Observatory are examined in the light of these developments.

The first part of this paper presents a revised and significantly enlarged pipeline/code for recovering the flare-rate/frequency distribution $\varphi(\nu)$ of a population of randomly flashing objects from the observed distribution of flare counts n_k (the number of stars with k registered flares). That is critical for reconstructing the flare rate distribution function, thus we must establish the total flare-star count in the sample by calculating the number of undiscovered flare stars n_0. The new code allows the use of the χ^2 test and the maximum likelihood method to significantly improve the estimate of the number of undiscovered flare stars n_0 (Ambartsumian, 1969) and the statistical properties of this estimate.

Two methods for recovering the flare-rate distribution $\varphi(\nu)$ of a stellar population are considered. The first method is the inverse-Laplace formulation from Ambartsumian (1978), applied to the discovery curve of first-flare events. The second method (Akopian, 2003) is the method of moments (MoM), improved and extended here to the full Pearson family of probability distributions. A comparative analysis of previously proposed methods is also presented.

In the second part of the study, the code was used to determine the flare rate distribution of flare stars in the Kepler telescope's field of view (hereinafter - Kepler stars). Both methods produce the same results for synthetic data. However, for the Kepler stars sample, they diverge significantly.

To address this problem independently of any specific form of the Pearson distribution and resolve discrepancies that have arisen between the two methods, a new approach has been proposed, in which the use of the numerical inverse Laplace transform plays a key role.

We have endeavoured to ensure that the structure of this article, in terms of content, corresponds as closely as possible to the structure of the code. This explains the somewhat unusual style of presentation. The paper is structured as follows. Section 2 outlines the key assumptions and approaches used in this study. Section 3 sets up the moment-transformation formulas and reviews the Pearson family of densities. Section 4 describes the MoM pipeline including the estimation of the silent population and ML refinement. Section 5 introduces Ambartsumian's inverse-Laplace formulation. Section 6 applies both methods to the Kepler stars (Yang et al., 2019) and quantifies their disagreement.

Section 7 discuss results and identified discrepancies. Section 8 concludes.

doi: https://doi.org/10.52526/25792776-26.73.1-39

2. Basic assumptions and approaches

A photometric survey of N stars observed for a time T produces, for each star j, an integer count K_j of detected flares. The counts $\{K_j\}$ are the raw data of stellar-activity statistics. Behind each star is a hidden intrinsic flare rate ν_j, and the population of rates $\{\nu_j\}$ is itself a sample from an unknown population density $\varphi(\nu)$. Recovering $\varphi(\nu)$ from the observed flare counts $\{K_j\}$ is the central inference problem of this paper.

The Poisson-mixture model is the standard framework. Given the rate ν_j, the count K_j is Poisson-distributed with mean $\nu_j T$:

$$\Pr(K_j = k \mid \nu_j) \;=\; \frac{(\nu_j T)^k}{k!}\, e^{-\nu_j T}. \tag{1}$$

The rate ν_j itself is drawn from $\varphi(\nu)$, so the marginal distribution of K over the population is

$$\Pr(K = k) \;=\; \int_0^\infty \frac{(\nu T)^k}{k!}\, e^{-\nu T}\, \varphi(\nu)\, \mathrm{d}\nu. \tag{2}$$

Eq. (2) defines the burst-count distribution. Recovering φ from observations of K is a deconvolution problem: we observe a mixture and must infer the mixing density.

Two approaches

This problem can be addressed using two different approaches.

Inverse Laplace transform. Ambartsumian (1978) proposed a statistical method for determining $\varphi(\nu)$ based on inverse Laplace transform. Ambartsumian's main idea was to determine the desired function using the chronology of discoveries of new flare stars. From a mathematical point of view, the key observation is that the rate of first-flare events, $m_1(t)$, equals $\int_0^\infty \nu\, e^{-\nu t}\, \varphi(\nu)\, \mathrm{d}\nu = \mathcal{L}[\nu\varphi(\nu)](t)$.

Method of moments (MoM). This method was proposed in (Akopian, 2003). The basic idea is to compute the sample central moments μ_{k_r} of K from the observed histogram, transform them via Eq. (6) below into the central moments μ_{ν_r} of φ, and then fit a parametric density (from the Pearson family) to those moments. This approach uses all of the data, weighting it heavily toward the high-K tail through the third and fourth moments.

The two approaches agree on data that are well-described by their assumed parametric family. However, they can disagree on observational data that depart from these parametric assumptions. The character of this disagreement serves as a useful model-diagnostic tool.

3. Theoretical framework

From flare-count moments to rate moments

The Poisson-mixture model (2) relates the r-th sample central moment of the observed counts, μ_{k_r}, to the corresponding moment of the rate distribution $\varphi(\nu)$, μ_{ν_r}, as follows:

$$\mu_{\nu_1} = \mu_{k_1}/T, \tag{3}$$
$$\mu_{\nu_2} = (\mu_{k_2} - \mu_{k_1})/T^2, \tag{4}$$
$$\mu_{\nu_3} = (\mu_{k_3} - 3\mu_{k_2} + 2\mu_{k_1})/T^3, \tag{5}$$
$$\mu_{\nu_4} = (\mu_{k_4} - 6\mu_{k_3} + 11\mu_{k_2} - 6\mu_{k_1} - 6\mu_{k_1}\mu_{k_2} + 3\mu_{k_1}^2)/T^4. \tag{6}$$

doi: https://doi.org/10.52526/25792776-26.73.1-39

Pearson family of densities

The Pearson family of probability density functions is a comprehensive system of continuous probability distributions developed by Karl Pearson (Pearson, 1895) consisting of all probability density functions $\varphi(y)$ that satisfy the differential equation

$$\frac{\mathrm{d}\varphi(y)}{\mathrm{d}y} = \frac{(y-a)\,\varphi(y)}{b_0 + b_1 y + b_2 y^2}. \tag{7}$$

The roots of the quadratic denominator $b_0 + b_1 x + b_2 x^2 = 0$ govern the mathematical properties and shape of the density. The discriminant $\Delta = b_1^2 - 4b_0 b_2$ classifies these distributions. The classical types are labelled I through VII. For our purposes, six are relevant: Types I, III, IV, V, VI, and the Normal as a boundary case. The coefficients of the ODE map onto the moments via

$$a = b_1 = -\frac{\mu_{\nu_3}(\mu_{\nu_4} + 3\mu_{\nu_2}^2)}{A}, \quad b_0 = -\frac{\mu_{\nu_2}(4\mu_{\nu_2}\mu_{\nu_4} - 3\mu_{\nu_3}^2)}{A}, \quad b_2 = -\frac{2\mu_{\nu_2}\mu_{\nu_4} - 3\mu_{\nu_3}^2 - 6\mu_{\nu_2}^3}{A}, \tag{8}$$

with $A = 10\mu_{\nu_2}\mu_{\nu_4} - 18\mu_{\nu_2}^3 - 12\mu_{\nu_3}^2$.

The dimensionless ratios $\beta_1 = \mu_{\nu_3}^2/\mu_{\nu_2}^3$ (squared skewness) and $\beta_2 = \mu_{\nu_4}/\mu_{\nu_2}^2$ (kurtosis) determine the type. The diagnostic quantity

$$\kappa = \frac{\beta_1\,(\beta_2+3)^2}{4\,(4\beta_2 - 3\beta_1)\,(2\beta_2 - 3\beta_1 - 6)} \tag{9}$$

classifies the regions: $\kappa < 0 \Rightarrow$ Type I (Beta on a finite interval); $0 < \kappa < 1 \Rightarrow$ Type IV (real-line density with complex roots of the denominator); $\kappa > 1 \Rightarrow$ Type VI (Beta-prime on $[L, \infty)$, heavy upper tail). The line $2\beta_2 - 3\beta_1 - 6 = 0$ is the Type III boundary (shifted gamma); $\kappa = 1$ is the Type V boundary (shifted inverse gamma); and the point $(\beta_1, \beta_2) = (0, 3)$ is the Normal.

Figure 1 shows representative densities for each type. Figure 2 maps the regions in the (β_1, β_2) plane.

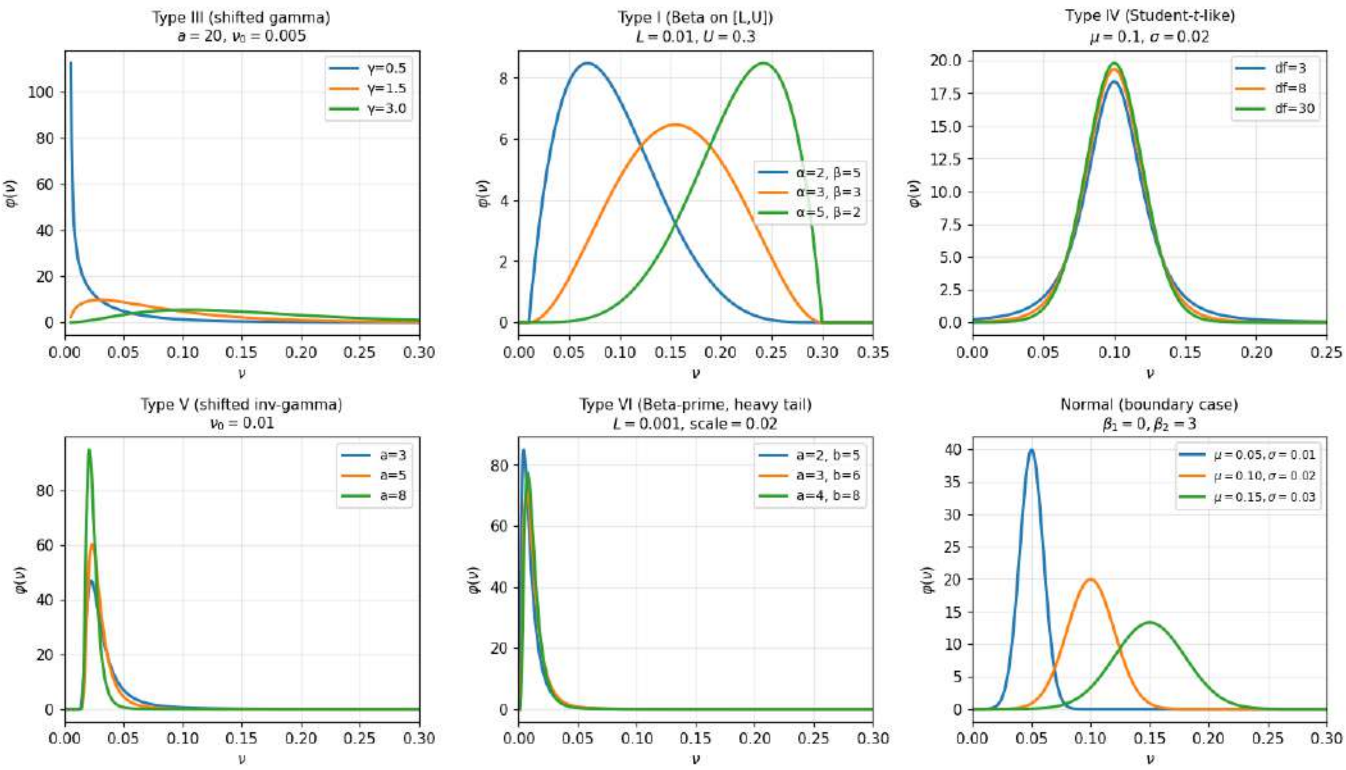

Figure 1: Representative densities of the six Pearson types plotted for parameters relevant to stellar flare rates (ν in day^{-1}). Top row: Type III (shifted gamma, monotone or unimodal depending on γ); Type I (bounded support $[L, U]$); Type IV (real-line symmetric or skew, Student-t when symmetric). Bottom row: Type V (shifted inverse gamma); Type VI (beta-prime, heavy upper tail); Normal as the boundary case.

doi: https://doi.org/10.52526/25792776-26.73.1-39

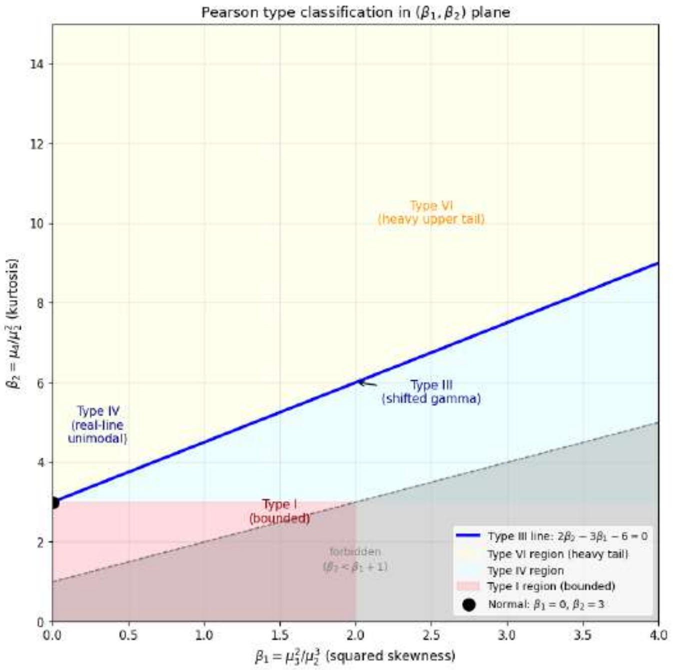

Figure 2: Pearson type classification in the (β_1, β_2) plane. The Type III line is $2\beta_2 - 3\beta_1 - 6 = 0$. Above it lies the Type VI region (heavy upper tail); below it the Type IV region; in the bounded-density part the Type I region. The Normal sits at $(0, 3)$. The forbidden region $\beta_2 < \beta_1 + 1$ is excluded by moment inequalities.

The special role of the Pearson Type III distribution

Type III (strictly speaking, a shifted gamma distribution) is

$$\varphi_{\rm III}(\nu) \;=\; \frac{a^\gamma}{\Gamma(\gamma)}\,(\nu-\nu_0)^{\gamma-1}\,e^{-a(\nu-\nu_0)}, \quad \nu \geq \nu_0. \tag{10}$$

Its parameters are recovered directly from the first three moments:

$$a = \frac{2\mu_{\nu_2}}{\mu_{\nu_3}}, \qquad \gamma = a^2\,\mu_{\nu_2}, \qquad \nu_0 = \mu_{\nu_1} - \frac{\gamma}{a}. \tag{11}$$

The Laplace transform of Type III is elementary:

$$\mathcal{L}[\varphi_{\rm III}](t) \;=\; e^{-\nu_0 t}\left(\frac{a}{a+t}\right)^{\gamma}. \tag{12}$$

This makes Type III the only Pearson type for which both MoM recovery and inverse-Laplace recovery have closed analytical forms. Type V's Laplace transform involves the Bessel function K_a; Types I and VI involve confluent hypergeometric functions; The type IV distribution has no closed-form expression. For this reason, all our applications of Ambartsumian's formulation (Section 5) use Type III as the analytical smoothing function.

A reliable benchmark for checking the quality of any fitted density is the population mean rate,

$$\langle\nu\rangle \;=\; \int_0^\infty \nu\,\varphi(\nu)\,\mathrm{d}\nu \;=\; \mu_{\nu_1}. \tag{13}$$

For the Type III distribution, $\langle\nu\rangle = \gamma/a + \nu_0$. This quantity is robust against moderate misspecification of the parametric family — much more robust than the shape parameters themselves.

doi: https://doi.org/10.52526/25792776-26.73.1-39

4. MoM pipeline

Implementation and synthetic validation

The full implementation is available in the Jupyter notebook accompanying this paper. Given the numbers $\{n_k\}$ of stars with k flares (histogram), the pipeline performs the following steps:

1) Compute the sample moments μ_{k_r} from the histogram using standard unbiased estimators.

2) Transform them to the rate moments μ_{ν_r} via Eqs. (3)–(6).

3) Compute the Pearson coefficients via Eq. (8) and classify the distribution type via Eq. (9).

4) Apply the type-specific parameter recovery (e.g., Eq. (11) for Type III) and return $\varphi(\nu)$.

We have implemented closed-form parameter recovery for all six types.

Figure 3 shows the recovery accuracy for Type III on synthetic samples of increasing size N. The ground truth corresponds to the Pleiades-like parameters $(a, \gamma, \nu_0) = (873, 0.235, 9.11 \times 10^{-5})$ determined in (Akopian, 2003). The shaded bands represent the 16–84th percentiles over 30 Monte Carlo realizations. All three parameters converge to the input values for $N \gtrsim 10^3$.

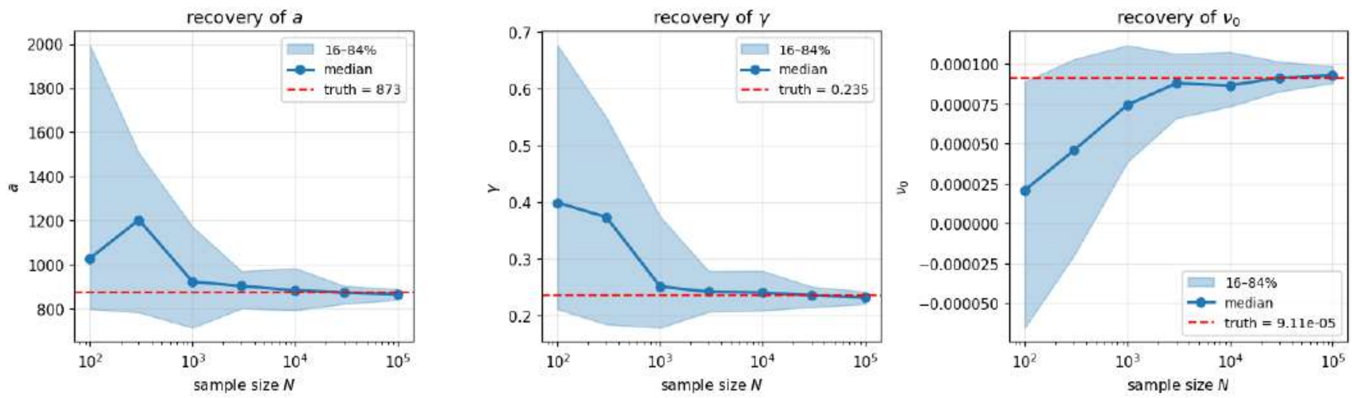

Figure 3: MoM recovery accuracy for Type III as a function of sample size. Blue curves: median (over 30 trials per N) of the fitted (a, γ, ν_0).

Estimating the "silent" population n_0 of undiscovered flare stars

The numbers $\{n_k\}_{k\geq 1}$ omit the truly silent stars ($k = 0$). However, to compute the moments correctly, we need an estimate of n_0. To this end, we utilize the Ambartsumian's estimator,

$$\hat{n}_0 \;=\; \frac{n_1^2}{2n_2}, \tag{14}$$

Two variance estimators for $\hat{n}_0$ are available. The first approach, proposed by Chao (1984), treats the observed counts as fixed, yielding

$$\mathrm{Var}_{\mathrm{Chao}}(\hat{n}_0) \;=\; n_2\left[\tfrac{1}{2}r^2 + r^3 + \tfrac{1}{4}r^4\right], \quad r = n_1/n_2, \tag{15}$$

whereas Bohning et al. (2008) refines the conditional (δ-method) variance by introducing a finite-sample correction:

$$\mathrm{Var}_{\mathrm{B}}(\hat{n}_0) \;=\; \frac{n_1^3}{n_2^2}\Big[1 + \tfrac{1}{4}\,\tfrac{n_1}{n_2}(1 - n_2/n)\Big], \qquad n = \textstyle\sum_{k\geq 1} n_k. \tag{16}$$

We adopt Eq. (16) by default and retain Eq. (15) as an alternative. To achieve greater robustness, we then perform a χ^2 optimization: we vary n_0 around $\hat{n}_0$ on a grid, refit the Pearson III distribution at

doi: https://doi.org/10.52526/25792776-26.73.1-39

each value, compute the predicted probability mass function (PMF), $\Pr(K = k)$, via the convolution of $\varphi_{\rm III}$ with a Poisson distribution, and minimize the Pearson χ^2 statistic between the predicted and observed histograms. The χ^2-best n_0 value is then selected as the final working estimate.

Maximum-likelihood refinement and model selection

The moment estimator is consistent but not fully efficient. A maximum-likelihood refinement, initialized at the moment-based values, typically tightens the parameter estimates by a factor of two to three. We employ a log-transformed parameterization, $\theta = (\log a, \log \gamma, \log \nu_0)$, and utilize the Nelder & Mead (1965) algorithm to maximize the zero-truncated log-likelihood function:

$$\log \mathcal{L} \;=\; \sum_{k \geq 1} n_k \log P_k(\theta) \;-\; N_{\rm obs} \,\log(1 - P_0(\theta)), \tag{17}$$

where $N_{\rm obs} = \sum_{k\geq 1} n_k$ and $P_k(\theta)$ is the predicted PMF.

For type selection among competing families (e.g., Type I vs. Type III vs. Type VI), we compare AIC(Akaike Information Criterion) and BIC (Bayesian Information Criterion). The AIC (Akaike, 1974) and BIC (Schwarz, 1978) are standard metrics used to select statistical models, and both are directly based on the Maximum Likelihood Estimate:

$$\mathrm{AIC} = 2k - 2\log \mathcal{L}, \qquad \mathrm{BIC} = k \log N_{\rm obs} - 2\log \mathcal{L}. \tag{18}$$

On the synthetic Pleiades sample from Akopian (2003) , this pipeline recovers Type III as the best-fit type with overwhelming AIC/BIC preference, and the ML-refined parameters land within 1σ of the input values for $N \geq 10^4$.

5. Ambartsumian's inverse-Laplace formulation

Derivation

As noted above, from a mathematical point of view, the key observation of Ambartsumian's inverse-Laplace formulation is that the rate of first-flare events, $m_1(t)$, equals $\int_0^\infty \nu\, e^{-\nu t}\, \varphi(\nu)\, \mathrm{d}\nu = \mathcal{L}[\nu\varphi(\nu)](t)$.

Obviously

$$\frac{m_1(t)}{m_1(0)} = \frac{\int \nu e^{-\nu t}\varphi(\nu) d\nu}{\int \nu \varphi(\nu) d\nu} = \frac{\int \nu e^{-\nu t}\varphi(\nu) d\nu}{\langle \nu \rangle} \tag{19}$$

so the question of determining $\varphi(\nu)$ reduces to inverse Laplace transform of the observed function $m_1(t)/m_1(0)$:

$$\varphi\left(\nu\right) = \frac{\langle \nu \rangle}{\nu} \mathcal{L}^{-1}\left[\frac{m_1(t)}{m_1(0)}\right] \tag{20}$$

In this article, we use two other, equivalent methods of representing a function $m_1(t)/m_1(0)$ using observational data:

- *Survival function.* Consider the survival function of the first-flare time. A star with rate ν has its first flare at an exponentially distributed time, so the probability that it has not yet flared by time t is $e^{-\nu t}$. Averaging over the population,

$$1 - \frac{n_{\rm disc}(t)}{N_{\rm tot}} \;=\; \int_0^\infty e^{-\nu t}\, \varphi(\nu)\, \mathrm{d}\nu \;=\; \mathcal{L}[\varphi](t). \tag{21}$$

doi: https://doi.org/10.52526/25792776-26.73.1-39

Here $n_{\rm disc}(t)$ is the cumulative number of stars that have flared at least once, and $N_{\rm tot}$ is the total number of flare stars in the population. Eq. (21) identifies the survival curve as the Laplace transform of φ at parameter t. Inverting gives φ. This formulation uses only the first-flare statistic and is sensitive to a different region of φ than the MoM.

- *Direct identity.* Note (Akopian & Parsamian, 2009) that (see subsection 6.5)

$$\frac{m_1(t)}{m_1(0)} = \frac{n_1(t)}{n(t)} \tag{22}$$

where $n\,(t)$ is the total number of flares detected up to t and $n_1\,(t)$ is the number of singly flaring stars. $n_1(t)$ and $n(t)$ are both counted directly from the observational data — no normalization by $N_{\rm tot}$ enters. This ratio is arguably the cleanest possible observable to feed into the Laplace-inversion.

In practice the survival data are discrete and noisy. The Talbot (1979) algorithm for numerical Laplace inversion requires $\mathcal{L}[\varphi]$ evaluable at complex arguments s, but we have it only at real t in the observation range. Ambartsumian's solution is to smooth the observed $S(t) = 1 - n_{\rm disc}(t)/N_{\rm tot}$ with a known analytical form whose Laplace inverse is given in closed form.

The Type III special case

By Eq. (12), the Type III Laplace transform yields

$$n_{\rm disc}(t) \;=\; N_{\rm tot}\left[1 - e^{-\nu_0 t}\left(\frac{a}{a+t}\right)^{\gamma}\right]. \tag{23}$$

This is a three-parameter nonlinear least-squares fit of the observed discovery curve. The fitted (a, γ, ν_0) are the parameters of φ, recovered without computing any moment of K.

The MoM uses all of $\{n_k\}$ and is dominated by the high-ν tail through the third and fourth moments. Ambartsumian's approach uses only first-flare times, weighted by $\nu\, e^{-\nu t}$ and therefore sensitive to a different region of φ. On data well- described by a single Type III the two methods agree. On heterogeneous data they disagree, and the character of the disagreement reveals the nature of the misspecification.

6. Distribution function of the flare rates of Galactic field flare stars using various methods: a comparative analysis

To address this problem, we used a catalogue of flaring stars compiled on the basis of observations from the Kepler space observatory (VizieR J/ApJS/241/29) (Yang et al., 2019) which lists 162,262 flare events on $N_{\rm cat} = 3420$ unique Kepler Input Catalog (KIC) stars. The flare-start times *Begin* span $T \approx 1460\ d$.

6.1. MoM: a time-evolution analysis

To probe the stability of the MoM fit, we apply it to 14 observation windows $T_w \in \{100, 200, \ldots, 1400\}$ d. At each window, we re-bin the data: for each star, we count the number of flares with `Begin` $\leq T_w$, build the histogram $\{n_k(T_w)\}$, estimate $n_0(T_w)$ via χ^2 optimization, and refit the Type III distribution. If φ were exactly a Pearson III distribution, the parameters should stabilize as T_w increases.

Figure 4 and Table 1 show the result. The shape parameters a and γ are remarkably stable across the 14 windows ($a \approx 16$–18, $\gamma \approx 0.67$–0.73). However, ν_0 consistently lands near $-5 \times 10^{-3}\ d^{-1}$. A Type III density with $\nu_0 < 0$ is not a valid probability density on $\mathbb{R}^+$ — its support would extend to negative rates.

doi: https://doi.org/10.52526/25792776-26.73.1-39

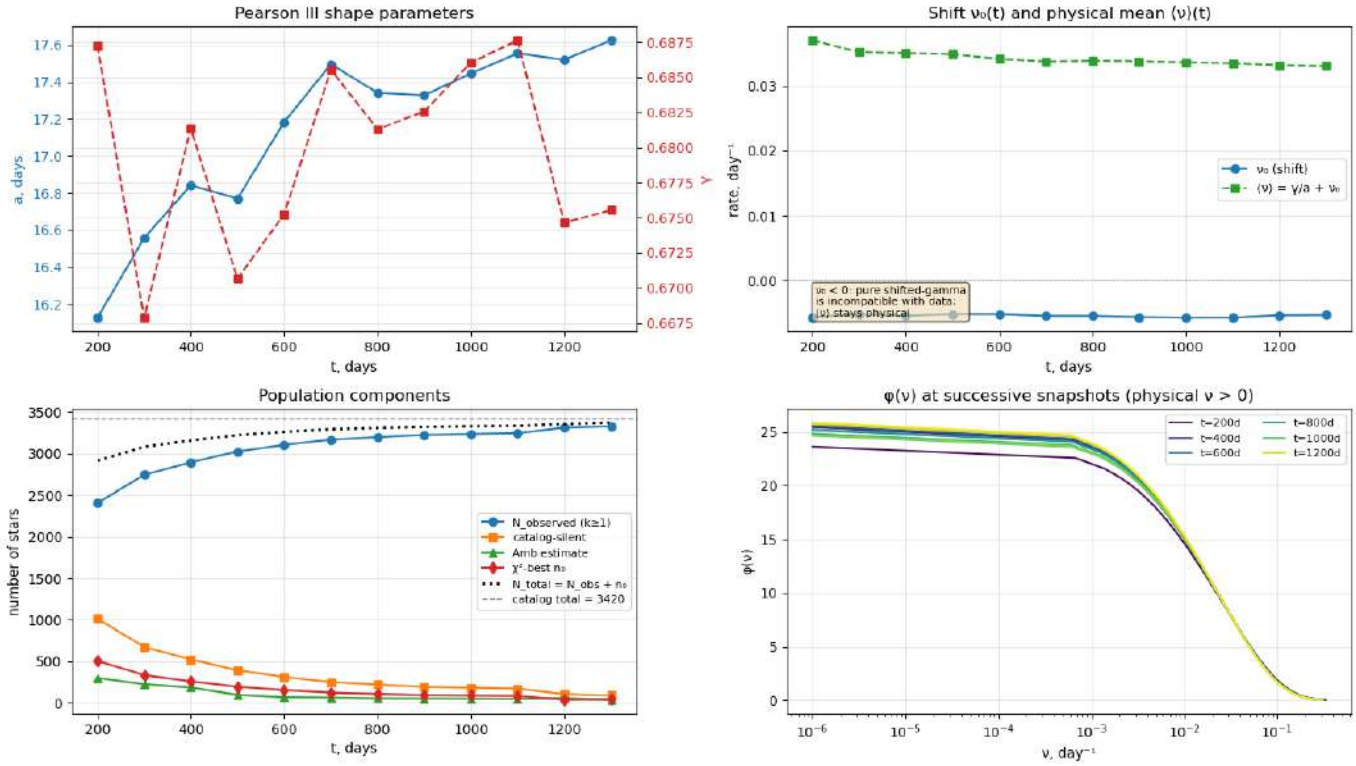

Figure 4: Time evolution of the MoM Pearson III fit on Kepler stars, applied at 12 observation windows $T_w \in \{100, \ldots, 1200\}$ d. Top left: $a(T_w)$; top right: $\gamma(T_w)$; bottom left: $\nu_0(T_w)$; bottom right: 12 and the Ambartsumian's estimates of n_0. The shape parameters (a, γ) stabilize quickly but ν_0 settles at a clearly negative value — an unphysical shift signalling that the data are not drawn from a single Pearson III.

Table 1: Time evolution of the MoM Pearson III fit on Kepler stars applied at observation windows $T_w \in \{200, \ldots, 1200\}$ d

t,	N_{obs}	$n_0(\text{cat})$	$n_0(\text{Amb})$	$n_0(\chi^2)$	N_{tot}	a	γ	ν_0
200	2406	1014	303	507	2913	16.1	0.687	-5.64×10^{-3}
400	2895	525	187	262	3157	16.8	0.681	-5.43×10^{-3}
600	3105	315	72	157	3262	17.2	0.675	-5.16×10^{-3}
800	3197	223	57	111	3308	17.3	0.681	-5.45×10^{-3}
1000	3236	184	54	92	3328	17.4	0.686	-5.72×10^{-3}
1200	3312	108	61	42	3354	17.5	0.675	-5.34×10^{-3}

Although the Laplace transform formula, Eq. (12), remains formally well-defined, it no longer represents the Laplace transform of any proper density.

This negative ν_0 value provides the first diagnostic indicator, demonstrating that the sample moments are internally consistent with a Pearson III distribution, but no such density can function as a valid probability density on the positive half-line. The high-ν tail of φ (which governs μ_3 and μ_4) demands a particular pair of (a, γ) parameters that does not match the low-ν behavior (which dictates the offset).

6.2. Ambartsumian's approach

We now apply the Ambartsumian's fit via Eq. (23) to the Kepler stars discovery curve over the full observation window $T_w = 1456$ d, with $N_{\text{tot}} = N_{\text{cat}} = 3420$ held fixed.

The result (Figure 5) is striking. The analytical fit reproduces the discovery curve to within better than 1% in RMS. The fitted parameters are $a = 12.0$, $\gamma = 0.33$, and $\nu_0 = +1.7 \times 10^{-3}\ d^{-1}$. Most importantly, ν_0 is positive; hence, the recovered density is a proper probability density on $\mathbb{R}^+$. The Ambartsumian's formulation perceives the data differently from the MoM and finds a perfectly physical Type III distribution,

doi: https://doi.org/10.52526/25792776-26.73.1-39

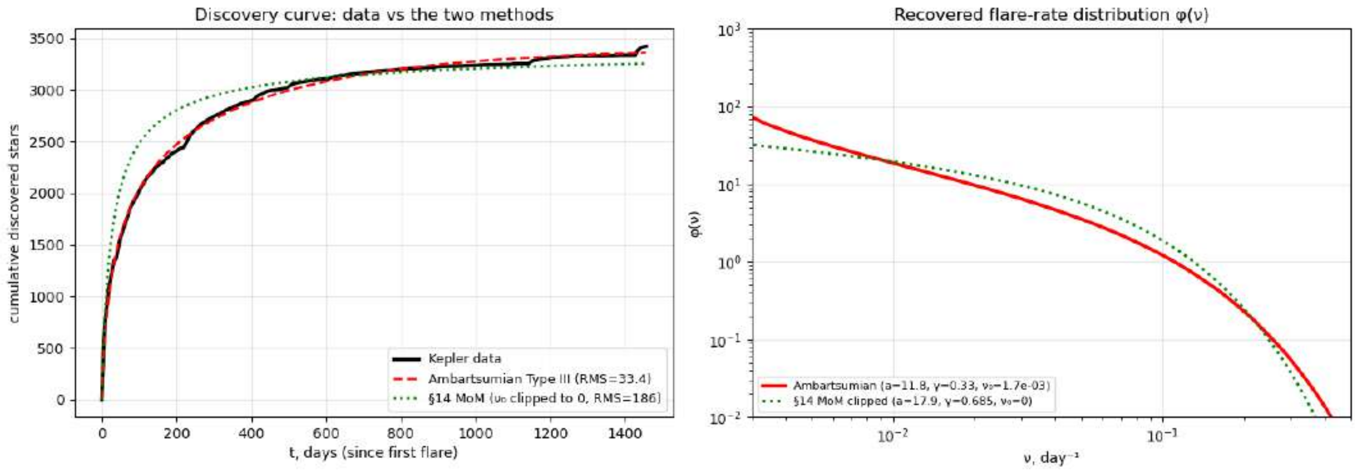

Figure 5: Type III fit to the Kepler stars discovery curve over the full observation window. Left panel: observed cumulative number of discovered stars (black) and the analytical fit (red dashed). The fit is excellent (Root Mean Square (RMS) = 33 stars out of 3420, i.e., $\sim 1\%$). The χ^2-best ν_0 value obtained from the MoM (green dotted) yields a much worse fit to the discovery curve because a negative $\nu_0 < 0$ in that case is mathematically inconsistent with the discovery-curve interpretation. Right panel: the recovered distribution $\varphi(\nu)$. Ambartsumian's approach yields a physically valid Type III distribution with $\nu_0 = +1.7 \times 10^{-3}\ d^{-1}$. The numerical inverse Laplace transform of the fitted analytical $\mathcal{L}[\varphi]$ (black dots) reproduces the analytical curve to within $< 1\%$, validating the `mpmath` Talbot implementation.

while the MoM applied to the same data returns an inconsistent model.

A useful cross-check can be performed at this stage: although the two methods yield different shape parameters, they agree on the population mean rate $\langle \nu \rangle$ to within 15% (0.029 d^{-1} from the Ambartsumian's method vs. 0.033 d^{-1} from the MoM). This is the only quantity that survives the methodological disagreement, confirming it as the most robust statistic of the population.

6.2.1. Dual time evolution.

We can repeat the Ambartsumian's fitting procedure at each T_w (Figure 6) and place the results alongside the evolution of the MoM estimates.

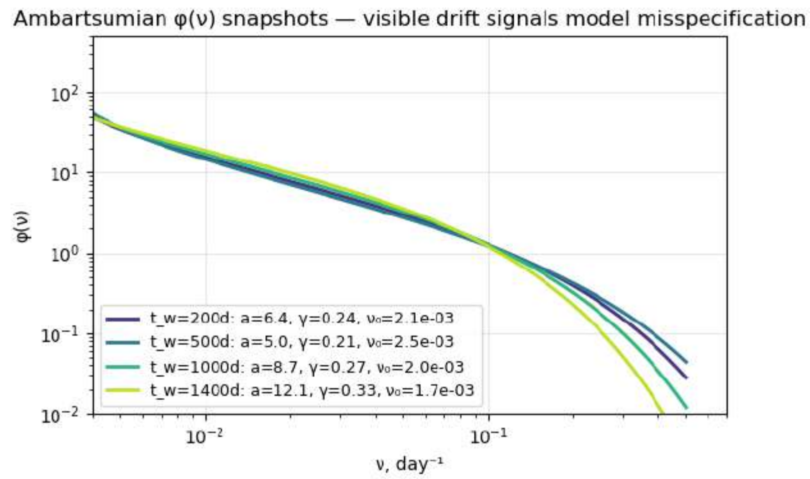

Figure 6: Ambartsumian's fitting procedure at each T_w

Figures(6, 7) provides the second diagnostic. The MoM (green) yields stable (a, γ) values throughout, but results in $\nu_0 < 0$ at every T_w. Conversely, Ambartsumian's approach (red) yields $\nu_0 > 0$ across all windows, but the shape parameters drift smoothly with T_w: a increases from 3.6 at $T_w = 100\ d$ to 12.1 at $T_w = 1400\ d$, while γ shifts from 0.16 to 0.33. This drift is overall monotonic, except for a small, transient

doi: https://doi.org/10.52526/25792776-26.73.1-39

non-monotonic feature at $T_w < 500$ d that reflects the limited information content of the early discovery curve.

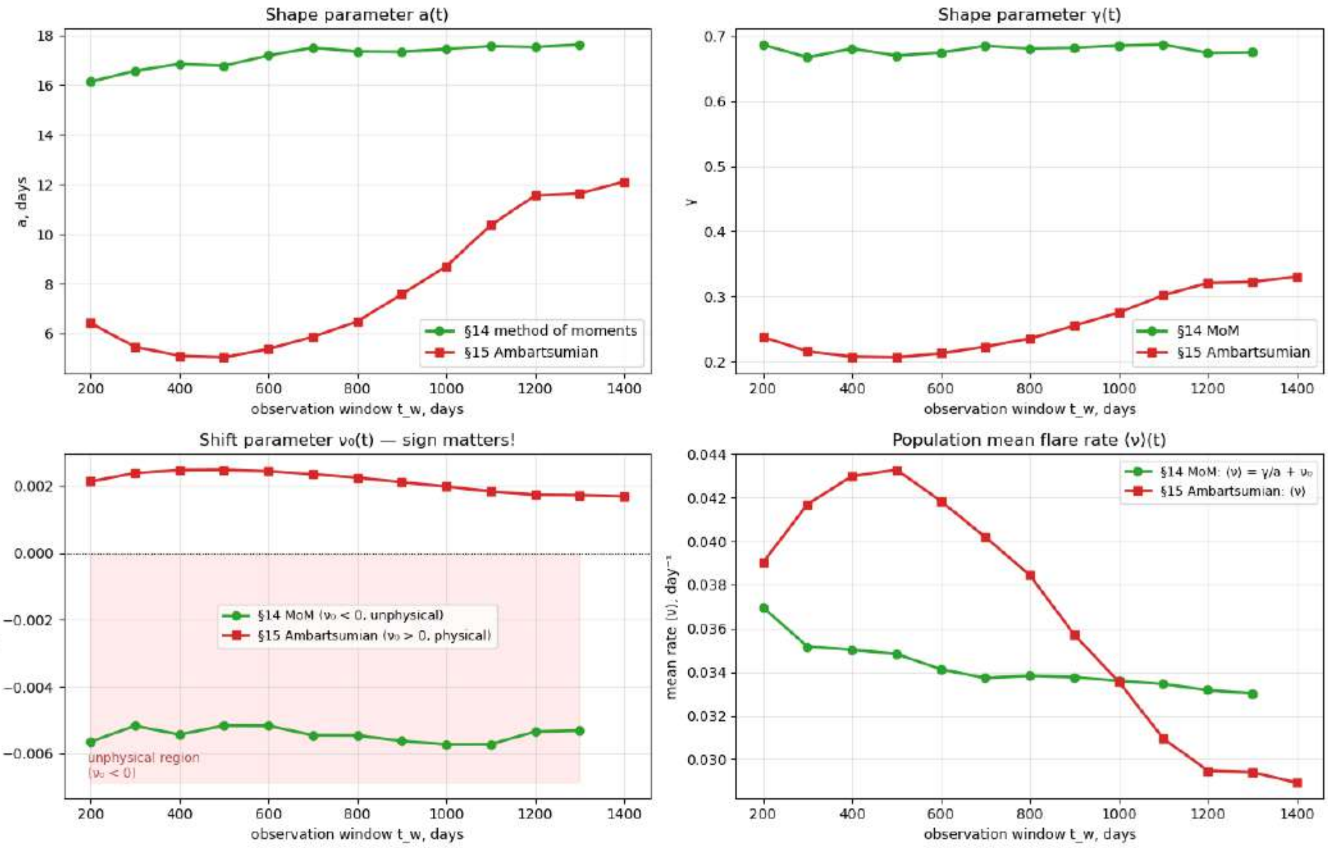

Figure 7: Side-by-side time evolution of the MoM fit (green) and the Ambartsumian's fit (red) at 13 observation windows $T_w \in \{200, \ldots, 1400\}$ d on the Kepler stars. Top left: $a(T_w)$. Top right: $\gamma(T_w)$. Bottom left: $\nu_0(T_w)$ — the shaded red region is the unphysical $\nu_0 < 0$ regime, in which the moment method sits throughout. Bottom right: population mean rate $\langle\nu\rangle(T_w)$. Both methods agree on $\langle\nu\rangle$ at $T_w = 1400$ d to $\sim 15\%$, but disagree on shape parameters throughout.

Both diagnostics — the unphysical ν_0 value from the MoM and the parameter drift in Ambartsumian's approach — point toward the same conclusion. The Kepler stars sample is not drawn from a single Pearson III distribution. Instead, the data possess an additional structure that neither parametric fit fully captures, and the two estimators reveal this underlying structure from distinct perspectives.

6.3. Two-component Pearson III mixture

The minimal extension is a weighted mixture of two Type III densities:

$$\varphi(\nu) \;=\; w\,\varphi_{\text{fast}}(\nu; a_1, \gamma_1, \nu_{0,1}) + (1-w)\,\varphi_{\text{slow}}(\nu; a_2, \gamma_2, \nu_{0,2}). \tag{24}$$

Because the Laplace transform is linear, it follows from (12) that:

$$1 - \frac{n_{\text{disc}}(t)}{N_{\text{tot}}} \;=\; w\,e^{-\nu_{0,1}t}\left(\frac{a_1}{a_1+t}\right)^{\gamma_1} + (1-w)\,e^{-\nu_{0,2}t}\left(\frac{a_2}{a_2+t}\right)^{\gamma_2}. \tag{25}$$

The fit has seven parameters $(w, a_1, \gamma_1, \nu_{0,1}, a_2, \gamma_2, \nu_{0,2})$ and a non-convex landscape, so we use eight random restarts from physically motivated initial conditions.

The shape parameter γ_2 of the slow component is weakly constrained by the discovery curve but strongly constrained by the flare-count histogram n_k. A star with a flaring rate ν produces, on average, $\langle k\rangle = \nu T$ flares over the baseline T. Consequently, the observed histogram excess at $k \approx 17$–23 demands a slow

doi: https://doi.org/10.52526/25792776-26.73.1-39

population centered near $\nu \approx k/T \approx 1.2 \times 10^{-2}$ d^{-1}, while reproducing a broad excess (rather than a sharp peak) requires $\gamma_2 \sim 0.6$. Fitting this mixture model directly to n_k yields an excellent match to the histogram ($\chi^2_{\rm PMF} \approx 77$) with a mixing weight of $w = 0.79$. The resulting parameters comprise a fast component ($a_1 = 12.0$, $\gamma_1 = 0.35$, $\langle\nu\rangle_1 = 3.3 \times 10^{-2}$ d^{-1}, corresponding to a $\sim$ 30-day mean recurrence interval) and a broad slow component ($a_2 = 51$, $\gamma_2 = 0.57$, $\langle\nu\rangle_2 = 1.1 \times 10^{-2}$ d^{-1}, corresponding to a $\sim$ 87-day interval).

Fit criterion	γ_2	$\langle\nu\rangle_{\rm slow}$	RMS$_{\rm disc}$	$\chi^2_{\rm PMF}$
discovery-curve only	$\to 0$	5×10^{-3}	**22.5**	2100
histogram only	0.57	1.1×10^{-2}	119	**77**
joint (equal weight)	0.60	6×10^{-3}	28	294

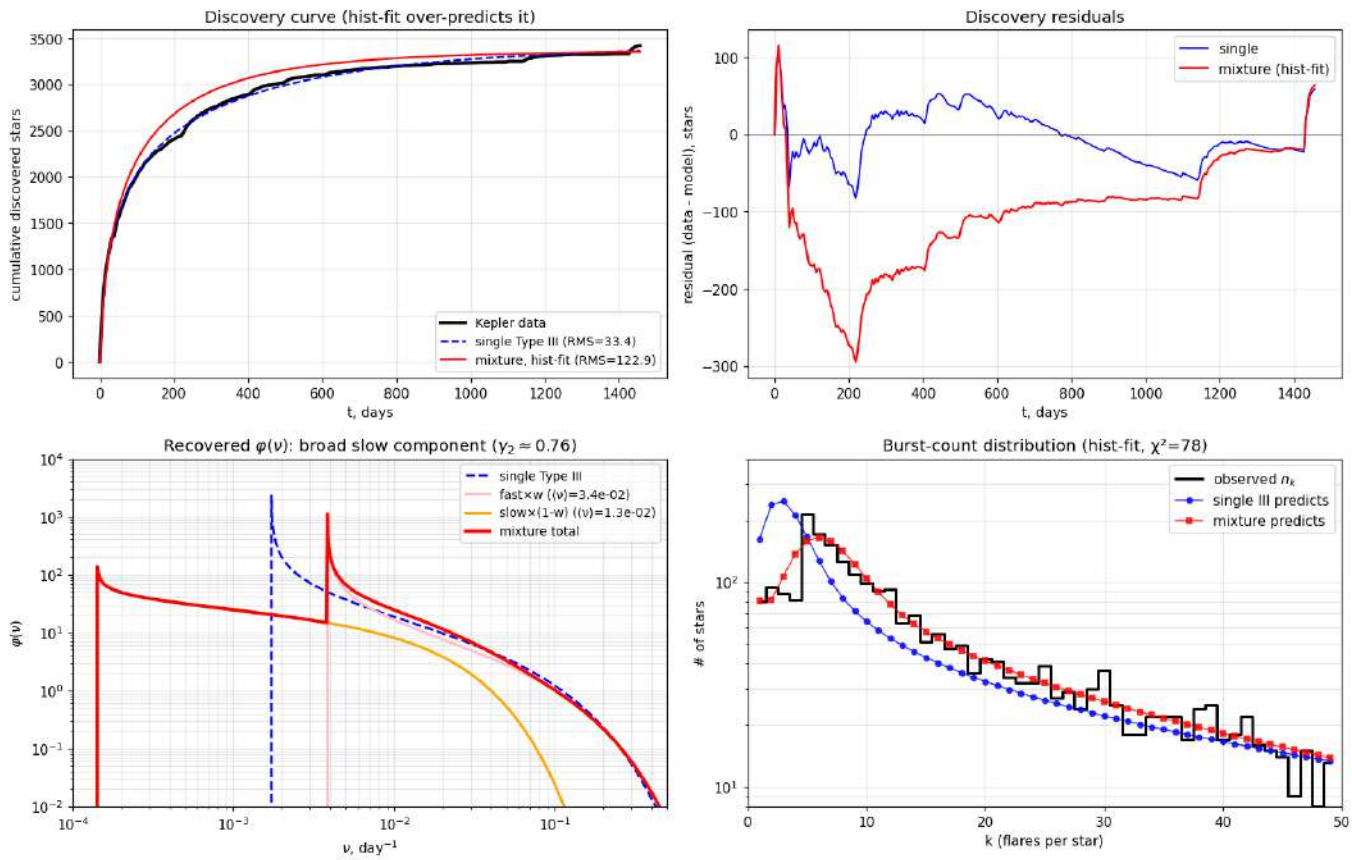

Figure 8: Two-component Type III mixture fit to the Kepler stars, fitted to the flare-count histogram n_k. Top left: discovery curve $n_{\rm disc}(t)$ (the histogram-best fit over-predicts it). Top right: discovery-curve residuals. Bottom left: recovered $\varphi(\nu)$, showing the broad slow component ($\gamma_2 \approx 0.57$). Bottom right: flare-count distribution n_k — the mixture (red) matches the data across all k, whereas a single Type III (blue) cannot.

6.3.1. The discovery–histogram discrepancy

An important finding of this work is that no single two-component Type III mixture can fit both observable features simultaneously. The histogram-best fit, characterized by its broad slow component, over-predicts the discovery curve at early times (Fig. 8): stars with intermediate flaring rates of $\nu \sim 10^{-2}$ d^{-1} produce the correct total flare count k by the end of the mission, yet they are discovered (i.e., their first flare is detected) later than a pure Poisson process at that rate would predict.

Either way, this discrepancy demonstrates that Kepler stars flare statistics cannot be fully captured by a static rate distribution $\varphi(\nu)$ under pure Poisson assumptions.

doi: https://doi.org/10.52526/25792776-26.73.1-39

6.4. Model-independent recovery

The mixture analysis presented above still constrains the analysis to the Pearson III functional form for each component. To obtain a model-independent reconstruction of $\varphi(\nu)$, we now employ non-Pearson analytical smoothers to fit the discovery curve and subsequently perform a numerical inversion.

6.4.1. Choice of smoothers, fit-and-invert pipeline

We investigate three analytical forms characterized by distinct qualitative behaviors:

$$S_{\mathrm{SE}}(t) = \exp(-c\,t^{\beta}) \qquad \text{(stretched exponential, 2 parameters),} \tag{26}$$

$$S_{\mathrm{Alg}}(t) = (1 + (ct)^{\alpha})^{-\beta} \qquad \text{(algebraic, 3 parameters),} \tag{27}$$

$$S_{\mathrm{Prony}}(t) = w\,e^{-\lambda_1 t} + (1-w)\,e^{-\lambda_2 t} \qquad \text{(two exponentials, 3 parameters).} \tag{28}$$

For $0 < \beta < 1$, S_{SE} represents the Laplace transform of a one-sided β-stable density (of the Mittag-Leffler type). S_{Alg} inverts to a non-elementary continuous density, whereas S_{Prony} inverts to a discrete two-point distribution, $w\,\delta(\nu - \lambda_1) + (1-w)\,\delta(\nu - \lambda_2)$, and is included here as a degenerate limiting case. None of these three smoothers corresponds to a member of the Pearson family.

Table 2: Non-Pearson smoothers fit to the Kepler stars discovery curve, and Pearson III re-fits of the numerically inverted φ.

Smoother	parameters	RMS (stars)	Pearson III refit of inverted φ		
			a	γ	ν_0
Stretched exp	$c = 0.072$, $\beta = 0.545$	25.6	27.5	2.22	~ 0
Algebraic	$c = 10^{-5}$, $\alpha = 0.555$, $\beta = 41$	25.6	20.9	1.56	~ 0
Two-exp Prony	$w = 0.52$, $\lambda_1 = 3.2 \times 10^{-2}$, $\lambda_2 = 2.6 \times 10^{-3}$	56.2	—	—	—
Type III (ref.)	$a = 12$, $\gamma = 0.33$, $\nu_0 = 1.7 \times 10^{-3}$	33.2	—	—	—

For each smoother, we fit the analytical expression to the observed Kepler stars survival curve, $S(t) = 1 - n_{\mathrm{disc}}(t)/N_{\mathrm{cat}}$, using nonlinear least squares. Next, we employ the Talbot algorithm implemented in the `mpmath` library to numerically invert the fitted analytical form into $\varphi(\nu)$ on a logarithmic ν-grid. Finally, we fit a Pearson III distribution to the recovered $\varphi(\nu)$ profile via weighted least squares in $\log\varphi$ space, evaluating the proximity of the standard Pearson III family to the fully data-driven distribution shape. The results are presented in Figure 9 and summarized in Table 2.

6.4.2. Key findings

Three key findings can be inferred from these data:

First, the non-Pearson smoothers provide a better fit to the discovery curve than the Type III distribution, despite using either the same number of parameters or only one extra parameter (the RMS residual drops to 26 for both the stretched exponential and algebraic smoothers, compared to 33 for Type III). This indicates that the standard Type III functional form is not preferred by the empirical data.

Second, the stretched-exponential and algebraic recoveries yield nearly identical reconstructed profiles for $\varphi(\nu)$, despite originating from radically different functional forms in t-space. The recovered distribution φ is unimodal, centered near $\nu \sim 2 \times 10^{-3}\ d^{-1}$, and features a prominent high-ν tail. This shape is qualitatively distinct from the direct Type III fit, which decreases monotonically from the boundary value $\nu_0 = 1.7 \times 10^{-3}\ d^{-1}$.

Third, the Pearson III distribution re-fit to the recovered φ yields $\gamma > 1$ in both cases. A Type III distribution with $\gamma < 1$ is monotonically decreasing (a decaying Gamma distribution), whereas $\gamma > 1$

doi: https://doi.org/10.52526/25792776-26.73.1-39

produces a true interior mode. Consequently, the data-driven shape can indeed be accommodated within the Pearson III family, but strictly in the $\gamma > 1$ parameter regime — not the $\gamma \sim 0.3$ region where both the MoM and the direct fit artificially converge. Thus, while the parametric family itself is sufficiently flexible, standard fitting methods that operate directly on raw moments or the raw survival curve $S(t)$ fail to locate the physically correct parameter region.

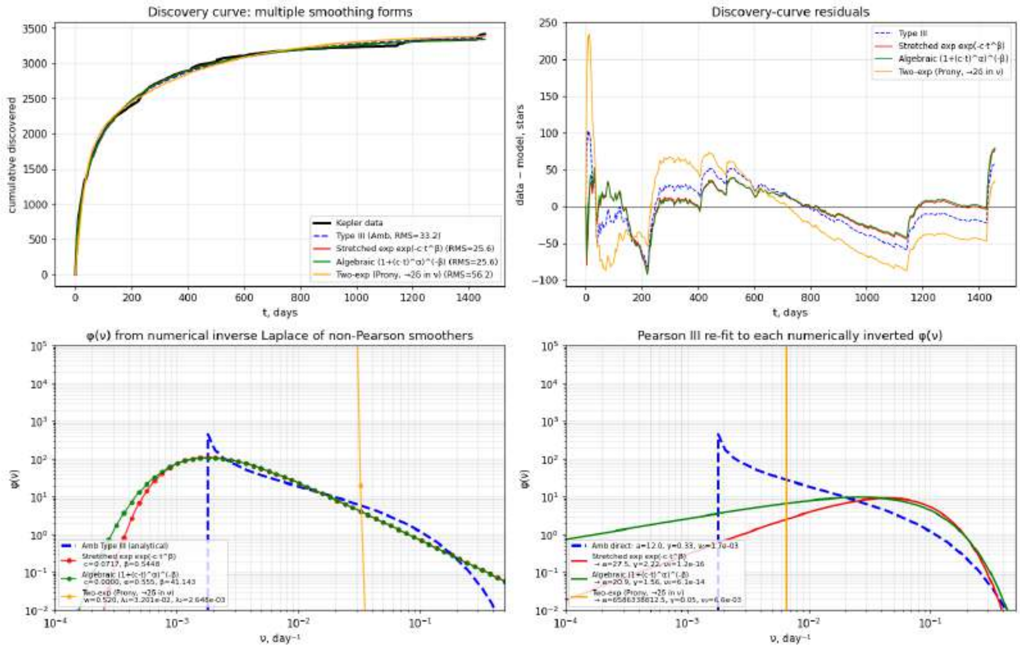

Figure 9: Model-independent inverse-Laplace recovery on Kepler stars. Top left: discovery curve and four fits — Type III (blue dashed, RMS= 33), stretched exponential (red, RMS= 26), algebraic (green, RMS= 26), two-exponential Prony (orange, RMS= 56). Top right: residuals on a common scale. Bottom left: $\varphi(\nu)$ from numerical inverse Laplace of each smoother, on a logarithmic ν-axis. Bottom right: Pearson III re-fits to each numerically inverted φ, compared to the direct Type III. The stretched-exp and algebraic recoveries (red, green) give a peaked $\varphi(\nu)$ centered near $\nu \sim 2 \times 10^{-3}\ d^{-1}$ — qualitatively different from the monotonically decreasing Type III.

6.4.3. Stability of model-independent recovery

We can repeat the model-independent recovery at each observation window T_w and ask: does the recovered shape change with T_w? If the recovery is genuine, the answer should be *no*; if it is a method artifact (like the Type III drift of Section 6.1), the answer would be *yes*.

Figure 10 delivers the cleanest possible demonstration. The stretched-exp parameters vary by only 5–15% across all 14 windows; the four snapshots of $\varphi(\nu)$ at $T_w = 200, 600, 1000, 1400\ d$ are nearly superimposed. The mean rate $\langle\nu\rangle$ from the model-free φ stays flat at $\sim 0.031\ \mathrm{d}^{-1}$ across all windows. The peak position of φ stays at $\sim 2 \times 10^{-3}\ d^{-1}$.

Compare with the Type III evolution (Figure 7): a varies by 70%, γ by 70%, ν_0 by 70%, $\langle\nu\rangle$ by 65%. The model-free recovery is roughly an order of magnitude more stable in every comparable summary statistic (Table 3). This is the third diagnostic. The data have a stable underlying $\varphi(\nu)$ that the model-independent recovery captures well. The drift of the Type III fit, identified in Section 6, is therefore confirmed to be a model artifact — the Pearson III family with $\gamma < 1$ is wobbling under the load, while the data themselves do not change.

6.5. Recovering using the identity: $m_1(t)/m_1(0) = n_1(t)/n(t)$

All the analyses so far rely on the discovery curve $n_{\mathrm{disc}}(t)/N_{\mathrm{tot}}$ — which means committing to a value of N_{tot}. There is a much cleaner observational route to the Laplace-pair function.

doi: https://doi.org/10.52526/25792776-26.73.1-39

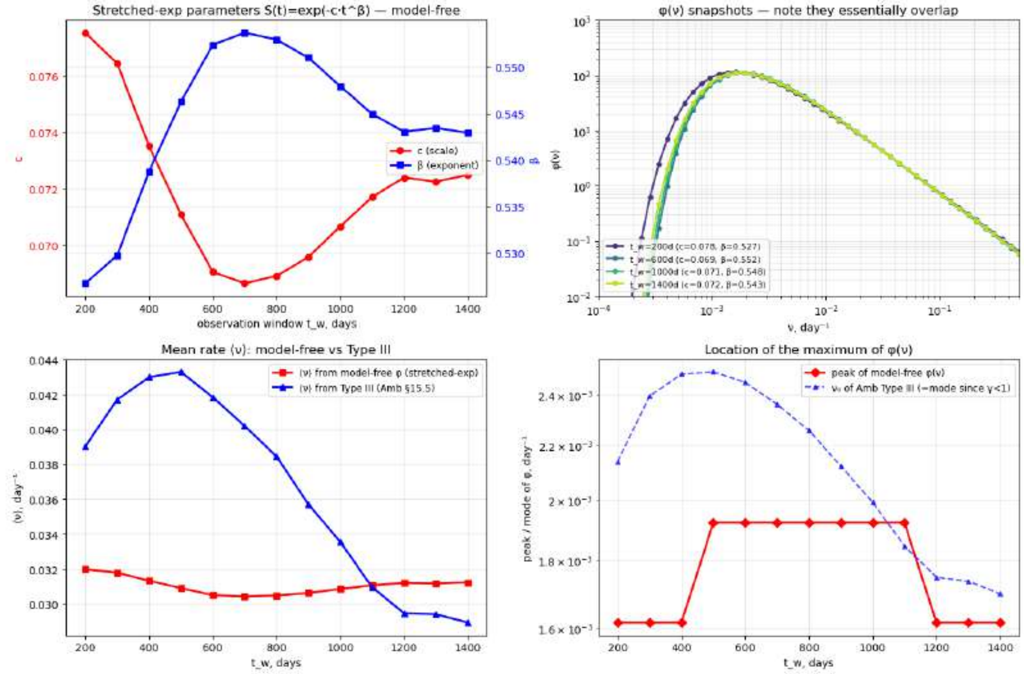

Figure 10: Time evolution of the model-independent recovery via stretched- exponential smoothing. Top left: fitted smoother parameters c (red, left axis) and β (blue, right axis) across T_w. Top right: four snapshots of recovered $\varphi(\nu)$ at $T_w = 200, 600, 1000, 1400$ d — note how the snapshots nearly overlap. Bottom left: mean rate $\langle\nu\rangle$ from the model-free φ (red squares) vs. the same from Type III (blue triangles). Bottom right: peak position of φ vs. T_w for both methods. The model-free recovery is roughly an order of magnitude more stable across T_w than the Type III recovery.

Table 3: Stability of recovered quantities across $T_w \in [100, 1400]$ days for two reconstruction methods.

Quantity	model-free (stretched exp)	Type III (Ambartsumian)
Shape parameter 1	c: 0.069–0.078 (13% range)	a: 3.6–12.1 (70% range)
Shape parameter 2	β: 0.527–0.555 (5% range)	γ: 0.16–0.33 (70% range)
Peak / mode of φ	1.6–1.9×10^{-3} (17%)	ν_0: 1.7–3.5×10^{-3} (70%)
Mean rate $\langle\nu\rangle$	3.04–3.20×10^{-2} (5%)	2.89–4.88×10^{-2} (65%)

Define

$$n_1(t) = \#\{j : \text{star } j \text{ has flared exactly once by time } t\}, \tag{29}$$

$$n(t) = \sum_j K_j(t), \quad \text{the cumulative flare count up to } t. \tag{30}$$

For a single star with hidden rate ν_j, the probability of exactly one flare in $[0, t]$ is $\Pr(K_j = 1 \mid \nu_j) = \nu_j t\, e^{-\nu_j t}$. Summing over the population and taking expectations:

$$\mathbb{E}[n_1(t)] \;=\; N \int_0^\infty \nu t\, e^{-\nu t}\, \varphi(\nu)\, \mathrm{d}\nu \;=\; N\, t\, m_1(t), \tag{31}$$

where $m_1(t) = \int \nu e^{-\nu t} \varphi(\nu) \mathrm{d}\nu$. Likewise $\mathbb{E}[n(t)] = N\, t\, \langle\nu\rangle = N\, t\, m_1(0)$, since the expected total count is the expected rate per star times Nt. Dividing,

$$\frac{n_1(t)}{n(t)} \xrightarrow[N\to\infty]{} \frac{m_1(t)}{m_1(0)}. \tag{32}$$

The identity holds in the large-N limit. Both numerator and denominator are counted directly from the catalog — no N_{tot} appears.

doi: https://doi.org/10.52526/25792776-26.73.1-39

The function $R(t) = m_1(t)/m_1(0) = \mathcal{L}[\nu\varphi(\nu)](t)/\langle\nu\rangle$ is the Laplace transform of $\nu\varphi(\nu)/\langle\nu\rangle$. Inverting it gives $\nu\varphi(\nu)/\langle\nu\rangle$, from which φ follows by dividing by ν and renormalizing. The recovery pipeline is now:

1) compute $R(t) = n_1(t)/n(t)$ directly from the catalog,

2) fit a non-Pearson analytical form to $R(t)$,

3) numerically invert via Talbot to obtain $u(\nu) \propto \nu\varphi(\nu)$,

4) divide by ν and normalize: $\varphi(\nu) = u(\nu)/\nu \cdot Z$ with $\int \varphi \, d\nu = 1$.

At no stage do we need to know N_{tot}. If the catalog has missing truly-silent stars, or if the survey selection function is non-trivial, the R-route is unaffected — both n_1 and n scale with the observed population in the same way.

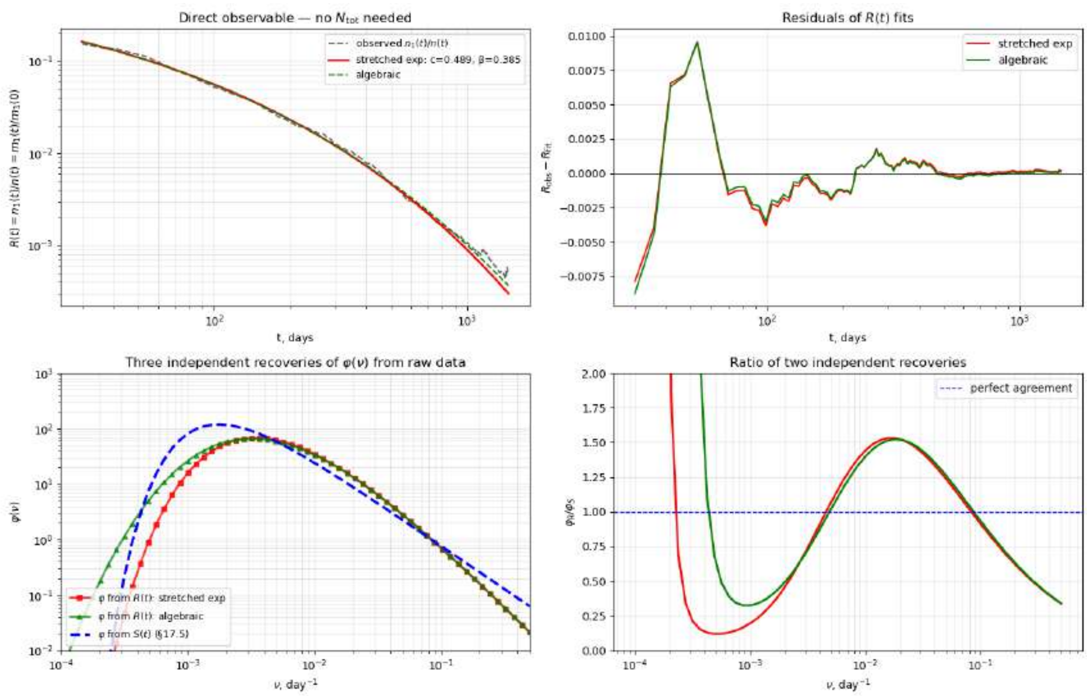

Figure 11: Direct $R(t) = n_1(t)/n(t)$ recovery on Kepler stars. Top left: observed $R(t)$ (black dots) and two analytical fits — stretched exponential (red), algebraic (green dashed). The two fits are visually indistinguishable on the log-log plot. Top right: residuals. Bottom left: three recoveries of $\varphi(\nu)$ — from $R(t)$ via stretched exp (red), from $R(t)$ via algebraic (green), and from $S(t)$ via stretched exp (blue dashed). Bottom right: ratio φ_R/φ_S with y-axis clipped to $[0, 2]$, showing the structured pattern of disagreement.

Figure 11 shows the result. We compute $n_1(t)$ and $n(t)$ efficiently from sorted first- and second-flare times using $n_1(t) = N_{\text{disc},1}(t) - N_{\text{disc},2}(t)$, where $N_{\text{disc,k}}(t)$ is the number of stars with at least k flares by time t. The ratio $R(t)$ is well-fit by both the stretched exp ($c = 0.49$, $\beta = 0.39$) and the algebraic form, with RMS residual $\sim 10^{-3}$ in R over five decades.

The bottom-left panel of Figure 11 compares three independent recoveries of $\varphi(\nu)$:

- from $R(t) = n_1(t)/n(t)$ (no N_{tot}) using stretched exp;
- from $R(t)$ using algebraic;
- from $S(t) = 1 - n_{\text{disc}}(t)/N_{\text{cat}}$ (with $N_{\text{tot}} = 3420$ fixed) using stretched exp.

In the bulk of φ, all three agree to within a factor of 1.5 — a remarkable cross-check given that they use fundamentally different observables. The bottom-right panel quantifies the disagreement as a structured pattern (Table 4). The R-route gives less mass at the low-ν shoulder ($\nu \sim 5 \times 10^{-4}\ d^{-1}$, ratio ~ 0.1), crosses

doi: https://doi.org/10.52526/25792776-26.73.1-39

the S-route at the peak of φ ($\nu \sim 4 \times 10^{-3}\ d^{-1}$), rises to a $\sim 50\%$ excess in the bulk ($\nu \sim 2 \times 10^{-2}$, ratio ~ 1.5), and falls again in the high-ν tail (ratio ~ 0.3 at $\nu \sim 0.4$).

Table 4: Structured pattern of disagreement between R-route and S-route recoveries.

ν regime (d^{-1})	φ_R/φ_S	Reading
$\lesssim 2 \times 10^{-4}$	diverges (clipped)	numerical-inversion noise; do not interpret
$\approx 5 \times 10^{-4}$	~ 0.1 (minimum)	R-route assigns less mass at the low-ν shoulder
$\approx 4 \times 10^{-3}$	crosses 1	two routes cross near the peak of φ
$\approx 2 \times 10^{-2}$	~ 1.5 (maximum)	R-route assigns more mass at the bulk
$\gtrsim 10^{-1}$	~ 0.3	R-route mildly underestimates the heavy tail

The two routes use the same underlying φ but with different Laplace weightings:

- $S(t) = \mathcal{L}[\varphi](t)$ — weight $e^{-\nu t}$, equal at $t = 0$ and progressively concentrating on low ν as t grows;
- $R(t) = \mathcal{L}[\nu\varphi(\nu)](t)/\langle\nu\rangle$ — extra factor ν in the weight, so it concentrates on high-ν stars at every t.

The two-parameter smoothers fit each observable as well as they can but cannot capture every feature. When the same simple analytic form is forced to model two differently-weighted views of φ, it produces two different best-fit Laplace shapes, whose inversions agree only in the bulk. The systematic shape of the disagreement — too little mass at the shoulder, too much in the bulk, slightly too little in the tail — is the expected signature of a single simple smoother trying to model a bimodal $\varphi(\nu)$ (cf. Section 6.3).

7. Discussion

7.1. Cross-model comparison: time evolution of n_k and discovery curves

We have recovered four different rate distributions $\varphi(\nu)$:

1. **MoM** — Pearson III by the MoM (a=17.9, γ=0.685, ν_0 clipped to 0 since the raw fit gave $\nu_0 < 0$);
2. **Ambartsumian** — analytical Type III from the survival curve;
3. **mixture** — two-component Pearson III, fitted to the flare-count histogram;
4. **model-independent** — stretched-exponential survival $S(t) = e^{-ct^{\beta}}$, inverted to $\varphi(\nu)$ by Talbot (1979) algorithm.

Each φ predicts **two** observables, both flowing from the Laplace transform $L(t) = \int \varphi(\nu)e^{-\nu t}\,d\nu$:

- **discovery curve** $n_{\text{disc}}(t) = N\,[\,1 - L(t)\,]$ (time of first flare); or $n_1(t)/n(t)$
- **flare-count histogram** $n_k(T) = N \int \varphi(\nu)\,\text{Poisson}(k; \nu T)\,d\nu$ (total count by time T).

Comparing how each model tracks the **observed** time evolution of both quantities is the sharpest test: a φ that fits one observable but not the other (or fits at one T_w but drifts at another) is revealed immediately. This is the discovery/histogram discrepancy seen across all four models at once (Figures 12, 13).

doi: https://doi.org/10.52526/25792776-26.73.1-39

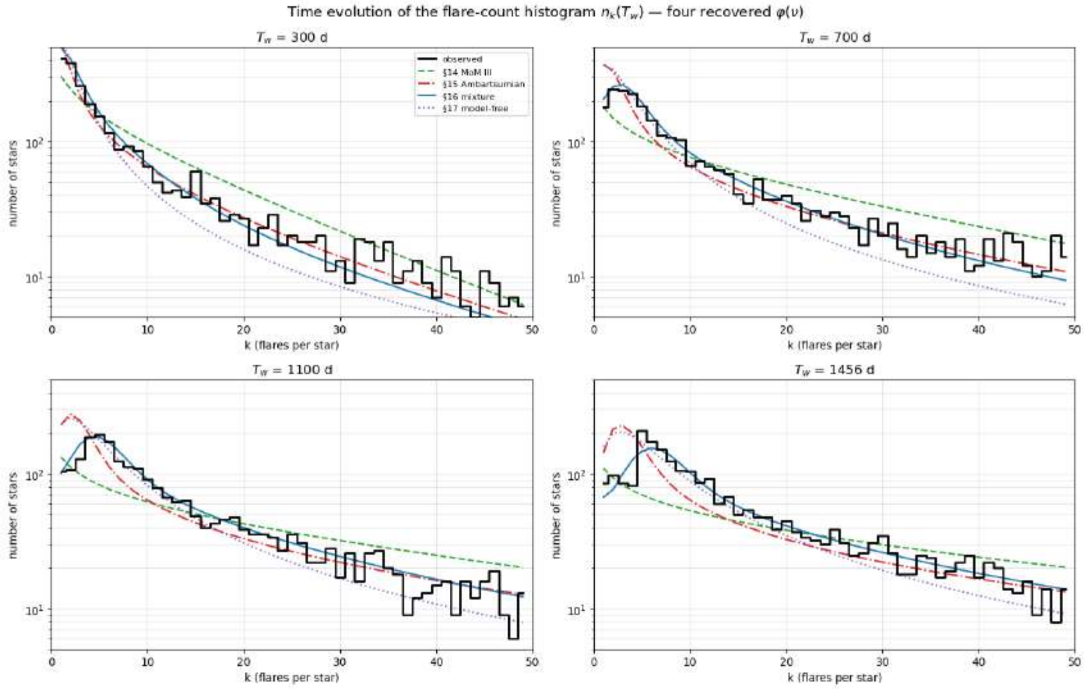

Figure 12: Cross-model comparison: time evolution of n_k

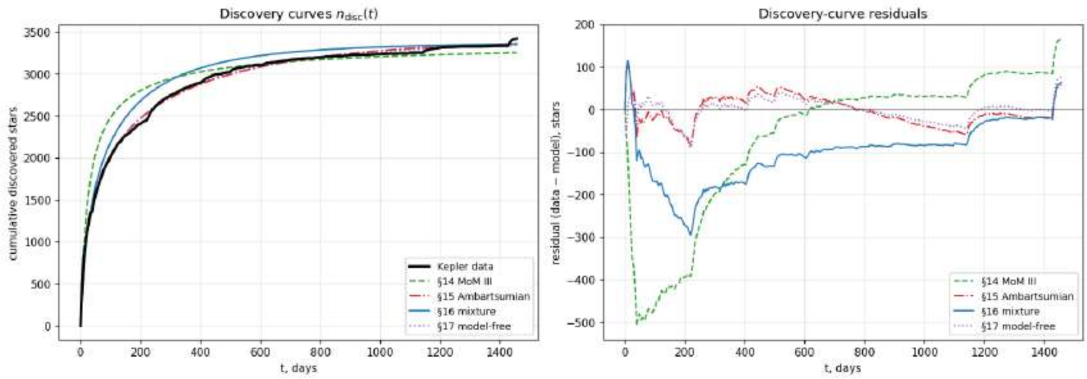

Figure 13: Cross-model comparison: discovery curves

7.2. Revealed discrepancies

The pipeline provided three independent diagnostic metrics, each leading to the same conclusion: the Kepler stars flare-rate distribution is a smooth, peaked density with a long high-ν tail, and cannot be modeled as a single Pearson III in any natural parameter regime:

1. The MoM fit yields an unphysical $\nu_0 < 0$ (Section 6). This provides the most direct mathematical evidence that no Type III density can internally match the observed moments.

2. Although the Type III fit yields a physical ν_0, the resulting parameters (a, γ) drift as a function of the observation window T_w (Figure 7) . Under Ambartsumian's approach, a correctly specified model would produce window-independent parameters; thus, this drift quantifies the degree of model misspecification at each T_w.

3. Employing non-Pearson analytical smoothers followed by numerical inversion (Section 6.4) yields a consistent recovered φ across two independent functional forms, which remains stable across all observation windows (Figure 10, Table 3). The recovered φ is peaked, with the maximum located near $\nu \sim 2 \times 10^{-3}\ d^{-1}$. A Pearson III re-fit of this stable φ falls into the $\gamma > 1$ regime, where the Type III distribution itself becomes a peaked density. This confirms that while the distribution family is sufficiently flexible, direct moment- or discovery-curve fits converge on the wrong region of the parameter space.

doi: https://doi.org/10.52526/25792776-26.73.1-39

7.3. The mixture interpretation

The two-component mixture described in section 6.3 is consistent with the picture outlined above. A fast component (mean rate $\sim 6 \times 10^{-2}\ d^{-1}$, $\sim 87\%$ of stars) accounts for the active flarer population, plausibly dominated by M-dwarfs. The slow component (average frequency $\sim 10^{-3}$, $\sim 13\%$ of stars) describes flares on stars with an effective temperature close to that of the Sun (Figure 14).

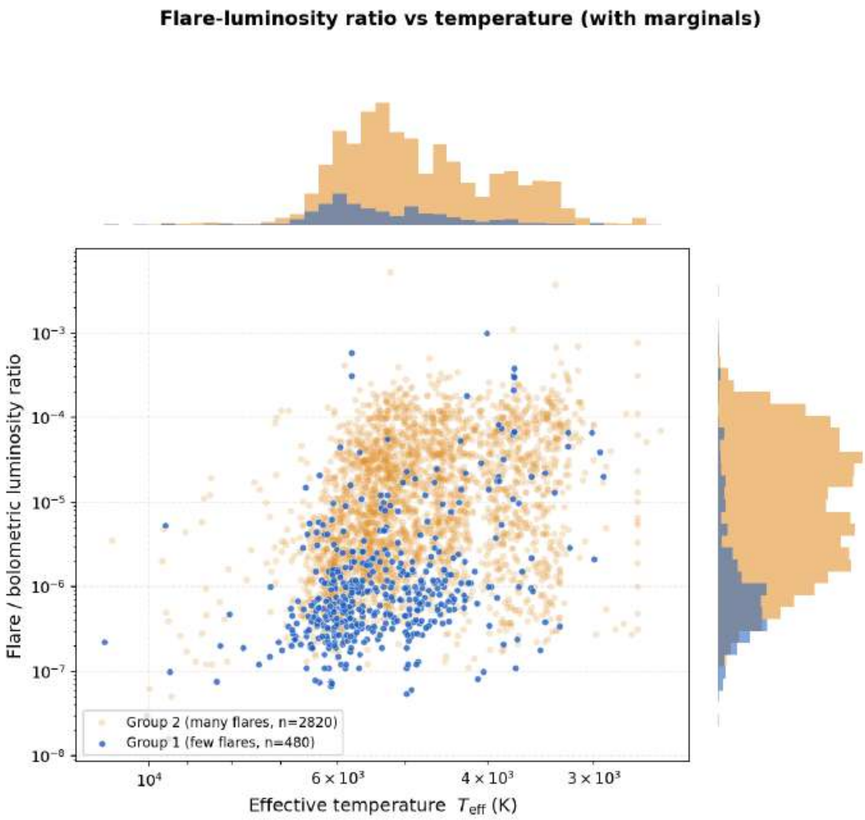

Figure 14: Flare-luminosity ratio vs temperature

The mixture decomposition reproduces the discovery curve dramatically better than the single Type III ($\Delta\mathrm{AIC} = +300$), and cures the negative ν_0 pathology. Its remaining weakness is in the flare-count tail at $k > 20$, where super-active stars with $\nu \gtrsim 0.2\ d^{-1}$ contribute and neither Pearson III component extends. This is the only piece of misspecification that the two-component mixture does not address.

7.4. Cross-validation by independent observables

The $R(t) = n_1(t)/n(t)$ analysis of Section 6.5 provides the most reliable of the available recovery tests. The two routes — through $S(t)$ requiring N_{tot}, through $R(t)$ requiring nothing beyond the raw catalog — give recovered $\varphi(\nu)$ that agree in the bulk to within a factor of 1.5. The structured pattern of residual disagreement is itself informative: it has exactly the shape expected when a single simple smoother is forced to model a bimodal distribution. Used together, the two observables would constrain the recovery much more tightly than either alone.

8. Conclusion

An improved and significantly extended pipeline/code is presented for reconstructing the flare rate distribution $\varphi(\nu)$ in a population of objects generating random flares.

The pipeline was used to determine the distribution of flare rate among flare stars within the Kepler telescope's field of view. The pipeline includes the MoM extended to the full Pearson family, the inverse-

doi: https://doi.org/10.52526/25792776-26.73.1-39

Laplace approach of Ambartsumian, the Pearson III mixture model, and a fully model-independent numerical inversion via non-Pearson smoothers. On synthetic data the methods agree at the percent level, but on the sample of flare stars from the Kepler field of view disagree in informative ways. The nature of these discrepancies reveals the structure of the underlying distribution: a smooth density curve with a peak shifted towards values of $\nu \sim 2 \times 10^{-3}\ d^{-1}$, with a long tail in the region of high ν values.

The most important methodological result is that three independent diagnostics (negative ν_0, parameter drift, model-free stability) converge on the same conclusion. Together they form a robust diagnostic chain that is much more informative than any single statistic.

The identity $m_1(t)/m_1(0) = n_1(t)/n(t)$ provides the cleanest possible observational realization of the Laplace-pair function — purely from the catalog, with no commitment to N_{tot}. The agreement between S-route and R-route recoveries provides the strongest possible cross-check available without ground truth.

Future work will extend the mixture to three components, use joint (S, R) fitting to tighten the low-ν shoulder, and apply the same pipeline to other flare catalogs (TESS, K2) where the observation geometry differs and the model-independent recovery can be tested across instruments. Given the statistical basis of the methods presented, it is to be hoped that they will also prove useful in other fields of natural science and statistics.

References

Akaike H., 1974, IEEE Transactions on Automatic Control, 19, 716

Akopian A. A., 2003, Astrophysics, 46, 58

Akopian A. A., Parsamian E. S., 2009, Astrophysics, 52, 322

Ambartsumian V. A., 1969, Stars, Nebulae, and Galaxies. Publishing House of the Armenian Academy of Sciences

Ambartsumian V. A., 1978, Astrophysics, 14, 209

Bohning D., Suppawattanabodee B., Kusolvisitkul W., Viwatwongkasem C., 2008, Journal of Statistical Planning and Inference, 138, 1017

Chao A., 1984, Scandinavian Journal of Statistics, 11, 265

Nelder J. A., Mead R., 1965, Computer Journal, 7, 308

Pearson K., 1895, Philosophical Transactions of the Royal Society of London Series A, 186, 343

Schwarz G., 1978, The Annals of Statistics, 6, 461

Talbot A., 1979, IMA Journal of Applied Mathematics, 23, 97

Yang H., Liu J., Qiao E., Zhang H., Gao Q., Zhang Y., 2019, The Astrophysical Journal Supplement Series, 241, 29

doi: https://doi.org/10.52526/25792776-26.73.1-39

Communications of BAO, Vol. 73, Issue 1, 2026, pp. 59-63

Satellite system of M31 and dark energy

H. A. Harutyunian * and A. A. Torosyan

Byurakan Astrophysical Observatory, 0213, Armenia

Abstract

The structural features of the Andromeda satellite galaxy system are examined. Their configuration clearly contradicts the assumption that they formed randomly from a uniform distribution of primordial matter. In contrast, we propose a scenario that emerges when the evolutionary role of dark energy is taken into account. The disintegration of a protogalactic baryonic clump of matter is proposed as the primary mechanism for the formation of all Local Group galaxies. M31, from which the Milky Way separated, was most likely the first of the two giant galaxies in the Local Group to form. This is supported by the fact that M31 is larger than our galaxy, the diameter of its satellite system is larger than that of the Milky Way, and the known flattened satellite structures of both galaxies are aligned parallel to the line connecting their parent galaxies. As a supporting argument, the blueshift of the spectra of Andromeda's satellites is shown to be inversely correlated with their luminosity.

Keywords: *Dark energy, Local Group of galaxies, Andromeda galaxy, satellite system: structural features, formation scenario.*

1. Introduction

In our previous work, we examined the blueshift of the neighboring galaxy M31. To this end, we used the results of analyses on the physical consequences of baryonic matter interacting with dark energy carriers. This approach is based on the following well-known observational data and laws of physics—the building blocks upon which the entire paradigm is built. The first building block is the acceleration of the expansion of the Universe and the introduction of the concept of dark energy into science. The second building block is the inevitable recognition of the interaction between the dark energy carrier and baryonic matter, which became the key to their discovery on cosmological scales. The third important link is the laws of thermodynamics, which govern energy exchange processes in interactions among various physical systems.

Since all baryonic objects, starting from baryons themselves and atomic nuclei and up to stars and galaxies, exist as a whole due to negative total energy, such interactions lead to the transfer of some non-zero amount of energy to baryonic objects. At the macro and mega levels of the cosmic hierarchy, this additional energy increases the kinetic energy of the corresponding system. This very effect is clearly seen in the universe's expansion behavior. In the microworld, it simply reduces the binding energy, increasing therefore the baryonic and nuclear masses. Mass growth at the nuclear level leads to the spectral blueshift for the corresponding energy terms. The statement formulated here and the linked predictions are based on the interpretation of physical laws. No laboratory experiment can reveal this effect if the process is slow and beyond the possibilities of modern measuring methods. However, cosmic distances and time intervals enable one to trace the predicted effects, if any.

It is easy to understand that the rate of the evolutionary change of baryonic matter depends on the ratio of dark energy to the object's maintenance energy. The higher this ratio, the more intensive the evolution process. In our view, the most significant result of the study of the rate of evolution is the conclusion that within a family of physically similar objects, the massive ones evolve more slowly. More precisely, the evolution rate is lower for more massive objects, provided that the average density is constant or at least decreases more slowly than the inverse square root of the mass. This estimate was obtained for spherical objects, but it holds to some accuracy for other configurations as well.

Previously, we compared the masses and sizes of our galaxy and M31 to show that M31 is twice the size of the Milky Way with nearly the same mass. This means, according to the criterion above, M31 is evolving

*hhayk@bao.sci.am, Corresponding author

doi: https://doi.org/10.52526/25792776-26.73.1-59

faster than our galaxy. Therefore, assuming these two galaxies formed simultaneously or resulted from the fragmentation of a parent object, we can conclude that M31 has advanced further in its evolutionary history than our galaxy. M31's longer evolutionary path is also supported by its lower activity, lower rate of star formation, and nova explosions. The physical mechanism presented here explains the blueshift of M31 without involving the Doppler effect and the galaxy's movement toward us. In this paper, we study the satellite system of the Andromeda galaxy to find additional facts backing our concept.

2. The structural features of the Local Group of galaxies.

The bulk of the Local Group of galaxies is concentrated in its two main members, the Milky Way and M31. Traditionally, this group, like other groups and galaxies, is believed to have formed by successive mergers of dwarf galaxies formed immediately after the Big Bang. The observed blueshift in M31's spectrum is interpreted as its motion toward our galaxy, with an inevitable future collision that will form a single supermassive galaxy that will engulf all dwarf galaxies, sooner or later.

However, studies show (Harutyunian, 2024) that dark energy radically changes the adopted interpretation. And here, one circumstance comes to the forefront, one that is almost always neglected for some unknown reason. This circumstance is that the carrier of dark energy, whatever it is, interacts with baryonic matter. It is precisely the discovery of Corollary A that, since dark energy is purely positive, during such interactions, baryonic structures, which have negative total energy at all hierarchical levels, gain a non-zero amount of energy. Moreover, since the interaction is continuous and energy is cumulative, it accumulates in these structures over time.

It is obvious, from a general physical point of view, that injecting excess energy into any equilibrium baryonic structures renders them nonequilibrium. Adding positive energy to the energy balance of a given structure primarily reduces its binding energy. Gravitational systems, including clusters of galaxies and planetary systems, must expand. At the level of baryons and atomic nuclei, a decrease in binding energy reduces the mass defect and increases the mass. The transformation occurring in the microworld ultimately manifests itself as an increase in the mass of all baryonic objects and the entire baryonic universe. The increase in mass and decrease in binding energy ultimately require energy release by ejecting clumps of matter and/or dividing the object with excess energy into pieces. A similar process continues for each decaying part.

Research shows that the satellites of both our Galaxy and the Andromeda Galaxy are not randomly distributed in space, contrary to predictions of the prevailing cosmological theories. Their distribution is highly anisotropic, forming ordered structures. In both cases, dwarf galaxies orbit their parent galaxies synchronously within thin disks (Pawlowski, 2018). A strictly anisotropic distribution of satellites was first discovered in our Galaxy in mid 70s of the last century (Kunkel & Demers, 1976, Lynden-Bell, 1976).

The first attempt to model the Milky Way's satellite system using cosmological models was made based on the then-known positions of 11 satellites (Kroupa et al., 2005). The authors concluded that the satellite system is strictly aligned in a narrow plane oriented nearly perpendicular to the Milky Way's disk. After considering the positions of all known satellites, the authors rejected with 99.5 percent confidence the hypothesis that the satellite positions could be derived from an isotropic distribution.

The mentioned detailed analysis of the spatial satellites of the Milky Way showed that these galaxies are better understood as precursors of the so-called dark matter configurations (Kroupa et al., 2005). As model calculations show, such well-defined, extensive, and long-lived thin satellite planes are extremely unlikely in standard cosmological simulations of cold dark matter. That is, the authors believe that they cannot be considered dwarf galaxies of cosmological origin, in which dark matter dominates. Moreover, studies of the spatial distribution of all known satellites, including the newly revealed fainter ones, again confirmed a flat distribution (Metz et al., 2007, Pawlowski et al., 2012).

In the paper (Ibata et al., 2013), the authors have concluded that a subgroup of Andromeda's satellites, comprising approximately 50 percent of the entire population, forms a flat configuration (99.998 percent significance). The diameter of this formation is approximately 400 kpc, and the thickness is no more than 14.1 kpc (99 percent confidence level). The radial velocities of these satellites have the same direction of rotation relative to their parent galaxy. Remarkably, the revealed plane has a unique orientation relative to the Milky Way. It (approximately) includes the pole of our Galaxy's disk, as well as the Milky Way's position vector relative to Andromeda. Figuratively speaking, it is extremely thin, almost perpendicular to the Milky Way's disk, and extends precisely in its direction.

doi: https://doi.org/10.52526/25792776-26.73.1-59

A recent study (Conn et al., 2013) examined the spatial structure of the M31 satellite system. Using a sample of 27 M31 satellites and M31 itself, they concluded that the satellite distribution, when considered as a whole, is no flatter than would be expected from a random distribution of equal sizes. However, the disk consisting of 15 satellites turned out to be very significant and strikingly thin, with a root-mean-square thickness of only 12.3 kpc. This disk is oriented approximately edge-on to the Milky Way. It turned out that this disk is also roughly orthogonal to the disk-shaped structure in the Milky Way satellite system and closely corresponds to the giant stellar stream of M31.

Analysis of the observed asymmetry in the spatial distribution of M31 satellites shows that it is significantly greater than would be expected from a random distribution. Moreover, 20 of the 27 satellites appear to be on the Milky Way side. This remarkable asymmetry is most pronounced in the subset of satellites that form a thin disk.

Since the entire scientific methodology of modern cosmology and cosmogony is built on two well-known hypotheses: the Kant-Laplace concept of the formation of baryon structures and Lemaitre's idea of the primeval atom (dubbed the Big Bang thanks to Fred Hoyle's sarcasm), the interpretation of the formation of any cosmic configuration is inevitably based on them. It is this approach that leads to many paradoxes when considering real cosmic structures and their coexistence at different eras of cosmic history. Each JWST discovery, for example, dating back to the early stages of the universe's evolution, necessitates introducing some new "free parameters" to reconcile prevailing concepts with observational surprises.

We observe the same situation in relation to the aforementioned disks and their orientations. There is no doubt that the random formation of such "coordinated" kinematic structures from independently generated fragments within the halos of two massive galaxies is extremely unlikely. It requires a specifically developed scenario. Such structures can form if they are already encoded in the properties of the material they are composed of, which previously had been united within a single body with a strict internal structure.

In a previous paper (Harutyunian & Torosyan, 2024), we demonstrated that observational data on the physical parameters of M31 are consistent with the hypothesis of baryonic matter evolution under the influence of dark energy. The most significant conclusion was that M31 may actually exhibit a Doppler redshift relative to the Milky Way due to its removal, and the observed blueshift in its spectrum may be the result of an evolutionary effect superimposed on the Doppler effect. This could occur if the baryonic matter in our neighboring galaxy has undergone a longer evolution path than that of our galaxy.

Since M31 is approximately 2.5 million light-years away, we see the evolutionary state of its baryonic matter at that distance. On the other hand, according to Hubble's law, at that distance it should have had a recession velocity of approximately 50 km/sec. Although we believe this value may be reduced, it is nevertheless clear that, in that case, for the observed velocity of -122 km/sec, M31's evolutionary blueshift should be at least -170 km/sec. Considering also that the evolutionary shift per million years is approximately -2 km/sec (see Harutyunian, 2021), it turns out that in terms of the evolution of baryonic matter, M31 is 85 million years ahead of our galaxy. This is a relatively small value compared to the ages of M31 and the Milky Way, but its "fingerprints" are nevertheless clearly visible in the spectrum of the neighboring galaxy.

3. Correlation between satellites' stellar magnitudes and their blueshifts.

As noted in the previous paragraph, within the framework of the considered paradigm of the evolution of baryonic matter and the formation of cosmic structures under the influence of dark energy, any group of objects is formed as a result of the decay of a clot of matter, which is a proto-object of a higher hierarchical class. This proposal diametrically contrasts with the generally accepted scenario of object formation through mergers at all levels, beginning with the synthesis of heavy atomic nuclei through fusion, stars, and planets—due to the compression of gas and dust clouds—and galaxies through merging and cannibalism. The decay of baryonic clumps is a consistent process at all hierarchical levels of the universe. As a result of this decay, an object of a higher hierarchical class can form objects of its own class and lower classes. Moreover, the distribution of the decay products across classes is governed by the parent object's structural features.

The above, if correct, means that statistically less massive objects are either the same age as more massive ones or younger. This means that their evolutionary path is either the same length as that of massive objects or shorter. However, on the other hand, the rate of evolution is greater for less massive objects since evolution is more difficult at larger values of the following parameter introduced as a measure

doi: https://doi.org/10.52526/25792776-26.73.1-59

of stability (MoF, see, for example, (Harutyunian, 2024):

$$\eta \sim \left(M\rho^2\right)^{2/3} \sim \left(\frac{M}{R}\right)^2, \tag{1}$$

where M, ρ and R are mass, density, and radius of an object. Evidently, the MoF gets larger with mass if the mass of an object grows faster than its radius.

Let's apply the above-mentioned to the system of the Andromeda galaxy. We previously showed that interaction with a dark energy carrier increases the nuclear mass of atoms. Therefore, one of the most easily detectable evolutionary changes should be a blueshift of the object's spectrum, according to the Rydberg relation:

$$\frac{1}{\lambda_{mn}} = RyZ^2\left(\frac{1}{m^2} - \frac{1}{n^2}\right) \tag{2}$$

where

$$Ry = \frac{\mu e^4}{8\varepsilon_0^2 h^3 c} \tag{3}$$

is the Rydberg constant and $\mu$is the derived mass of the atomic nuclei and electron. The remaining designations are also generally accepted.

Since, according to relation (1), low-mass galaxies should evolve faster than more massive ones, this effect should be more pronounced for them. However, it should be taken into account that, within this paradigm, satellites form much later than their host galaxies, which, for a host galaxy much more massive than its satellite, provides sufficient time for evolution. However, even in this case, given the enormous difference between masses, we expect the effect to be statistically visible in our small sample. That is, we expected a statistically significant gradient of increasing blueshift with decreasing luminosity (mass) of the galaxies in our sample.

For our statistical analysis, we use the richest data on the galaxies of the Local Group, which are presented in the paper published one and a half decades ago (McConnachie, 2012). The data pertain to all galaxies in the Local Group, 33 of which are designated as true members of the M31 family, including the Andromeda Galaxy itself. Of these galaxies, only 22 have the required parameters—absolute magnitudes and galactocentric velocities. Namely, these galaxies were used. We first directly calculated the correlation coefficient between these parameters without any preliminary sample processing. A simple calculation yielded a value of -0.44 for this coefficient, which, as expected, is negative but cannot be considered sufficiently convincing. When M31 is excluded from the sample, the desired coefficient increases up to -0.5.

Clearly, there may be a spread in the satellites' ages, which makes it difficult to detect the underlying trend, if any. Therefore, our next step was to average the magnitudes and corresponding velocities over intervals of one magnitude. This immediately revealed a more pronounced correlation. In the first case, when the parent galaxy is taken into account, the correlation coefficient amounts to -0.64. In the second case, it increases to -0.83, which indicates an unconditional correlation. Moreover, the dispersion of velocities increases for the faintest satellites. In the context of the concept we are considering, this means that their evolutionary paths are of completely different lengths, or, in other words, they are of completely different ages.

It is noteworthy that the correlation we obtained here repeats the one we had found earlier for the Virgo and Fornax clusters of galaxies (Harutyunian et al., 2019). The analogous analyses for the mentioned clusters have given -0.90 and -0.64, respectively. Interestingly, the correlation coefficient for the mentioned clusters becomes much more significant when calculated only for galaxies with velocities below the cluster's average. It has a very intriguing physical meaning that follows from the applied physical mechanism. The fact that some regularity, which was found for clusters with statistically significant samples of objects, is sharply exhibited in a much smaller sample speaks in favor of the regularity's universal nature.

4. Conclusion and perspectives.

We continue studies of the manifestation of baryonic matter evolution using observational data of objects and systems of various hierarchical levels of the Universe. The Andromeda galaxy satellite system is a baryonic structure, possessing several features unexpected from the traditional viewpoint. This makes this system a suitable "laboratory" for testing theoretical predictions and hypotheses. Many recently discovered structural features pose complex challenges for researchers and are considered unique due to the lack of

doi: https://doi.org/10.52526/25792776-26.73.1-59

analogs. They will remain so until other similar structural features are discovered, definitively demonstrating their natural existence within the new paradigm of baryon structure formation.

This paper analyzes two features of the Andromeda Galaxy's satellite system. The first has been studied in detail by many researchers. This feature is the flat structure of the satellite system, which is oriented toward the Milky Way. Moreover, most of the satellites are located on the side of our galaxy relative to M31. Clearly, a random distribution of satellites in circumgalactic space cannot explain such a low-entropy structure. Therefore, the researchers who discovered and are studying this still unique structure are developing various intricate scenarios for interpreting it within the framework of traditional extragalactic cosmogony.

Our approach to the formation and evolution of cosmic structures is quite different from the prevailing hypothesis. It is based on observational data and a consistent application of the laws of modern physics. This approach inevitably leads to the conclusion that, at all hierarchical levels of the universe, baryonic structures interact with the carrier of dark energy, thereby continuously receiving energy, which makes these structures unstable and simultaneously increases their mass. This approach returns us to Ambartsumian's cosmogonic concept (Ambartsumian, 1961), where the main direction of evolution is decay and expansion. This concept has been largely forgotten today for two reasons. The first is the impossibility of the stable existence of superdense matter of the required mass. The second concerns the source of the required energy. In the summary of the Santa Barbara Conference on the "Instability of Systems of Galaxies", devoted to Ambartsumian's hypothesis, it is mentioned: "The first is the mechanism whereby such tremendous amounts of energy can be released - energy equivalent roughly to the total annihilation of a globular cluster, or to the radiation from a million stars over their whole lifetimes" (Neyman et al., 1961). Now, 65 years later, the storage of this energy is widely known. That is dark energy.

Within our paradigm, the entire Local Group of galaxies has been formed as a result of the disintegration of a single clump of baryonic matter and the successive ejections of secondary objects (satellites) from the two most massive objects (M31 and our Galaxy). We reached this conclusion (Harutyunian & Torosyan, 2024) by hypothesizing that the blueshift of M31's spectrum is not Doppler-induced but is evolutionary. This would imply that the Andromeda Nebula has undergone a longer evolutionary path than our Galaxy. The data presented in the previous paper, at least, do not contradict our concept.

Here, we further develop our idea, arguing that the two main galaxies of the Local Group resulted from the disintegration of a proto-object into two parts. A more probable scenario is that the clump of matter from which the Milky Way formed was ejected from the core of M31. The following facts support this assertion. Not only is M31 twice the size of our galaxy, but the diameter of its satellite system is also at least twice that of the Milky Way. Therefore, it's not surprising that both planes of these systems are aligned with the line connecting the nuclei of the two galaxies. We will discuss this in more detail in a future paper.

References

Ambartsumian V. A., 1961, Astron. J. , 66, 536

Conn A. R., et al., 2013, Astrophys. J. , 766, 120

Harutyunian H. A., 2021, Astrophysics, 64, 435

Harutyunian H. A., 2024, Astrophysics, 67, 506

Harutyunian H. A., Torosyan A. A., 2024, Communications of the Byurakan Astrophysical Observatory, 71, 68

Harutyunian H. A., Grigoryan A. M., Khasawneh A., 2019, Communications of the Byurakan Astrophysical Observatory, 66, 25

Ibata R. A., et al., 2013, Nature. , 493, 62

Kroupa P., Theis C., Boily C. M., 2005, Astron. Astrophys. , 431, 517

Kunkel W. E., Demers S., 1976, in Dickens R. J., Perry J. E., Smith F. G., King I. R., eds, Vol. 182, The Galaxy and the Local Group. p. 241

Lynden-Bell D., 1976, Mon. Not. R. Astron. Soc. , 174, 695

McConnachie A. W., 2012, Astron. J. , 144, 4

Metz M., Kroupa P., Jerjen H., 2007, Mon. Not. R. Astron. Soc. , 374, 1125

Neyman J., Page T., Scott E., 1961, Astron. J. , 66, 633

Pawlowski M. S., 2018, Modern Physics Letters A, 33, 1830004

Pawlowski M. S., Pflamm-Altenburg J., Kroupa P., 2012, Mon. Not. R. Astron. Soc. , 423, 1109

doi: https://doi.org/10.52526/25792776-26.73.1-59

Low-mass M-type eclipsing variable star found in the third catalogue of DFBS late-type stars

G. R. Kostandyan*[1], K. K. Gigoyan†[1], and K. S. Gigoyan‡[1]

[1]INAS RA V. Ambartsumian Byurakan Astrophysical Observatory (BAO), Byurakan 0213, Aragatzotn Province, Armenia

Abstract

Based on the Transiting Exoplanet Survey Satellite (TESS) phased light curve, we confirm the eclipsing type variability nature for low-mass M-dwarf DFBS J095623.83+064801.9, as presented in the third version of the DFBS (Digitized First Byurakan Survey) catalog of late-type stars (LTSs). We present the most important physical parameters of this object from the Gaia Data Release 3 (DR3) catalog and TESS catalogs.

Keywords: *Variables: Algol-type eclipsing variables: Gaia and TESS data*

1. Introduction

Variable stars are classified into several broad classes: pulsating, eclipsing, rotating, eruptive, cataclysmic, and others. Each class of variable stars is divided into several subclasses. In more detail, the improved system of variability classification is presented by the authors of the "General Catalogue of Variable Stars" (GCVS) (Samus' et al., 2017). An overview of variable stars in general, the techniques for discovering and studying them, and a description of the main types are also presented in John Percy's book (Percy, 2007) and in papers by Drake et al. (2014, 2017)

There are three basic classes of eclipsing variables, based solely on the overall light curve shape: EA (Algol), EB (Beta Lyrae), and EW (W Ursae Majoris) types. Eclipsing binaries include contact, semi-detached, and detached systems.

In recent years, there have been many searches of eclipsing variable stars. Large-scale surveys significantly increased the number of eclipsing variable stars. A catalog of 1292 low-mass, short period eclipsing binaries is presented by Oddo et al. (2026). A large number of eclipsing binary candidates based on Gaia Data Release 3 (DR3) are presented by Mowlavi et al. (2023) and collaborators. An updated catalog of 4680 northern eclipsing binaries with Algol-type light curve morphology was presented by Papageorgiou et al. (2018). Data for more than 40,000 eclipsing binary candidates identified by the ASAS-SN, were also presented by Rowan et al. (2022). Xiong et al. (2023) published data for 56 eclipsing binaries selected from the LAMOST Medium-Resolution Survey (MRS). Data for 4584 TESS (Transiting Exoplanet Survey Satellite, Ricker et al., 2014, 2015) eclipsing binary stars were published by (Prša et al., 2022). The catalog of eclipsing binaries found in the Entire Kepler data was reported by David et al. (2016). Many papers are devoted to the study of individual eclipsing variables.

As part of the M dwarf research program, we analyzed phase-dependent light curves for all DFBS M dwarfs (Gigoyan et al., 2025), using the Pre-search of Data Conditioning Simple Aperture Photometry (PDCSAP) at the Mikulski Archive for Space Telescopes (MAST). While analyzing the TESS data, we discovered an Algol-type light curve of the M dwarf DFBS J095623.83+ 064801.9.

This paper is organized as follows. Section 2 presents the TESS light curve for the M dwarf DFBS J095623.83+064801.9. Section 3 presents Gaia DR3 low-resolution spectra for this object. Section 4 considers photometric data and important physical parameters. We discuss the results obtained for this object and provide concluding remarks in Section 5.

*kostandyan@bao.sci.am, Corresponding author

†kgigoyan@bao.sci.am

‡karengigoyan@bao.sci.am

doi: https://doi.org/10.52526/25792776-26.73.1-64

Table 1. TESS Observations of DFBS J095623.83+064801.9 from the MAST

DFBS Number	TESS target name	Data of observations	Exposure length (sec.)
J095623.83+064801.9	TIC 377129640	2021-11-07	120

2. TESS light curve.

The Transiting Exoplanet Survey Satellite is NASA‘s ongoing Astrophysics Explorer Mission, designed to detect exoplanets around the nearest M dwarfs, which are ideal for follow-up observations and further characterization. TESS was launched on April 18, 2018, and its prime mission (PM) ran from July 26, 2018, to July 4, 2020. TESS observed nearly 73% of the sky across 26 observing “Sectors” during its two-year PM. TESS monitored bright stars with a 2 minute short cadence and provided full-frame images every 30 minutes. The wide red bandpass of the TESS cameras (600-1000 nm) enables TESS to detect Earth and super-Earth-sized exoplanets transiting M dwarfs.

Table 1 presents TESS observational data for M dwarf DFBS J095623.83+064801.9 from the MAST. We downloaded the PDCSAP light curves for these stars from the MAST (on-line access available at https://mast.stsci.edu/portal/Mashup/Clients/Mast/Portal.html/) using the lightcurve package (Barentsen et al., 2019).

Figure 1 shows the TESS SAP (Simple Aperture Photometry) light curve for object DFBS J095623.83+064801.9. We estimate the orbital period P = 0.762631 d for this object, using Box Least Squares (BLS) (Kovács et al., 2002).

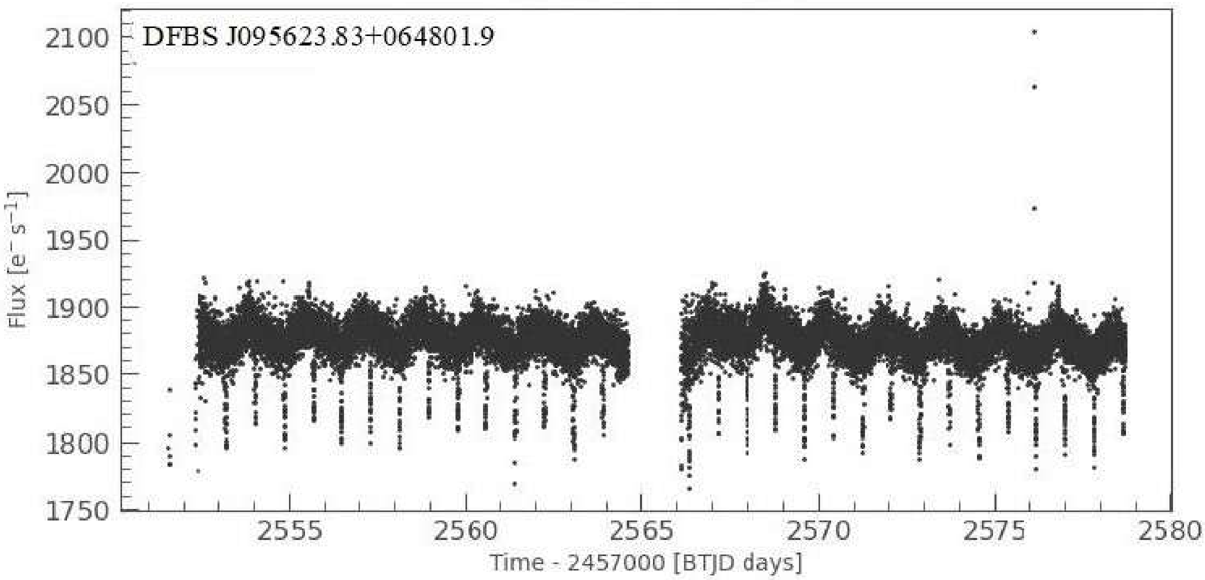

Figure 1. DFBS lr spectral shape (A) and Gaia DR3 BP/RP spectra (B) for new confirmed M giant DFBS J035851.35+700544.9. G mag =12.679, T_eff = 3269 K, TIC Catalogue number is 85987534.

3. Gaia DR3 spectra.

In Figure 2 we present Gaia Data Release 3 (Gaia Collaboration, Vallenari et al., 2023) low-resolution spectra (De Angeli et al., 2023a) (CDS VizieR Catalog I/355/spectra) for M dwarf DFBS J095623.93+064801.9.

4. Photometric data. Important stellar parameters: Gaia DR3 and TESS Input Catalog Data.

Gaia DR3 (Gaia Collaboration, Vallenari et al., 2023) provides high-precision astrometry, three-band photometry, radial velocities, effective temperatures, and information on numerous astrophysical parameters

doi: https://doi.org/10.52526/25792776-26.73.1-64

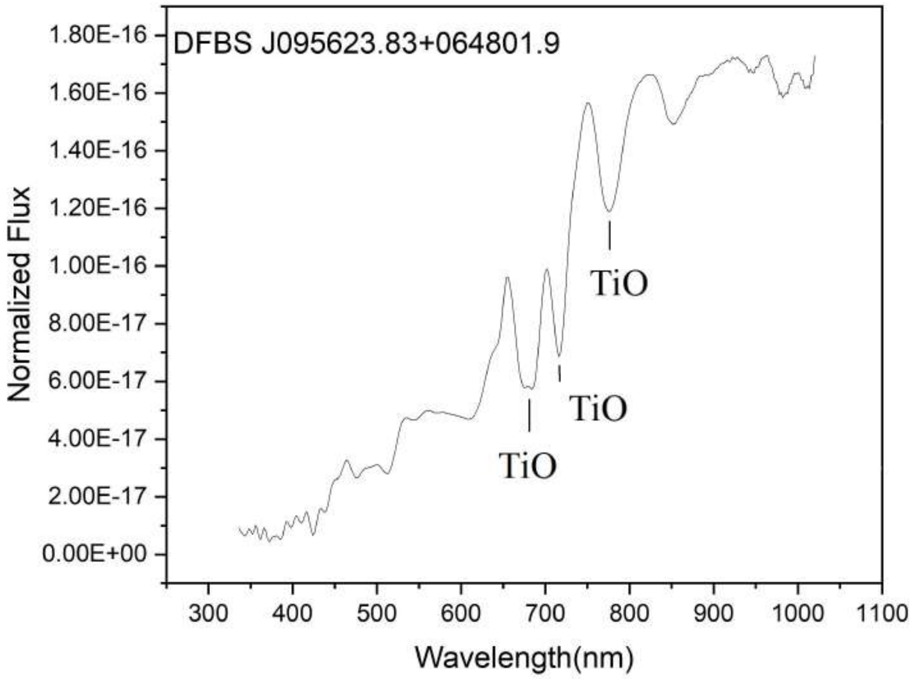

Figure 2. Gaia DR3 BP/RP lr spectra of M dwarf DFBS J095623.83+064801.9. The absorption broadbands of the TiO molecule in the range 600-800 nm are indicated. Spectral subclass can be estimated as M2-M3.

Table 2. Some Important Gaia DR3 Data for DFBS M Dwarfs

DFBS Number	Gaia DR3 Name	G-mag	BP mag	BP-RP mag	R (pc)
J095623.83+064801.9	3850549957388322816	13.643	15.023	2.536	87.11

for approximately 1.8 billion sources brighter than G = 21.0 magnitude (CDS Vizier Catalog I/355/gaiadr3). Table 2 provides important Gaia DR3 data for DFBS J095623.83+064801.9. We provide distance information from Gaia EDR3 by Bailer-Jones et al. (2021).

The Gaia G-band absolute magnitudes can be estimated as M(G) = + 8.942 for DFBS J095623.83+064801.9. This is typical for M2 – M3 dwarfs (Carmo et al., 2020, Gaia Collaboration et al., 2018) (see the website at https://www.pas.rochester.edu/∼emamajek/spt/ for more details).

Table 3 also includes other important parameters, such as effective temperature, stellar mass, and radii in solar units, for three DFBS M dwarfs from the TESS Input Catalog (Version 8.2, TIC V8.2 (Stassun et al., 2019), CDS Vizier Catalog IV/39/tic82).

5. Summary And Future Works

Eclipsing binary stars are very important in stellar astrophysics for a variety of reasons. The discovery and characterization of Algol-type eclipsing binaries provide an opportunity to improve our understanding of the structure of low-mass stars (defined as M ¡ 0.8 M (Carmo et al., 2020, Kroupa et al., 2013, Stassun et al., 2019). In this work, we present important physical parameters for Algol-type eclipsing binary DFBS J095623.83+064801.9, confirmed as low-mass M dwarfs in the third DFBS catalog of late-type stars. The

Table 3. TIC Catalog Important physical parameters for M dwarf DFBS J095623.83+064801.9

DFBS Number	Teff (K)	Radius (M_{Sun})	Mass (M_{Sun})	Luminosity (M_{Sun})
J095623.83+064801.9	3413	0.543	0.539	0.03609

doi: https://doi.org/10.52526/25792776-26.73.1-64

subtype is M2-M3.

In the future, high-spatial-resolution CCD imaging and speckle interferometry will allow us to study the nature of the companions around these objects in more detail.

Acknowledgements

We thank the anonymous referee for constructive comments that greatly improved the quality of this manuscript. This paper includes data collected by the TESS mission. This work was supported by the Victor Ambartsumian Research Grant (VA Grant 2025-2026) from the National Academy of Sciences of the Republic of Armenia (NAS RA). This research has made use of the SIMBAD database, operated at CDS, Strasbourg, France. This work has made use of data from the European Space Agency (ESA) mission Gaia (https://www.cosmos.esa.int/gaia/), processed by the Gaia Data Processing and Analysis Consortium (DPAC; https://www.cosmos.esa.int/web/gaia/dpac/consortium). This research has made use of the NASA/IPAC Extragalactic Database (https://ned.ipac.caltec.edu). This publication makes use of data products from the Two Micron All Sky Survey, which is a joint project of the University of Massachusetts and the Infrared Processing and Analysis Center/California Institute of Technology, funded by the National Aeronautics and Space Administration and the National Science Foundation.

References

Bailer-Jones C. A. L., Rybizki J., Fouesneau M., Demleitner M., Andrae R., 2021, Astron. J. , 161, 147

Barentsen G., et al., 2019, KeplerGO/lightkurve: Lightkurve v1.6.0, doi:10.5281/zenodo.3579358

Brown A. G. A., et al., 2021, Astron. Astrophys. , 649, A1

Carmo A., Ferreira Lopes C. E., Papageorgiou A., Jablonski F. J., Rodrigues C. V., Drake A. J., Cross N. J. G., Catelan M., 2020, Mon. Not. R. Astron. Soc. , 498, 2833

Carrasco J. M., et al., 2021, Astron. Astrophys. , 652, A86

David T. J., et al., 2016, Astron. J. , 151, 112

De Angeli F., et al., 2023a, Astron. Astrophys. , 674, A2

De Angeli F., et al., 2023b, Astron. Astrophys. , 674, A2

Drake A. J., et al., 2014, Mon. Not. R. Astron. Soc. , 441, 1186

Drake A. J., et al., 2017, Mon. Not. R. Astron. Soc. , 469, 3688

Gaia Collaboration et al., 2018, Astron. Astrophys. , 616, A10

Gigoyan K. S., Mickaelian A. M., 2012, Mon. Not. R. Astron. Soc. , 419, 3346

Gigoyan K. S., Mickaelian A. M., Kostandyan G. R., 2019, Mon. Not. R. Astron. Soc. , 489, 2030

Gigoyan K. S., et al., 2021, Astrophysics, 64, 20

Gigoyan K. S., Sarkissian A., Kostandyan G. R., Gigoyan K. K., Meftah M., 2025, Mon. Not. R. Astron. Soc. , 539, 223

Kovács G., Zucker S., Mazeh T., 2002, Astron. Astrophys. , 391, 369

Kroupa P., Weidner C., Pflamm-Altenburg J., Thies I., Dabringhausen J., Marks M., Maschberger T., 2013, in Oswalt T. D., Gilmore G., eds, , Vol. 5, Planets, Stars and Stellar Systems. Volume 5: Galactic Structure and Stellar Populations. p. 115, doi:10.1007/978-94-007-5612-0˙4

Mowlavi N., et al., 2023, Astron. Astrophys. , 674, A16

Oddo D., Dragomir D., Powell B. P., Kostov V. B., Han T., 2026, Astrophys. J. , 996, 82

Papageorgiou A., Catelan M., Christopoulou P.-E., Drake A. J., Djorgovski S. G., 2018, Astrophys. J. Suppl. Ser. , 238, 4

Percy J. R., 2007, Understanding Variable Stars

Prusti T., et al., 2016, Astron. Astrophys. , 595, A1

Prša A., et al., 2022, Astrophys. J. Suppl. Ser. , 258, 16

Ricker G. R., et al., 2014, in Oschmann Jacobus M. J., Clampin M., Fazio G. G., MacEwen H. A., eds, Society of Photo-Optical Instrumentation Engineers (SPIE) Conference Series Vol. 9143, Space Telescopes and Instrumentation 2014: Optical, Infrared, and Millimeter Wave. p. 914320 (arXiv:1406.0151), doi:10.1117/12.2063489

Ricker G. R., et al., 2015, Journal of Astronomical Telescopes, Instruments, and Systems, 1, 014003

Rowan D. M., et al., 2022, Mon. Not. R. Astron. Soc. , 517, 2190

Samus' N. N., Kazarovets E. V., Durlevich O. V., Kireeva N. N., Pastukhova E. N., 2017, Astronomy Reports, 61, 80

Stassun K. G., et al., 2019, Astron. J. , 158, 138

Vallenari A., et al., 2023, Astron. Astrophys. , 674, A1

Xiong J., et al., 2023, Astron. J. , 165, 30

doi: https://doi.org/10.52526/25792776-26.73.1-64

Pulsars and Millisecond Pulsars IV: From Subroutine Validation to Population Synthesis in NBODY6++GPU

Maria Rah*[1,3], Rainer Spurzem[2,3,4], Areg Mickaelian[1], and Francesco Flammini Dotti[5,6,7]

[1]NAS RA V.Ambartsumian Byurakan Astrophysical Observatory (BAO), Byurakan, Armenia
[2]Kavli Institute for Astronomy and Astrophysics, Peking University, Beijing, China
[3]The Silk Road Project at the National Astronomical Observatory, Chinese Academy of Sciences, Beijing, China
[4]Astronomisches Rechen-Institut, ZAH, University of Heidelberg, Heidelberg, Germany
[5]Department of Physics, New York University Abu Dhabi, Abu Dhabi, UAE
[6]Center for Astrophysics and Space Science (CASS), New York University Abu Dhabi, Abu Dhabi, UAE
[7]Dipartimento di Fisica, Sapienza, Università di Roma, Rome, Italy

Abstract

Direct N-body codes such as NBODY6++GPU can solve the dynamical evolution of globular clusters with great accuracy, yet historically uses simple models: spin period, spin-down rate, and magnetic field strength are never updated once a neutron star forms. Earlier works in this series identified this gap, proposed a seven-scenario framework (S1–S7) covering the full range of pulsar evolutionary channels, and demonstrated the absence of pulsar tracking in an existing cluster simulation. Here we bring together three subsequent stages that solve this gap. A pulsar evolution subroutine was first tested in isolation across all seven scenarios, with two independently written codes agreeing to better than 0.1% over more than two thousand compared values, and reproducing accretion-driven spin-up for the first time within this framework. The validated framework was then embedded directly into NBODY6++GPU, and test integrations spanning timescales from under a Megayear up to a Gigayear show that the resulting period-period derivative distribution already resembles the pattern seen in real globular cluster pulsar populations. Finally, an early production test followed ten neutron stars self-consistently through the integrated code over roughly 28 Myr, uncovering that most of them pass through at least one episode of backward evolution, a behaviour that only becomes visible when spin parameters are sampled at every simulation step rather than inferred afterwards. Taken together, these results show that pulsar physics can now evolve as an integral part of cluster dynamics rather than a separate bookkeeping exercise, setting the stage for a full production run at $N = 250{,}000$.

Keywords: *Pulsars, Millisecond Pulsars, N-body simulations, NBODY6++GPU, Spin Evolution, Magnetic Fields, Globular Clusters.*

1. Introduction

Globular clusters are unusually efficient factories for millisecond pulsars: their dense cores drive close stellar encounters that assemble and disrupt binaries far more often than in the Galactic field, and the resulting mass transfer episodes can spin a neutron star up from a period of seconds to a few milliseconds (Alpar et al., 1982, Bhattacharya & van den Heuvel, 1991). Several hundred of such pulsars are now known across the Galactic globular cluster system (Bagchi et al., 2025), with new discoveries continuing to emerge from targeted surveys of individual clusters (Chen et al., 2023, Dai et al., 2020, Padmanabh et al., 2024). Direct N-body integrators are, in principle, the ideal tool for following this process, since they track every stellar encounter, binary formation event, and mass-transfer episode self-consistently. In practice, however, codes such as NBODY6++GPU (Wang et al., 2015, 2016) treat neutron stars as inert masses after formation: nothing in the code records how their spin or magnetic field responds to the dynamical history that the star actually experiences. Earlier papers in this series laid the groundwork for closing this gap. A statistical census of observed cluster pulsars exposed how little of their diversity current simulations could explain (Rah et al., 2024); a classification of neutron star evolution into seven physically distinct scenarios, spanning isolated spin-down, wide binaries, accretion-driven recycling, and dynamical encounters, provided

*mariarah.astro@bao.sci.am, Corresponding author

doi: https://doi.org/10.52526/25792776-26.73.1-68

a concrete target for implementation (Rah et al., 2025a); and a worked example within an existing cluster simulation confirmed that no trace of this physics was present in the code output at all (Rah et al., 2025b).

The present paper reports on three further steps that, taken together, turn this framework into a working part of NBODY6++GPU. The first step (Rah et al., 2025a) tested the seven scenarios as isolated field stars, checking each one against an analytical solution or an observationally motivated benchmark and cross-checking two independently written implementations against each other. The second step carried the validated prescriptions into the full N-body code itself, adding the bookkeeping needed to track spin and field evolution for every neutron star at every timestep, and confirming that short and long test runs produce spin-down and recycling behaviour consistent with the standalone results. The third step used the newly integrated code to follow an early population of neutron stars all the way through a short cluster simulation, providing the first direct look at how spin parameters respond to a live dynamical environment rather than an idealised one. Section 2 summarises the standalone validation and its main quantitative results. Section 3 describes the integration into NBODY6++GPU and the qualitative agreement it produces with the observed pulsar population. Section 4 presents the first population-tracking results, including a diagram that traces ten neutron stars through their full observable history. Section 5 closes with the implications of these results for the forthcoming full-scale production run.

2. Standalone Validation of the Pulsar Subroutine

Before any pulsar physics is allowed to run inside a live cluster simulation, the codes implementing it must first be shown to behave correctly on their own. The subroutine developed for this purpose was tested outside NBODY6++GPU (Wang et al., 2015, 2016) entirely, under seven monitored configurations chosen to isolate the seven specific physical processes intended: an isolated young pulsar spinning down under magnetic braking (S1); an isolated millisecond pulsar evolving under a very weak torque (S2); a low-mass X-ray binary in which accretion competes with and eventually overcomes magnetic braking (S3); a millisecond pulsar embedded in the kind of dense, high-velocity-dispersion environment expected in a cluster core (S4); a millisecond pulsar with a wide, dynamically inert companion (S5); and two compact-binary configurations, neutron star–neutron star and neutron star–black hole, evolved under dipole spin-down alone while their orbital coupling is left for future work (S6, S7), consistent with the rich phenomenology of binary neutron star dynamics documented in globular clusters (Sigurdsson & Phinney, 1995). Table 1 summarises the initial conditions and dominant physics of each case.

Table 1. The seven standalone test scenarios used to validate the pulsar subroutine, with representative initial conditions and the physical process each one isolates.

ID	Configuration	B_0 (G)	Dominant physics
S1	Young isolated pulsar	1×10^{12}	Dipole spin-down + field decay
S2	Isolated MSP	5×10^{8}	Weak-torque spin-down
S3	Accreting LMXB	3×10^{8}	Accretion-driven spin-up
S4	MSP in a dense core	3×10^{8}	Environmental torque (subdominant)
S5	MSP with a wide companion	4×10^{8}	Negligible tidal coupling
S6	NS–NS compact binary	5×10^{11}	Dipole spin-down; GW deferred
S7	NS–BH compact binary	5×10^{11}	Dipole spin-down; GW deferred

Each scenario was evolved for 100 Myr in two entirely independent codes, and the two were compared point by point at every Myr across the magnetic field, period, and period derivative. Across all seven scenarios (101 timesteps and three physical quantities per scenario) this comparison spans more than two thousand matched values, and the two implementations agree to within a few parts in ten thousand for the period and period derivative, and to within one part in a million for the magnetic field, well inside the precision expected of two independently coded integrators.

Beyond this numerical cross-check, each scenario was also compared against an independent physical expectation. S1 reproduces the closed-form dipole spin-down solution (Ostriker & Gunn, 1969) to the same sub-percent precision once a redundant field-decay term, of the kind discussed for accreting and isolated neutron stars alike (Konar & Bhattacharya, 1997, Pons et al., 2009), identified during testing was removed. S2 settles into a characteristic spin-down age near one Gyr, matching the population of millisecond pulsars seen in 47 Tucanae (Baumgardt & Vasiliev, 2021, Lorimer & Kramer, 2004). S4 and S5 confirm that neither a dense cluster environment (Verbunt & Freire, 2014) nor a wide, tidally coupled binary companion (Bildsten & Cutler, 1992) measurably perturbs the dipole-dominated evolution, with environmental torques

doi: https://doi.org/10.52526/25792776-26.73.1-68

contributing a few hundredths of a percent of the total at most. S6 and S7 spin down identically under the currently implemented physics, as expected, since their gravitational-wave (Peters & Mathews, 1963) and tidal terms are intentionally deferred rather than active.

The most demanding test is S3, where the subroutine must not merely avoid breaking but actively reproduce a qualitatively different behaviour: sustained spin-up rather than spin-down. Early attempts produced spin-up on a timescale of about a year, seven orders of magnitude faster than physically reasonable, tracing back to an accretion-torque coefficient that had not been brought into a consistent system of units. Once corrected to match the standard Ghosh & Lamb prescription (Ghosh & Lamb, 1979), the same scenario settles into a spin-up episode lasting roughly a hundred Myr and asymptotes to a period near the neutron-star breakup limit of one millisecond, with the accretion torque exceeding the magnetic braking torque by a factor of order ten throughout the active phase, consistent with the timescales expected for recycling in low-mass X-ray binaries (Tauris & Savonije, 1999). This is, to our knowledge, the first time this transition has been reproduced from first-principles torque balance within this validation framework, and it establishes that the subroutine is capable of driving a neutron star through the full recycling process rather than only slowing one down.

Taken together, the seven scenarios show that the framework reproduce every qualitatively distinct regime it is meant to capture, agrees with independent analytical and observational benchmarks wherever those exist, and does so identically across two separately written implementations. This is the baseline of confidence required before the same physics is allowed to run, unsupervised, inside a full NBODY6++GPU cluster integration (Spurzem & Kamlah, 2023), which is the subject of the next section.

3. Integration into NBODY6++GPU

Passing standalone validation is a necessary but not sufficient condition: the same physics must then survive being embedded inside a live, million-particle-capable code (Kamlah et al., 2022) without breaking either the subroutine or the surrounding integrator. Other groups have pursued parallel efforts to embed simplified pulsar spin-up prescriptions into direct N-body and related codes (Song et al., 2025, Ye et al., 2019). Here, this required adding a dedicated data block to NBODY6++GPU to carry each neutron star's spin period, magnetic field, birth conditions, and current scenario alongside the usual dynamical variables, and hooking the subroutine into the points in the code where a neutron star forms or enters a mass-transferring binary, following the existing stellar and binary evolution prescriptions already built into the code (Hurley et al., 2000, 2002). The framework now records a full spin history, position, velocity, and scenario label for every tracked object at each simulation output step, giving direct access to quantities that were previously invisible to the code entirely.

Two regimes were used to check that the integration preserves the standalone behaviour once the subroutine is exposed to a real dynamical environment rather than fixed test conditions. Short integrations of order a hundred Myr reproduce the spin-down tracks expected for young and weakly evolving pulsars, with wide binaries (separations of order a few AU) and moderate cluster core densities ($\rho_c \sim 10^5\ M_\odot\,\mathrm{pc}^{-3}$, Rah et al. 2025b) leaving spin evolution essentially unchanged, exactly as found in the standalone tests. Longer integrations extending toward a Gyr allow the recycling channel to operate for the first time inside a dynamical simulation, together with dynamical exchanges and, in a small number of cases, compact-binary coalescence (Chattopadhyay et al., 2020). The resulting period-period derivative distribution, built up self-consistently from the live cluster rather than imposed by hand, already falls into the same regions of parameter space as the observed young-pulsar and millisecond-pulsar populations in real globular clusters, without any parameter having been tuned to make this happen. The integrated code is now stable up to particle numbers well beyond what is needed for the next stage of this project (Kamlah et al., 2022, Spurzem & Kamlah, 2023), clearing the way for the population-tracking results presented in Section 4.

4. First Population-Tracking Results

With validation complete at both the standalone and the integrated level, an early test run provides the first direct look at how the subroutine behaves for a real, if small, population of neutron stars evolving inside a live cluster. The simulation used $N = 5{,}000$ particles with a core radius $r_c \approx 0.47$ pc and tidal radius $r_t \approx 52$ pc, placing it firmly in the globular cluster regime, with stellar masses drawn from a standard initial mass function (Kroupa, 2001), and was evolved for a total of 28.13 Myr of physical time, during

doi: https://doi.org/10.52526/25792776-26.73.1-68

which ten neutron stars appeared and were tracked continuously, together accounting for several hundred recorded output steps. Only three of the seven scenarios (Rah et al., 2025a) were triggered under these conditions: isolated spin-down (S1), wide-binary evolution (S5), and impulsive merger-or-kick events (S7). The remaining four require either a longer integration time, higher stellar densities than reached in this test model, or specific companion types not yet present; that this fourth and only fully successful iteration of the integrated test series (N = 5,000, 28 Myr), markedly shorter and smaller than the standalone 100 Myr scenario tests of Section 2, cannot yet supply; this is expected, and is exactly what the forthcoming production run at $N = 250{,}000$ is designed to remedy.

The ten objects fall naturally into seven distinct evolutionary sequences depending on which scenarios they pass through and in what order (Table 2). At one extreme, three neutron stars never leave the isolated spin-down regime over their much shorter individual observable windows (roughly 0.6 Myr for one object and under 0.1 Myr for the other two, since they appear only late in the run); at the other, one object cycles through five separate scenario transitions within only a few Myr, moving from isolation into a binary, through an impulsive encounter, back into a binary, and finally settling again, a stochastic sequence of encounters rather than a designed outcome. The full set of trajectories spans spin periods from about five to a hundred milliseconds and surface fields from roughly 1.7×10^8 to 10^9 G, placing every tracked object in the recycled or mildly recycled regime and, crucially, above the pulsar death line throughout the simulation: none of the ten objects is ever driven into a state where radio emission would be expected to switch off.

Table 2. The seven scenario sequences identified among the ten neutron stars of the test run, ordered from the most dynamically active to the most quiescent.

Group	Scenario sequence	Objects
1	S1→S5→S7→S5→S1→S5	1
2	S1→S5→S7→S5 (or →S1)	2
3	S1→S5→S7→S1	1
4	S1→S5	1
5	S1→S7→S5→S7→S1	1
6	S7→S1	1
7	S1 only	3

The most notable outcome of this test is not any single trajectory but a pattern that cuts across most of them: a majority of the ten neutron stars pass through at least one episode that moves them *backward* along the usual recycling path rather than forward (Figure 1). In some cases this shows up directly in the spin parameters, as when a single impulsive encounter pushes an already partially recycled object back toward longer periods within one output step. In other cases it shows up as a reversion in scenario label itself, when a binary is disrupted and the neutron star returns permanently to isolated spin-down after only a brief accretion episode. In still other cases the assigned S-scenario label never changes at all, yet the underlying spin parameters jump abruptly in response to a dynamical encounter too weak to cross any classification threshold, a level of detail that would be invisible to any method that assigns spin evolution after the fact rather than tracking it at every timestep. None of this behaviour was anticipated when the scenarios were first defined, and it could only be found by sampling spin parameters as frequently as the dynamical simulation itself is sampled, which is precisely what the integration described in Section 3 makes possible for the first time.

5. Discussion and Conclusions

Across the three stages summarised here, pulsar physics has moved from an absent feature of NBODY6++GPU (Wang et al., 2015, 2016) to a working, tested component of it. The seven standalone scenarios established that the underlying physical prescriptions are correct and mutually consistent between two independently written codes; the integration into the full code showed that this correctness survives contact with a live, dynamically evolving cluster rather than only idealised test conditions; and the first population-tracking run demonstrated that ten neutron stars can be followed continuously through a real simulation, occupying exactly the recycled and mildly recycled region of parameter space expected for globular cluster pulsars and remaining active radio emitters throughout. Taken together, these results mean that a neutron star's spin and magnetic history are no longer a missing dimension of an N-body cluster simulation, but a quantity computed alongside its position and velocity at every timestep.

doi: https://doi.org/10.52526/25792776-26.73.1-68

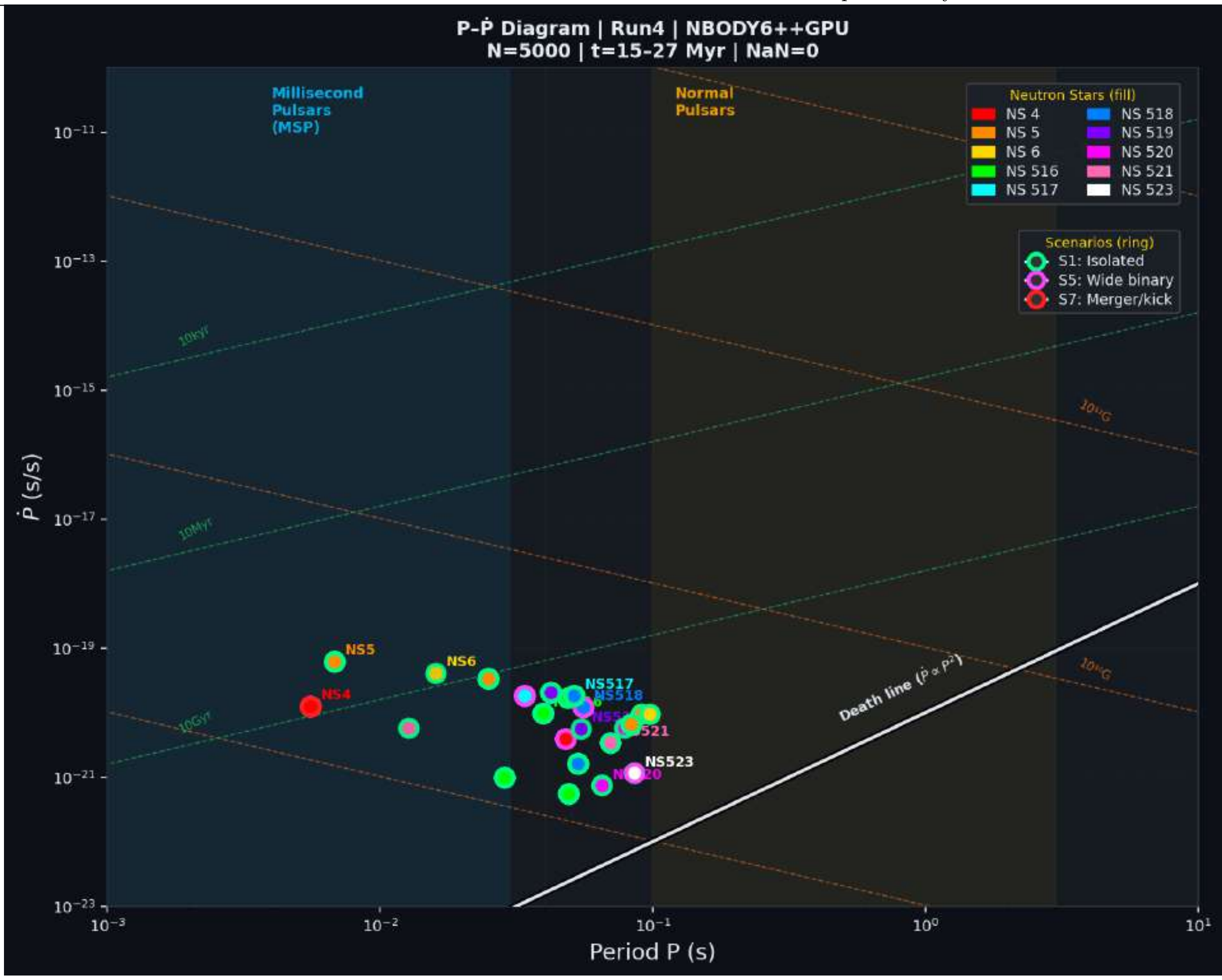

Figure 1. Period-period derivative diagram for all ten neutron stars tracked in the test run (N = 5,000, $t \approx$ 15–27 Myr). Each point is one recorded output step; fill colour identifies the neutron star and ring colour marks the active scenario at that step (S1: isolated spin-down; S5: wide binary; S7: merger or kick). Diagonal dashed lines show loci of constant characteristic age (green) and constant surface field (orange); the solid line is the pulsar death line. All ten objects remain in the recycled and mildly recycled regime throughout the simulation and stay above the death line at every tracked step, while several trajectories visibly double back on themselves, the direct graphical signature of the regression episodes described above.

The most unexpected outcome of this early test is not that the subroutine works, but what it reveals once it does: a majority of the tracked neutron stars pass through at least one episode in which they move backward along the usual recycling sequence, whether through a sudden change in spin parameters, a reversion to a simpler evolutionary state after a binary is disrupted, or a spin-parameter jump too small to register as a change in scenario at all. None of these behaviours were built into the subroutine by design; they emerge only because spin evolution is now sampled at the same cadence as the dynamical simulation itself, rather than reconstructed afterward from a coarser record. This suggests that some fraction of the isolated and partially recycled pulsars observed in real clusters may carry a disrupted or interrupted recycling history that a purely forward-evolving model would never produce, a possibility that only becomes visible through this kind of fully integrated tracking.

The natural next step is to repeat this exercise at a scale where all seven scenarios, not only three of them, have a realistic chance to occur. The present test used a comparatively small and short-lived cluster, which is why the accreting, tidally synchronised, and magnetar-like channels were never triggered; a longer, denser environment is needed to populate them. We are therefore preparing a production run at N = 250,000 particles extending to roughly 100 Myr of cluster evolution, an environment expected to be dense enough and long-lived enough for every one of the seven scenarios to appear and be tracked in full, and large enough to support a statistically meaningful comparison with the observed pulsar populations of real globular clusters. This production run will form the basis of the population-synthesis results that complete the next stage of this dissertation project.

doi: https://doi.org/10.52526/25792776-26.73.1-68

Acknowledgements

M.R. gratefully acknowledges the academic and financial support received from the Byurakan Astrophysical Observatory (BAO) throughout her Ph.D. studies, and the hospitality of the NAOC Silk Road Project.

References

Alpar M. A., Cheng A. F., Ruderman M. A., Shaham J., 1982, Nature, 300, 728

Bagchi M., et al., 2025, The Open Journal of Astrophysics, 8, 154251

Baumgardt H., Vasiliev E., 2021, Monthly Notices of the Royal Astronomical Society, 505, 5957

Bhattacharya D., van den Heuvel E. P. J., 1991, Physics Reports, 203, 1

Bildsten L., Cutler C., 1992, The Astrophysical Journal, 400, 175

Chattopadhyay D., Stevenson S., Hurley J. R., Rossi L. J., Flynn C., 2020, Monthly Notices of the Royal Astronomical Society, 494, 1587

Chen J., et al., 2023, The Astrophysical Journal, 948, 84

Dai S., Johnston S., Kerr M., Camilo F., Cameron A., Toomey L., Kumamoto H., 2020, The Astrophysical Journal Letters, 888, L18

Ghosh P., Lamb F. K., 1979, The Astrophysical Journal, 234, 296

Hurley J. R., Pols O. R., Tout C. A., 2000, Monthly Notices of the Royal Astronomical Society, 315, 543

Hurley J. R., Tout C. A., Pols O. R., 2002, Monthly Notices of the Royal Astronomical Society, 329, 897

Kamlah A. W. H., et al., 2022, Monthly Notices of the Royal Astronomical Society, 511, 4060

Konar S., Bhattacharya D., 1997, Monthly Notices of the Royal Astronomical Society, 284, 311

Kroupa P., 2001, Monthly Notices of the Royal Astronomical Society, 322, 231

Lorimer D. R., Kramer M., 2004, Handbook of Pulsar Astronomy. Vol. 4

Ostriker J. P., Gunn J. E., 1969, The Astrophysical Journal, 157, 1395

Padmanabh P. V., et al., 2024, Astronomy & Astrophysics, 686, A166

Peters P. C., Mathews J., 1963, Physical Review, 131, 435

Pons J. A., Miralles J. A., Geppert U., 2009, Astronomy & Astrophysics, 496, 207

Rah M., Mickaelian A., Flammini Dotti F., Spurzem R., 2024, Communications of the Byurakan Astrophysical Observatory, 71, 351

Rah M., Spurzem R., Flammini Dotti F., Mickaelian A., 2025a, Communications of the Byurakan Astrophysical Observatory, 72, 55

Rah M., Spurzem R., Flammini Dotti F., Mickaelian A., 2025b, Communications of the Byurakan Astrophysical Observatory, 72, 279

Sigurdsson S., Phinney E. S., 1995, The Astrophysical Journal Supplement Series, 99, 609

Song Y., Chattopadhyay D., Hurley J., Spurzem R., Dotti F. F., Wu K., 2025, Modelling Millisecond Pulsar Populations in Globular Clusters with NBODY6++GPU (arXiv:2511.08850), https://arxiv.org/abs/2511.08850

Spurzem R., Kamlah A., 2023, Living Reviews in Computational Astrophysics, 9, 3

Tauris T. M., Savonije G. J., 1999, Astronomy & Astrophysics, 350, 928

Verbunt F., Freire P. C. C., 2014, Astronomy & Astrophysics, 561, A11

Wang L., Spurzem R., Aarseth S., Nitadori K., Berczik P., Kouwenhoven M. B. N., Naab T., 2015, Monthly Notices of the Royal Astronomical Society, 450, 4070

Wang L., et al., 2016, Monthly Notices of the Royal Astronomical Society, 458, 1450

Ye C. S., Kremer K., Chatterjee S., Rodriguez C. L., Rasio F. A., 2019, The Astrophysical Journal, 877, 122

doi: https://doi.org/10.52526/25792776-26.73.1-68

Introduction

Editorial board *

NAS RA V. Ambartsumian Byurakan Astrophysical Observatory (BAO)

The International Conference Astronomical Heritage of the Middle East 2 (**AHME-2**) will take place from 6-10 October 2025 in the National Academy of Sciences (NAS) in Armenia. This will be the second such meeting; we had a very successful meeting, **AHME 2017**, with the participation of astronomers and many other specialists. This way, we make these meetings regular for BAO and Armenia, as Armenia is one of the cradles of Astronomical Heritage, and BAO hosts a UNESCO "Memory of the World" Documentary Heritage (Markarian Survey). We bring together astronomers and many other specialists from related fields. The Conference is devoted to the role of Astronomy in Culture and other fields of human activity, as well as to the development of these fields due to the knowledge obtained from the Universe. In the modern era, Astronomy is probably the field of science that plays a leading role in the formation and development of inter- and multi-disciplinary sciences. For a long time, Astrophysics has reached a high level of development; recently, new scientific disciplines have been created, such as Astrochemistry, Astrobiology, Planetary Science or Planetology ("Astrogeology"), Astroinformatics, and Astrolinguistics. Archaeoastronomy plays an important role in culture and in the heritage of nations, chronologies and calendars created on the basis of astronomical knowledge. Cultural Astronomy also plays an important role in the development of scientific (Astro) tourism and scientific journalism. The meeting is aimed at developing problems in astronomy-related interdisciplinary sciences in the countries of the European and Asian regions and at preparing a basis for further possible collaborations through presentations of available modern knowledge in various areas of culture by experts from different professions and through joint discussions.

Figure 1. *Left panel* - Celestial Maps of Gegham Mountain; *right panel - the ancient observatory of Karahunj.*

.

The history of Astronomy in Armenia goes back to ancient times. Since ancient times, Armenians have accumulated astronomical knowledge and left this heritage in the forms of rock art, ancient observatories, calendars and chronology, records of astronomical events, medieval sky maps, astronomical terms in the language, etc. Nowadays, Armenia is one of the more developed countries in an astronomical sense as well, though by terms of its economic level, Armenia is among the developing countries, and it is located in a region (Middle East) where efforts are needed to develop and promote Cultural Astronomy.

The following topics were covered at the meeting:

*combao@bao.am

- Review and discuss the Astronomical Heritage of the Middle East to summarize available data;
- Review and discuss individual items of Astronomical Heritage;
- Learn about related major current and upcoming projects and studies;
- Learn and discuss how Astronomical Heritage can change our understanding of history;
- Discuss access, data mining, analysis, visualization, etc., related to Astronomical Heritage;
- Discuss access, data mining, analysis, visualization, etc., related to Astronomical Heritage;
- Discuss the future of studies by joint efforts of Astronomers, Historians, Archaeologists, and other experts;
- Discuss and homogenize the presentation of available information on webpages, etc.

During the Conference, an Astronomical Festival (AstroFest-2025) will be organized on 8 October, where dozens of scientists, students, and others will visit BAO and meet scientists, writers, poets, composers, and artists.

This issue of BAO Communications presents the proceedings of the **AHME-2** meeting. All included articles have undergone a rigorous peer-review process.

Universe in Armenian Rock Art and Mythology

G. Vardumyan[1,2] and K. Tokhatyan*[1,2]

[1]NAS RA Institute of History
[2]Yerevan Brusov State University, Armenia

Abstract

The Universe, celestial bodies and luminaries, and the sky have been reflected in Armenian petroglyphic art and mythological conceptions since the earliest times. Throughout millennia, representations of the Universe, embodied in depictions of the Milky Way, the Sun, stars, and other celestial luminaries and bodies, have found vivid expressions in Armenian petroglyphs. Numerous rock carvings dating from the VII-III mill. BC, discovered on the slopes of the Aragats, Geghama, Vardenis, Syunik, and Vayots Dzor Mountain ranges, as well as at other sites throughout Armenia, depict solar, lunar, and astral motifs. The Universe found expression in Armenian rock carvings not only through depictions of celestial bodies but also through ritual scenes reflecting the veneration of higher supernatural powers.

Cults of gods and goddesses personifying the Sun and the Moon, planets of the solar system, and constellations, myths about the Milky Way, and many archeological artifacts, prove the high level of interpretation of the Universe in Ancient Armenian culture. Mythological representations of the Universe were further embodied in images of Patriarch Gods and in cosmogonic narratives connected with the Sun, the Moon, the Milky Way, and the stars. Over the millennia, a rich corpus of solar, lunar, and astral deities emerged within Armenian mythological thought, traces of which have been preserved in the Armenian epic “Sasna Tsrer”. Certain cosmological beliefs and mythological motifs have also survived in transformed forms within Armenian ethnographic traditions, remaining part of popular culture and folk belief up to the present day.

Keywords: *Armenia, Aratta, Ara, Aram, eponyms, Hayk, Movses Khorenatsi, mythology, rock art, patriarch, Urartu*

1. Introduction

Human interest in the celestial sphere evolved in response to the practical and symbolic significance of astronomical observations and developed through the perception of an interconnected relationship between cosmic phenomena and terrestrial life. From the earliest times, the people inhabiting the Armenian Highlands engraved images of the Sun, the Moon, stars, and constellations on rocks, as well as representations of the Milky Way, thereby expressing their cosmological perceptions and conceptions of the Universe. Solar disks with radiating rays, crescent moons, stars, and constellations, as well as stylized solar symbols and eternity signs, constitute a significant part of Armenian rock carvings.

Over time, these depictions came to include scenes reflecting cultic practices and rituals, attesting to the development of the mythological beliefs and cosmological concepts of our ancestors. Alongside the development of mythological thought, images of gods and goddesses embodying the Sun, the Moon, and the stars began to emerge, accompanied by beliefs and narratives concerning their origins and place within the cosmic order. Later, these cosmological and mythological conceptions were reflected in diverse spheres of Armenian culture, including the historical tradition of ethnogenesis, divine pantheons, cultic practices and rituals, ethnographic realities, temple architecture, and other manifestations of cultural heritage.

2. The Sun and celestial phenomena in rock art

The conceptual basis of Sun worship among the Armenians, as among many other ancient peoples, were rooted in the recognition of the indispensable role of solar light and heat in sustaining life. Such

*karen.tokhatyan@gmail.com, Corresponding author

doi: https://doi.org/10.52526/25792776-26.73.1-76

perceptions emerged during the earliest stages of human civilization and reflected an awareness of humanity's dependence on the Sun as the primary source of vital energy on Earth. Occupying a central place in Armenian spirituality and cultural consciousness, the Sun has found vivid expression in the symbolic language of rock art. Numerous carvings from the Geghama Mountains feature solar and luminous imagery, including representations of the solar disk with radiating rays and stylized depictions of the Sun in the form of the swastika (Fig. 1). In Armenian tradition, the swastika (kerkhach – "whirled cross") is perceived as an intermediary symbol linking the eternity sign and the cross.

Symbols of Eternity, rooted in the perception of the Sun as a manifestation of eternal cosmic order, are encountered on numerous monuments throughout India, Greece (including the Trojan cultural tradition), Italy, particularly on Etruscan ceramics, the Near East, the Caucasus, etc. (Khanzadyan et al., 1973). In the Armenian Highlands, the swastika functioned as a solar symbol and was associated with a supreme celestial deity identified with the Sun, the source of creation, light, and divine fire. The petroglyphic repertoire further includes numerous circular symbols of eternity adorned with revolving rays. Such motifs occur both independently and as constituent elements of more complex iconographic compositions.

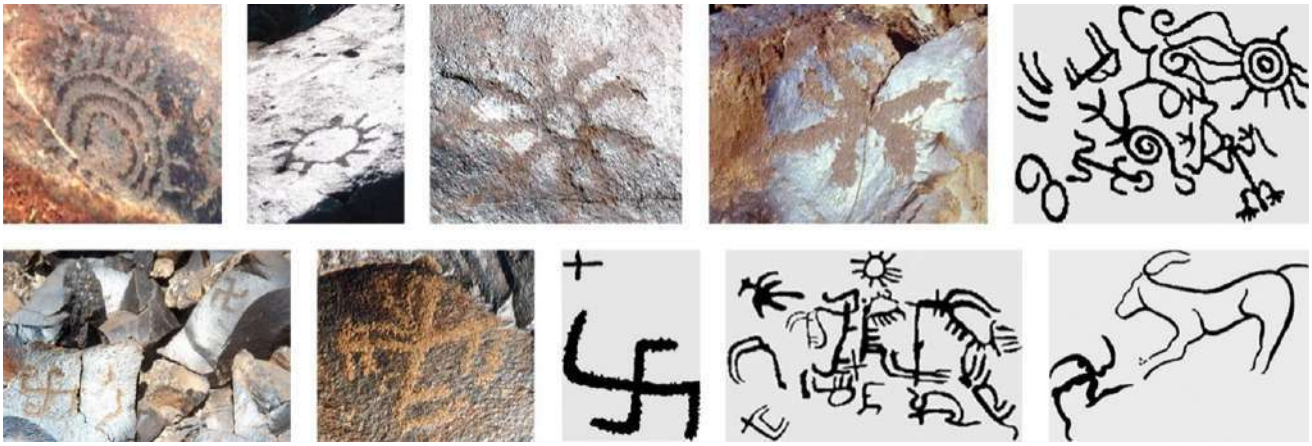

Figure 1: Petroglyphs: Sun, swastika, and stars in rock-carvings.

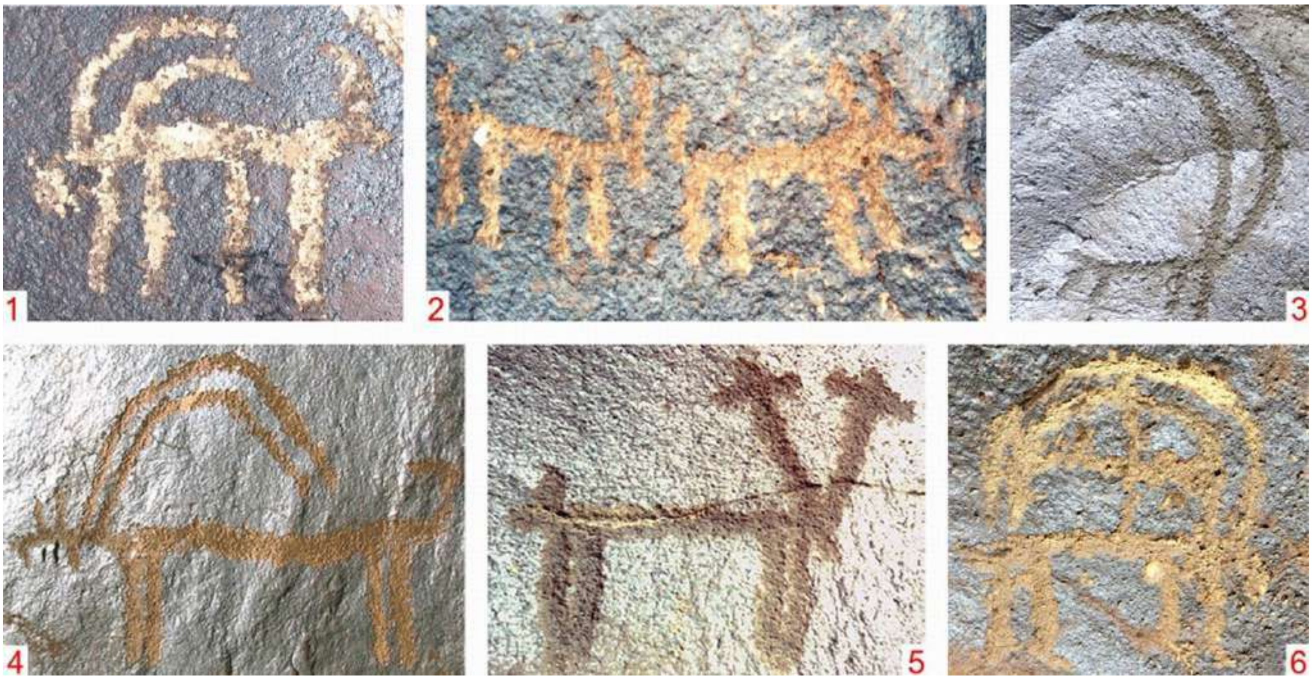

Figure 2: Petroglyphs: mountain goats (Geghama Mountains).

Among the Armenian petroglyphs, representations of mountain goats are particularly numerous and significant. These figures have often been interpreted as symbols of celestial luminous phenomena, especially lightning, which, in ancient Armenian cosmological conceptions, were associated with the dynamic power of the Sun (Fig. 2). Depictions of extraordinary goats — characterized by multiple limbs or horns — along

doi: https://doi.org/10.52526/25792776-26.73.1-76

with other mythical beings, frequently occur alongside zoomorphic and anthropomorphic images that have been interpreted as solar deities (Martirosyan, 1981, Martirosyan & Israelyan, 1971, Tokhatyan, 2025).

The rock art corpus further includes birds shown facing a solar disc or fire symbol, dragon, winged creatures with radiating appendages, winged horses, and other fantastic animals, reflecting a rich symbolic and mythological tradition connected with celestial phenomena.

Snake- and dragon-shaped motifs constitute another significant category within the corpus of Armenian petroglyphs. These representations have commonly been interpreted as symbolic expressions of celestial phenomena, including thunder, lightning, and rain, and are closely linked to ancient notions of the heavenly waters. As such, they appear to reflect a mythological worldview in which serpentine and dragon-like beings mediated the relationship between the celestial and terrestrial realms.

Closely connected with the veneration of thunder, lightning, and water are the so-called vishaps or vishapakars ("dragon stone"), distinctive megalithic monuments of the Armenian Highland, generally dated to the III–II mill. BC (Fig 3). Found exclusively within this region, they are typically situated near springs, lakes, irrigation systems, and other water sources. These monuments are predominantly fashioned in the shape of fish or bulls and are widely regarded as material expressions of ancient religious beliefs associated with water, fertility, and atmospheric phenomena (Bobokhyan et al., 2015).

Figure 3: Vishap stele.

The petroglyphs also contain a variety of cultic and ritual scenes that provide insight into ancient religious beliefs and practices. There are numerous cultic representations that testify to the worship of celestial and cosmic powers (Fig. 4–5). Such scenes reflect a worldview in which supernatural forces associated with the heavens were regarded as fundamental determinants of both natural processes and human existence and daily life.

3. Constellations and Milky Way in rock art

A unique place among the Armenian rock engravings is held by depictions of constellations, among which the representations of Aquila and Gemini in the ancient astronomical complex of Sevsar (near Lake Sevan, at an altitude of 2,670 m) are particularly significant (Fig. 6). These images testify to a certain level of development of astronomical thought in ancient Armenia, further confirmed by the celestial observation sites of Metsamor (IV-II mill. BC, 35 km southwest of Yerevan) and Zoratsqar (IV-I mill. BC, 3 km north of

doi: https://doi.org/10.52526/25792776-26.73.1-76

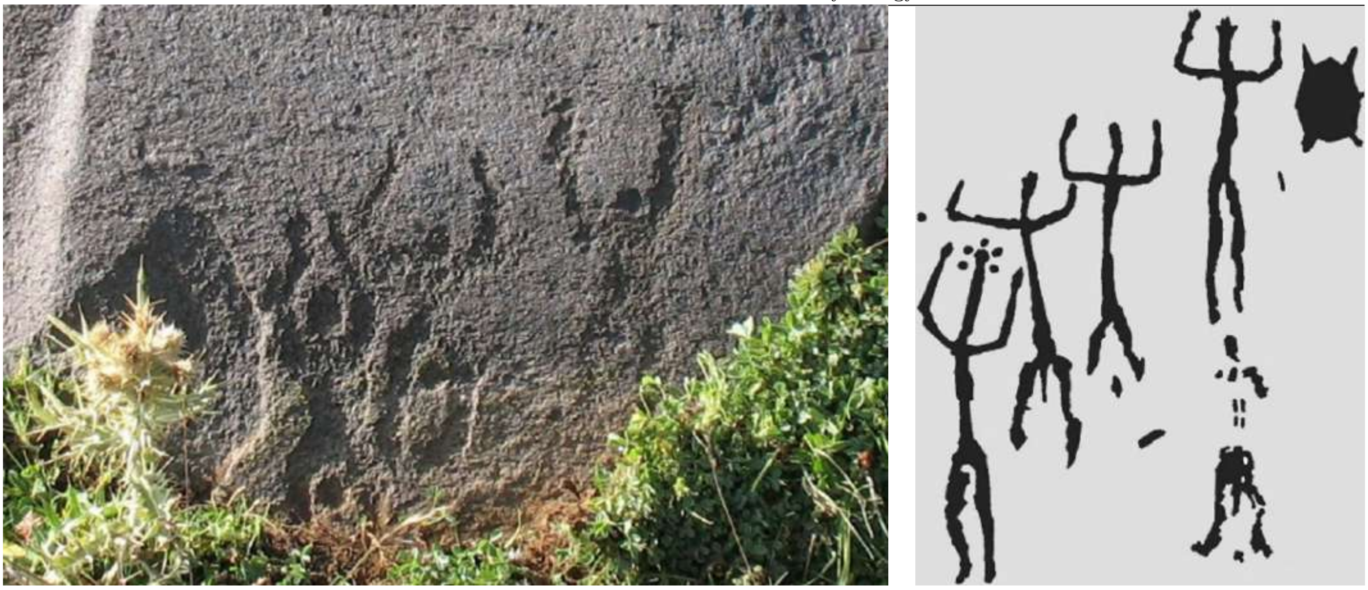

Figure 4–5: Petroglyphs: worship of Heaven (Geghama and Syunik Mountains).

Sisian, Syunik Province). The zodiac constellations were later discussed by Anania Shirakatsi (VII Ce.), an eminent Armenian philosopher and scholar whose extant works cover such fields as mathematics, astronomy, geography, calendar, and related disciplines (Anania Shirakatsi, 1940).

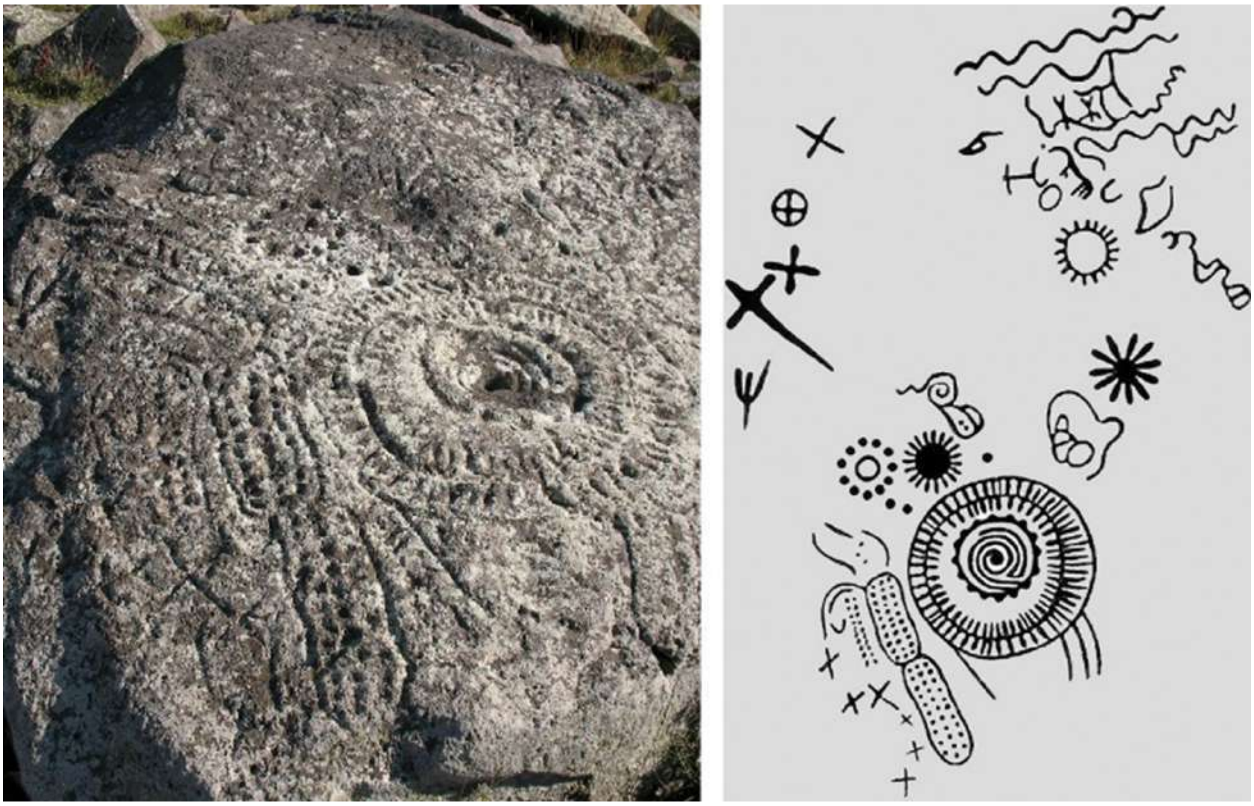

Figure 6: Petroglyps: constellations Aquilla, Gemini (Sevsar), Milky Way.

The Milky Way also found a reflection in Armenian cosmological thought (Fig. 7–8). Anania Shirakatsi, in his "Cosmology and Calendar", has offered a remarkably accurate scientific explanation of the phenomenon, describing the Milky Way *"as a vast multitude of distant, faintly shining stars"* (Anania Shirakatsi, 1940).

4. Moon in rock-carvings

The Moon is also represented in the petroglyphs, generally occupying the upper part of many compositions. Of particular interest is one example that appears to illustrate the phases of the Moon.

doi: https://doi.org/10.52526/25792776-26.73.1-76

Figure 7–8: Petroglyph: Milky Way (Sevsar); Moon phases (Geghama Mountains).

Armenian petroglyphic art is likewise rich in depictions associated with lightning and thunder spirits. These powerful atmospheric phenomena were a frequent and awe-inspiring presence in the lives of ancient peoples, and it was therefore natural for them to become embodied in the figures of thunder-wielding deities within various religious traditions, such as Zeus, Aramazd, Indra, etc.

The symbolic repertoire of Armenian rock art further reflects a wide range of religious and mythological concepts, including the veneration of motherhood and fertility, the cult of ancestors, the worship of deities and cultural heroes, beliefs associated with divine twins and benevolent spirits, as well as conceptions of time, calendrical cycles, and the cosmic order. These themes collectively attest to the richness of the spiritual world and cosmological imagination of ancient Armenia.

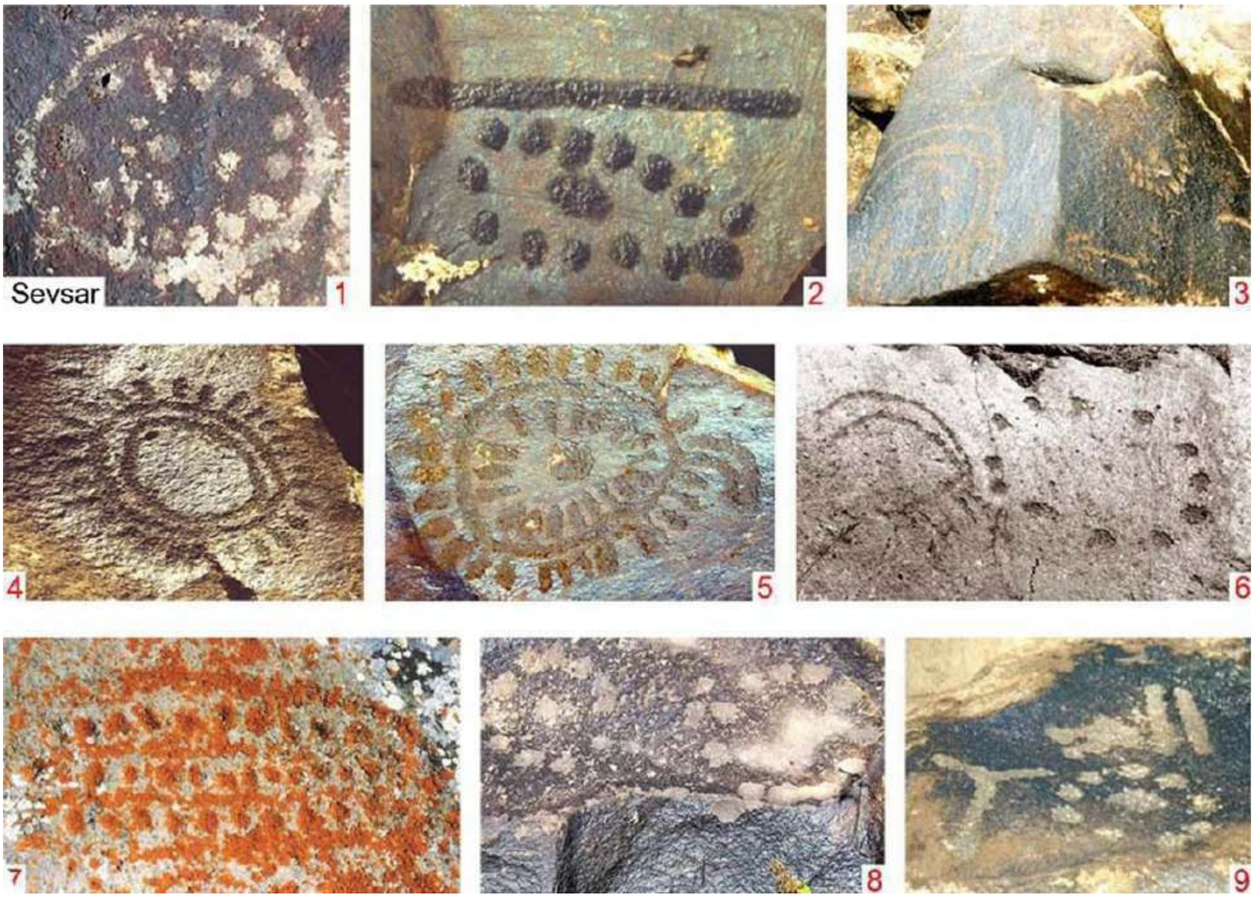

Figure 9: Calendars in petroglyphs (Geghama Mountains, Sevsar).

doi: https://doi.org/10.52526/25792776-26.73.1-76

5. Calendars in rock art

Time and its constituent units of measurement, which form the basis of calendrical reckoning, are intimately linked to ancient cosmological conceptions. Since the measurement of time was inseparable from observations of celestial phenomena, calendrical concepts occupied an important place in ancient cosmological thought. Numerous petroglyphs preserve representations of temporal cycles and their units of reckoning, attesting to the close relationship between astronomical observation, the perception of cosmic order, and the development of early calendrical systems. This relationship is reflected in numerous petroglyphic representations, where symbols associated with temporal cycles and celestial movements appear to embody early understandings of the structure and order of the Universe. There are a number of 12-month years, 31-day months, and 364-day annual calendars in petroglyphs (Fig. 9). Anania Shirakatsi has also addressed the calendar and the computation of time, distinguishing between the different dimensions of celestial and terrestrial time (Anania Shirakatsi, 1940).

6. Patriarch god Hayk – constellation Orion

Alongside the evidence of petroglyphs, ancient Armenian conceptions of the celestial and cosmic order and their relationship to human existence were reflected in mythological traditions and embodied in the images and attributes of the deities (Vardumyan, 2020).

The earliest significant connection between the Universe and Armenian mythology can be traced to the formative stages of Armenian ethnogenesis. This tradition exhibits features of the so-called *historization* of myth and *mythologization* of history, whereby historical memory is preserved and transmitted through mythic narratives.

Movses Khorenatsi, the Father of Armenian historiography (V Ce.), writes about Haykids and their heroic deeds in his "History of Armenia". These narratives are associated with the **Haykazuni** dynasty, regarded in Armenian tradition as the legendary founders of Armenia and the prefathers of the Armenian people. The earliest and most prominent among them was Hayk, the legendary archer and patriarch of the Armenian nation, depicted as a mighty and invincible hunter armed with a broad bow and long arrows. According to tradition, Patriarch Hayk led a struggle against the tyrannical Babylonian ruler Bel, defeated him in battle, and, following this celebrated victory, established the land of Hayk – **Hayq**, the ancestral homeland of the Armenians. Armenian historical tradition further links the ethnonym **Hay** and the country name **Hayastan** – the self-designations by which Armenians and their homeland are known to this day, to the patriarch Hayk, who was revered as both an epic hero and a deified ancestral figure – progenitor god. And from that time on *"our country is called Hayk' after the name of our ancestor Hayk"* (Movses Khorenatsi, 1978).

The archer motif and the swastika symbol may have been perceived as identical or functionally equivalent representations of a celestial shooter. In Armenian astral tradition, the constellation of Hayk, identified with Orion, is situated in relation to the constellation of Taurus in a manner corresponding to the mythological narrative. This alignment may be interpreted as iconographic evidence of the cult of Patriarch Hayk and the veneration of the celestial constellation bearing his name (Fig. 10).

7. Patriarch solar gods: Aram and Ara

The Armenian words for the Sun – Arev, Aregak – are traditionally considered to derive from the root *Ar (Areg or Aregnazan* is the name of the solar hero in Armenian fairy tales, preserving ancient motifs within the corpus of Armenian folk tradition).

Numerous Armenian names and terms have likewise been associated with this root, foremost among them the name of Aram, the second patriarch and eponymous ancestor of the Armenians. In his History of Armenia, Movses Khorenatsi recounts the legend of Aram, who, like Hayk, wages successful campaigns against foreign enemies. He expands the borders of the country in all directions and becomes so powerful and renowned that *"by his name all races call our land: like the Greeks, Armenia, and the Persians and Syrians, Armenik'"* (Movses Khorenatsi, 1978). According to this historical tradition, it was after Aram that neighboring peoples came to designate the land as Armenia and its inhabitants as Armenians.

In Armenian tradition, the root Ar is also linked to the name of the sacred mountain Ararat. The highest peak of the Armenian Highlands – Mount Ararat (5165 m) – revered by Armenians and all Christians alike,

doi: https://doi.org/10.52526/25792776-26.73.1-76

Figure 10: Patriarch Hayk: sculpture in Yerevan; photo of Orion constellation.

is identified in biblical tradition as the mountain upon which Noah's Ark came to rest after the Deluge: *"On the seventeenth day of the seventh month, the ark came to rest on the mountains of Ararat"* (Bible, Genesis, 84).

Earlier Mesopotamian flood traditions likewise associate the salvation of humankind with the Armenian Highlands. In Sumerian epic literature of the early III mill. BC, the land of Armenia is identified as Aratta, a distant and prosperous country whose inhabitants are portrayed as valiant warriors. According to these traditions, they are described as inhabitants of the Land of Sacred Rites *"Those who stood in the midst of the flood, when the waters swept away everything"* - a passage that has been interpreted as preserving memories of an ancient deluge and the survival of humanity upon the mountains of Ararat (Kramer, 1952).

Figure 11: Mountains Hatis, Araler, Aragats.

The names of the mountains Aragats and Araler (Fig. 11) are traditionally associated with the name

doi: https://doi.org/10.52526/25792776-26.73.1-76

of the dying and resurrecting god Ara. Movses Khorenatsi also writes about one of Aram's descendants, Ara the Handsome, King of Armenia, who rejected the love of "dissolute and lascivious" Shamiram, queen of Assyria, and declined her offer to ascend the Assyrian throne. She became "exceedingly angry" and attacked Armenia with war, during which Ara was killed. In the original version of the legend, Ara was reborn (as Egyptian Osiris, Phrygian Attis, Greek Adonis, etc.) Ara's legend indicates the importance of the worship of dying and rising deities as mythic personifications of sunrise and sunset, as well as the hibernation of nature in winter and awakening in spring. Ara does not accept Shamiram's passionate love and remains faithful to his country and queen Nuard (Movses Khorenatsi, 1978), with whom they constitute the male (solar) and female (lunar) beginnings in Armenian mythology. Mount Aragats, the highest peak in present-day Armenia, is regarded in Armenian folklore as the throne of Ara, where he was believed to reside following his resurrection. Mount Araler, whose silhouette resembles that of a reclining human figure, has been interpreted in popular belief as the body of the slain King Ara. In the Armenian linguistic tradition, the word Ararich signifies Creator, reflecting the semantic association of the root Ara- with concepts of creation and generative power. The figure of Ara was likewise associated with the planet Mars (Hrat), reflecting a parallel with the identification of the Greek god Ares and the Roman god Mars with the red planet.

Summarizing all the above-mentioned evidence concerning the Haykazuns, it should be emphasized that they symbolize Hayk'–Armenia as the ancestral cradle of the Armenian nation and have endured in historical tradition as deified forefathers.

8. Cosmogonic myth – Vahagn vishapaqagh

The Sun energy and the four elements of the Universe – Air, Fire, Water, and Soil – generate, sustain, and transform the forms of life and their creatures on Earth. An original weave of all these natural elements demonstrates the environment that gives rise to the ancient Armenian Sun-god **Vahagn**. In the song of "Vahagn's Birth,'preserved in Movses Khorenatsi's "History of Armenia", who had the pleasure of listening to the bards in one of the Armenian provinces reported that they were singing:

Heaven was in travail, earth was in travail, / The purple sea was also in travail,
In the sea, travail also gripped the red reed. / From the tube of the reed came forth smoke,
From the tube of the reed came forth flame. / From the flame, a blond young boy ran out.
He had fire hair, and had flame beard, / And his eyes were suns (Movses Khorenatsi, 1978).

The song describes the birth of Vahagn through a powerful convergence of cosmic and elemental forces. Solar energy and the four primordial elements of the Universe – Air, Fire, Water, and Earth – are traditionally regarded as the fundamental forces that generate, sustain, and transform life on Earth. The intricate interaction of these natural elements is vividly reflected in the mythological environment from which the ancient Armenian solar god Vahagn emerged (Toporov, 1977).

Vahagn's image combines several layers of mythology: solar divinity, warrior god, thunder hero, and cosmic protector. Solar aspect is complemented by his epithet ***Vishapaqagh*** ("Dragon-Slayer"), by which he was revered, as he defeated the dragon symbolizing darkness. The title reflects his role as the divine hero who defeats the forces of chaos and darkness represented by the dragon (Fig. 12). The solar aspect is also reflected in this function: he does not merely fight dragons; he restores cosmic order, bringing light against darkness (Vardumyan, 1991).

In Armenian mythology, the Milky Way occupies a distinctive place in the celestial imagination. Anania Shirakatsi records an ancient tradition concerning the ancestral hero Vahagn. According to the myth, Vahagn stole straw from Barsham, the legendary progenitor of the Assyrians, in order to provide warmth for his people during a harsh winter. As he fled, strands of straw scattered across the sky, leaving a luminous trail that came to be known as the **Straw-Thief's Path** (*Hardagoghi chanaparh*), the traditional Armenian name for the Milky Way. This etiological myth explains the celestial phenomenon by linking it to the cultural hero's beneficent act on behalf of his people (Anania Shirakatsi, 1940).

doi: https://doi.org/10.52526/25792776-26.73.1-76

Figure 12: Sculpture of Vahagn in Yerevan.

Figure 13: Van Lake, sunset.

9. Solar myths

The region of Van in ancient Armenia constituted one of the principal centers of solar veneration. According to legend, the Sun was envisioned as a golden-haired youth who traversed the heavens in a golden chariot during the day. At sunset, he was believed to descend into Lake Van, where he bathed and rested throughout the night, renewing his strength for his daily celestial journey (Fig. 13). Another major center of solar worship was the region of Ayrarat, the largest province of historical Armenia, situated around Mount Ararat. In Armenian folk tradition, the summit of Ararat is portrayed as the place where the Sun pauses to rest during its passage across the sky, further underscoring the mountain's sacred association with solar mythology and cosmological beliefs.

doi: https://doi.org/10.52526/25792776-26.73.1-76

Figure 14–15: Haldi on fresco (Erebuni) and on bronze votive plaque; statuette of Theisheba.

10. Lunar myth

Armenian folklore also preserves a number of myths concerning the Moon. One such legend recounts that, when the Moon was still a little girl, her mother was preparing dough to bake bread. Impatient to eat the freshly baked bread, the child repeatedly urged her mother to hurry. Exasperated by her daughter's persistent demands, the mother finally slapped her cheek with a dough-covered hand. According to the legend, the marks left by this doughy slap remained forever visible on the Moon's face, providing a mythical explanation for the dark patterns observed on the lunar surface.

11. Planet and sky deities

In the Kingdom of Ararat, commonly known as Urartu (also referred to as Biainili or the Van Kingdom, IX–VI Ce. BC), celestial bodies and natural phenomena were closely integrated into the religious worldview and represented through divine personifications. The deities of the supreme triad and their consorts were associated with major celestial powers: **Haldi (aldi)** was linked to the planet Jupiter, **Theisheba (Teišeba, Theispas)** to thunder and lightning, and **Shivini (Šiuine)** to the Sun (Badalyan, 2015, Hmayakyan, 1990).

The concept of the Tree of Life occupied a prominent place in cosmological thought, symbolizing the connection between the celestial realm of Heaven (Eden) and the terrestrial and subterranean worlds. As a cosmic axis, it embodied the unity of the Universe and the dynamic relationship between its divine, earthly, and underworld domains (Fig. 14–15).

Within the Urartian pantheon, other celestial bodies of the Solar System were likewise identified with specific deities. **Ardi (^{D}ardi)** was associated with Mercury, **Sardi (^{D}sardi)** with Venus, **Melardi (^{D}melardi)** with the Moon, and **Tzinuardi (^{D}ṣinuiardi)** with Saturn. The element ardi, meaning "star," appearing in all of these divine names, reflects the astral character of their cults (Hmayakyan, 1990).

Urartian religious thought also developed the concept of the Tree of Life, a powerful cosmological symbol representing the connection between the celestial and terrestrial realms (Fig. 17). It reflected an advanced cosmological understanding in which the Universe was perceived as a unified system of divine, celestial, and earthly forces. Associated with Haldi, the supreme deity, the sacred tree functioned as a symbolic bridge between Heaven and Earth, expressing the idea of cosmic balance, divine protection, and the eternal renewal of life. In iconography, the Tree of Life often appears together with winged divine symbols, sacred animals, and royal figures, suggesting that it was not simply a botanical image but a representation of cosmic

doi: https://doi.org/10.52526/25792776-26.73.1-76

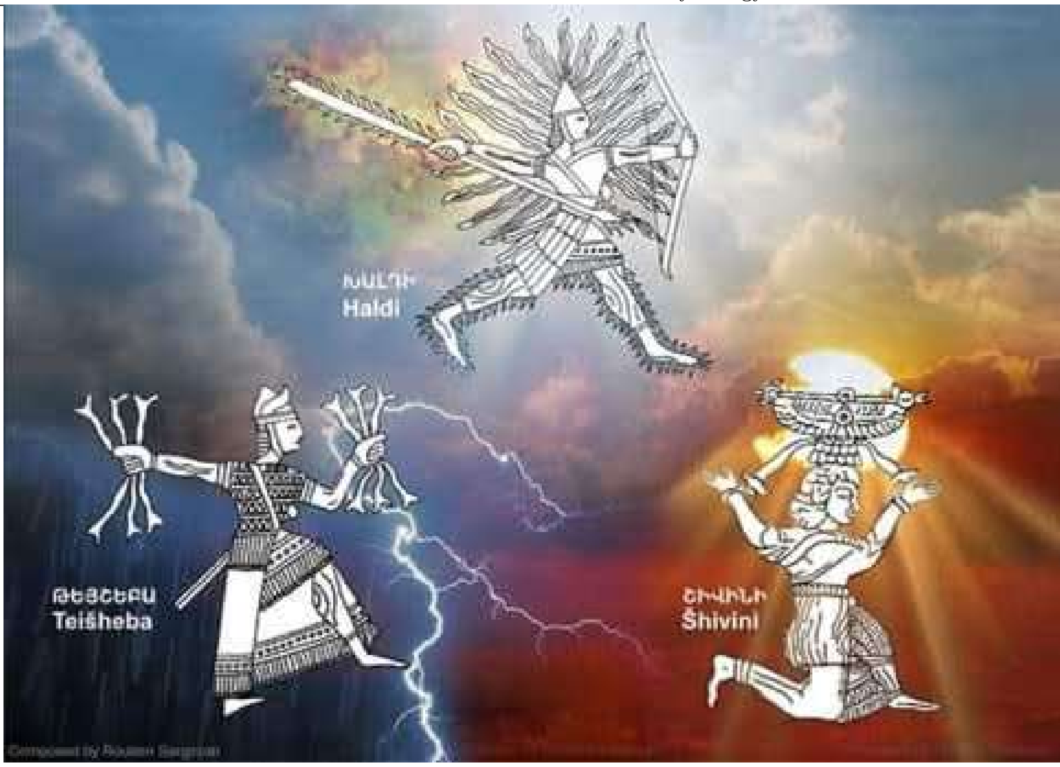

Figure 16: The supreme triad: Haldi, Theysheba, Shivini.

structure and divine presence.

Figure 17: Fresco: Tree of Life (Voskeblur, in Eriza).

In Ervandid-Artashesid-Arshakid (Orontid–Artaxiad–Arsacid) periods of Armenian history (VI Ce. BC – 301 AD), the supreme deity of the Armenian pantheon, Aramazd, was associated with the planet Jupiter. **Aramazd** and his consort **Anahit** were regarded as the patron deities of all creation, governing both the celestial and terrestrial realms (Fig. 18–19, left panel). The most revered Armenian Mother Goddess, Anahit, was described as Gold-haired and Gold-fingered, with the symbolism of gold reflecting solar radiance and the divine power of the Sun. Their daughter **Astghik**, whose name means 'star' in Armenian, was identified with Venus – the brightest and most beautiful celestial body visible in the morning and evening skies – and was worshiped as the goddess of love and beauty (Fig. 18–19, right panel). Aramazd's divine messenger, **Tir**, the patron of wisdom, knowledge, writing, and sciences, was associated with the planet Mercury (Alishan, 1895, Melik-Pashayan, 1963, Vardumyan, 2010).

A prominent solar deity was **Mihr**, whose cult had ancient origins rooted in the worship of fire and

doi: https://doi.org/10.52526/25792776-26.73.1-76

Figure 18–19: Goddesses: Bronze head of Anahit; statuette of Astghik.

Figure 20: Mher's Door (Van).

the sacred household hearth. He represented the Armenian counterpart of the Indo-Iranian divine figures – Vedic Mitra, Zoroastrian Mithra, and Roman Mithras. However, unlike these traditions, the cult of Armenian Mihr continued to survive for a much longer period, and its echoes are preserved in the images of the epic heroes **Great Mher** and **Little Mher** of the medieval Armenian epic tradition (VII–IX Ce.). Great (Senior) Mher was described as possessing extraordinary strength: he tore apart the lion that had deprived his kin of life and, for this heroic feat, received the epithet **Aryutsadzev**, meaning "lion-shaped" or "lion-like". Later, he was transformed into the figure of Lion Mher, a symbolic embodiment of solar power. Great Mher was associated with the rising Sun and the dawn, while his grandson Little (Junior) Mher, was connected with the setting Sun and twilight. At the end of the epic, Junior Mher withdrew into the **Raven-Rock**, also known as **Mher's Door** (identified by some traditions with the Haldian Gates near the fortress of Van), because he was outraged by the injustice prevailing in the world (Fig. 20). He remains there with his fiery horse, awaiting the time when justice, peace, and prosperity will be restored on Earth

doi: https://doi.org/10.52526/25792776-26.73.1-76

(Daredevils of Sassoun, 1966). According to legend, within Mher's stone sanctuary there is a rotating Wheel of Fate suspended from the Heavens, symbolically preserving the connection between the Cosmos and the Earth, and, in a broader sense, between the celestial realm and the epic heroes (Vardumyan, 2014).

Figure 21: Trndez.

12. Luminaries in ethnography

The Sun occupied a central place in the complex of beliefs and concepts associated with the celestial sphere. Certain ethnographic traditions have preserved elements of solar worship into the present day. One such example is the Christian feast of the Presentation of Jesus at the Temple, which is believed to have absorbed certain elements of the pre-Christian festival of Trndez – the ritual celebration of the Sun's symbolic rebirth, associated with the birthday of Mihr on the 14^{th} of Mehekan (February). The feast continues to be observed today by the Armenian people and the Armenian Apostolic Church. Its central ritual involves newlyweds dancing around the fire and jumping over the flames, symbolizing the wish for a prosperous family life, fertility, and the blessing of children (Fig. 21).

13. Luminaries in iconography

The Greek historian and military commander Xenophon, in his work Anabasis, records that during the festivals dedicated to Mihr in Armenia, a great number of stallions were sacrificed, as the horse was regarded as one of the principal symbols of the Sun (Fig. 22–23). Xenophon himself is said to have offered his own horse to the chief of an Armenian village so that it could be sacrificed to the Solar Deity (Xenophon, Anabasis,, IV).

14. Luminaries in architecture

One of the sanctuaries dedicated to Mihr, the only surviving pre-Christian temple in Armenia, is located in Garni – the summer residence of the Armenian kings – and represents a remarkable monument of I Ce. pre-Christian architecture[1]. The Garni temple embodies the ancient concept of the sacred connection

[1] After Armenia adopted Christianity as the state religion in 301 AD, numerous pagan temples were destroyed as part of the religious transformation of the country. The temple of Garni, however, survived, most likely due to its function as a royal sanctuary and architectural monument. During the medieval period, the structure suffered damage from earthquakes and eventually collapsed in 1679. It was later reconstructed in 1969–1975 based on the surviving architectural elements and archeological evidence.

doi: https://doi.org/10.52526/25792776-26.73.1-76

Figure 22–23: Solar symbols: Lion on relief in Commagene; Horse – fresco in Erebuni.

Figure 24: Garni temple.

between the celestial and terrestrial worlds (Fig. 24).

A magnificent archaeological monument is the Commagene pantheon, constructed in 62 BC by the Armenian king Antiochus I of the Ervanduni (Orontid) dynasty on the slopes of Mount Nemrut in the Armenian Taurus (Fig. 25). The monumental stone sculptures of deities – Aramazd, Mihr, Vahagn, Anahit – and Antiochus himself, together with the colossal heads of the Lion and the Eagle, symbols of royal authority, are situated on the eastern and western terraces of an artificial tumulus approximately 50 m high. The entire sculptural ensemble, including the deities, the king, and the symbolic animals, was arranged in harmony with the movement of the Sun: facing the celestial luminary at dawn and witnessing its departure at sunset, thus reflecting the ancient veneration of the rising and setting Sun.

15. Summary

The Universe, with its celestial bodies and phenomena, has left a profound imprint on Armenian culture throughout the millennia. The earliest manifestations of cosmic perceptions can be traced to rock art, where numerous representations of the Sun, Moon, planets, constellations, and the Milky Way have been preserved. Over time, these ideas found expression in mythology through the cults of solar, lunar, astral, and

doi: https://doi.org/10.52526/25792776-26.73.1-76

Figure 25: Commagene pantheon.

other deities, reflecting the advanced level of cosmological understanding and interpretation of the Universe in ancient Armenian culture. The image and concept of the Universe were also manifested in various cultural spheres, including the calendar system, folklore, divine pantheons, iconography, architecture, and ethnographic traditions. Concepts of the Universe and its celestial manifestations continued to be reflected in the Armenian worldview, mentality, and cultural heritage throughout different historical periods, from antiquity to the present day.

References

Alishan G., 1895, Ancient Faith or Pagan Religion of Armenians. Venice, "St. Lazaro", 525 p., (in Arm.)

Anania Shirakatsi 1940, Cosmography and Calendar. Yerevan, "Haypethrat", 96 p., (in Arm.)

Badalyan M., 2015, The Supreme Triad of the Urartian Pantheon (cult, symbols, iconography), on the basis of archaeological sources. Candidate thesis, Yerevan. "IAE of NAS RA", 299 p., (in Arm.)

Bible, Genesis 8:4,

Bobokhyan A., Gilibert A., Hnila P., 2015, Archaeology of Vishap Stones. The Vishap Stone Stelae. Yerevan, "IAE of NAS RA", p. 269-39, (in Arm.)

Daredevils of Sassoun 1966, The Armenian Epic by Leon Surmelian. London, "George Allen & Unwin", 251 p.

Hmayakyan S., 1990, The State Religion of the Kingdom of Van. Yerevan, "Academy of Sciences of Armenia", 191 p., (in Arm.)

Khanzadyan E., Mkrtchyan K., Parsamyan E., 1973, Metsamor. Yerevan, "Academy of Sciences of Arm. SSR", 215 p., (in Arm.)

Kramer S. N., 1952, Enmerkar and the Lord of Aratta. Philadelphia, "University of Pennsylvania", 88 p.

Martirosyan H., 1981, The Petroglyphs of the Geghama Mountains. Yerevan, "Academy of Sciences of Arm. SSR", 128 p., (in Arm.)

Martirosyan H., Israelyan H., 1971, The Petroglyphs of the Geghama Mountains. Yerevan, "Academy of Sciences of Arm. SSR", 66 p., (in Arm.)

Melik-Pashayan K., 1963, The Cult of Goddess Anahit. Yerevan, "Academy of Sciences of Arm. SSR", 165 p., (in Arm.)

Movses Khorenatsi 1978, History of the Armenians (trans. and comment. on the literary sources by Robert W. Thomson). Cambridge, Massachusetts, London, 411 p.

Tokhatyan K., 2025, Petroglyphs of Armenia. Yerevan. "Gitutyun", 520 p., (in Arm.)

Toporov V., 1977, On the Reflection of an Indo-European Myth in the Ancient Armenian Tradition. Historical-philological journal. Yerevan, № 3, p. 88-106, (in Russ.)

Vardumyan G., 1991, Pre-Christian Cults of Armenians, Armenian Ethnography and Folklore. Vol. 18. Yerevan, "Academy of Sciences of Armenia", p. 61-146, (in Russ.)

doi: https://doi.org/10.52526/25792776-26.73.1-76

Vardumyan G., 2010, La antigua religión y la mitología, Historia del Pueblo Armenio. Barcelona, “Originarte Diseño-inpresion SL”, p. 431-435

Vardumyan G., 2014, The Sun God Mihr – the Patron of Goodness and Justice among the Armenians. ”The Problems of the History of Armenia”, Yerevan, “Institute of History NAS RA”, 15, p. 3-19, (in Russ.)

Vardumyan G., 2020, Ancient Armenian Cosmogonic and Theogonic myths, Studies on Culture along the Silk Road. Vol. 2. Budapest, p. 167-183

Xenophon, Anabasis, IV, 35. 98

doi: https://doi.org/10.52526/25792776-26.73.1-76

Istanbul and Kandilli Observatories as the Astronomical Heritage of Türkiye

S. Fisek *[1,2,3] and S. Alis[1,2]

[1]Department of Astronomy and Space Sciences, Faculty of Science, Istanbul University, 34116 Istanbul, Türkiye
[2]Istanbul University Observatory Research and Application Centre, 34116 Istanbul, Türkiye
[3]Kandilli Observatory and Earthquake Research Institute, Geodesy Department, Astronomy Laboratory, Boğaziçi University, 34684 Istanbul, Türkiye

Abstract

This paper explores the historical evolution and scientific contributions of two cornerstone institutions of Turkish astronomy: the Kandilli Observatory and the Istanbul University Observatory. By examining their origins—ranging from the late Ottoman era to the early years of the Republic—this work highlights their roles in establishing modern astronomical research in Türkiye. The paper details their historical instrumentation, significant manuscript collections, and the continuous solar observation datasets that remain vital for global heliophysics research today. Furthermore, it discusses their current educational initiatives and their role in bridging Türkiye's rich astronomical heritage with future endeavors, such as the Eastern Anatolia Observatory (DAG).

Keywords: *Astronomical Heritage, Cultural Heritage, Science History*

1. Introduction

The foundations of modern astronomical research in Türkiye are deeply rooted in two primary institutions: the Kandilli Observatory and the Istanbul University Observatory. These two observatories hold great significance in terms of the nation's scientific heritage. It is important to emphasize that Kandilli was established prior to the foundation of the Republic, whereas the Istanbul University Observatory was founded shortly after. Together, these institutions laid the crucial foundations for the astronomical research that Türkiye carries out today.

To fully understand this scientific heritage, one must trace its origins back to the 16th century. In 1574, Murad III became the Sultan of the Ottoman Empire. During his reign, the empire's chief astronomer, Taqi al-Din, petitioned the Sultan to finance the construction of a great observatory that would rival Ulugh Beg's famous observatory in Samarkand. The Sultan approved the project, and its construction was completed in 1577, making it a contemporary of Tycho Brahe's Uraniborg Observatory. However, this pioneering institution was short-lived; according to some sources, the observatory was demolished by the Sultan's order because a comet observed in the sky during that period was superstitiously believed to be connected with certain unfortunate events. Today, the legacy of this early endeavor is honored by a quadrant displayed in the building located at the approximate site of the original observatory (Figure 1)[1].

Following this historical interruption, the foundations of modern institutional astronomy began to re-emerge during the late Ottoman Empire with the establishment of the Imperial Observatory. Initially founded with a primary focus on meteorology to predict weather events and storms, historical documents and published materials clearly indicate that there were also ambitions to expand its scientific role into astronomy. The observatory operated at various locations, primarily carrying out meteorological and seismological measurements (Benoist, 2009). However, following the unrest and uprisings of 1909, the building housing the observatory was damaged[2]. This pivotal event eventually led to the search for a new, permanent location, marking the beginning of a new era for what would become the Kandilli Observatory.

*sfisek@Istanbul.edu.tr, Corresponding author

[1]https://web.astronomicalheritage.net/show-entity?identity=184&idsubentity=1

[2]http://www.koeri.boun.edu.tr/eng/tarih_eng.htm

doi: https://doi.org/10.52526/25792776-26.73.1-92

Figure 1. Commemorative quadrant model marking the approximate site of the first Ottoman observatory, founded by Taqi al-Din (1575-1580), reproduced in 2009 by the Turkish Astronomical Society (TAD), UNESCO National Commission of Türkiye, and Koç University to celebrate the International Year of Astronomy.

2. Kandilli Observatory

2.1. Origins and Relocation

The modernization of the observatory is inextricably linked to the appointment of Fatin Gökmen (known as Fatin Hoca) in 1910. Following the destruction of the Rasathane-i Amire during the political turbulence of 1909, the Ottoman administration sought to rebuild its scientific infrastructure (Benoist, 2009). Gökmen was tasked with selecting a site that would provide the atmospheric stability and isolation necessary for precise astronomical and geophysical measurements. He selected Icadiye Hill on the Asian side of the Bosphorus, utilizing an existing fire watchtower as the initial structural core of the new Kandilli Observatory. By 1911, the institution was operational, marking a shift from a purely meteorological station to a multi-disciplinary research center focused on astronomy and geophysics[3].

2.2. Astronomical Instrumentation

A cornerstone of Kandilli's scientific heritage is the purchase of a 20cm equatorial telescope from the German firm Carl Zeiss. Ordered in 1918 during the final stages of World War I, the telescope's delivery was significantly delayed by the post-war geopolitical environment and the subsequent transition from the Empire to the Republic. The instrument finally arrived in Türkiye in 1925, but the construction of a specialized dome to house it required nearly another decade. The telescope became fully operational in 1935. This instrument was not merely a tool for observation but a symbol of the young Republic's commitment to state-of-the-art astrophysical research, allowing for higher precision in celestial mechanics and solar studies.

Building upon this historical foundation, the observatory is currently expanding its observational capabilities. The institution operates a modern 35 cm aperture telescope, which is presently deployed on a mobile basis. Equipped with a CMOS camera, this instrument is actively utilized for a variety of research campaigns, primarily focusing on target of opportunity (ToO) and follow-up observations. In the near future, this telescope will be permanently housed in its own dedicated building. This strategic installation aims to ensure the continuity of regular, systematic night-time observations at Kandilli.

2.3. Observational Heritage

The most distinctive feature of Kandilli's astronomical activity is the unwavering continuity of its solar research. Systematic observations began in 1947, and remarkably, the historical Carl Zeiss telescope remains in active observational status today. A cornerstone of this scientific routine is the commitment to daily data collection: every single day with clear skies, researchers perform meticulous hand-drawings of sunspots and monitor solar activity.

[3] http://www.koeri.boun.edu.tr/new/en/history

doi: https://doi.org/10.52526/25792776-26.73.1-92

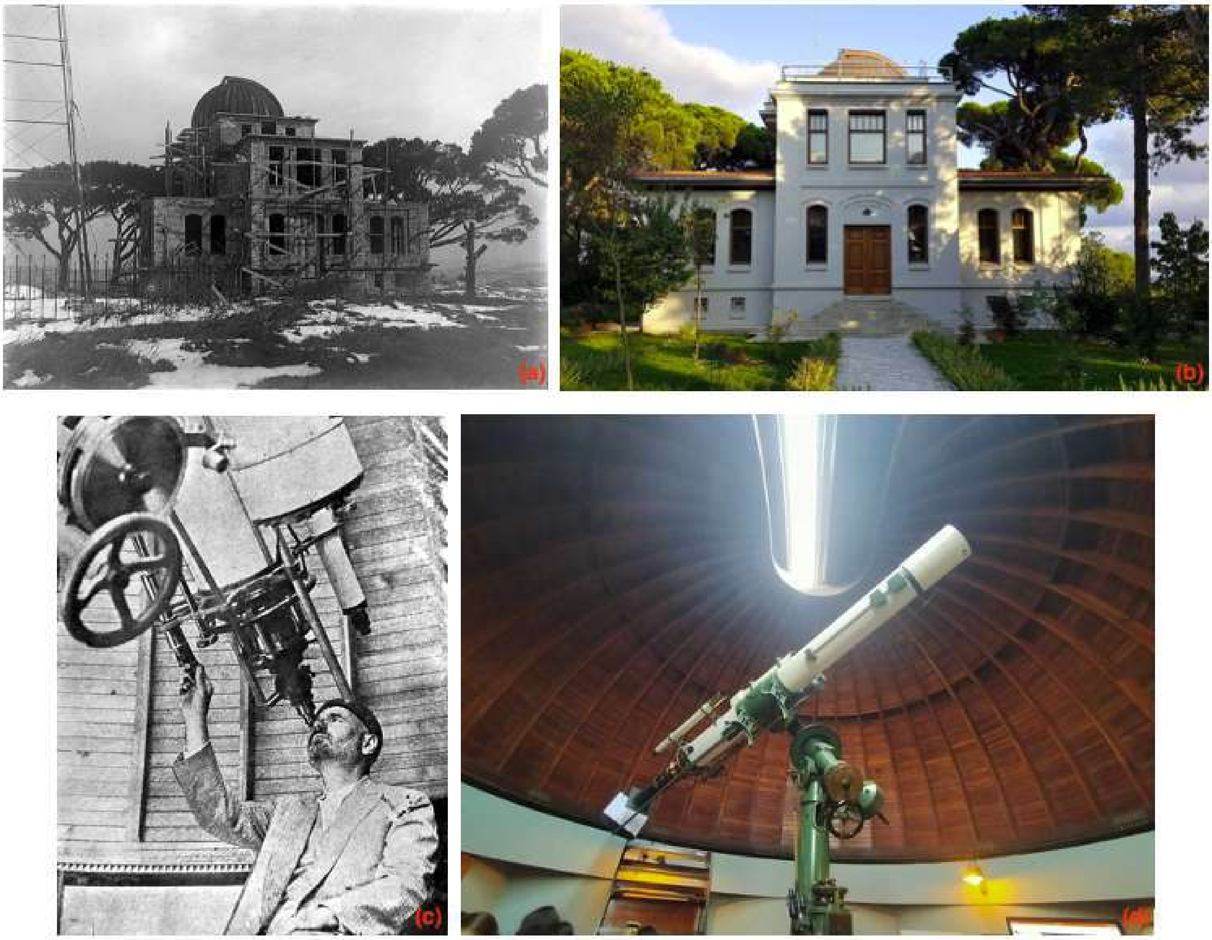

Figure 2. (a) The Kandilli Observatory building during its construction phase. (b) The current appearance of the historical building. (c) Fatin Gökmen seen observing through the telescope. (d) An interior view of the dome, featuring the historical 20 cm aperture Carl Zeiss telescope.

This persistent effort has culminated in a digital and physical archive spanning over 80 years. In the context of "Astronomical Heritage," this dataset is not merely a relic of the past but a vibrant, growing resource. It serves as a critical baseline for modern solar physics, allowing for the cross-calibration of historical records with data from space-based observatories. By maintaining this daily ritual of observation, Kandilli ensures that its heritage remains a living component of global solar cycle research[4].

2.4. The UNESCO Manuscript Collection

One of Kandilli's most profound contributions to the history of science is its preservation of classical Islamic and Ottoman scientific thought. Under Fatin Gökmen's guidance, the observatory amassed a collection of 1,339 rare manuscripts dating from the 11th to the 20th century. This collection includes seminal works by scholars such as Ali Qushji, Al-Biruni, and Taqi al-Din, covering mathematics, astronomy, and geography. In recognition of its universal value, the collection was inscribed in the UNESCO Memory of the World Register in 2001[5]. This status formally acknowledges Kandilli not just as a site of observation, but as a global guardian of scientific history.

2.5. Transition to Boğaziçi University

In the wake of the 1983 university reorganization in Türkiye, the institution was integrated into Boğaziçi University, becoming the Kandilli Observatory and Earthquake Research Institute (KOERI)[6]. While the institute gained international renown for its seismological and tsunami warning capabilities, the Astronomy

[4] https://astronomi.bogazici.edu.tr/tr/archives
[5] https://www.unesco.org/en/memory-world/kandilli-observatory-and-earthquake-research-institute-manuscripts
[6] http://www.koeri.boun.edu.tr/new/en

doi: https://doi.org/10.52526/25792776-26.73.1-92

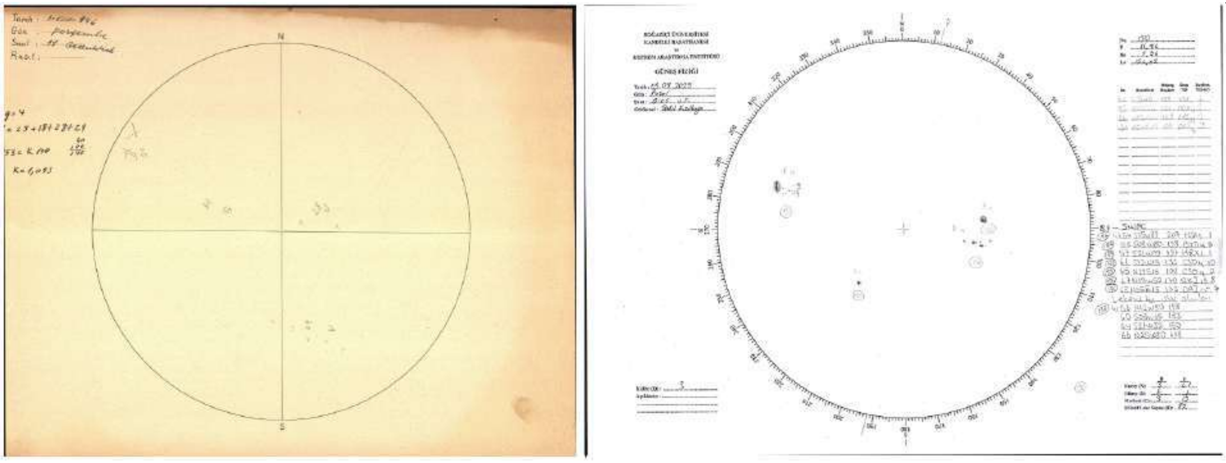

Figure 3. (left) The earliest known solar observation sheet, recorded in 1946. (right) A present-day example of a solar observation sheet, recorded in 2025 at the Kandilli Observatory.

Laboratory[7] remains the custodian of its astronomical legacy. Today, the laboratory balances its historical solar observation duties with new educational roles, housing a vast collection of historical astronomical instruments and serving as a key site for public outreach and scientific literacy.

3. Istanbul University Observatory

3.1. The University Reform in 1933

While Kandilli represents the transition of astronomical heritage from the Ottoman era, the Istanbul University Observatory stands as the first observatory and astronomy department established after the founding of the Republic. Its inception was intrinsically tied to the 1933 University Reform, a monumental step aimed at modernizing higher education and scientific research in Türkiye (Bilsel, 1943) which was initiated by Atatürk (Reisman, 2006). As part of these comprehensive academic developments, the Faculty of Science and the Department of Astronomy were established, marking the creation of the first astronomy department in the country. The observatory was subsequently constructed on the university's main campus, situated near its iconic main entrance gate, physically and symbolically placing astronomy at the heart of the new academic structure (Figure 5).

3.2. Migrated Scientists and the Legacy of Wolfgang Gleissberg

The intellectual foundation of the newly established department was profoundly shaped by the influx of European scholars. Specifically, German scientists of Jewish origin, who had fled Nazi persecution in the 1930s (Widmann, 1973), played a crucial role in the development of the astronomy department and the establishment of the observatory (Gunergun & Kadioglu, 2006). Erwin Finlay-Freundlich is the founder of the department and the observatory. Wolfgang Gleissberg, Erich Karl Weber, Hans Rosenberg, and Thomas Royds were scholars who worked at Istanbul University Observatory. Among these pioneering figures, Wolfgang Gleissberg is particularly notable. Gleissberg served Istanbul University for 24 years between 1934 and 1958, implementing rigorous academic standards and training a foundational generation of Turkish astronomers. The pedagogical impact of this era was far-reaching; graduates trained under Gleissberg and his colleagues later contributed significantly to the establishment and advancement of other astronomy departments and observatories across Türkiye (Alis, 2019). In 1982, an honorary doctorate was awarded to Gleissberg for his contributions to the Istanbul University Observatory and to the Astronomy Department at a ceremony organized in the Turkish consulate in Frankfurt (Menteşe et al., 2002).

3.3. The 1935 State Decree and Historical Instrumentation

The physical realization of the observatory required substantial governmental backing, underscoring the state's vision for scientific progress. In 1935, a state decree was issued authorizing the purchase of a major

[7] https://astronomi.bogazici.edu.tr/tr

doi: https://doi.org/10.52526/25792776-26.73.1-92

Figure 4. Calendar of the Gregorian year 1527-1528 (933-934 Hijri) dedicated to Sultan Süleyman the Magnificent, No:333 in Kandilli's manuscripts collection.

telescope and the formal establishment of the observatory. This financial and administrative commitment was a difficult yet highly significant decision for the newly founded Republic, directly shaping the future of scientific research in the country. The primary instrument acquired was a multi-telescope mount featuring a 30 cm aperture astrograph at its center. In its early decades, this large astrograph was heavily utilized for night-time observations, equipped with a specialized chamber for capturing celestial data on photographic glass plates.

3.4. Continuous Scientific Operations

Although the 30 cm astrograph is no longer actively used for night-time observations, the observatory has successfully adapted its historical infrastructure to maintain its scientific relevance. Today, two other telescopes mounted alongside the historical astrograph remain in active service (Figure 5). These instruments are dedicated strictly to solar observation, specifically targeting the Sun's photosphere and chromosphere layers. Mirroring the rigorous data collection practices at Kandilli, solar observations at Istanbul University are carried out every day when the sky is clear. This ongoing operational status ensures that the facility functions not merely as a museum of early Republican science, but as an active observatory continuously contributing to long-term astronomical data collection[8].

Early systematic sunspot observations at the Istanbul Observatory were reported in internal observatory publications, reflecting the institution's commitment to continuous solar monitoring. Besides several individual solar events and focused analysis, the observatory published the sunspot observations systematically starting from the 1950s (e.g., The Sunspot Observations Made in 1955) (Yılmaz, 1956). The complete list of publications of the observatory can be found in Menteşe et al. (2002) which is published in Turkish but provides a comprehensive historical record[9].

Beyond solar observations with historical telescopes, the institution maintains a strong focus on academic training and contemporary night-time observations. Currently, to provide astronomy students in the department with practical night-time observational experience, a modern telescope IST40 with a 40 cm aperture is installed within the main building. Although primarily utilized for educational purposes to enhance students' observational skills, this telescope is also actively used for various targeted scientific observations (Devecioğlu et al., 2024, Eryılmaz et al., 2023, Ötken et al., 2025, Sağlam et al., 2022). Furthermore, to over-

[8] https://astronomi.istanbul.edu.tr/arsiv.php

[9] https://astronomi.istanbul.edu.tr/tanitim/tarihce/kurgunastro.pdf

doi: https://doi.org/10.52526/25792776-26.73.1-92

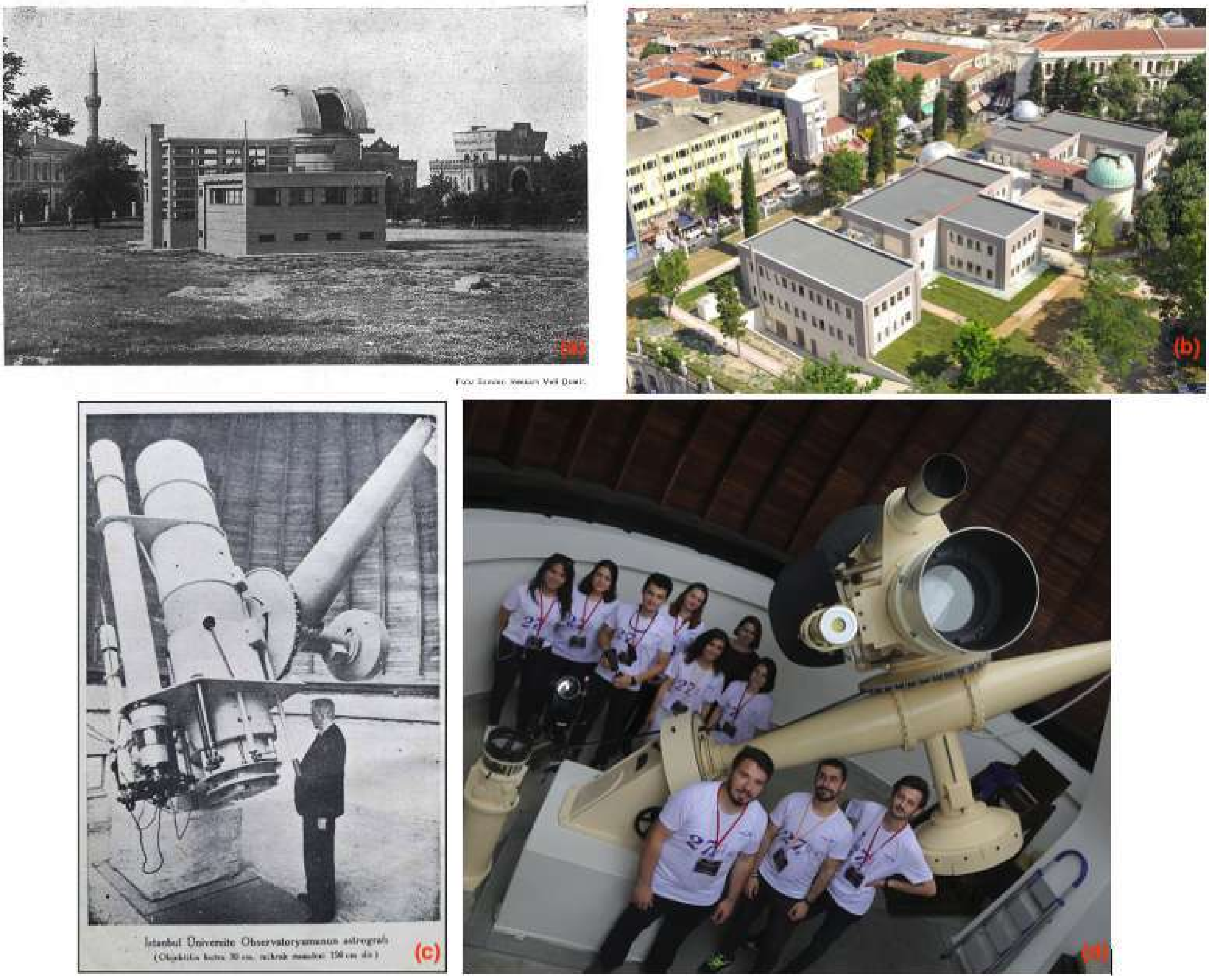

Figure 5. (a) A view of the observatory during its founding years at the main campus. (b) A present-day view of the Istanbul University Observatory and the Astronomy Department. (c) An observer seen with the historical telescope inside the dome. (d) Present-day astronomy department students alongside the historical telescope.

come the observational limitations imposed by light pollution, Istanbul University Observatory[10] operates an advanced 60 cm aperture telescope IST60 located in Çanakkale. This telescope is capable of functioning in both remote-control and fully robotic modes (Aliș et al., 2020), significantly expanding the department's modern research capabilities[11](Figure 7).

In addition to the optical telescope infrastructure, the Istanbul University Observatory has recently expanded its observational capabilities into the domain of high-energy solar physics through the establishment of the Space Weather Monitoring Center[12]. Developed within the scope of the National Space Program coordinated by the Turkish Space Agency (TUA)[13], this initiative represents the latest technological evolution of the institution's 80-year legacy of solar activity tracking. The core of this project is the Mirya-μ1 Cosmic Ray (Muon) Detector[14]. Following its initial testing and calibration at the Istanbul University facilities, the instrument was relocated to the Eastern Anatolia Observatory (DAG) campus in Erzurum. Positioned at an altitude of 3150 meters, this facility now operates as Turkey's first Space Weather Monitoring Station (Dag et al., 2025).

[10] https://gozlemevi.istanbul.edu.tr/en/_
[11] https://cdn.istanbul.edu.tr/FileHandler2.ashx?f=astrbolumu.pdf
[12] http://ist60.istanbul.edu.tr/mirya/info/
[13] https://tua.gov.tr/tr
[14] http://ist60.istanbul.edu.tr/mirya/

doi: https://doi.org/10.52526/25792776-26.73.1-92

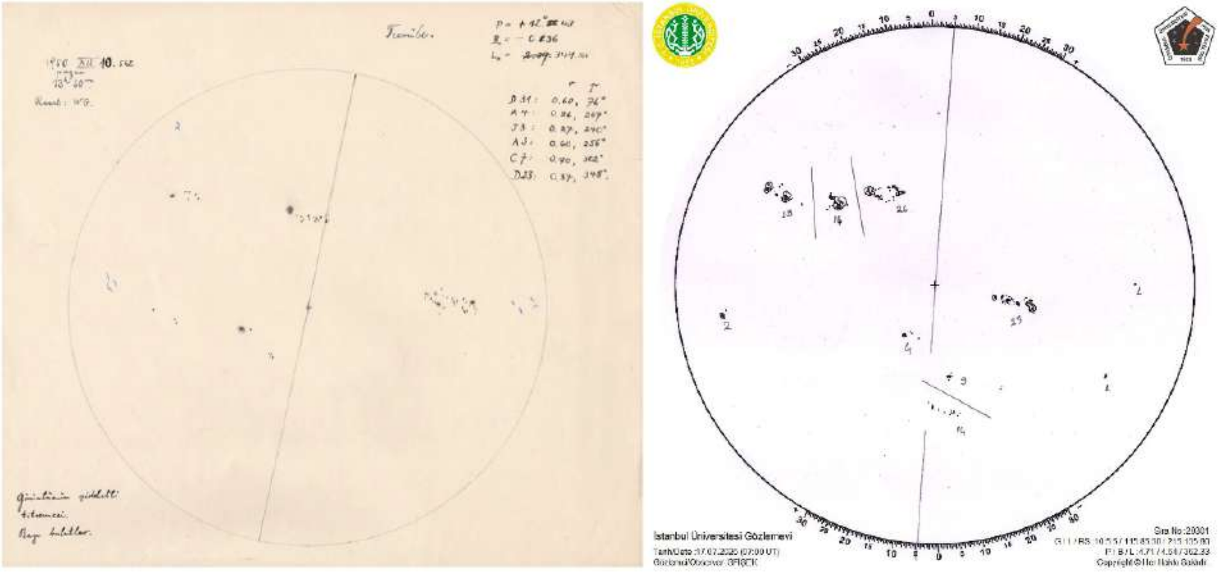

Figure 6. (left) A historical solar observation sheet, recorded in 1950. (right) A present-day example of a solar observation sheet, recorded in 2025 at the Istanbul University Observatory.

4. The Data Heritage: 80-Year Solar Archive

The fundamental scientific legacy of both Kandilli and Istanbul University Observatories extends far beyond their historical architecture and vintage instrumentation; it is rooted in their systematic and continuous data collection. Since the 1940s, both institutions have maintained a continuous series of solar photospheric observations (Figures 3 and 6). By recording daily sunspot counts, coordinates, and morphological classifications, these observatories have generated a very large and highly valuable longitudinal dataset. In the context of astronomical heritage, this archive serves as a critical baseline for analyzing long-term solar cycle variations, offering indispensable historical data for contemporary researchers investigating trends in solar minima and maxima over the past century.

While photospheric drawings constitute the core of the historical archives, both observatories have also contributed to the documentation of solar chromospheric activity. Although these observations were occasionally interrupted, systematic records obtained using Hα and Ca II filters complement the photospheric dataset and extend the temporal coverage of solar activity indicators. The transition from photographic plates to digital CCD imaging at Istanbul University Observatory represents not a change in scientific scope but an effort to preserve and sustain the continuity, consistency, and accessibility of this long-term solar archive in the modern era.

A crucial aspect of scientific heritage is its accessibility to the global research community. Neither institution treats its historical data as a closed, static museum exhibit. Instead, both the scanned historical photosphere observations and the ongoing daily digital observations are systematically cataloged and made publicly accessible on the websites of the two observatories[15] [16]. By adhering to open science principles, this digital archive represents a remarkable scientific data heritage that contributes significantly not just to the local scientific community in Türkiye, but to global.

5. Education and Public Outreach

Kandilli Observatory serves as a crucial interface between the scientific community and the general public, dedicating considerable resources to science communication. The institution opens its facilities to school and student visits on a weekly basis, providing structured tours of its seismology, meteorology, and astronomy laboratories. To enhance public scientific literacy, particularly regarding natural disasters, the observatory offers experiential learning through both on-site and mobile earthquake simulators. Furthermore, the institution maintains its astronomical public engagement by organizing specialized night-sky observation events during significant celestial occurrences and major institutional milestones, such as the activities held for its

[15] https://astronomi.bogazici.edu.tr/tr/archives
[16] https://astronomi.istanbul.edu.tr/arsiv.php

doi: https://doi.org/10.52526/25792776-26.73.1-92

Figure 7. (left) An interior view of the dome featuring the IST40 telescope, located at the university main campus in Beyazıt, Istanbul. (right) An interior view of the dome featuring the IST60 telescope, located at the Ulupınar Observatory, Çanakkale.

150th anniversary.

Istanbul University Observatory operates a highly active public engagement and educational program, hosting more than one hundred visiting students every weekday. The institutional infrastructure supporting this outreach includes a digital planetarium (Alis et al., 2024), which houses a library of over ten specialized educational films. Visitors are also provided access to the historical dome and the departmental archives, specifically the Gleissberg Astronomy Collection. Named in recognition of Wolfgang Gleissberg's foundational contributions, this collection exhibits historical astronomical instruments, telescopes, mechanical clocks, calculators, etc. Additionally, since 2017, the observatory has successfully institutionalized a public engagement initiative known as "Observation Nights," held on the last Friday of every month, which integrates academic seminars with guided night-sky observations.

Beyond public outreach, Istanbul University Observatory's facilities serve as crucial tools for advanced scientific training. Undergraduate students in the astronomy department actively utilize both the planetarium and the telescopes for practical exercises, effectively bridging the gap between theoretical coursework and applied observational astronomy. Furthermore, the observatory functions as a key training center for the Turkish National Astronomy and Astrophysics Olympiad Team[17]. During specialized training camps hosted at the observatory, the team extensively utilizes the planetarium's advanced simulation capabilities to prepare for international competitions.

The operational sustainability of these extensive outreach and educational programs heavily relies on the human power provided by student clubs at universities. Established in 1991, the astronomy student club Amateur Astronomers Club (AAK, in Turkish Amatör Astronomlar Kulübü[18]) at Istanbul University has actively organized scientific and public events for over three decades. From an academic perspective, these organizations play a critical role in capacity building. They provide undergraduate students with essential practical experience in observational techniques, seminar organization, and science communication, thereby significantly boosting academic motivation. A prominent example of this long-standing tradition is the "May Fest", which has been held continuously since the club's founding in 1991. In 2026, the 35th festival will be organized from 6 to 8 May 2026. Ultimately, these student-driven initiatives function as a vital mechanism for carrying the nation's astronomical heritage forward, ensuring the continuous training of future scientists.

Regarding student engagement at the Kandilli Observatory, the situation is shaped by its specific institutional framework. Since Kandilli is structured as a post-graduate research institute, and given its physical distance from the main campus of Boğaziçi University on the European side of Istanbul, the daily presence of undergraduate students is naturally limited. Consequently, its student body consists predominantly of post-graduate researchers.

[17] https://olimpiyat.astronomi.org
[18] https://aak.istanbul

doi: https://doi.org/10.52526/25792776-26.73.1-92

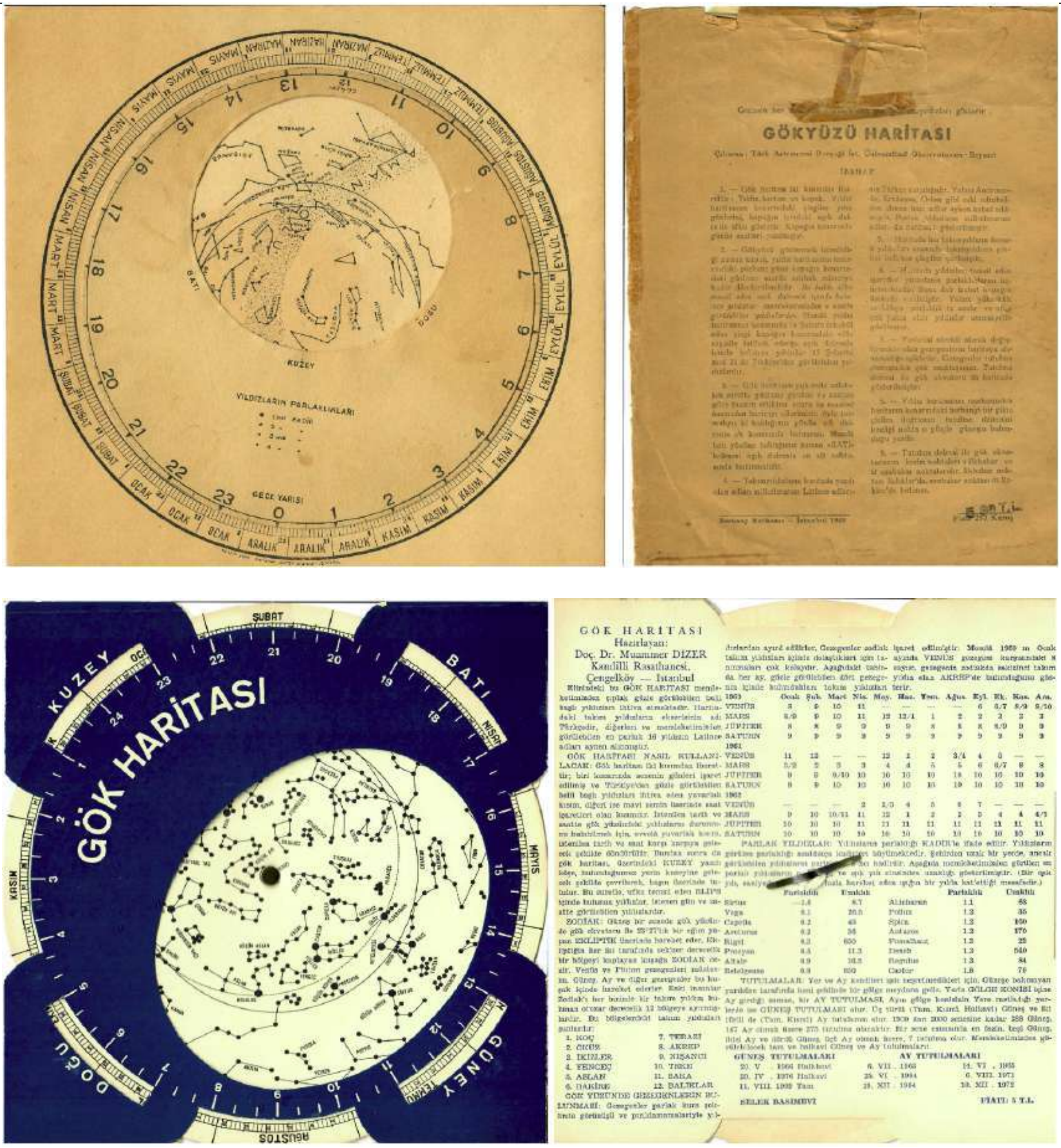

Figure 8. (top) The front and back covers of the sky atlas prepared in 1960 in collaboration with Istanbul University Observatory and the Turkish Astronomical Society. (bottom) The front and back covers of the sky atlas prepared by the Kandilli Observatory in 1960.

6. Conclusion

In conclusion, the astronomical heritage of Türkiye is not defined merely by the preservation of historical instruments or architectural landmarks, but by the sustained continuity of scientific inquiry. Kandilli and Istanbul University Observatories exemplify the concept of "living heritage," maintaining uninterrupted solar observation programs for more than eight decades while continuously adapting their scientific practices to evolving technological and educational contexts.

The preservation of this long-term solar archive represents both a major scientific asset and a methodological challenge. In particular, the extraction of quantitative information from decades of hand-drawn sunspot records has become an active area of research. Recent advances in machine learning and computer vision now enable the digitization and systematic analysis of these historical datasets, transforming archival material into high-precision, temporally extended data products. In this way, historical observations are being reintegrated into modern solar physics, effectively bridging past and present methodologies.

Equally central to the institutional identity of both observatories is their long-standing commitment to the democratization of scientific knowledge. This mission has historically been realized through the production of publicly accessible educational materials, including printed sky atlases. As illustrated in Figure 8, both Kandilli Observatory and Istanbul University Observatory independently prepared detailed sky maps around 1960, aimed at facilitating public engagement with astronomy. These efforts, carried out

doi: https://doi.org/10.52526/25792776-26.73.1-92

in part in collaboration with organizations such as the Turkish Astronomical Society (TAD)[19], reflect a sustained institutional philosophy in which public outreach and scientific literacy are regarded as integral components of astronomical practice. Today, this tradition continues through digital platforms that provide open-access data and educational resources.

By combining long-term data stewardship, public engagement, and the continuous training of new generations of researchers, these observatories have played a foundational role in shaping Türkiye's modern astronomical community. The academic culture and observational expertise cultivated over decades have directly contributed to the development of contemporary scientific infrastructure.

This legacy finds its most prominent modern expression in national-scale initiatives such as the Eastern Anatolia Observatory (Doğu Anadolu Gözlemevi, DAG), operating under the Türkiye National Observatories[20], and in the advancement of indigenous instrumentation projects, including the Mirya-μ1 detector. These developments demonstrate how historical institutions continue to inform and support cutting-edge astrophysical research.

Ultimately, Kandilli and Istanbul University Observatories serve as dynamic bridges between past and present, ensuring that the scientific vision, observational discipline, and human capital established in the early Republican era remain actively engaged in the advancement of 21st-century astronomy.

Acknowledgements

SF is grateful for the hospitality of the Byurakan Astrophysical Observatory staff. Authors acknowledge the support from the Istanbul University Observatory Research and Application Center and the Boğaziçi University Kandilli Observatory and Earthquake Research Institute.

References

Alis S., 2019, Astronomical Society of the Pacific Conference Series, 520, 95

Alis S., Saygaç A. T., Yelkenci F. K., 2024, Communicating Astronomy with the Public Journal, 34, 33

Aliș S., et al., 2020, Turkish Journal of Astronomy and Astrophysics, 1, 759

Benoist C., 2009, in Wolfschmidt G., ed., Cultural Heritage of Astronomical Observatories: From Classical Astronomy to Modern Astrophysics. pp 115–120

Bilsel C., 1943, İstanbul Üniversitesi Tarihi. Istanbul University Press, https://iupress.istanbul.edu.tr/book/istanbul-universitesi-tarihi/home

Dag M. K., Guver T., Gurkan G., et al. 2025, Advances in Space Research, 76, 1906

Devecioğlu E. E., Beyaz C., Toy Z., Eryılmaz M. İ., Dalkılıç Y., Bayram M. B., Bașara S., 2024, Turkish Journal of Astronomy and Astrophysics, 5, 9

Eryılmaz M. İ., et al., 2023, Turkish Journal of Astronomy and Astrophysics, 4, 5

Gunergun F., Kadioglu S., 2006, Osmanli Bilimi Arastirmalari (Studies in Ottoman Science), 8, 135

Menteşe H. H., Esenoğlu H. H., Çalışkan H., 2002, Technical report, History of the Istanbul University Astronomy and Space Sciences Department (1933–2000), https://astronomi.istanbul.edu.tr/tanitim/tarihce/kurgunastro.pdf. İstanbul University Observatory, https://astronomi.istanbul.edu.tr/tanitim/tarihce/kurgunastro.pdf

Ötken S., Özel S., Bayram M. B., Kelkitli İ. Z., İçen M., Erol Z., Toy Z., Demirel B., 2025, Turkish Journal of Astronomy and Astrophysics, 6, 14

Reisman A., 2006, Turkey's Modernization: Refugees from Nazism and Atatürk's Vision. New Academia Publishing, Washington, DC

Sağlam M. T., et al., 2022, Turkish Journal of Astronomy and Astrophysics, 3, 8

Widmann H., 1973, Exil und Bildungshilfe: Die deutschsprachige akademische Emigration in die Türkei nach 1933. Peter Lang, Frankfurt am Main

Yılmaz F., 1956, Review of the Faculty of Science, University of Istanbul, Series C, 21, 110

Yılmaz F., 1969, İstanbul Üniversitesi Fen Fakültesi Mecmuası, Seri C, 34, 165

[19] https://www.tad.org.tr
[20] https://trgozlemevleri.gov.tr

doi: https://doi.org/10.52526/25792776-26.73.1-92

Communications of BAO, Vol.73, Issue 1, 2026, pp.102-106

Ancient Georgian Cultural Heritage: Archaeoastronomy and Ethnocosmology

I. Simonia *

The School of Natural Sciences and Medicine, Ilia State University, Tbilisi, Georgia

Abstract

The processes of accumulating knowledge about celestial bodies and phenomena are considered. Certain elements of the ancient Georgian astronomical worldview are discussed. Archaeoastronomical and ethnocosmological aspects of the problem are described. Examples of the astronomical projection of the ancient Georgian heritage are presented.

Keywords: *astronomy, archaeoastronomy, ethnocosmology, cultural heritage, Georgia*

1. Introduction

Since prehistoric times, humans have been fascinated by celestial phenomena. Bright celestial bodies, their repetitive appearances and configurations, impressed ancient humans, inspiring their desire to understand and respect them. Gradually, ancient people realized that the bright celestial bodies—the Sun and the Moon—could serve as useful guiding lights in time and space, allowing humans to prepare for periods of heat or drought, cold or moisture. Bright, rising, and setting celestial bodies provided ancient humans with precise directions for spatial movement in mountainous and valley terrain. The phenomena observed in the sky and the positions of bright luminaries were imprinted in the ancients' memory as empirical knowledge that could be consulted as needed. The empirical knowledge accumulated in this way about the appearance, movement, and mutual configurations of bright luminaries was passed on and enriched from generation to generation, which, in turn, was transformed into an ancient cultural heritage in the form of oral narratives and simple drawings (signs, direct images of lights, etc.) inscribed and carved on stones, rocks, in caves, and other material surfaces near the places of habitation of ancient humans. Later, enriched with empirical knowledge, ancient people shifted from the casual contemplation of celestial phenomena to their conscious observation and anticipation of the appearance of bright bodies, with the goal of using these phenomena to regulate daily life. The transformation of ancient humans from passive contemplators of celestial phenomena to practical observers was also expressed in the fact that the ancients no longer limited themselves to recording the rising of stars over the horizon but began to build simple stone structures with the goal of "capturing" and precisely recording the first appearances of bright bodies in the elements of these structures: in windows, openings, and crevices where the first bright rays of the rising Sun and the silvery light of the Moon could penetrate. Fixing the rise of bright luminaries in the elements of stone constructions allowed the ancients to accurately determine the onset of warm and cold seasons. Later, landscape features were added to stone constructivism; for example, a rising full moon over a high mountain peak, whose light penetrates the stone opening only for a short time during a given period. This kind of landscape constructivism became a reliable tool for the ancients' orientation in time, which was very important for agriculture. The Sun and the Moon became the main deities of the ancients, so the places, sites, and locations of stone structures gradually acquired another meaning—that of special religious buildings. There, people worshiped bright luminaries, their guides through time and space. Myths and legends were formed by the ancients in the context of celestial phenomena, bright luminaries, and their worship. All of this today constitutes a valuable cultural heritage of ancient peoples and civilizations in the form of material artifacts, legends, and oral narratives. Interdisciplinary methods of archaeoastronomy and ethnocosmology allow us to uncover previously unknown layers of this ancient cultural heritage.

*iraklisimonia@yahoo.com

doi: https://doi.org/10.52526/25792776-26.73.1-102

Figure 1. Avranlo. Credit: K. Jelia.

2. Ancient Georgian cultural heritage. Archaeoastronomical aspects

All of the above also applies to the South Caucasus, particularly Georgia. Considering the landscape and climatic conditions of Georgia, as well as the ancient agricultural traditions of the Georgians, it can be fairly concluded that ancient Georgians were interested in, understood, and used celestial phenomena for practical purposes since prehistoric times (Georgobiani, 1971, Simonia, 2001, 2019, Simonia et al., 2009). In the eastern and western parts of Georgia (called in ancient times Caucasian Iberia and the kingdom of Colchis, respectively), numerous megalithic structures and their fragments, built by the ancients for various purposes, including religious and ceremonial ones, have been preserved. A certain part of these constructions could be used for observations of celestial bodies – rises and sets of the Sun, the Moon and bright stars. Megalithic complexes, structurally oriented to the north, could have been used to record short periods of time during observations of circumpolar, never-setting stars and constellations. Megaliths in the astronomical context apparently had a dual purpose: as purely observation platforms, structures and simultaneously as religious-ceremonial centers. Considering the fact that the main deities of the ancient Georgians were the Moon, the Sun, and Venus, one can conclude that observations of the risings of these luminaries were primarily used to record time periods, seasons of warmth and cold. This refers to both ordinary risings of luminaries, as well as cheliacal and acronic ones. Simonia (2001) was the first to examine the astronomical significance of the megalithic monument, Gokhnari, and the possible connection of the ancient legend of Amirani with this monument. The concepts of starry practicality and solar stations were proposed. This megalithic complex actually represents a multifunctional ritual and observation center of the Bronze Age, where the ancients worshipped their luminary gods and observed the first rays of the rising Sun to determine time. Simonia & Jijelava (2015) examined, among other things, the functioning of megalithic complexes the Abuli and Shaori solar stations, where the ancients performed their religious ceremonies and observed the sunrises in the days of the summer and winter solstices. Another very interesting megalithic complex, possibly of astronomical significance, is Avranlo, also located in southern Georgia, at an altitude of 1,640 meters above sea level. This large megalithic complex consists of three elements arranged in tiers according to a circle, square, and rectangular symmetry (Zukhbaia, 1975). This megalithic complex still awaits archaeoastronomical study (Fig. 1). However, it should be noted that not every megalithic complex characterized by regular geometric constructivism can have astronomical significance. The landscape of eastern and western Georgia, with its rugged terrain and mountainous and high-altitude relief, encouraged the ancients to utilize these natural features to observe and record the risings and setting of bright luminaries. Gradually, man-made constructivism was added to natural constructivism, when the ancients began to enrich and integrate unified structures into the terrain of a particular area, such as individual menhirs and their rows, various cromlechs, and other megalithic elements, with the goal of “uniting” mountain peaks and depressions with stone devices (if not tools) for (at that time, of course) recording astronomical phenomena, such as the appearance of the Moon as a ”hill” over a specific mountain peak or the ”landing” of a bright

doi: https://doi.org/10.52526/25792776-26.73.1-102

star (such as Sirius) in a specific mountain depression.

Figure 2. Kvatsantsalia. From the public domain www.about.ge.

Given the diversity of Georgia's mountain landscape, it can be assumed that the ancients had a fairly wide range of capabilities for creating artificial-natural "instruments" for observing the appearance and movement of bright luminaries. Since travel by land and sea during the Bronze Age and early antiquity was a difficult and time-consuming task, it can be concluded that for people living at a distance, for example, 180 kilometers, communication and the transfer of knowledge were time-dependent processes. This means that tribes, communities, and settlements separated by tens of kilometers (mountains and valleys) needed to develop their own methods for acquiring knowledge about celestial phenomena. Different regions of the eastern and western parts of Georgia are characterized by their own unique relief. In other words, each tribe or community must have had its own observation platform, megalithic instrument, built-into the landscape, with which it would be possible to accurately fix the sunrise on the day of the solstice and other celestial phenomena. Is this why the mountainous and valley regions of Georgia are so rich in megalithic artifacts and their fragments? The answer to this question must be sought in an interdisciplinary manner, at the intersection of the results and methods of archaeology, ethnography, and astronomy. Thus, the ancients, not far from each other, separated by a mountain ridge, could have had slightly different ideas about celestial phenomena. For those who lived in the field, a specific bright star rose above the horizon even before sunrise, and for those living 12 kilometers to the west, behind the mountain, it would appear an hour later, already at an altitude of approximately 15°, with a slightly different azimuth in the rays of the rising sun. For farmers in fields with a horizon close to the mathematical horizon, the rising of the luminaries differed slightly from the rising of the highlanders. This is because the horizons of the latter were contoured by the outlines of mountain ridges and valleys, clearly situated above the mathematical horizon. For the ancient Georgians, one can mainly speak of the development of mountain-horizon astronomy. At the same time, the celestial phenomena observed by these ancient people were somewhat influenced by the lag factor, proportional to the angular height of the local mountains and depressions. Of course, for the ancients living in the lowlands of Georgia and by the Black Sea, the pattern of rising luminaries was standard—rising above a small circle of the celestial sphere (below the mathematical horizon). The peculiarities of the celestial phenomena observed by the ancients were reflected in their applied arts in drawings, ornaments on stone, metal, and ceramics. In the western part of Georgia (ancient Colchis), in the Mingrelia region, on Mount Kvira is located the irregularly shaped monolith Kvatsantsalia. The width of the conventional sides of the monolith is about 1.5 meters, and the height is approximately 3 meters. The remarkable thing about the Kvatsantsalia monolith is that it stands on one support, a small "leg" or slab, which ensures its vibrational stability. A light touch or a slight wind causes the monolith to oscillate, accompanied by a rhythmic sound. Legends indicate that the speaking monolith Kvatsantsalia was a source of inspiration and predictions for the Lunar priests (Kobalia, 2023). Kvatsantsalia, translated from Georgian, literally means a swaying or rocking stone. We hypothesize that the Kvatsantsalia monolith was used by the ancients as an astronomical

doi: https://doi.org/10.52526/25792776-26.73.1-102

“instrument” and a ceremonial object. In particular, the ancients could observe the appearance of a weak shadow from Kvatsantsalia at the moment of the rising of the ”harvest” Moon—the closest full Moon to the autumnal equinox. Thus, the appearance of a weak shadow of Kvatsantsalia of the appropriate shape and direction was a sign for the ancients indicating the need for harvesting. Here at the Kvatsantsalia, the ancients could celebrate this important date with appropriate ceremonies, as an integral part of the worship of their main deity, the Moon (Fig. 2). On the territory of Georgia, many small metal artifacts from the Bronze Age and antiquity were discovered, symbolizing directly or indirectly bright luminaries and celestial phenomena in general (Simonia & Simonia, 2005). Research of the cultural heritage of Georgia in the context of archaeoastronomical interdisciplinarism is important for understanding the culture and science of the ancients.

3. Ancient Georgian cultural heritage: ethnocosmological aspects

The ethnocosmological beliefs of ancient Georgians have reached us in the form of material artifacts, as well as in the ideas, direct and indirect knowledge of celestial bodies contained in oral narratives, legends, and myths. Moreover, knowledge of the stellar world, which has found its way into Georgian myths and legends, is often characterized by its systematic nature, comprehensively reflecting the ancients’ understanding of the universe as a whole. For example, narratives about the Earth and the Moon; the Sun, the Moon, and stars; the multiplicity of bright stars and their movements, etc. This means that the ancients observed and noted the peculiarities of the rising and setting of celestial bodies, their mutual configurations in the sky, and changes in appearance, for example, the phases of the Moon, etc. The ancients sought to organize what they saw in the sky, giving it universal significance—the Sun and the Moon, bright planets, and stars—as a kind of precise mechanism above the heads of ancient people. In our opinion, the cosmology of the ancient Georgians, which described their understanding of the universe as a whole, was based on the empirical knowledge of the ancients about the movement of the sun, the Moon, and the bright planets (primarily Venus) relative to the stars. Their cosmological concepts could have stimulated the regular measurement of time. For example, the ”fast” Moon, which rotated in a month, and the ”slow” Sun, which returned to the same point in the sky only after a year, is both the systematic nature of the universe and the precise counter of time: days, months, and years. The cosmological ideas of the ancient Georgians are well woven into folklore. As Javakhishvili (1908) showed, in the western Georgian region of Mingrelia (and some other regions), the following names for the bright luminaries were common: Tuta, Taxa, Juma, Tsa, Vobi, Sabateni, bzha, which translated means: the Moon, Mars, Mercury, Venus, Jupiter, Saturn, The sun, respectively. Why exactly this order of luminaries existed should be the subject of a separate study. Here we note that the first Moon and the last Sun seem to encompass this row of planets, opposing night and day, speed and slowness. Here we can see the system, universal concepts of the ancient Georgians. It’s worth noting that the Georgians’ systematic understanding of the world of planets and stars was complemented by the systematic nature of their way of life, ceremonies and rituals, and even the orientation of their homes, where structural elements in the form of small windows were aligned with the points on the horizon where the rising sun appeared on the days of the summer and winter solstice. This testifies to the ancients’ extensive observational experience, knowledge, and desire to see the world as a unified whole, where rational humans play a vital role. They worship their luminary gods, utilize light and heat, count days and nights, and anticipate the coming and going of springs and fall. Farmers in ancient Georgia often linked celestial phenomena (sunrises, moon phases, etc.) and climatic phenomena (wind and rain seasons) into a unified understanding of the world around them. Moreover, they tried to use celestial phenomena to predict the weather, crop quality, and other factors important to their lives. According to Tsotsanidze (1987), in ancient times, farmers in Tusheti (a region of Georgia) used to say: ”The Moon will tell about many things, in particular about bad weather, heat and cold. The waning of the Moon - the beginning of its waning - often corresponds to bad weather. The weather that accompanies the appearance of the waxing crescent will last until the beginning of the Moon waning. If the crescent of the young Moon is turned upward, there will be good weather - a month of drought, but if the crescent is tilted down, there will be bad weather – a month of rain.

If in winter the Moon is surrounded by a ”fence”, that is, if the full Moon is surrounded by a luminous halo, expect severe frosts”; “In the starry sky ”deer flight” - a pale whitish strip seen on the northern side, a sign of clear weather”; “If in the morning the sky turns red, the weather will deteriorate”. This figuratively speaking astro-climatic material is quite rich and characteristic of many oral narratives from various regions of Georgia. It is curious that here, too, the cosmologism of the ancient Georgians prevails,

doi: https://doi.org/10.52526/25792776-26.73.1-102

linking weather phenomena with the bright luminaries of the sky, which, in their opinion, govern the world order. Generally speaking, Georgian ethnographic materials are enriched with astronomical and ethnocosmological elements. Unfortunately, ethnographic materials of Georgia published by various authors in the form of articles and monographs are of an irregular nature within the interests of ethnocosmology. Therefore, it seems appropriate: 1) to work through the already published layer of ethnographic material within the framework of the interests of ancient astronomy; 2) to prepare and carry out expeditions to populated areas, primarily high-mountain regions of Georgia, with the aim of accumulating ethnographic material; 3) to systematize, interpret, and publish the obtained results in the form of a separate monograph. A project of this kind could shed new light on the ethno-cosmological and observational experiences of Georgians that have come down to us from ancient times. It should not be forgotten that Georgian folk poetry and chants are also enriched with references to the Sun, the Moon, and other bright luminaries. In various regions of Georgia, both in the east and the west, people still remember the popular names of luminaries, asterisms, and astronomical phenomena. For example, "mzebudoba" – nesting sun, or "Mravalai" and "Khomli" – popular names for the Pleiades cluster. Many Georgian historical traditions and events were associated with these names (Simonia et al., 2008). Research of the cultural heritage of Georgia in the context of ethnocosmological interdisciplinarism is important for understanding the culture and science of the ancients.

4. Conclusion

In this work, we have examined some archaeoastronomical and ethno-cosmological elements of the ancient Georgian cultural heritage. Megalithic constructions, small artifacts of various shapes and purposes, oral narratives and legends, and Folk names of stars and planets, preserved from ancient times, clearly testify to the astronomical knowledge and cosmological beliefs of the Georgians of those eras. We examined only a small portion of the material, focusing on the instrumental capabilities and systematic nature of the ancient Georgian worldview. These materials, artifacts, and data are scattered and little studied, awaiting the application of new methods, systematic analysis, and subsequent generalization. It would be advisable to prepare and implement special research projects devoted to the development of astronomy in antiquity, both in the eastern and western parts of Georgia.

References

Georgobiani G., 1971, Bulletin of Abastumani Astrophysical Observatory, 40, 207, [in Georgian]

Javakhishvili I., 1908, History of the Georgian Nation, 1, 100, [in Georgian]

Kobalia N., 2023, The Mosaic of the Moon: Essay on Megrelian Mythology and Ethnography. Tbilisi, Intelekti Publishing, [in Georgian]

Simonia I., 2001, Journal of Astronomical History and Heritage, 4, 59

Simonia I., 2011, in Corsini E. M., ed., Astronomical Society of the Pacific Conference Series Vol. 441, The Inspiration of Astronomical Phenomena VI. p. 487

Simonia I., 2019, in Farmanyan S. V., Mickaelian A. M., McKim Malville J., Bagheri M., eds, Astronomical Society of the Pacific Conference Series Vol. 520, Astronomical Heritage of the Middle East. p. 59

Simonia I., Jijelava B., 2015, in Ruggles C. L. N., ed., , Handbook of Archaeoastronomy and Ethnoastronomy. p. 1443, doi:10.1007/978-1-4614-6141-8˙138

Simonia I., Simonia T., 2005, in Metal Artifacts As a Mirror of Ancient Georgian Astronomical World View. Current Studies in Archaeoastronomy. Conversations Across Time and Space. Selected papers from the Fifth Oxford International Conference at Santa Fe. pp 435–440

Simonia I., Simonia T., 2011, in Corsini E. M., ed., Astronomical Society of the Pacific Conference Series Vol. 441, The Inspiration of Astronomical Phenomena VI. p. 409

Simonia I., Ruggles C., Chagunava R., 2008, Journal of Astronomical History and Heritage, 11, 213

Simonia I., Ruggles C., Bakhtadze N., 2009, Journal of Astronomical History and Heritage, 12, 235

Tskhakaia D., 1959, History of Mathematical Sciences in Georgian from Ancient Time until the 20th Century. PGeorgian SSR Academy of Sciences, Tbilisi, [in Russian]

Tsotsanidze G., 1987, From Giorgoba to Giorgoba: Ethnographic Excursions into Tusheti's Recent Past. Sabchota Sakartvelo Publishing, Tbilisi, [in Georgian]

Zukhbaia V., 1975, The Stone Pages of Kartli's Life. Sabchota Sakartvelo Publishing, Tbilisi, [in Georgian]

doi: https://doi.org/10.52526/25792776-26.73.1-102

Communications of BAO, Vol. 73, Issue 1, 2026, pp. 107-116

Astronomical Simulation of UNESCO World Heritage Sites with Stellarium

Georg Zotti *

VRVis Vienna Research Center for Visual Computing, Vienna, Austria

Abstract

An accurate desktop planetarium program can be of great importance for research and explanations in cultural astronomy. The author has developed virtual archaeoastronomy in the free and open-source desktop planetarium "Stellarium". This paper summarizes 15 years of development and highlights applications where the sky and architecture over UNESCO world heritage had to be simulated.

Keywords: *Desktop planetarium, Stellarium, astronomical phenomenology, virtual archaeoastronomy*

1 Introduction

Astronomy is often seen as the oldest science, and it has certainly driven development of other sciences and mathematical methods. Archaeoastronomy deals with the oldest traces of "human engagement" with celestial phenomena, much of which has been expressed in form of structural orientation of built monuments like tombs or temples (Ruggles, 2015).

Some of these monuments and also other landscape features or human cultural achievements have gained importance and acknowledgement from cultural heritage protectors, with UNESCO the most prominent example, for their respective unique values. Ruggles & Cotte (2010, 2017) have collected information about heritage sites of astronomical interest, either of archaeoastronomical value or of value in context of the development of modern astronomy.

As part of research and outreach activity, an accurate and visually appealing simulation engine for astronomical phenomenology is important. This author is part of the Stellarium development team and has improved it over the last 15 years to become a versatile desktop planetarium application for cultural astronomy research and outreach. This paper highlights a few of the developments and applications to UNESCO World Heritage sites.

2 Celestial simulation

Astronomy is a discipline where computation has a long tradition. A tedious but important work of earlier times was the computation and release of an annual almanac for astronomical observation, and especially astronomical navigation purposes. The introduction of mechanized and later electronic computers has greatly eased this task, and the wide availability of programmable pocket calculators and later desktop computers has made the creation of astronomy programs possible (e.g., Zotti, 1996).

For public explanations of planetary phenomena, a century ago the optomechanical planetarium was developed, a dedicated auditorium room with hemispherical dome projection surface and a specialized projector in its center which projects thousands of stars visible to the unaided eye, the Milky Way, Sun, Moon and the major planets. While these have meanwhile seen numerous upgrades to become full-dome electronic cinemas, computer programs have been developed which allow the same explanatory demonstrations on the average desktop computer system (Zotti, 2015).

In summer of 2000, Fabien Chèreau started developing such a desktop planetarium: Stellarium. He decided to create it as free and open-source community project with a handful of co-developers distributed

*Georg.Zotti@vrvis.at

doi: https://doi.org/10.52526/25792776-26.73.1-107

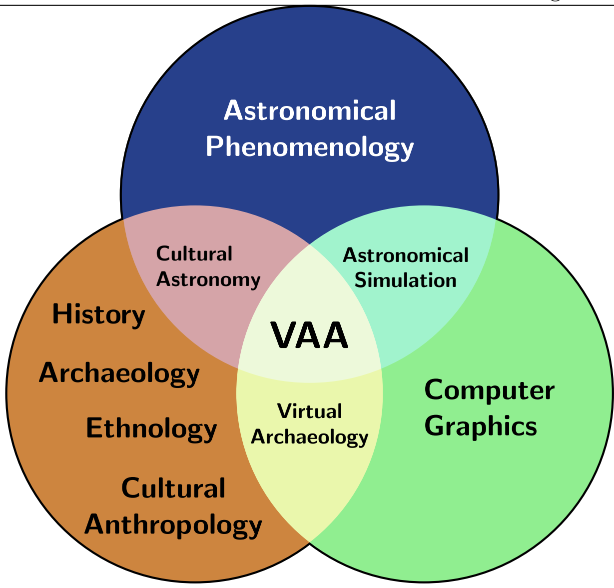

Figure 1: The multidisciplinary nature of Virtual Archaeoastronomy (VAA)

around the globe. Its numerous features which span from driving GOTO telescopes to showing constellation patterns of various cultures gained much attraction among amateurs and astronomy popularizers.

For a research project around potential astronomical orientation in Neolithical circular ditch systems ((Pásztor et al., 2015, Zotti & Neubauer, 2015), ASTROSIM 2008-12) this author needed a good visualisation system. Unfortunately Stellarium at that time was not accurate for historical research, but its open-source nature allowed inspection, corrections, and ultimately the addition of many features which have made Stellarium an almost perfect system for research and dissemination of historical sky views (Zotti & Wolf, 2022, Zotti et al., 2021).

During these years, the present author was involved in several archaeological and archaeoastronomical research projects, some of which also involved sites on the UNESCO world heritage list.

2.1 Scenery3D: Virtual Archaeoastronomy in Stellarium

During ASTROSIM, Zotti & Neubauer (2012) and Zotti (2016) introduced the first round of relevant changes towards virtual archaeoastronomy in Stellarium. This combines three very different research fields: archaeology, astronomical phenomenology and computer graphics (Fig. 1). An important part of virtual archaeology is the creation of virtual 3D models to test hypotheses on the appearance of long-lost buildings. The investigation of potential astronomical components like main axes, view corridors or light-and-shadow phenomena requires adding accurate astronomical models, which are, apart from solar position, generally absent from architectural visualisation systems.

2.2 Why simulate?

It might seem desirable to study the astronomy or sky views from a site of archaeological or historical significance on the actual site. However, this might not provide the relevant observations due to several reasons.

1. Many sites are fragile and should not be visited too frequently to perform the observations necessary to ascertain the postulated importance of astronomical observations.

2. The sky has changed over time. Precession changed rising/setting points (azimuths) of stars, and changes in the obliquity of Earth's axis changed those points for Sun and Moon.

3. Moreover, in urban or near-urban environments, the horizon line may have been changed by modern buildings, and especially the overall impression of the sky has largely been altered by adverse effects of excessive artificial light at night, i.e., light pollution, removing almost all stars and especially the Milky Way from urban skies. A new danger is already threatening even scientific ground-based professional astronomy in the form of uncontrolled growth of "satellite constellations" which also for visual observers have destroyed the solemnity of a natural starry sky.

doi: https://doi.org/10.52526/25792776-26.73.1-107

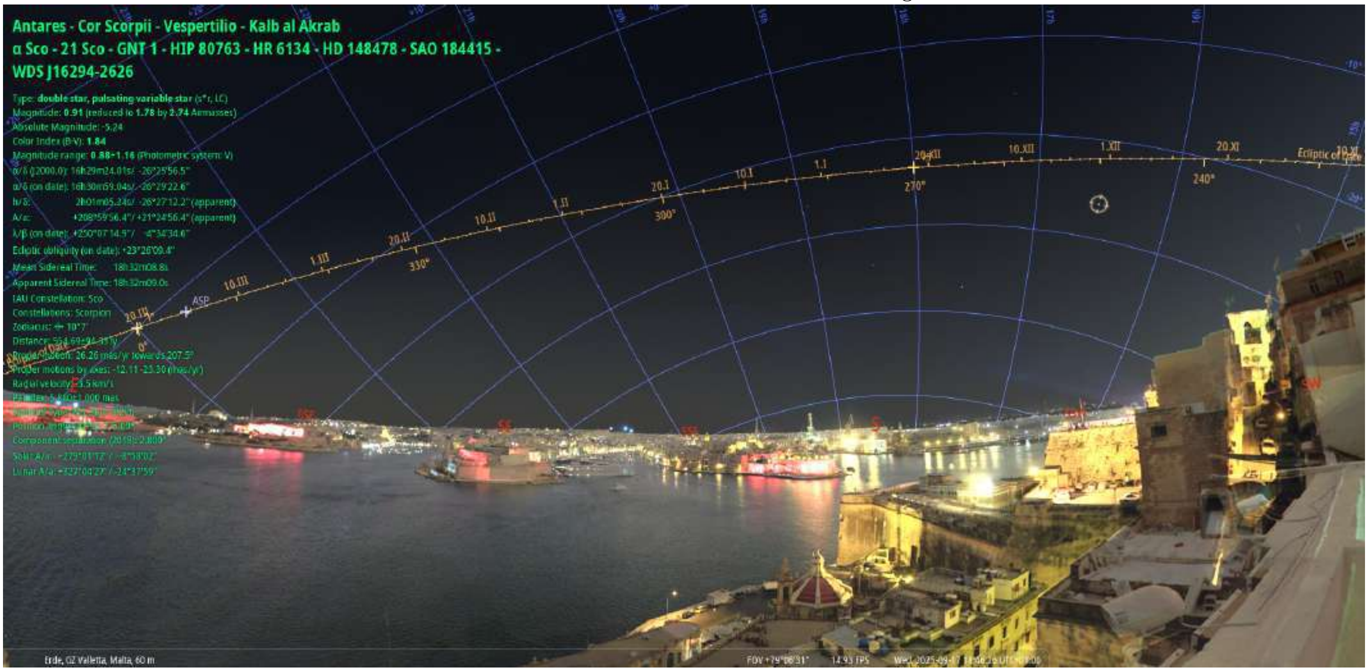

Figure 2: Nocturnal sky over the UNESCO world heritage site of Valletta, Malta. Light pollution diminishes stellar visibility. A dedicated night light layer in Stellarium simulates detailed artificial light at night.

In addition, some celestial cycles, e.g., the Meton Cycle or similar nodal cycle of the Moon, or the orbital motion of Saturn, require decades of observational activity. This can be tremendously sped up by simulation using current high-quality ephemeris models.

3 Stellarium and Astronomical World Heritage

Desktop planetarium programs nowadays allow the inclusion of a panorama photograph or artificial panorama which, when correctly created, allows to accurately discern features along the horizon like mountains or conspicuous rock formations which may relate to important horizon events like solstitial sunrises, sunsets, minor or major standstill moonrises/moonsets (the extreme points in the Lunar orbit repeating in a 18.6 year pattern) or stellar events in the period the observation would have taken place. Obviously, in urban areas, modern buildings would have to be removed from the image, or an artificial panorama can be rendered which depends only on a digital terrain model without buildings. Some websites[1] even allow downloading of landscape files particularly for Stellarium. However, those are usually created from SRTM data and cannot model small details in the nearby environment.

3.1 Light pollution

The sky over many historical sites close to current human settlements has been greatly changed by artificial outdoor lighting. Stellarium can be used to illustrate the effect by globally reducing stellar visibility. Zotti & Wuchterl (2016) introduced the addition of a night light layer to Stellarium's horizon panoramas, with UNESCO heritage site Valletta, Malta, as example (Fig. 2).

3.2 Analyzing astronomical orientation of human-made structures

Frischer et al. (2016) investigated the orientation of a temple in the Villa of Roman emperor Hadrian, the UNESCO WH site Tivoli. An architectural model of a building tentatively named the Antinoeion of which only traces remain today, embedded in a digital terrain model that includes the nearby mountains to the east, was configured as Stellarium 3D scenery. We could identify corroborating evidence for setting this temple into an egyptianizing context that involves the Sun: the entrance axis of the building is in line with

[1] HeyWhatsThat: https://heywhatsthat.com, Peakfinder: https://www.peakfinder.com, Skyliner: https://archaeoastronomyireland.github.io/skyliner. The author has developed a Google Earth-based workflow at https://gzotti.github.io/panoCam.html

doi: https://doi.org/10.52526/25792776-26.73.1-107

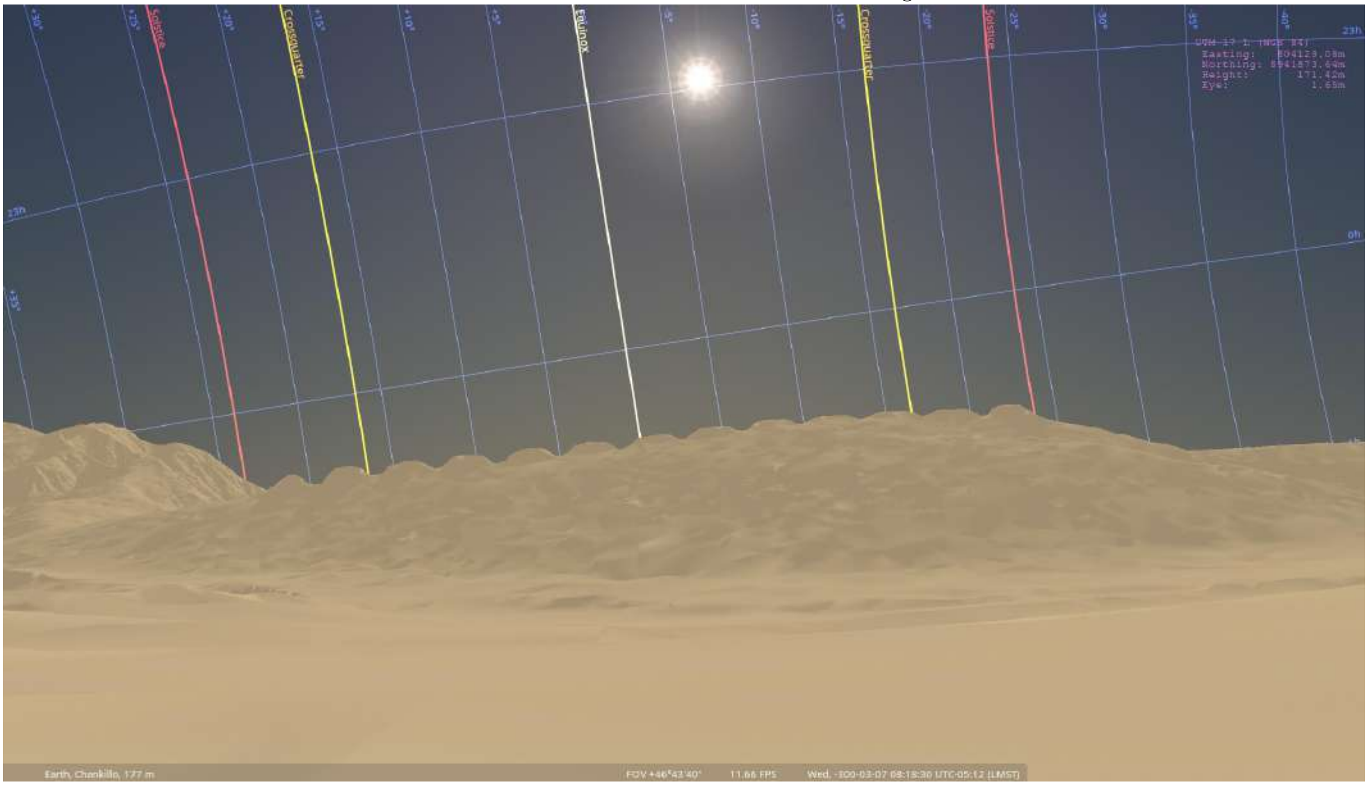

Figure 3: The 13 towers of Chankillo, Peru, cover the range of sunrises when observed from the end of a corridor in a temple. The lines indicate diurnal tracks of the sun at the solstices (red), equator (white) and intermediate dates called "cross-quarter days".

the point of sunrise on summer solstice behind the mountains, so that the statue in the central niche would have been illuminated by the first rays of the rising sun in the days around solstice.

Another very fine example was a 3D model gained from a laser scan of the prehistoric temple of Mnajdra, Malta, courtesy of Heritage Malta. During the SEAC 2014 conference, attendants visited this temple to experience equinoctial sunrise, where the first rays of the sun as it climbed over the nearby terrain ridge falls inside along the entrance axis. Putting the 3D temple model on a piece of Lidar-based digital terrain model, the geometrical light and shadow effects recorded in photographs taken on that date could be accurately replayed, finally indicating that Scenery3D held its promises (Zotti et al., 2021, Figs. 4&5).

Lidar based landscape models have been a game changer for archaeology since the 2000s. The ability to digitally remove vegetation has allowed the discovery of structures hidden in forested areas for centuries, or to create highly detailed 3D models of extended terrain. The principal workflow for model creation for Stellarium was described by Zotti (2019).

A large structure of archaeoastronomical relevance is the UNESCO Astronomical World Heritage site of Chankillo near the coast of northern Peru (Ghezzi & Ruggles, 2015). 13 towers, dated to the 3rd century BC, have been erected along the crest of a ridge. Observed from the end of a corridor in a temple to the west, the sun always rises along the horizon area covered by the towers (Fig. 3).

The extent of this model is huge, however. The Lidar-based terrain is surrounded by SRTM-based terrain of the Andes where the mountains can still be seen tens of kilometres away. And here a limitation of most 3D landscape modelling must be conceded: buildings are placed onto 2D coordinates in the Cartesian UTM (or other) survey grid. Earth curvature is happily ignored, and faraway mountains in the 3D model appear definitely too high when attempting to accurately recreate observations along the horizon. In such cases, use of a classical panorama is recommended, either from photographs (which may however miss mountains on hazy days; see Fig. 6) or from dedicated programs like Horizon (Smith, 2020) – or see section 4.1 for another approach.

Stonehenge is likely the most iconic example of a prehistoric built structure connected to astronomy, and it is on the list of UNESCO world heritage. The latest discoveries from an ongoing project (Gaffney et al., 2018) were presented in an exhibition in Austria, which included full-size replica of the stone circle's central Sarsen "horseshoe" combined with a 25×4 m screen on which Stellarium was used as "Skyscape Planetarium" to present a narrated automated show lasting over 20 minutes (Zotti et al., 2017). On special

doi: https://doi.org/10.52526/25792776-26.73.1-107

Figure 4: Stellarium used on a big screen in an exhibition about Stonehenge. While in daily use a scripted 20-minute story about the Stonehenge landscape was told, during special "flashlight tours" for children, a manual operation mode allowed using it for nocturnal ambience and the iconic summer solstice sunrise.

occasions the museum provided "flashlight tours" for school children who were guided through the dark museum where the starry sky was shining through the stones, and where they found a sleeping "man from the past", an actor who first acted grumpy, but later helped explaining exhibit pieces in his own (unknown) language enhanced with pantomime. The tour ended after twilight was setting in (initiated by the author with Stellarium's then-new RemoteControl plugin on a small tablet) and the group welcomed the iconic summer solstice sunrise within the horseshoe with a little music and dance guided by the "man from the past" (Fig. 4).

Another problem was also solved for a landscape like Stonehenge for which a temporal sequence or "phases" have been identified. When exploring a 3D model in Stellarium, loading a large model representing a different phase disrupts the immersive experience. Zotti et al. (2018) introduced "phased models" which include several versions of the model, and Stellarium's own time control governs the appearance of the appropriate components, to avoid showing, e.g., the early Neolithic timber circle phase under a much later Bronze-age sky.

Archaeological reconstructions can be found as 3D models in some online repositories, which can be configured to be shown in Stellarium following instructions in Stellarium's User Guide. A major problem with most of these models is a lack of proven georeferencing (ground coordinates), so care is advised before trusting any unverified download and drawing wrong conclusions.

4 Advanced Virtual Archaeoastronomy

The 3D sceneries in Stellarium were developed with geometrical analysis of architectural monuments and nearby landscape features in mind. They do not attempt to provide photorealistic simulation of landscapes with vegetation, wind, moving (terrestrial) objects, flowing water or animals enriching the scene. For such tasks, modern game engines provide building blocks for the development of "game realistic" environments. The most popular game engines include Unity and the Unreal Engine. *Serious Gaming* utilizes computer gaming technology for non-recreational purposes. Users typically explore their environment in the first person perspective. In an outdoor landscape environment, the sky often plays a background role only, and in the simplest scenarios is formed by six tiles of a cube, forming a static *skybox*, which are quickly rendered ahead of, and later partially overpainted by the actual scene. More advanced environment modules may provide atmospheric effects like moving clouds or even rain, or a "Sun" light source that can be arbitrarily

doi: https://doi.org/10.52526/25792776-26.73.1-107

Figure 5: The Virtual Instrument Park demo application which shows the combination of Stellarium and the Unity game engine (Zotti, 2021). The user can operate virtual reconstructions of Ghazan Khan's 14th century instruments re-used from Mozaffari & Zotti (2012). In the background a virtual reconstruction of Ulugh Beg's Samarqand observatory (15th century is visible) which users can also explore (Zotti & Muzaffari, 2020). Ambient effects like seasonal vegetation or bird sounds enhance the simulation atmosphere. The sky background is provided by Stellarium.

positioned in the sky as the developer finds useful. "Night sky" modules are commercially available, but even if some are based on real star positions, they often lack sufficient astronomical accuracy (or just don't provide relevant information in the accompanying documentation).

Zotti (2014) and, more exhaustive, Zotti & Neubauer (2019) presented results of their research on Neolithic circular ditch systems in a Unity-based environment with a self-made sky module which included the Sun and the about 9000 stars from the Yale Bright Star Catalog, and which was sufficient to illustrate the final results which were astronomically much less spectacular than originally anticipated (Zotti & Neubauer, 2015, 2023). Unfortunately Unity's proprietary web player browser plugin which allowed guided user visits was removed soon after the project was finished, limiting further project outreach to a few screenhots or pre-recorded animations. This also shows the importance of using open systems for long-time use in the rapidly developing computer game industry.

In the context of astronomical simulation, this author has further experimented with Unity and co-developed a module which combines it with Stellarium in multiple technical modes of operation (Zotti et al., 2020). The simplest mode 1 only creates predefined skyboxes and provides data for the three shadow casting natural luminaries, Sun, Moon and the planet Venus. These can then be mixed appropriately to provide scene illumination similar to what is available in Stellarium/Scenery3D, while the simulation designer may include whatever interaction with scene objects or ambience elements (seasonally changing vegetation, birds singing in the trees, . . .) is required. This mode is also appropriate for providing Unity-based simulations on websites[2].

The other modes require running an instance of Stellarium on the same Windows PC as the Unity-based simulation application. Mode 2 connects the simulation via Stellarium's RemoteControl plugin and sends commands that influence settings in Stellarium, and then triggers the generation of six new skybox

[2]The author has made the Instrument Park available at https://gzotti.github.io/InstrumentPark/index.html

doi: https://doi.org/10.52526/25792776-26.73.1-107

tiles which get loaded to update the current skybox, and a text file with data on Sun, Moon, and Venus. Other settings can still be changed with a quick task switch to Stellarium. The advantage of this mode is the availability of all graphical features and improved capabilities that Stellarium provides at the time of simulation, so that future updates in Stellarium not necessarily require updates in the simulation program (as long as the communication protocol is not changed). A disadvantage of all skybox-based methods however is the limited angular resolution of the skybox tiles which are usually created with 2048^2 or at best 8192^2 pixels resolution. Zooming into the terrain, e.g. to observe a sunrise or sunset, will show this limitation. For the Sun, an actual 3D sphere has been placed into the simulation which enhances observability.

The most immediate mode 3 uses a camera-mounted virtual canvas in the scene on which the output of Stellarium is first displayed before overpainting it with simulation output. The view direction is transferred to Stellarium, which renders a new output to be displayed on the virtual canvas. When the camera (viewer, virtual character) in the Unity based simulation is not moving in the scene, this provides an almost "live view" into Stellarium, and zooming in will also enlarge details in the Stellarium-generated canvas content, which enables the user to observe celestial motions in connection with the simulation scene. Moving around in the scene will however cause a notable frame delay of the sky background. On a PC screen this may be acceptable for research in virtual archaeology, however, this frame delay will make application in setups with VR headsets very problematic.

Zotti (2021) presents this in a demo application, the "Virtual Instrument Park", where visitors can experience the Vienna "Sterngarten" (a modern public observing installation designed to learn about horizon astronomy; the model was originally created by the author for and is available as demo scenery in Stellarium), several virtual reconstructions of observational instruments which had been used in Maragha in the early 14th century re-used from earlier work (Mozaffari & Zotti, 2012, Zotti & Mozaffari, 2010), and devices related to and including Ulugh Beg's 15th century observatory in Samarqand (UNESCO World Heritage) reused from Zotti & Muzaffari (2020).

The user can walk around in a "game-realistic" virtual landscape, observe the sky being reflected in an undulating water surface, and can take actual observations with the old instruments, guided by on-screen instructions (Fig. 5). Some instruments have constructive elements linked to their geographical latitude, so when approaching them, the user is secretly transported to Rayy (Iran) or Samarqand (Usbekistan) as necessary. To decorate the game-like environment, the ground is covered in grass which can change according to the season (solar longitude) to show frost, fresh green or dried summer grass, the visual perimeter is decorated with trees, and bird voices have been planted into the trees. Also the user creates a stomping sound while walking.

4.1 Mitigating the Earth Curvature problem

The scene setup in Scenery3D and most Unity-based applications consists of buildings and landscape features on an otherwise flat surface in Cartesian coordinates. The user can at best read UTM grid coordinates of the current view position. However, any two-dimensional map suffers from its principal simplification of flattening out a piece of Earth's near-spherical surface. For large scenes and far-away horizons, it would be desirable to take earth curvature into account. NAOJ (2022) have developed a system which first utilizes a QGIS plugin to preprocess 300×300 km of a digital terrain model into a curved shape which is then used as game terrain in Unity. When moving in the central part of the game terrain the mountains on the outer area therefore appear properly shifted downward by earth curvature (Fig. 6 left). Unfortunately the reprojecting makes accurate placement of otherwise properly georeferenced scene objects difficult because their UTM coordinates do no longer fit. The simulation connects to Stellarium with a method derived from the one by Zotti et al. (2020). A complete solution might have to involve geocentric Cartesian coordinates and dynamic computation of the local vertical, and developing a complete workflow around these tasks.

4.2 Point Clouds

The natural file format after a laser survey are point clouds, and the creation of meshes is often a challenge. If mesh generation is not part of the processing and no more than a quick check regarding astronomical orientation is possible within some project, you can utilize an extension of the free web based point renderer Potree (Schütz et al., 2020). This program can render large georeferenced point clouds in a web browser window. Again, a skybox can be utilized to enclose the scene with a static background that may include sky and enclosing panorama. If a sky view from a small part of the model is enough, you

doi: https://doi.org/10.52526/25792776-26.73.1-107

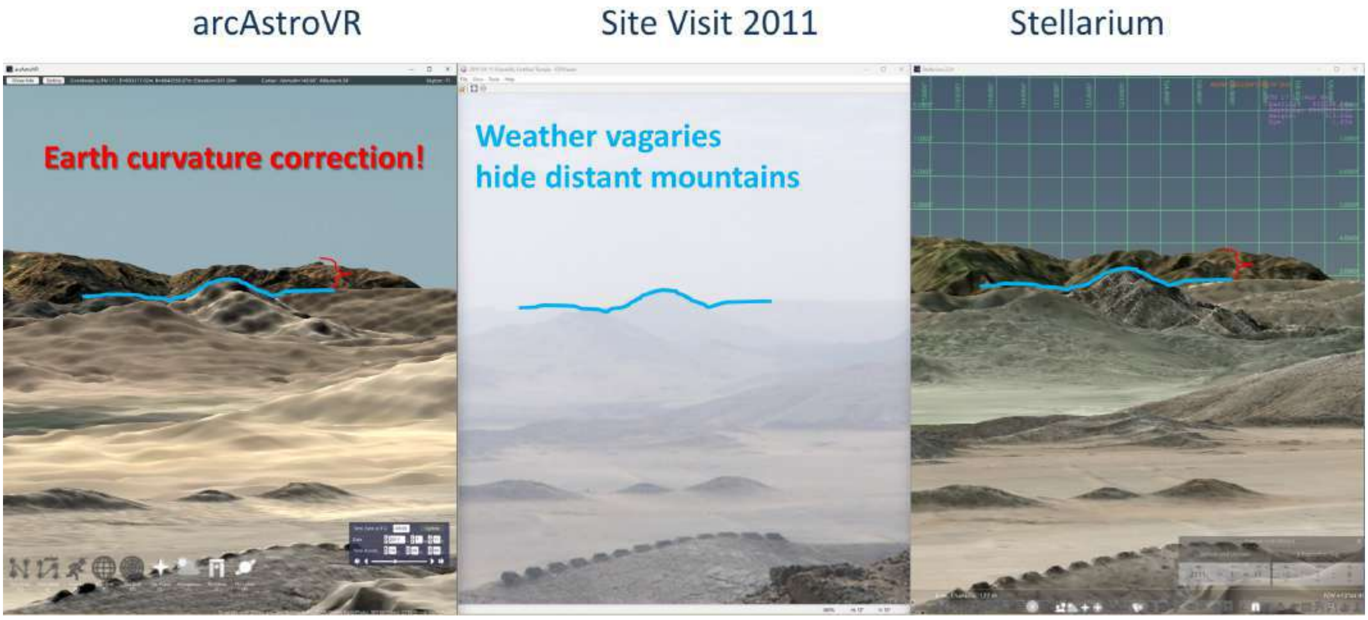

Figure 6: Chankillo, Peru. View over the fortified temple (lower right) and the ridge with 13 towers towards the east. Comparing photo from a site visit (center) with views in Stellarium/Scenery3D (right) and arcAstroVR (left), which itself uses a Skybox from Stellarium. Both simulations show mountains which are no longer visible in the photograph due to atmospheric haze. While the model in Stellarium cannot cope with earth curvature, the terrain in arcAstroVR is processed into a curved shape. The red indicators are of the same size and show the difference in horizon elevation of a few tenths of a degree. It depends on the use case whether this matters, but users ahould be aware of the principal issue.

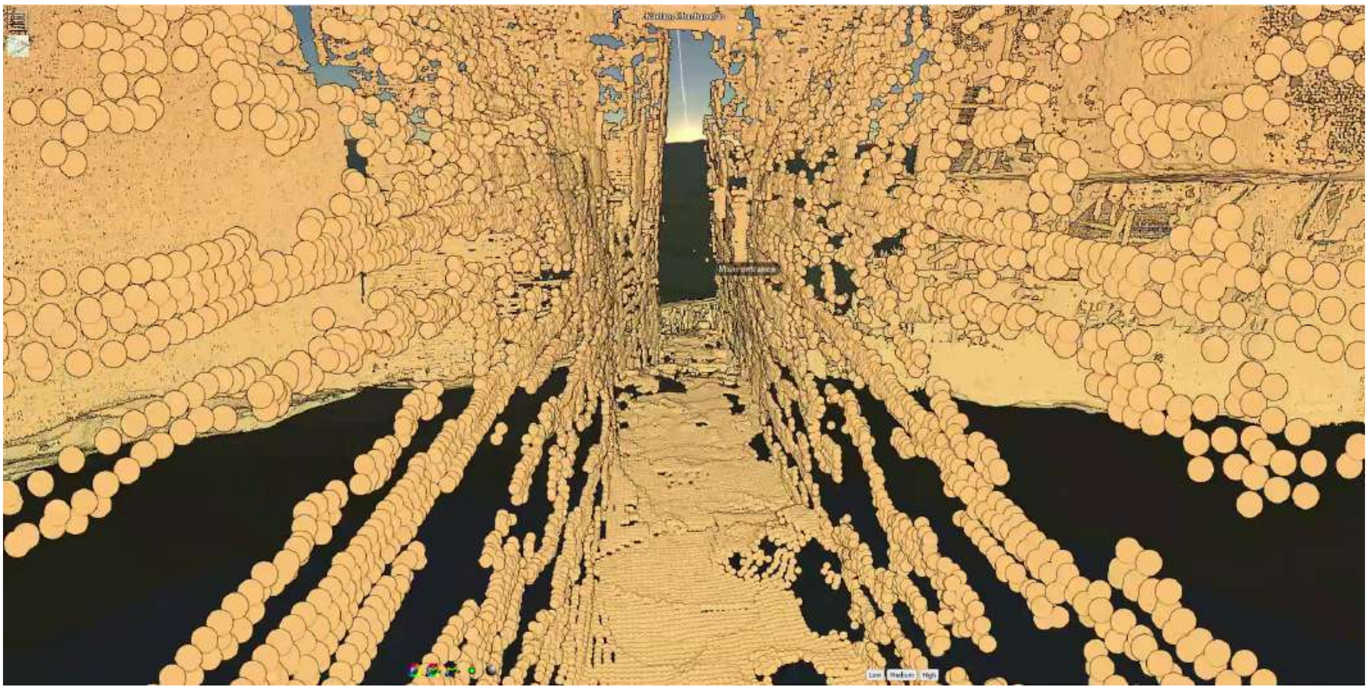

Figure 7: Visualisation of a Laser scan of Kuelap, Peru, in Potree with a skybox created in Stellarium (Zotti et al., subm). The narrow main (southerly eastern) entrance corridor points towards the sunrise azimuth on the day of zenith passage, which also announces the rainy season. Through the entrance you can see the diurnal path of the sun on this day rising above the mountain in the skybox view created in Stellarium. According to 17th century literature, stars and sky observations were important to the Chachapoya, although most details have been lost.

doi: https://doi.org/10.52526/25792776-26.73.1-107

can create a static panorama with Horizon (Smith, 2020) for this viewpoint and use this in Stellarium to create relevant skyboxes with a built-in script. The author's fork of the official repository[3] allows re-loading skyboxes on the fly, and enables Potree users to analyze their data for possible connections to astronomical observations.

Zotti et al. (subm) describe this application for investigations around the Chachapoya fortified settlement of Kuelap, now another UNESCO world heritage site in Peru (Fig. 7). A tower-like building with an opening in the roof had previously been interpreted as zenith observatory. Our new finding of entrance orientation towards sunrise on the day of zenith passage further corroborates interest of the Chachapoya in celestial observation.

5 Discussion

Virtual archaeology has numerous applications in archaeology and historical research for analyzing, understanding and explaining human-made buildings and their natural environment. While architects are often interested in interaction with sunlight and many architectural simulation systems can simulate the sun, the other celestial objects are often neglected and require dedicated software. Most workflows and software presented in this paper are free and open-source and run on most desktop computers, and thus are accessible to all. While technology has been greatly improved in the past 20 years, it requires interdisciplinary interest to bring these systems to good use.

Both astronomy and archaeology often raise public interest and can attract many visitors to exhibitions or public events. Archaeoastronomy is a topic of considerable interest. The astronomy is accessible to typical amateur astronomers and, if well explained, to most exhibition visitors or attendants of public presentations who are interested in the value astronomical phenomena had in the lives of earlier human cultures. However, claims about the astronomy of prehistoric cultures and dating of archaeological structures so that they appear relevant in astronomical context should be reverified in accordance with archaeological dating methods.

While technology for virtual archaeoastronomy is now available, archaeological data are rarely released to the public in a format complete enough for integration to Stellarium or for other use by the interested public. It has been observed that some official authorities' archives store files in proprietary vendor formats which become obsolete within a few years. Those are advised to use well-documented open formats, else digital data which has been collected to help preserving and protecting ancient structures are useless well before significant changes can be seen around the recorded sites.

To allow others experience at least some aspects of the interesting landscape around Chankillo without travelling, Ghezzi and Ruggles agreed to let this author release the 3D scenery created for them as seen in Figure 3 to the public. It can be downloaded from the 3D sceneries repository on the Stellarium website[4], and it is to be hoped that more datasets usable for explaining sites of archaeoastronomical interest can be collected in the future (e.g., Zotti et al., 2024).

Acknowledgements

The core team of Stellarium consists of 3 voluntary developers. Further development of Stellarium depends on continued support by a community of backers and sponsors on OpenCollective. Translation into over 80 languages is the effort of community translators.

References

Frischer B., Zotti G., Mari Z., Vittozzi G. C., 2016, Digital Applications in Archaeology and Cultural Heritage (DAACH), 3, 55

Gaffney V., et al., 2018, Archaeological Prospection, pp 1–15

Ghezzi I., Ruggles C. L. N., 2015, in Ruggles C. L. N., ed., , Vol. 1, Handbook for Archaeoastronomy and Ethnoastronomy. Springer Reference, New York, Chapt. 62, pp 807–820, doi:10.1007/978-1-4614-6141-8˙75

Mozaffari S. M., Zotti G., 2012, Journal of the American Oriental Society, 132, 395

NAOJ 2022, arcAstroVR, https://arcastrovr.org/en/index.html (Accessed 2026-01-10)

Pásztor E., Barna J. P., Zotti G., 2015, in Ruggles C. L., ed., , Vol. 2, Handbook for Archaeoastronomy and Ethnoastronomy. Springer Reference, New York, Chapt. 113, pp 1317–1326, doi:10.1007/978-1-4614-6141-8˙127

Ruggles C. L., ed. 2015, Handbook for Archaeoastronomy and Ethnoastronomy. Springer Reference, New York

[3] https://github.com/gzotti/potree/tree/gz_skyboxExtension

[4] https://stellarium.org/en/scenery3d-collection.html

doi: https://doi.org/10.52526/25792776-26.73.1-107

Ruggles C., Cotte M., 2010, Heritage Sites of Astronomy and Archaeoastronomy in the context of the UNESCO World Heritage Convention. ICOMOS and IAU, Paris

Ruggles C., Cotte M., 2017, Heritage Sites of Astronomy and Archaeoastronomy in the context of the UNESCO World Heritage Convention, Volume 2. Ocarina Books Ltd and ICOMOS and IAU, Bognor Regis and Paris

Schütz M., Ohrhallinger S., Wimmer M., 2020, Computer Graphics Forum, 39, 13

Smith A., 2020, Horizon, http://agksmith.net/horizon/index.html

Zotti G., 1996, in Mucke H., ed., Report on the XII. International Planetarium Directors Conference. Budapest-Wien-Praha, p. 15

Zotti G., 2014, Mediterranean Archaeology and Archaeometry, 14, 271

Zotti G., 2015, in Ruggles C. L., ed., , Vol. 1, Handbook for Archaeoastronomy and Ethnoastronomy. Springer Reference, New York, Chapt. 29, pp 445–457, doi:10.1007/978-1-4614-6141-8˙32

Zotti G., 2016, Mediterranean Archaeology and Archaeometry, 16, 17

Zotti G., 2019, in Henty L., Brown D., eds, Visualising Skyscapes: Material Forms of Cultural Engagement with the Heavens. Routledge Studies in Archaeology. Routledge, pp 35–54

Zotti G., 2021, in Draxler S., Lippitsch M. E., Wolfschmidt G., eds, SEAC Publications, Vol. 1, Harmony and Symmetry (Proc. SEAC2018). tredition, Hamburg, Chapt. 10.1, pp 420–429

Zotti G., Mozaffari S. M., 2010, in Pigatto L., Zanini V., eds, Astronomy and its Instruments before and after Galileo. CLEUP, Padova, pp 157–168

Zotti G., Muzaffari S. M., 2020, Journal for the History of Astronomy, 51, 255

Zotti G., Neubauer W., 2012, in Ioannides M., Fritsch D., Leissner J., Davies R., Remondino F., Caffo R., eds, Lecture Notes in Computer Science Vol. 7616, Progress in Cultural Heritage Preservation. Springer, Heidelberg, pp 170–180, doi:10.1007/978-3-642-34234-9˙17

Zotti G., Neubauer W., 2015, in Pimenta F., Ribeiro N., Silva F., Campion N., Joaquinito A., Tirapicos L., eds, SEAC2011 Stars and Stones: Voyages in Archaeoastronomy and Cultural Astronomy. No. 2720 in BAR International Series. Archaeopress, Oxford, pp 188–193

Zotti G., Neubauer W., 2019, Virtual Archaeology Review, 10, 90

Zotti G., Neubauer W., 2023, in Schier W., ed., Berliner Archäologische Forschungen, Vol. 21, Rondels revisited: Recent research on Neolithic circular enclosures in Central Europe 5000-4500 cal. BC.. Verlag Marie Leidorf GmbH, Rahden/Westfalen, pp 343–355

Zotti G., Wolf A., 2022, Journal of Skyscape Archaeology, 8, 332

Zotti G., Wuchterl G., 2016, in Silva F., et al., eds, The Materiality of the Sky: Proc. SEAC 2014. Sophia Centre Press, pp 197–203

Zotti G., Schaukowitsch F., Wimmer M., 2017, in Henty L., et al., eds, Culture and Cosmos Vol. 21, The Marriage of Astronomy and Culture: Theory and Method in the Study of Cultural Astronomy (Papers from the 2016 SEAC Conference). Culture and Cosmos & Sophia Centre Press, Lampeter, Ceredigion, Wales, pp 269–281, http://www.cultureandcosmos.org/pdfs/21/CCv21_17Zotti.pdf

Zotti G., Schaukowitsch F., Wimmer M., 2018, Mediterranean Archaeology and Archaeometry, 18, 523

Zotti G., Frischer B., Fillwalk J., 2020, Studies in Digital Heritage, 4, 51

Zotti G., Hoffmann S., Wolf A., Chéreau F., Chéreau G., 2021, Journal for Skyscape Archaeology, 6, 221

Zotti G., Reijs V., Rennie E., Carty A., 2024, in Wolfschmidt G., ed., Nuncius Hamburgensis: Beiträge zur Geschichte der Naturwissenschaften, Vol. 53, Der Mensch im Kosmos: Lebenswelten und Kosmologien. — Man within the Cosmos: Lifeworlds and Cosmologies. (Proc. Annual Meeting of the Gesellschaft für Archäoastronomie, Weimar 2023). tredition, Ahrensburg bei Hamburg, pp 88–102

Zotti G., Kucera M., Bornik A., Höller J., subm., in , Proc. SEAC 2023, Sept. 6-8, 2023

doi: https://doi.org/10.52526/25792776-26.73.1-107

Communications of BAO, Vol. 73, Issue 1, 2026, pp. 117-120

Astronomical Terminology in Ancient Armenian and Early Armenian Cosmology

Harutyunian H.A. *

Byurakan Astrophysical Observatory, 0213, Armenia

Abstract

This paper examines traditional astronomical terminology preserved in the Armenian language and discusses its significance for reconstructing early Armenian cosmological concepts. Armenian names of the planets are compared with their ancient Greek counterparts, revealing similarities in the original descriptive meanings assigned to these celestial objects. The myth of Vahagn, one of the principal deities of the ancient Armenian pantheon, is examined as an early cosmological narrative preserved in Armenian tradition. Particular attention is given to the description of his birth, in which the four classical elements—air, earth, water, and fire—appear as fundamental components of the surrounding world. The study demonstrates that language and mythology can serve as valuable sources for investigating early astronomical and cosmological ideas.

Keywords: *History of astronomy, language: Armenian language, Planets: Armenian names, ancient cosmology: Vahagn, birth of Vahagn: four elements.*

1. Introduction

Ancient astronomical knowledge has reached us through a variety of sources, including archaeological monuments, written texts, oral traditions, and language itself. Among these sources, language occupies a special position because it preserves concepts and terms that may have originated many centuries before their written documentation. The analysis of ancient terminology can therefore provide valuable information about the development of early scientific and cosmological ideas.

All ancient societies developed, independently or through interaction with neighbouring cultures, systems of knowledge related to the structure of the surrounding world. This knowledge included the identification and naming of celestial objects, legends explaining their origins, and fundamental concepts describing the organization of the universe.

The Armenian people, as one of the ancient indigenous populations of the South Caucasus and the Armenian Highlands, naturally developed their own understanding of the sky and the phenomena observed in it. These ideas were transmitted through different forms of cultural memory. The earliest evidence may be found in petroglyphs and other archaeological monuments. Numerous astronomical representations have been discovered in the mountains of Armenia. Among the surviving archaeoastronomical monuments, the stone structure of *Zorats Qarer*, often referred to as the Armenian Stonehenge, and the ancient observation site of Metsamor occupy a special place. These monuments have been extensively discussed in the works of Elma Parsamyan, Paris Herouni, Grigor Brutyan, Karen Tokhatyan, Hayk Malkhasyan, and other researchers.

In the present paper, we draw attention to another source of ancient astronomical knowledge: language itself. A language that develops together with its speakers preserves numerous traces of historical experience, including terminology related to the natural world. Comparative linguistic analysis can therefore reveal information about the origin, development, and antiquity of astronomical concepts preserved in Armenian.

The paper first examines traditional Armenian planetary terminology in comparison with ancient Greek names, then discusses cosmological concepts preserved in the myth of Vahagn and the traditional Armenian interpretation of the Milky Way.

*hhayk@bao.sci.am

doi: https://doi.org/10.52526/25792776-26.73.1-117

2. Names of planets

Planets were among the first celestial objects recognized by ancient observers as distinct from the fixed stars. When observing the night sky, people noticed that several bright star-like objects changed their positions relative to the background of stars. This apparent motion distinguished them from other celestial bodies and required a special terminology.

The ancient Greeks called these objects *planētai asteres*, meaning “wandering stars,” or simply *planētai*, “wanderers.” The modern term “planet” derives from this Greek designation.

The Armenian term for a planet, *molorak*, is linguistically different but conveys a remarkably similar concept. The word may be translated as “one who is lost,” “wandering,” or “astray.” In this sense, it reflects the same fundamental idea: an object that does not follow the fixed and regular pattern of the stars but appears to move along an unusual path across the sky.

Notably, the ancient Greeks did not initially use the mythological names Mercury, Venus, Mars, Jupiter, and Saturn for the planets. Actually, these are the third set of names, which represent the Romanized names of Greek deities. Before the mythological names became widespread, the planets were often designated by descriptive terms related to their apparent appearance in the night sky, including their brightness, color, and luminosity.

The traditional Greek names of the five planets were *Stilbon* for Mercury, *Phosphoros* for Venus, *Pyroeis* for Mars, *Phaethon* for Jupiter, and *Phainon* for Saturn. These names can be interpreted as descriptions of various aspects of celestial light: shining, bringing light, fiery appearance, brilliance, and visibility.

Interestingly, the Armenian language has preserved traditional planetary names that express very similar concepts. Alongside the internationally adopted Roman mythological names, Armenian astronomical terminology includes *Paylatsou*, *Lousaber*, *Hrat*, *Loosntag*, and *Yerevak*.

One can compare the names in two languages to reveal that the meanings of these Armenian names correspond closely to the descriptive meanings of the ancient Greek terms. *Paylatsou* refers to shining or glittering, *Lousaber* to the bringing of light, *Hrat* to fire or fiery appearance, *Loosntag* to a luminous or light-related attribute, and *Yerevak* to visibility or brilliance.

Table 1. Traditional descriptive names of the planets in ancient Greek and Armenian traditions.

Planet	**Greek name**	**Meaning**	**Armenian name**	**Meaning**
Mercury	*Stilbon*	Shining	*Paylatsou*	Glittering
Venus	*Phosphoros*	Light-bringer	*Lousaber*	Light-bringer
Mars	*Pyroeis*	Fiery	*Hrat*	Fire-related
Jupiter	*Phaethon*	Bright	*Loosntag*	Crown of light
Saturn	*Phainon*	Shining	*Yerevak*	Visible, brilliant

Evidently, they are similar, and the similarity between these two traditions is noteworthy. However, the available historical and linguistic evidence does not allow us to determine whether the Armenian and Greek terms are directly connected, whether one tradition influenced the other, or whether both preserve elements inherited from an earlier cultural background. Nevertheless, the preservation of such descriptive astronomical terminology in Armenian demonstrates that these concepts were deeply rooted in the ancient perception of the night sky.

The comparison presented in Table 1 demonstrates that both Greek and Armenian astronomical traditions preserved descriptive names reflecting the visual characteristics of planets observed in the night sky. These names are not merely arbitrary designations but an attempt to describe and classify celestial phenomena according to their observable properties.

Moreover, the preservation of such terminology in the Armenian language provides evidence that astronomical observations formed an important part of the ancient cultural and intellectual tradition. Language, in this case, acts as a historical record, preserving traces of how ancient observers interpreted the celestial world around them.

3. The Myth of Vahagn as an Early Cosmological Narrative

Ancient myths often contain early attempts to explain the origin and structure of the surrounding world. Although these narratives are fundamentally different from scientific theories, they preserve important

doi: https://doi.org/10.52526/25792776-26.73.1-117

information about how ancient societies perceived natural phenomena and the organization of the cosmos.

Elements of such early cosmological thinking can be found in Armenian oral traditions, folk narratives, and epic literature. Among these sources, the legend of Vahagn occupies a special place. Vahagn was one of the principal deities of the pre-Christian Armenian pantheon and was associated with thunder, lightning, fire, courage, and victory. His epithet in Armenian *Vishapakagh*, usually translated as "Dragon Slayer" or "Dragon Reaper," reflects his mythical role as a hero confronting cosmic chaos.

The etymology of the name Vahagn has been discussed in connection with ancient Indo-European linguistic roots. One interpretation associates the first part of the name with the Indo-European root *vah-*, meaning "to carry" or "to bring," while the second part is connected with *Agni*, the ancient Indo-Aryan deity of fire. According to this interpretation, the name Vahagn may be understood as "the bringer of fire."

This interpretation corresponds well with the famous account of Vahagn's birth, preserved by Movses Khorenatsi (Movses of Khoren, 410-490 CE), in which the god emerges from a fiery element with hair and a beard resembling flames.

Movses Khorenatsi wrote the most comprehensive medieval historical account of Armenia in the fifth century CE. His work combines historical traditions with mythological narratives and is the earliest known written source to preserve the legend of Vahagn.

Only two fragments of the much longer song about Vahagn have survived. Both fragments are related to the structure of the surrounding world and therefore provide valuable evidence about ancient Armenian cosmological imagination.

The first fragment describes the birth of Vahagn: It tells how Vahagn was born and goes like this:

In travail were heaven and earth,
In travail, too, the purple sea
The travail held in the sea the small red reed.
Through the hollow of the stalk came forth smoke,
Through the hollow of the stalk came forth flame,
And out of the flame a youth ran!
Fiery hair had he,
Ay, too, he had a flaming beard,
And his eyes, they were as suns!

The description of Vahagn's birth contains a remarkable combination of natural elements that later became central components of ancient philosophical models of the physical world. The text mentions heaven, earth, sea, and flame as fundamental parts of the environment from which Vahagn emerges. These elements correspond to air, earth, water, and fire — the four classical elements that were later formulated in ancient Greek philosophy.

It is important to note that the presence of these elements in the Armenian myth does not necessarily imply a direct historical connection with Greek philosophical theories. Rather, it demonstrates that ancient cultures often attempted to explain the origin and structure of the world through a limited number of fundamental natural principles. The Armenian narrative preserves an early example of such cosmological imagination expressed through mythological language.

The concept of four fundamental elements became one of the most influential ideas in ancient Greek philosophy. Early Greek philosophers discussed the nature of the basic substances constituting the world, and Plato later used the term sounding as *stoicheîon* in connection with the classical elements: earth, water, air, and fire.

The terminology associated with these concepts also reflects interesting linguistic developments. The Greek word *stoicheîon* gave rise to the scientific term "element" in many languages, while in Russian the related word *stikhiya* acquired the meaning of a natural force or disaster. In Armenian, the word *tarr* expresses the meaning of "element," while the plural form *tarerq* is traditionally associated with natural forces or phenomena.

Unlike the first fragment, which describes the origin of a cosmic hero, the second narrative provides a mythological explanation of a visible structure in the night sky.

The second surviving fragment of the Vahagn legend concerns another remarkable astronomical phenomenon: the Milky Way. According to the legend preserved by Movses Khorenatsi, Vahagn stole straw from the Assyrian king Barsham during a cold winter night and carried it back to Armenia. While crossing

doi: https://doi.org/10.52526/25792776-26.73.1-117

the sky, some of the stolen straw was scattered along his path, creating the luminous band visible across the night sky.

This mythological explanation is reflected in the traditional Armenian name of the Milky Way, sounding *Hardagoghi chanaparh*, which can be translated as “the Way of the Straw Thief.” The name itself preserves a direct connection between a celestial phenomenon and the cultural narrative associated with its origin.

Interestingly, a similar association between the Milky Way and the concept of straw is preserved in Neo-Aramaic traditions. In Assyrian Neo-Aramaic, the Milky Way is known as *shvil tivna*, meaning “the way of straw,” while another traditional expression, *urha d’gannave*, refers to “the path of thieves.”

Although the exact historical relationship between these expressions remains uncertain, their similarity demonstrates the persistence of a shared symbolic interpretation of the Milky Way within the region’s cultural traditions.

The Armenian scholar Anania Shirakatsi (Anania of Shirak, 610–685 CE), one of the earliest medieval Armenian scientists, also mentioned the Milky Way in his works. Describing its nature, he referred both to the Greek astronomical terminology and to the traditional Armenian name, preserving the legend inherited from earlier generations.

However, Shirakatsi clearly distinguished between mythological interpretation and scientific explanation. He noted that the Milky Way was not actually composed of straw but consisted of countless stars, in agreement with the views of ancient scholars.

The examples discussed above demonstrate that ancient Armenian astronomical knowledge was preserved not only through written scientific texts but also through language, mythology, and traditional names. These sources provide valuable evidence for reconstructing how ancient societies observed and interpreted the sky. The existence of specific astronomical terms and narratives indicates that celestial phenomena were not only observed but also incorporated into the cultural memory of the Armenian people. Language thus represents a long-lasting record of humanity’s earliest attempts to understand the structure of the cosmos.

4. Conclusion

The examples discussed in this paper demonstrate that language can serve as a valuable historical source for reconstructing early astronomical and cosmological concepts. Unlike archaeological monuments or written scientific works, linguistic evidence is often preserved through continuous use over many generations and may retain traces of ancient observations and interpretations of the natural world.

The traditional Armenian names of the planets show that astronomical observations were incorporated into the linguistic system of ancient Armenian culture. The legend of Vahagn and the traditional name of the Milky Way further demonstrate how celestial phenomena were interpreted and preserved through mythology and oral tradition.

Words and terms do not appear randomly in a language. In ancient societies, the creation of a term usually reflected the need to describe, classify, or explain a particular phenomenon. Therefore, the existence and preservation of ancient astronomical terminology provide evidence that observations of the sky occupied an important place in the intellectual life of past cultures.

Further studies combining linguistic analysis, ancient texts, mythology, and archaeological evidence may reveal additional information about the earliest human attempts to understand the structure of the Universe. Such interdisciplinary research can contribute to a broader understanding of the development of astronomical knowledge and the cultural history of science.

doi: https://doi.org/10.52526/25792776-26.73.1-117

Temple of Apollo in Didyma: An Oracle as an Astronomical Instrument

Alper K. Ateş *

İSTEK Belde Schools Observatory, Üsküdar 34664 İstanbul

Abstract

In this conference communique, we summarise our findings on the orientation of the Temple of Apollo in Didyma, published in The Journal of Skyscape Archaeology in 2024. We suggest that the temple is carefully oriented towards the heliacal rising direction of Castor (α Gemini) at an azimuth of 55 degrees. Since in the Archaic and Hellenistic construction epochs the heliacal rise of Castor coincided with the summer solstice, Castor's sighting must have been used as the confirming signal for the beginning of the summer season. We believe the temple was oriented for Castor's early detection and, therefore, for the oracle's timing purposes.

1. Introduction

Since the dawn of archaeoastronomy, the celestial orientations of ancient Hellenistic temples have been a topic of interest. Beginning with Nissen (1907) and Penrose & Lockyer (1893), many scholars have suggested celestial objects as potential markers. Most of these suggestions have focused on the rising directions of constellations sacred to the particular cult. Particularly, Cygnus and Lyra have been primary choices for Apollo related cults due to the belief in the god's migration on the celestial swan and his gifting humans the first harp. Since most temples are oriented towards the east, many inadvertently align with the rising direction of one star pattern or another. Therefore, a scholar must be free of romantic ideas and support a claim, if it exists, with written information or strong data supported by leads from different disciplines. Aware of these facts, we present our study as the first proof of a precise stellar alignment.

Astronomical, architectural, religious, and etymological evidence indicates that the Temple of Apollo in Didyma is a unique structure aligned with a particular position of a specific star.

Figure 1. Temple of Apollo in Didyma (Image source: Public domain)

*aka.alper@gmail.com

doi: https://doi.org/10.52526/25792776-26.73.1-121

2. The Temple of Apollo: An Architectural Instrument

The Temple of Apollo in Didyma (see Fig. 1) is one of the most important religious sites of antiquity. According to tradition, a sacred spring had been revered long before the Hellenic colonisation of western Anatolia. Around the 6th century BC, an Archaic sanctuary was built on the site. This structure served a family of oracles named the Branchidae for 200 years until its destruction by the Persians during the Ionian Revolt. Today, only the stone paving floor and slabs surrounding the well have survived from this structure.

After Alexander the Great's conquest of the region, the temple was rebuilt in a grandiose fashion. The Hellenistic temple was planned to be 110x51m and built on three levels: the adyton (inner sanctum), the pronaos (where pilgrims received oracles), and the ground level (where the stadium and the sacrificial rotunda are located). The columns (21 on the North and South sides, 10 on the East and West) were planned to be 2 meters in diameter and 20 meters in height. The project was so ambitious and overwhelmingly expensive that it was never finished; for instance, out of 116 planned columns, only five were completed (three survive today). Still, pilgrims flocked to the site for 700 years until it was closed, along with other pagan temples, by Theodosius in the 4th century AD.

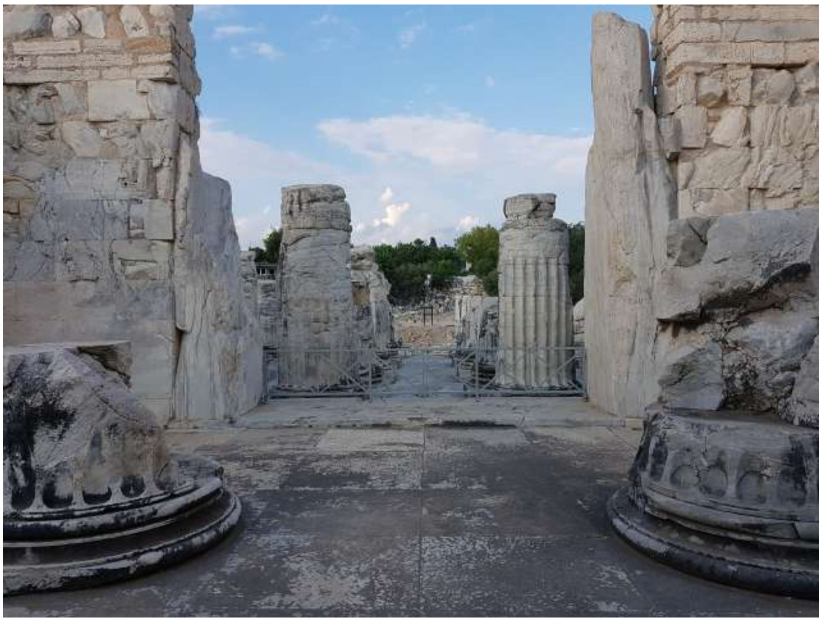

Figure 2. Temple axis is devoid of any terrestrial vantage points (Image by the author)

3. The Orientation Problem

The temple axis is directed towards a 55 degree azimuth. This was first reported by Köster in 2017 and confirmed by myself via GPS measurements in 2023. This is rather an enigmatic orientation with no visible terrestrial vantage point. Believing a structure of this magnitude could not be placed at a random direction, Glenn Maffia suggested a celestial orientation. According to Maffia, the name of the town Didyma (twins) could be a connection between the site and the rising direction of the zodiacal constellation Gemini. Tradition holds that Apollo and Artemis are the twin children of Zeus and Leda; thus, the Temple of Apollo might very well have been oriented towards the celestial twins.

However, this clue soon turned out to be misleading since most scholars of antiquity called the constellation "Dioscouri" (sons of god, after Castor and Polydeuces), not "Didymoi." According to Ulf Weber, Didyma is a native Carian name, very much like Idyma, Loryma, and Syndima; thus, the similarity is a coincidence. The astronomical evidence is also against Gemini, as the rising direction of the constellation is almost 20 degrees south of the temple axis. Once Gemini was eliminated, the two brightest celestial objects, the Sun and the Moon, were investigated. Rigorous simulations using the NASA Horizons tool and professional software quickly eliminated both as potential targets. Neither the Sun nor the Moon crossed the temple axis in any season. Similarly, for the bright planets, 55 degrees was too far from the ecliptic. These simulations also eliminated Apollo-related constellations Cygnus and Lyra, which rose too far north, thus only partially crossing the axis.

doi: https://doi.org/10.52526/25792776-26.73.1-121

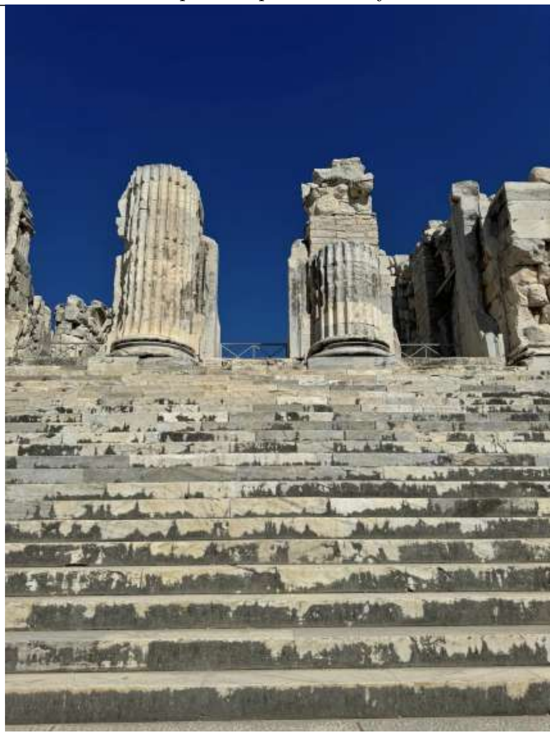

Figure 3. Cresmographeion window (Image by the author)

The final category of targets consisted of stars. A number of naked-eye stars do cross the temple axis, the brightest being Castor and Arcturus. At this point, an architectural detail offers a clue: the sacred open-air adyton is surrounded by massive walls, creating a secluded space. From the sacred spring, only a thin slice of sky can be seen through a specific "visibility window" created by the architectural layout. When observed from the naiskos (the small inner shrine housing the cult statue), the view is blocked in all directions except the temple axis flanked by two massive pillars bordering the chresmographeion (oracle room). This opening creates a 3.2° wide window. It is well known that stars are difficult to detect right over the horizon and must reach a certain altitude to be clearly visible. The unknown target probably had to climb to an altitude above 5 degrees at the azimuth of 55 degrees to be visible.

Figure 4. Castor as Apollo (Bode 1802)

4. Why Castor?

Out of two prominent stars, Castor appeared a more plausible target due to higher altitude and mythological resonance. Throughout history, the celestial twins have been called different names, including Castor,

doi: https://doi.org/10.52526/25792776-26.73.1-121

Pollux, Hercules, and even Helen of Sparta. Some ancient astronomers, including Ptolemy, frequently referred to the star Castor as "Apollo." This name was evident up to 16th-century celestial cartography, including Bayer's Uranometria (1603), Flamsteed's Atlas Coelestis (1729), and Bode's Vorstellung der Gestirne (1801). The name "Castor" gained wider acceptance only in the last 200 years.

Figure 5. Castor's transit through the cresmographeion window (Photo by the author)

The next issue was the significance of the 55-degree azimuth for Castor. Using Ates & Maffia (2024), Lockyer (1894), and Belokrylov et al. (2011) works, we reached the conclusion that the arcus visionis for Castor was at Δh = 14 degrees. During the Archaic and Hellenistic construction epochs, this condition was satisfied in late June during the summer solstice. In other words, Castor's heliacal rise — its first appearance in the dawn sky after a period of invisibility — coincided with the summer solstice. According to tradition, the oracles of Apollo functioned during summer months when the god returned from Boreas after his seasonal migration. Therefore, the summer solstice has long been the harbinger of Apollo's arrival to southern lands. In the Hellenistic period (c. 300 BC), Castor's heliacal rise occurred around June 28th, coinciding with the summer solstice. The star's appearance most likely served as a confirming sign due to the difficulty in estimating the Sun's position along the ecliptic precisely.

Castor's first appearance provided a high-resolution "trigger" for the priests to announce the return of Apollo from the land of the Hyperboreans and the reopening of the oracular season. Therefore, besides all the grandeur, the temple's most significant property appeared to be a subtle one: the narrow opening between the naiskos and the chresmographeion window acting as a natural telescope, shielding the observer from ambient light and predawn glow, which is essential for detecting a star during its heliacal rising. As days passed, the angular separation between the Sun and Castor increased. The star began to appear brighter and easier to detect due to increasing contrast with the background. This event created the illusion of the star emerging from the Sun's glare. Macrobius in Saturnalia gives the etymological root of Apollona as "hurling out of the rays"; this was what the priests were witnessing every year. After the star "hurled out" of the Sun, the oracles began delivering messages to the faithful. Castor's significance is also evident in Milesian coins, where an unmistakable star appears next to cult statues or Roman emperors. This symbolism must be due to an extraordinary reason, not a random ornament.

5. Correction for Precession

The Hellenistic temple axis deviates from the Archaic by 1°45'. This shift is clearly visible between the Archaic stone pavement and the Hellenistic building. The Archaic pavement aligns with the sacrificial rotunda, which used to be on the axis but is now slightly south. This shift can be explained by the Earth's axial wobble (precession). The heliacal rise of Castor shifted from an azimuth of approximately 56.5° in 600 BC to 55.1° in 300 BC. It appears that the star-sighting method was a generations-old tradition and the architects Paionius and Daphnis, aware of this knowledge, deliberately "re-calibrated" the temple to keep the star centered in the chresmographeion window for the new era. We do not expect them to have had modern astronomical knowledge about precession; therefore, they probably corrected what they thought was

doi: https://doi.org/10.52526/25792776-26.73.1-121

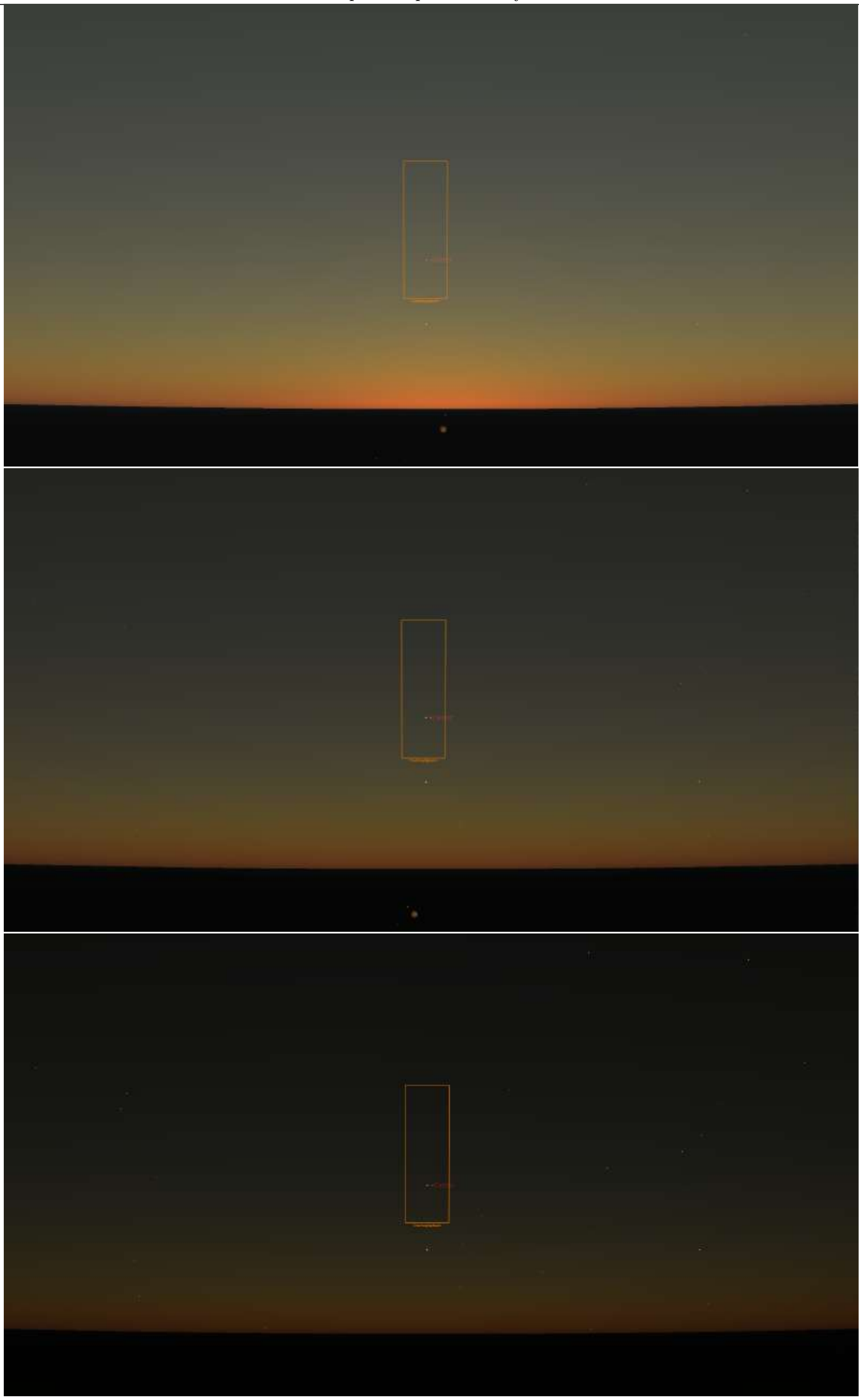

Figure 6. Castor's appearance between June30th-July 7th 3 sidereal days apart (Image by the author using StarryNight v.7)

an error made by the ancients. In either case, this correction is the first detection of precession, a century before Hipparchus.

6. Conclusion

The Temple of Apollo in Didyma is not just a religious center, but a monumental observatory. By aligning the architecture with the heliacal rising of Castor, the priests of Didyma could verify the arrival of the summer solstice with a degree of precision that solar observation alone could not match. The discovery of a precessional correction between building phases provides a ”smoking gun” for intentionality, revealing a sophisticated understanding of celestial mechanics hidden within the secretive traditions of the Apollo cult. The heliacal rise turns out to be an event exclusively witnessed inside protecting walls; we can only imagine the excitement of the priests in the days prior to the summer solstice and the joy brought by the first sighting.

References

Ates A. K., Maffia G., 2024, Journal of Skyscape Archaeology, 9(2), 181

Aveni A., 1972, American Antiquity, 37, 531

Belokrylov R. O., Belokrylov S. V., Nickiforov M. G., 2011, Bulgarian Astronomical Journal, 16, 50

Boutsikas E., 2011, Bulgarian Astronomical Journal, 115(2), 303

Köster J., 2017, DAI Abteilung Istanbul, 67, 373

Macrobius 2011. Saturnalia, vol. 1. Trans. R. A. Kaster. Loeb Classical Library 510, Harvard University Press

Maffia G., 2017, Faint Whispers from the Oracle. Knurów. Faint Whispers from the Oracle. Knurów, Poland: Aslan

Nissen H., 1907, Orientation.. Studien zur Geschichte der Religion, Berlin: Weidmann

Penrose F. C., Lockyer F. R. S., 1893, Phil. Trans. R. Soc. Lond.A, 184, 805

doi: https://doi.org/10.52526/25792776-26.73.1-121

Reviving Indigenous Star Names of the Middle East: Cultural Heritage in Modern Astronomy

Mohammad Sadegh Faghanpour *[1,2] and Saeed Jafari†[1,3,4,5]

[1]IAU OAE National Astronomy Education Coordinator for Iran, Tehran, Iran
[2]IAU Working Group on Star Names, International Astronomical Union
[3]International Decade of Indigenous Languages (IDIL 2022–2032), UNESCO
[4]Department of Linguistics, University of Kurdistan, Sanandaj, Iran
[5]IAU Commission C5 Cultural Astronomy, International Astronomical Union

Abstract

This review examines the revival of indigenous Middle Eastern star names as a resource for astronomy education and cultural preservation. It draws on the IAU Catalog of Star Names and recent reports of the IAU Working Group on Star Names (WGSN), considering 230 officially adopted names classified here according to Arabic, Persian, Sumerian, Hebrew, Turkish, Akkadian and Coptic origins. The review also describes educational infographics that combine astrophysical parameters with historical and linguistic context and were disseminated primarily through social media. Recent WGSN activity shows that standardisation now proceeds alongside the documentation of variant names, etymologies, cultural transfer, and visual traditions. Middle Eastern star names are therefore relevant to both scientific nomenclature and the preservation of intangible astronomical heritage. Their educational use is strongest when an adopted name is presented together with its historical source, linguistic development, and astronomical identification rather than as an isolated label.

Keywords: *cultural astronomy, star names, indigenous asterisms, astronomical nomenclature, intangible astronomical heritage*

1. Introduction

The night sky of the Middle East preserves a rich cultural heritage in indigenous star names, many of which have gradually faded from common use in modern astronomy education. In the catalogue snapshot reviewed for this article, 230 of more than 512 officially adopted names were assigned Middle Eastern origins and represented Arabic, Persian, Sumerian, Turkish, Hebrew, Akkadian and Coptic linguistic traditions. Reference works on modern star names show that many familiar forms entered scientific use through complex histories of translation, transcription and spelling standardisation (Kunitzsch & Smart, 2006). Reviving these names through educational materials can connect astronomy with history, language and cultural identity.

The WGSN was established to reduce ambiguity in scientific publications while preserving historical and cultural stellar nomenclature. Its recent work has moved beyond the standardisation of commonly used spellings toward the documentation of cultural variants, etymologies and names drawn from underrepresented traditions (Hoffmann et al., 025a). Research reported in 2025 further demonstrates that names and constellation figures often record cultural transfer and transformation across Arabic, Babylonian, Greek, Indian and Persian contexts (Hoffmann et al., 025b). This wider historical frame provides the basis for reviewing the Middle Eastern material and its educational use.

2. Review Scope and Educational Representation

2.1. Source Base and Classification

The review uses the IAU Catalog of Star Names, WGSN etymological documentation and the two recent accounts of the Working Group's activities and research findings (Hoffmann et al., 025a,b). Names

*ms.faghanpour@gmail.com, Corresponding author
†saeed.jafari72@gmail.com

doi: https://doi.org/10.52526/25792776-26.73.1-127

were grouped according to their documented linguistic and cultural origins. The categories were treated cautiously where an etymology remains uncertain or a name exists in several historical forms, since the WGSN describes its etymological record as a living resource that is revised when stronger evidence becomes available (Hoffmann et al., 025a).

2.2. Infographic Design and Dissemination

The reviewed educational materials use a standardised infographic template developed in Adobe Photoshop. Each infographic combines the constellation name and Hipparcos identification with apparent magnitude, spectral type, mass, radius, temperature and distance, followed by a short account of etymology and cultural context. The materials were disseminated mainly through social media for educators, students and the general public. Audience responses are mentioned only as contextual observations; they were not collected through a formal evaluation and are not treated here as evidence of educational effectiveness.

3. Middle Eastern Names in the IAU Catalogue

The catalogue snapshot contains 230 adopted names classified as Middle Eastern in origin, approximately 45% of the names reviewed for October 2025. The distribution includes 209 Arabic names, 7 Persian names, 6 Sumerian names, 3 Coptic names, 2 Hebrew names, 2 Turkish names and 1 Akkadian name. Arabic therefore dominates this group, a pattern consistent with the WGSN's broader etymological review and with the historical transmission of stellar nomenclature through Arabic astronomical literature (Hoffmann et al., 025a, Kunitzsch & Smart, 2006).

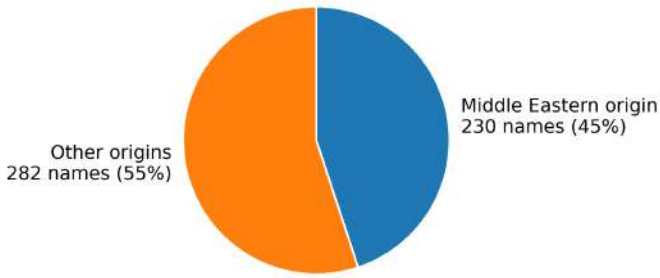

Figure 1. Proportion of adopted star names classified in this review as Middle Eastern in origin, October 2025.

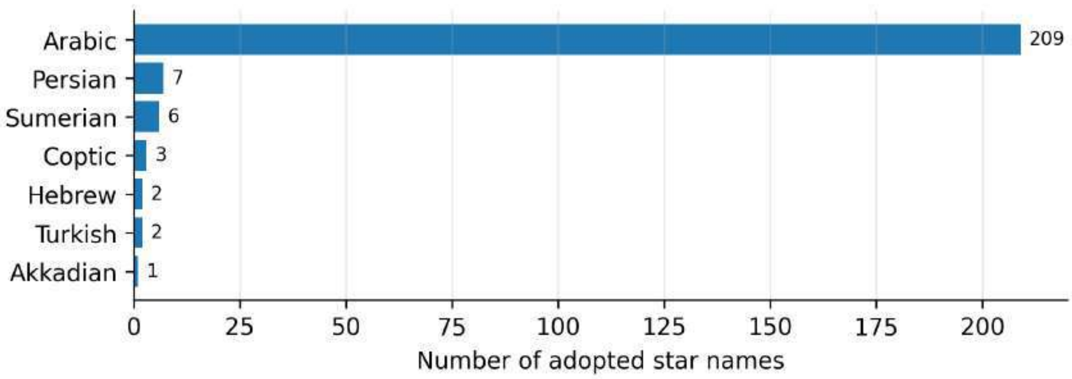

Figure 2. Distribution of Middle Eastern star names by linguistic and cultural origin.

doi: https://doi.org/10.52526/25792776-26.73.1-127

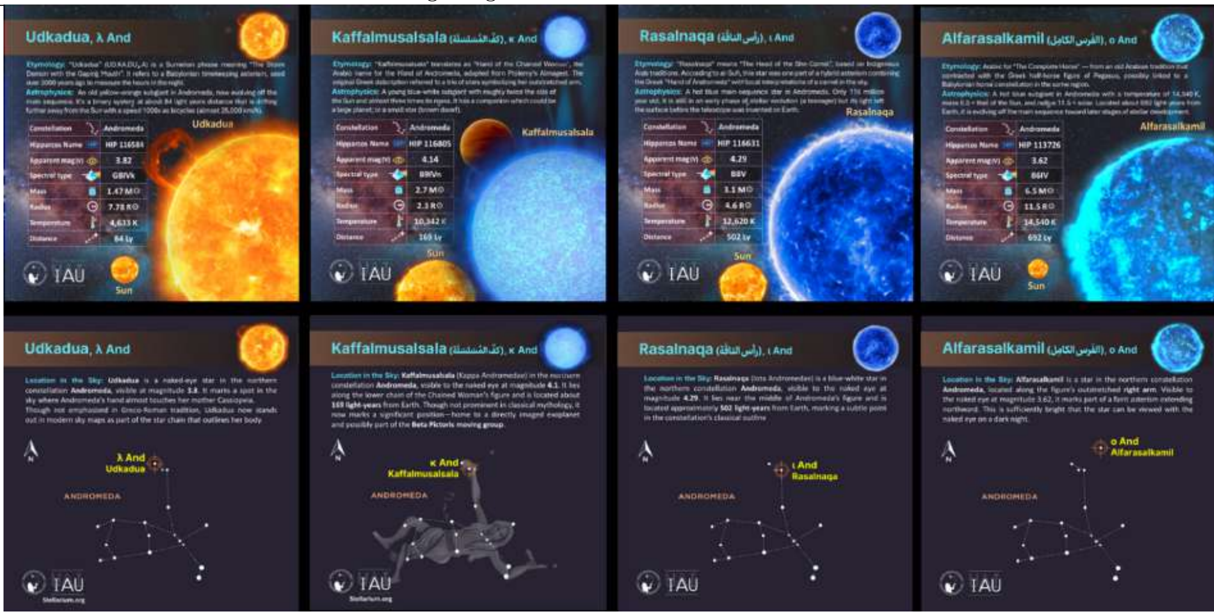

Figure 3. Examples of educational infographics developed for indigenous star names.

4. Discussion

The reviewed material highlights the historical role of Middle Eastern civilisations, especially the scholars and observational traditions through which earlier astronomical knowledge was preserved, translated and reorganised. Indigenous star names retain mythological, linguistic and historical layers of cultural memory, yet their value lies in more than the recovery of alternative labels. Recent WGSN practice separates official standardisation from the broader documentation of heritage: the All Skies Encyclopaedia records etymology, transformation, cultural transfer and visual representation for adopted and non-adopted names alike (Hoffmann et al., 025a,b). Educational resources should follow the same distinction and indicate uncertainty where derivations remain disputed or appear in several historical variants.

5. Future Directions

Future development may include a multilingual catalogue of Middle Eastern star names, an open-access educational database and collaboration with cultural and educational organisations. The WGSN's current encyclopaedia and naked-eye catalogue initiatives offer an appropriate scholarly framework for such work (Hoffmann et al., 025a,b). Additional resources for schools and public outreach should connect each name with a traceable historical source, a clear astronomical identification and an explanation suited to the intended audience.

References

Allen R. H., 1899, Star Names: Their Lore and Meaning. New York: G. E. Stechert

Hoffmann S. M., Vickers D., Mamajek E., et al. 2025a, Journal of Astronomical History and Heritage,, 28(1), 280

Hoffmann S. M., AlAjaji B. B., Shylaja B. S., et al. 2025b, Journal of Astronomical History and Heritage,, 28(4), 1026

Kunitzsch P., Smart T., 2006, A Dictionary of Modern Star Names: A Short Guide to 254 Star Names and Their Derivations. Sky Publishing, Cambridge, MA

Vickers E., et al. 2006, WGSN Task Group for Etymologies

doi: https://doi.org/10.52526/25792776-26.73.1-127

From Khayyām's Calendar to the Chartaqi: Bringing Persian Heritage into Astronomy Classrooms in Iran

Maryam Papari *[1,4] and Saeed Jafari†[1,2,3,4]

[1]International Decade of Indigenous Languages (IDIL 2022–2032), UNESCO
[2]World Space Week Association
[3]Department of Linguistics, University of Kurdistan, Sanandaj, Iran
[4]Commission C5 Cultural Astronomy, International Astronomical Union

Abstract

Iranian astronomy education often presents celestial concepts apart from the cultural materials through which communities have long interpreted the sky. This article examines how Mehr Observatory in Bushehr organised a programme around four resources, the Jalali calendar and seasonal festivals, Canopus as observed from southern Iran, astronomical imagery in Persian poetry and the Jereh Chartaqi. Between 2022 and 2025, 30,000 secondary-school students joined in observations, model building, literary interpretation, international exchange, and field-based inquiry. Evidence comes from activity records, student work, observation notes, and reflective discussions produced during implementation. The article asks how familiar heritage can become a disciplined route into astronomical reasoning and what organisational conditions make that work credible. The activities linked equinoxes, latitude, stellar motion, and solar orientation with regional practices; yet they also exposed gaps in teacher preparation, documentation, and tested learning resources. The programme indicates that heritage gains educational value when learners examine claims, construct representations, and connect local knowledge with astronomical evidence in class.

Keywords: *Astronomy Education; Astronomical Heritage; Cultural Heritage; Archaeoastronomy; Persian Heritage; Inquiry-Based Learning*

1. Heritage at the Edge of the Astronomy Classroom

Iran's astronomical heritage remains highly visible in public culture, yet its place in school astronomy is uneven. The Solar Hijri calendar begins at the vernal equinox, seasonal festivals organise civic life, and celestial imagery remains familiar through poetry, although classroom instruction often reduces the subject to definitions and diagrams detached from those settings. Jafari identified more than 200 local astronomy societies and centres, with amateur networks carrying a substantial share of public education after 2000 (Jafari, 2020). This separation produces the article's central question. How can Iranian heritage enter astronomy lessons as evidence-bearing material instead of mere decoration? Heritage scholarship recognises monuments, landscapes, practices and records as astronomical resources, but classroom use requires tasks that learners can observe, model and discuss critically (Belmonte & González-García, 2016, Ruggles, 2019).

Mehr Observatory in Bushehr developed the programme with student research centres, schools, and educational institutions, and the local setting shaped both content and organisation. Bushehr's southern horizon made Canopus observable, regional poetry gave Suhail a recognisable cultural voice, and nearby Fars supplied architectural remains for field inquiry. Coordination therefore involved suitable dates, access to locations, communication with teachers, and a sequence through which classroom interpretation could lead into observation or modeling.

The four strands addressed one educational problem through different astronomical questions. Calendar activities examined the solar year; Suhail turned latitude into a local constraint on visibility, and poetry required students to translate figurative descriptions into claims about motion or classification. The Jereh Chartaqi introduced orientation, modeling, and the limits of architectural interpretation. Astronomy Day

*maryam.papari99@gmail.com, Corresponding author
†saeed.jafari@spacegeneration.org

doi: https://doi.org/10.52526/25792776-26.73.1-130

in Schools and teacher preparation supported by the IAU Office of Astronomy for Education extended this work beyond one classroom (Pompea & Russo, 2020).

The evidence places clear limits on the conclusions. Activity records document implementation, participant reasoning, and questions generated during the work, but provide neither a controlled comparison nor a standardised learning test. The article therefore examines pedagogical design and changes in explanation, treating the records as evidence of process instead of proof of effectiveness. Such restraint matters in archaeoastronomy, where an attractive alignment may gain authority more quickly than archaeological evidence permits (Ruggles, 2015).

2. Setting, Records and Limits

Secondary-school students participated through Mehr Observatory and partner institutions in classrooms, at observation sites, and during heritage visits. The documentary base included observation notes, student models, presentations, photographs, field records, reports, and reflective discussions produced during teaching. Reviewing these materials together made it possible to reconstruct implementation and compare explanations offered at different stages without treating the records as a formal experimental dataset.

Across the different strands, the activity sequence retained a common structure: a familiar practice or artefact introduced the problem, students identified an astronomical claim, produced an observation or representation, and compared their interpretation with the available evidence. The closing discussion returned to the heritage source and distinguished supported relations, symbolic meanings, and questions requiring further research. The organisation nevertheless changed with the demands of the task. Calendar sessions used solar diagrams and date records; Canopus required suitable dates, a clear southern horizon, and attention to weather, whereas poetry relied on close reading and physical models, and the Chartaqi project required maps, craft materials, and a field visit.

The programme combined contextual, observational, inquiry, and experiential approaches, with each label describing the work students performed. Learners first encountered a problem in a recognisable setting and then used astronomy to examine it. This choice fits cultural approaches to scientific representation (Salimpour & Fitzgerald, 2024) and the astroEDU model, which expects learning goals, materials, and evidence to accompany an activity (Russo et al., 2015). Logistics consequently formed part of pedagogy, as an obstructed horizon, uncertain orientation, or undocumented source could weaken the investigation.

Using one instrument across all activities would have concealed differences among their outcomes and the forms of reasoning they elicited. Explanatory talk before and after observation was most informative for Canopus, whereas models and translations from metaphor to motion mattered more in the poetry work. In the Chartaqi investigation, measurements and competing interpretations carried greater value than a final answer. This mixed record supports an account of practice, but it also exposes missing rubrics, common prompts, and a central archive; future comparison will require shared timing and comparable forms of student response.

3. Khayyām's Calendar and Seasonal Practice

The calendar strand began with an object that students use daily but seldom examine astronomically. The Iranian calendar starts at the vernal equinox and follows the vernal-equinox year, whose present mean length is about 365.2424 solar days (Heydari-Malayeri, 2004). Nowruz linked the year's opening to the March equinox and Yalda directed attention to the winter solstice and changing daylight, with Tirgan and Mehregan extending the discussion toward seasonal memory and agriculture. Khayyām entered through the Jalali reform and the cultural record of the Nowruznameh, allowing calculation, history, and living practice to meet without becoming equivalent (Kennedy, 1963, Khayyam, 2012).

Students examined shadow length, sunrise direction, Earth-Sun models, and calendar comparisons so that broad praise of "ancient accuracy" could be replaced by testable relations. Which event begins the year? Discussion then moved to daylight extremes at the solstices, the effect of latitude on the Sun's apparent path, and the expectation of exactly twelve hours of day and night at the equinox. That expectation opened discussion of refraction and the apparent solar disk, and students considered how calendar maintenance depends on observation, calculation, and intercalation.

Participation in Astronomy Day in Schools gave several calendar sessions an international setting in which Iranian students presented Nowruz and Yalda, shared photographs of Haft-Sin and family gatherings,

doi: https://doi.org/10.52526/25792776-26.73.1-130

and compared latitude measurements with groups elsewhere. Explaining a local practice to peers who knew the same equinox through another season, calendar, or festival required students to make the astronomical relation explicit. Astronomy supplied a common reference for the exchange, although cultural responses to that reference remained distinct.

This strand clarified one condition under which a festival becomes educationally productive. The lesson first identified a measurable celestial relation and then returned to the cultural practice with greater precision, and international collaboration required students to present their own calendar, terms, and images instead of a generic cultural package. This emphasis on local authorship is consistent with participatory approaches promoted in international astronomy education (Russo & Gomez, 2015).

4. Suhail on the Bushehr Horizon

Canopus, known regionally as Suhail, gave the programme its most place-specific observation. With a declination near minus 53 degrees, the star culminates only about eight degrees above Bushehr's southern horizon, where haze, buildings and site choice can determine whether it is seen at all. Participants compared Bushehr with northern Iranian cities, predicted where Suhail would rise and how high it might appear, then used a celestial globe and horizon sketches to relate those predictions to latitude and declination. When the star appeared low in the south, the coordinate system acquired an immediate observational purpose.

Regional accounts associate Suhail's seasonal appearance with moderating summer heat, and facilitators used that association to separate stellar visibility, seasonal timing and the physical causes of temperature change. The discussion preserved the saying as evidence of sustained local attention to the sky, without converting it into a direct causal model. A verse by Fayez Dashti then gave the observation a literary and geographical frame.

> Suhail andar Yemen Bolghar suzad,
> Del-e ashegh ze hejr-e yar suzad...

The reference to Yemen led students back to the sky map, where they examined the star's southern association and its symbolic force in Bushehr. Recorded discussion after the observation contained a more differentiated vocabulary, with participants referring to latitude, declination, horizon altitude and season instead of treating "clear weather" as a complete explanation. The evidence remains qualitative, yet it identifies a plausible learning process in which local knowledge directed attention toward Suhail and direct observation required a coordinate-based account of its visibility.

5. Persian Poetry as Astronomical Evidence and Metaphor

Persian poetry offered a large archive, so selection required an explicit relationship between each verse and an astronomical task. Students first classified examples as observational reference, seasonal or cosmological interpretation, and symbolic use, which helped them identify the kind of claim being made before translating it into contemporary terms. Manuchehri Damghani's account of Banat al-Naśh and Polaris provided the clearest case for examining apparent motion.

> Hami bargasht gard-e Qotb-e Jaddi,
> Cho gard-e babzan morgh-e mosamman;
> Banat al-Naśh gard-e u hami gasht,
> Cho andar dast-e mard-e chap falakhan.

A ball attached to a string reproduced the sling image and supported the discussion of counterclockwise motion around the celestial pole. Khayyām's verse then shifted attention from direction to classification.

> Gāvi ast dar āsemān o nāmesh Parvin,
> Yek gāv-e degar nehofte dar zir-e zamin,

Students identified Pleiades and Taurus, then distinguished a physical star cluster from a conventional constellation figure. The verse showed the organising role of cultural naming in the night sky and the shift in classification when imagery was compared with observation. References to sa'd and nahs encounters introduced readings of planetary conjunctions, which students set beside the definition of an apparent close approach. Hafez's verse brought Venus into the interpretive exercise.

doi: https://doi.org/10.52526/25792776-26.73.1-130

Dar āsemān na 'ajab gar be gofte-ye Hafez,
Sorud-e Zohreh be raqs āvarad Masihā rā.

Students examined the planet's brightness and visibility alongside its association with music and beauty. Literary interpretation opened the problem, after which observation records and planetarium views tested claims about position and appearance. Poetry, therefore, worked as a language for setting astronomical questions, condensing direction, comparison, and memory into lines that could be unpacked through models and observation. Moving between these semiotic systems is central to astronomy learning (Salimpour & Fitzgerald, 2024).

6. Investigating the Jereh Chartaqi

The architectural strand centred on the Jereh Chartaqi in Fars, using the transcription adopted in Assasi's archaeoastronomical study for a square domed unit opened by four arches. Prominent in Iranian architecture from late antiquity, the form later appeared in religious and secular settings, with monumental early Sasanian examples at Firuzabad associated with Ardashir I. Mehr Observatory students selected Jereh through the National Student Scientific Research Competitions and gathered photographs, plans, and earlier interpretations before visiting, so fieldwork began from competing expectations about solar orientation.

Assasi's inventory includes 25 Iranian chartaqi and records incomplete archaeological documentation for several examples (Assasi, 2014). Students, therefore, separated observed orientation from calendrical function and distinguished a possible solar relation from evidence concerning builders or users, following Ruggles's warning that alignment alone carries limited explanatory weight (Ruggles, 2015). At the site, they recorded openings, orientation, and surviving fabric.

In class, cardboard scale models and phone flashlights approximated sunrise and sunset directions at equinoxes and solstices. Students marked illuminated surfaces and shadow boundaries, then identified measurements that required improvement. Would horizon altitude alter solar direction? The question also focused attention on model dimensions, the original form of the openings, and possible reconstruction, showing how a model can expose uncertainty as effectively as it illustrates a proposed alignment.

Preservation concerns emerged from the same inquiry, as damaged fabric and missing context reduce historical knowledge and later educational use. The Heritage of the Sky project had already received more than 200 photographs and gathered 250 people at its award event (Jafari et al., 2020); the Jereh work translated that public interest into a smaller exercise in documentation and interpretation.

7. Lessons from Implementation and Teacher Preparation

Coherence depended on a shared set of decisions concerning the heritage source, the astronomical relation open to examination and the limits of evidence. What evidence is available, and what remains interpretive? Requiring every connection to produce an observation, representation, or research question linked the calendar, stars, poems and monuments without forcing them into one method. Mehr Observatory organised observing conditions, communication with research centres and continuity between sessions; teachers contributed knowledge of students and schedules, and international partners supported ADiS comparisons. Iran's astronomy network offers considerable capacity, although resources and institutional support remain uneven (Jafari, 2020).

Teacher preparation presented the immediate constraint. A two-day Teacher Training Programme supported by the IAU Office of Astronomy for Education involved 20 primary teachers from Fars Province and Pasargadae, combining astronomy education and archaeoastronomy with a visit to Persepolis. Participants framed possible astronomical features as research questions, and their feedback indicated that literature and architecture had rarely entered earlier teaching.

Resource design raised a related issue. A heritage lesson requires verified sources, an age-appropriate task, local language, practical instructions, and a clear distinction between observation and interpretation. The Heritage of the Sky project showed the reach of storytelling and visual media through a national initiative organised by 20 communicators and outreach professionals (Jafari et al., 2020), but classroom use requires documented and reproducible goals.

Future work should prioritise a shared archive, common observation prompts, and modest evaluation tools. Brief explanation tasks before and after an activity could record conceptual change without converting

doi: https://doi.org/10.52526/25792776-26.73.1-130

each session into an experiment, and schools need procedures for field safety, site permission, and image records. Organisational memory must accompany cultural memory.

8. Conclusion

Taken together, the activities respond to a persistent separation in Iranian astronomy education, where abundant cultural materials rarely enter classroom accounts of the sky. Mehr Observatory organised four routes through the calendar: Canopus, poetry, and the Jereh Chartaqi; each began from a local or national reference and required observation, modeling, or critical comparison.

The strongest work used place and practice precisely. Bushehr's latitude made Suhail a low southern star; Persian verse supplied language for motion and grouping, the Chartaqi model brought uncertainty into architectural inquiry, and ADiS placed Nowruz and Yalda within international comparison. Different tasks, therefore, shared one evidential structure.

The records support a limited conclusion about pedagogical design, not a measured claim of effectiveness. More differentiated explanations appeared when familiar heritage led students toward an inspectable problem, and teachers required source criticism, activity design, and organisational support. Without those elements, heritage risks becoming decoration or unsupported history.

The next stage should preserve local character and strengthen documentation across partners through common prompts, samples of student work, and clearer criteria for interpretation. Persian heritage can enter astronomy classrooms as disciplined inquiry when evidence, context, and responsibility remain connected.

References

Assasi R., 2014, Doctoral dissertation, McGill University

Astronomy Day in Schools n.d., Astronomy Day in Schools, Website

Belmonte J. A., González-García A. C., 2016, Astronomy and World Heritage: Across Time and Continents. Cambridge University Press

Heydari-Malayeri M., 2004, preprint (arXiv:astro-ph/0409620)

Jafari S., 2020, Communications of the Byurakan Astrophysical Observatory, 67, 103

Jafari S., Kamkar A., Latani M., Akson A., Abdollahi M., Parsaeyan H., Khalili S. M., 2020, Communicating Astronomy with the Public Journal, 28, 47

Kennedy E. S., 1963, Journal of Near Eastern Studies, 22, 52

Khayyam U., 2012, Nowruznameh. Adib

Pompea S. M., Russo P., 2020, Annual Review of Astronomy and Astrophysics, 58, 313

Ruggles C. L. N., 2015, Handbook of Archaeoastronomy and Ethnoastronomy. Springer

Ruggles C. L. N., 2019, Astronomy & Geophysics, 60, 4.14

Russo P., Gomez E., 2015, Proceedings of the International Astronomical Union, 11, 458

Russo P., Gomez E., Heenatigala T., Strubbe L., 2015, Communicating Astronomy with the Public, 18, 4

Salimpour S., Fitzgerald M. T., 2024, Science & Education, 33, 405

doi: https://doi.org/10.52526/25792776-26.73.1-130

Grigor Brutyan's Discovery of the Ancient Proto-Haykian Calendar of the Armenians (9th Millennium BCE)

H. V. Pikichyan *

V. Ambartsumian Byurakan Astrophysical Observatory, Byurakan, Armenia

Abstract

A fundamental discovery made by the late astrophysicist and calendrical scholar Grigor Hambardzum Brutyan in the field of deciphering ancient Armenian calendars is briefly presented. Prior to his work, it was known that the Armenian calendar, inherited from the patriarch Hayk, consisted of a year composed of twelve 30-day months and five additional days known as "Avelyats" ("added" days). Through a detailed analysis of diverse ancient sources, he succeeded in demonstrating that an even older calendar had existed before it — a system which he termed the "Proto-Haykian" calendar. This discovery was later confirmed through the study of a material artifact dating to the 3rd millennium BCE — a polished clay vessel bearing impressed ornamental motifs. The "Proto-Haykian" calendar consisted of ten months of 30 days each, together with an additional transitional period of approximately 65–70 days that lay outside the principal calendrical cycle. In both calendrical systems, the principal annual festival was Navasard. It began with the heliacal rising of the venerated star, occurring seven days before the summer solstice — on June 14 in the modern calendar. The Proto-Haykian calendar was established in the 9th millennium BCE on the basis of the heliacal rising of Spica, the brightest star of the constellation Virgo, and was associated with the emergence of cereal cultivation. In contrast, the principal star of the Haykian calendar was Betelgeuse. In the Proto-Haykian system, the year commenced with the festival of Navasard, whereas during the supplementary period lying outside the formal structure of the year, the venerated star remained below the horizon and was therefore invisible in the night sky. In everyday social life, these days constituted a period associated with certain prohibitions and restrictions derived from mythological conceptions. In both the Proto-Haykian and Haykian calendars, the position of the principal festival, Navasard, remained fixed. The beginning of the year was likewise fixed in the former system, whereas in the latter it had already become movable.

Keywords: *Ancient calendrical systems; Haykian and Proto-Haykian calendars; Navasard festival; Armenian calendar; Archeoastronomy.*

1. A Brief Introduction to Grigor Brutyan's Study of the Armenian Calendar

Grigor Hambardzum Brutyan was born on June 28, 1955.This year he would have celebrated his 70th anniversary. After graduating from the Faculty of Physics of Yerevan State University with a specialization in astrophysics, he began working at the Byurakan Astrophysical Observatory in 1978. Initially, he focused on the observation and physics of variable stars and published several articles in this field. Starting in 1982, his scientific interests also turned toward issues of calendrical studies. At the Byurakan Astrophysical Observatory, the field of research on the history of Armenian astronomy and calendrical studies had previously been developed on the initiative of Viktor Ambartsumian through the works of Benik Tumanyan and Hayk Badalyan. Several monographs had already been written by them. Brutyan's calendrical studies were particularly devoted to the ancient Armenian Haykian calendar, as well as to the calendrical heritage of Anania Shirakatsi and Hovhannes Sarkavag. These studies were successively summarized in his three monographs:

*hovpik@gmail.com

doi: https://doi.org/10.52526/25792776-26.73.1-135

- The Calendar of the Armenians (1997),
- Anania Shirakatsi's "Kharnikhorran" (1998),
- The Chronological System of Hovhannes Sarkavag (1999).

He was also the author of the fundamental scholarly work that encompasses calendrical studies with encyclopedic breadth:

- Armenian Calendrics (2016).

In Brutyan's works, the numerous confused and often contradictory issues in the field of calendrical studies were thoroughly analyzed and brought into a unified and coherent framework, leading to a number of entirely new fundamental results. It is particularly important here to draw special attention to the estimate he obtained for the beginning of the Haykian calendar, determined through precise astronomical calculations — 2341 BCE. This age estimate, given from a temporal distance of more than 4,000 years, differs by only 151 years from the date proposed earlier by Ghevond Alishan -2492 BCE, and by merely one year from the estimate obtained by Mikayel Chamchian through the examination of historical and philological sources for the war between Hayk and Bel. At the same time, certain fundamental questions concerning the nature of the Armenian Navasard festival and the beginning of the New Year were also clarified. Through the analysis of the Haykian calendar and other related cultural materials, Brutyan also succeeded in uncovering the structure of an earlier calendar that had preceded the Haykian system. He conventionally termed it the "Proto-Haykian Calendar" and presented it in the article:

- On Certain Issues of the Armenian Calendar: The Structure of the Proto-Haykian Calendar, Etchmiadzin, 1996, Vol. 12, pp. 135–164

and was later summarized in the first of the above-mentioned monographs.

Figure 1. Grigor Brutyan

Brutyan established that, whereas the calendar inherited from Patriarch Hayk had a basic year consisting of 12 months of 30 days each, plus 5 additional days, known as "avelats" ("added" days) outside the basic year, the Proto-Haykian calendar comprised only 10 months of 30 days each as its basic year, along with an additional period of 65–70 days lying outside the basic year. In both calendars, the main festival of the year was Navasard, being an immovable festival beginning with the helical rising of the worshipped

doi: https://doi.org/10.52526/25792776-26.73.1-135

star, 7 days before the summer solstice, which corresponds in the present calendar to June 14. In the Proto-Haykian calendar, at the time of its founding in the ninth millennium BCE, the brightest star of the constellation of the Virgin (α Virginis) was worshipped, and by the 24th century BCE, the bright star of the constellation of Hayk (α Orionis), had become worshipped. In the Proto-Haykian calendar, the positions of the beginning of the year and the Navasard festival coincided, they were immovable, and were determined by direct observation of the star's helical rising.

In the Proto-Haykian calendar the main year began with the Navasard festival and during the days lying outside the basic year, the venerated star was located below the horizon, that is, it was not visible in the night sky. In the life of society, these days — stemming from mythological perceptions — constituted specific periods of restrictions. In the Haykian calendar the position of the main festival of the year, the Navasard, was also left unmoved, but the beginning of the 360-day cycle of the 12-month main year and 5 additional days outside it became mobile.

The discovery of the Proto-Haykian calendar, which resulted from Brutyan's examination of the calendrical sources in Armenian literature and of materials from folk tradition, later also received material confirmation. Indeed, archaeologists brought to Brutyan's attention a decorated clay bowl, known as Kreghan, dated to the third millennium BCE. After detailed investigations, Grigor Brutyan demonstrated that the Kreghan is in fact a material carrier of calendrical information. He presented the results of his many years of research in the following articles:

- Ancient Armenian Calendrical Concepts According to the Analysis of the Decorative Patterns of the Kreghan from the 28th–27th Centuries BCE, Bazmavep, 2007, pp. 149–163,
- The Beginning of the Armenian Proto-Haykian Calendar, Bazmavep, 2016, Nos. 3–4, pp. 11–63.

After that, Grigor Brutyan summarized the results of his research on the Armenian calendars in a concise yet systematic form in the semi-popular monograph published by the Byurakan Astrophysical Observatory,

- The Armenian Calendar from Its Origins to the Present (2018).

This book was intended for students and specialists interested in the history of Armenia and the development of its calendars.

He later presented the complete scientific decipherment of the Khreghan calendar in his still-unpublished, extensive monograph entitled

- The Early Bronze Age Armenian Calendar According to the Decorative Patterns of the Kreghan from Keti.

As the editor of that book, I will present — with minor modifications — an excerpt from the "Editor's Preface" placed at the beginning of the monograph, where a concise yet substantive outline of this fundamental work is given.

2. Excerpt from the Editor's Preface to Grigor Brutyan's Then-Unpublished Monograph

The reader is presented with the late Grigor Hambardzum Brutyan's sixth and final monograph, which is the fruit of more than twenty years of his scholarly research. During his lifetime, he prepared the book for publication three times — in 2007, 2011, and 2016 — yet never had the opportunity to see it realized. In the meantime, up until his passing on April 11, 2021, Grigor Brutyan continued to enrich the study with new results, revealing further essential aspects of the problem. The version of the book now presented is the copy that Brutyan last prepared for publication in 2019 and revised in 2020.

The book is devoted to the study of one of the two groups of decorative patterns on the Kreghan, a black-burnished ceramic vessel from the Early Bronze Age (33rd–30th centuries BCE), preserved in the Shirak Regional Museum. The Kreghan was discovered in 1974 in Shirak, in Tomb No. 8 of the Keti burial ground, and belongs to the Shengavit (Kura–Araksian) culture. The artifact was presented to Brutyan in 1987 by the museum's director, Hamazasph Khachatryan. He initially expressed this view orally, and in the 1990s also published an article suggesting that the decorative pattern apparently had a calendrical significance. It

doi: https://doi.org/10.52526/25792776-26.73.1-135

is incised on moist clay by means of impression and includes several distinct symbolic designs. Among them are arranged 365 dot-like marks. The examination and interpretation of the decorative pattern by Brutyan were carried out in several stages, each of which required approximately a decade of research work.

1) In the first stage, the initial assumption — that this was indeed a calendar — was confirmed, and the fundamental structure of that calendar was established. It was revealed that the overall structure of this calendar was similar to that of the "Proto-Haykian" calendar, which Brutyan had previously discovered by an independent line of research through the study of Armenian literary sources, folklore, and other cultural evidence.

2) In the second stage, a detailed examination of the individual motifs of the decorative pattern was carried out. A wide range of Armenian cultural materials was employed — including mythology, epic poetry, folktales, ethnography, archaeology, archaeoastronomical knowledge and concepts, as well as megalithic monuments. During this stage, the meteorological, botanical, zoological, and geographical characteristics of the Armenian natural environment were also taken into account. By comparing this rich body of material, and when necessary, examining the surviving fragments of the cultural heritage of neighboring peoples, Brutyan was able to reconstruct in detail the internal structure of the calendar impressed on the Kreghan. As a result, the reconstructed structure of the Kreghan calendar was presented in the form of a table, using the dates of the modern Gregorian calendar.

Figure 2. Kreghan

doi: https://doi.org/10.52526/25792776-26.73.1-135

3) The third stage was devoted to the correlation of the surviving Armenian day names and month names, and a thorough logical analysis clearly demonstrated the direct identity of the two calendars — the Kreghan calendar and the Proto-Haykian calendar.

4) In the fourth stage, he was able to determine the starting point of the Proto-Haykian calendar with an accuracy of only 80 days. It was found to have begun with the solar rising of Spica, the principal star of the Virgo constellation (whose name in Armenian means *"Ear of Grain"*), occurring seven days before the summer solstice in 9000 BCE, and was associated with the onset of grain-sowing practices in society.

Thus, it became clear that the vessel itself, as a material carrier of the calendar, dates to the late 4th millennium BCE, yet it has nevertheless preserved information about a calendar originating as far back as the 9th millennium BCE.

The basis of Brutyan's decipherment was:

- the discovery of a meaningful connection between the process of grain sowing and the traditional meanings of the names of a certain group of constellations, as well as
- the discovery of the essence of the main Armenian festival, Navasard, as a holiday connected with the summer solstice, the ripening of autumn-sown wheat, and the start of the year.

In the course of his investigation of the problem, Brutyan also made extensive use of certain features related to the geology, fauna, flora, and climate of the Armenian Highlands, drawing on the well-known results of distinguished domestic and foreign researchers in these fields.

Truly, one can be amazed by the wide range and depth of Brutyan's knowledge, by the skill and clear reasoning with which he used it, and by the remarkable persistence he showed in solving the problem. In his calendrical studies, Brutyan consistently applied the concept of the so-called "inverse problem". Such an approach directly stems from his training in physics and mathematics. The idea of the "inverse problem," as the great Viktor Ambartsumian noted—having applied it widely in his fundamental astrophysical research—traces back to Johann Kepler and Isaac Newton. In this approach, true understanding is achieved by keeping away from, as much as possible, any initial pre-assumptions, even widely accepted views and assumptions. In the process of scientific research, one proceeds only from a detailed and careful analysis of the available reliable facts (the observed regularities), includes only indisputable truths, and, when necessary, includes additional relevant information from other fields. On this basis, building a realistic line of reasoning, one proceeds step by step from the observed effect toward the underlying cause of the phenomenon under study.

Brutyan's working style is consistent with this approach and can serve as a practical guide for research work in the field. It is not by accident that Hayk Malkhasyan, a researcher of the Department of Historical and Cultural Astronomy headed by Brutyan, has achieved remarkable progress in recent years by continuing the archaeoastronomical investigations at the Zorats Karer complex that he had begun together with Brutyan. As a result, Brutyan's interpretations concerning the Kreghan vessel and the Proto-Haykian calendar were not only practically validated and refined, but also shed new light on the understanding of Navasard — the ancient principal holiday of the Armenians.

It is important to note that the knowledge obtained at Zorats Karer concerning astronomical observation instruments, the mythological perception of celestial bodies, and the ancient calendrical culture has already assumed the role of a cornerstone in the field of studying renowned monuments and cultural heritage attributed to later periods in other parts of the world.

The present monograph further incorporates a comprehensive overview of the author's scholarly legacy, prepared at my request by Hayk Malkhasyan, Head of the Department of Cultural Astronomy at the Byurakan Astrophysical Observatory, and dedicated to the memory of the late Grigor Hambartsum Brutyan.

3. Conclusion

The discovery of the Proto-Haykian calendar by Grigor Brutyan, the detailed decipherment and verification of its structure through the study of the ornamentation of a Bronze Age ceramic calendrical artifact, and the determination of the epoch of its origin constitute a major achievement in contemporary Armenian calendrical scholarship.

doi: https://doi.org/10.52526/25792776-26.73.1-135

Communications of BAO, Vol. 73, Issue 1, 2026, pp. 140-150

Ancient perceptions of the Pleiades

Ray P. Norris *[1,2]

[1]Australia Telescope National Facility, CSIRO Space & Astronomy, P.O. Box 76, Epping, NSW 1710, Australia
[2]Western Sydney University, Locked Bag 1797, Penrith, NSW 2751, Australia

Abstract

The Pleiades cluster is prominent in many cultures. Curiously, many cultures call it the Seven Sisters while acknowledging that most people only see six stars. They then have stories to explain why only six are visible. Similar stories about the Pleiades are found around the world and are shared by cultures (e.g., Australian Aboriginal and Classical Greek) that have had no cultural contact, even indirect contact, for tens of thousands of years. These curious details suggest the stories may date back to the time when early humans left Africa. This paper is part of a larger study to catalogue ancient references to the Pleiades, to help trace the history and evolution of the ancient myths and artefacts that refer to the Pleiades. This paper has a particular focus on material from Armenia and its surrounding region.

Keywords: *Pleiades; history of astronomy;* ~~*Aboriginal astronomy ; mythology*~~

1. INTRODUCTION

The Pleiades, or Seven Sisters, is an open stellar cluster of young stars formed about 115 to 125 million years ago (Stauffer et al., 1998, Ushomirsky et al., 1998), and is shown in Fig. 1. They are surrounded by a blue reflection nebula resulting from a passing interstellar cloud of dust, moving at 18 km s^{-1} relative to the stars of the cluster (White & Bally, 1993).

The Pleiades are important in many cultures around the world, from ancient Chinese records through to the present day (e.g. Allen, 1899, Avilin, 1998, Burnham, 1978, Dempsey, 2009, Krupp, 1994, Kyselka, 1993, Sparavigna, 2008). In this paper, I use the term "Pleiades" to refer to the astronomical stellar cluster and the term "Seven Sisters" to refer to the human perception of the cluster.

The most widely-known version of the Seven Sisters story comes from classical Greek mythology (e.g. Homer, 850), in which the Seven Sisters are named after the seven Pleiades sisters, who were the daughters of

*ray.norris@csiro.au

Figure 1. The Pleiades, showing the names of the seven brightest stars.

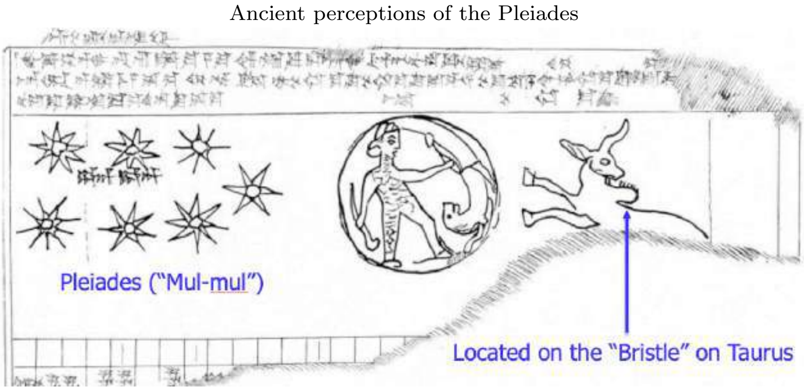

Figure 2. The Pleiades ("mulMul") depicted in the Babylonian Seleucid tablet, VAT 7851, taken from Verderame (2016). The seven stars of the Pleiades are shown on the left, and their position is on the "bristle" of the bull, Taurus, shown on the right.

Atlas and Pleione. After being forced by Zeus to hold up the sky, Atlas was unable to protect his daughters, who were being pursued with lustful intentions by Orion the hunter. To save them, Zeus transformed them into stars.

Very similar stories about the Pleiades and Orion are found in many other cultures. For example, many Australian Aboriginal cultures associate the constellation Orion with a virile man or a group of young men, and many have stories in which the Orion-man is trying to chase and rape the Seven Sisters (e.g. Johnson, 2011, Massola, 1968, Mountford, 1976, Norris, 2016, Norris & Norris, 2009, Pascoe & Norris, 2026).

For example, the Anangu people in central Australia call Orion Nyiru and say that he is chasing the Seven Sisters (Kunkarunkara). A typical version of the story[1] is that Nyiru chased the sisters from northern Australia past Uluru (Ayers Rock) until they hid in Walinynga Cave in South Australia. Nyiru manages to capture and rape the youngest sister, but the other sisters escape from the cave, rescue the seventh sister, and fly up into the sky. This rescued sister is the "missing" star.

In some versions of the story, the bright star Aldebaran, between Orion and the Pleiades, is a dingo dog that tries to protect the girls from Orion.

These same elements are found in many other stories around the world, suggesting a common origin.

1.1. This paper

In this paper, I examine evidence for ancient representations of the Pleiades, with a particular focus, given the location of this conference at Byurakan Observatory, on the area around Armenia. This is an important area for the history of astronomy, given its proximity to Mesopotamia, where our constellations are said to have originated around 1000-3000 BCE (Rogers, 1998), and to Gobekli Tepe, which may be our oldest ($\sim$ 9000 BCE) astronomically-aligned building (e.g. Malkhasyan, 2024).

Section 2 of this paper describes the earliest images that may represent the Pleiades, and Section 3 discusses why most people only see six stars in the "Seven Sisters". Section 4 discusses the similarity of the Seven Sisters stories from around the world, and Section 5 describes the phylogenetic analysis of the Seven Sisters stories. Section 6 discusses the evidence for early representations of the Pleiades in the region around Armenia, and Section 7 presents the Conclusions.

2. The Earliest images of the Pleiades

The oldest known reliable representation of the Pleiades (or "mulMul") is said to be from the Babylonian Seleucid tablet, VAT 7851, dated to about 300 BCE (Verderame, 2016), shown in Fig. 2. The fact that this tablet shows the seven stars of the Pleiades in roughly the right positions, shows their position on the back of Taurus, and refers to them in the text lends credibility to this claim.

The next oldest reliable reference to the Pleiades is in Ptolemy's Almagest (Ptolemy, 150), published in about 150 CE. That listed four of the stars of thr Pleiades and their positions, but an image was not made until the Persian astronomer Abd al-RaḥmānAl Sufi produced his book Kitāb ṣuwar al-kawākib ("The Book

[1] https://songlines.nma.gov.au/walinynga-rock-art/0/

doi: https://doi.org/10.52526/25792776-26.73.1-140

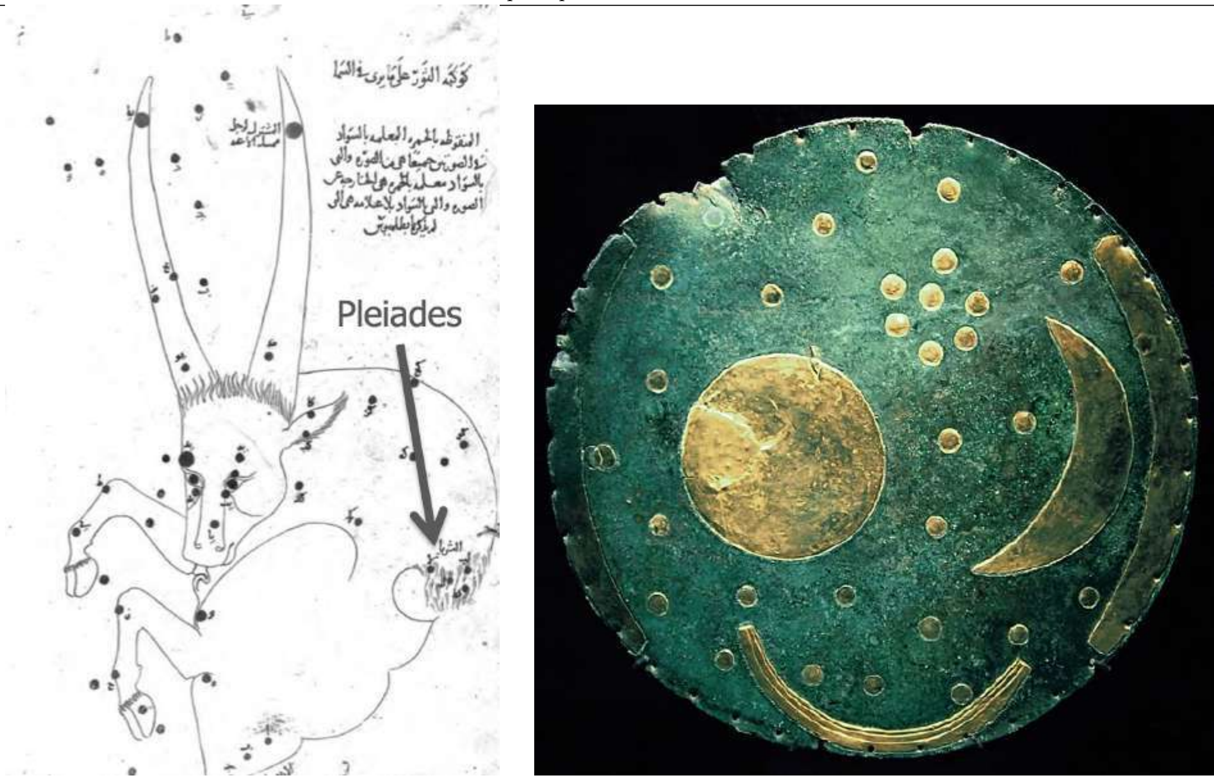

Figure 3. (left)The Pleiades depicted in Al Sufi's Kitāb ṣuwar al-kawākib ("The Book of Fixed Stars"). Like the Babylonian tablet, the seven stars of the Pleiades are shown on the "bristle" of Taurus. (right) The Nebra disk , dated to ∼1600 BCE, which is said to show the seven stars of the Pleiades above the sun and moon.

of Fixed Stars"), in 964 CE (Al-Sufi, 964). Like the earlier Babylonian tablet, Al Sufi shows the Pleiades on the bristles on the back of Taurus, as shown in Fig. 3(left).

A possibly older image is the Nebra disk, shown in Fig. 3(right), which was found in Germany in 1999 and is dated to ∼ 1600 BCE (Pasztor, 2015). Above a circle and a crescent which are said to represent the Sun and Moon are seven dots which are said to represent the Pleiades. However, the dots are not arranged in a shape that resembles the Pleiades, and there is no other information suggesting a connection with the Pleiades, so the identification of these dots with the Pleiades seems tenuous.

Even older, and even more controversial, is an image from the Lascaux caves in France dated to about 20,000 BCE. Six dots above an antioch (an ancient, and now extinct, member of the cow family) are suggested by Rappenglück (1997) to represent the Pleiades on the shoulders of Taurus, as shown in Fig. 4.

In defence of this suggestion, the six dots really do resemble the six obvious stars of the Pleiades, and they are shown on the shoulder of Taurus, just as the Al Sufi image shown in Figure 3. It can even be argued that there is a double dot at the position of Atlas/Pleione. On the other hand, archaeologists have pointed out that there are many other dots amongst the cave painting which do not seem to represent stars, and, most crucially, these images were painted some 17,000 years before the constellation of Taurus was thought to have been defined in Mesopotamia. Thus, if this suggestion were correct, it would necessitate a major rewrite of the early history of astronomy, and we have no other evidence of these constellations at that early date. So this suggestion must remain speculative unless more evidence is found to support it.

Another potentially older image may be found in the rock art at Marra Wonga, Australia (Taçon et al., 2022), with a probable date of about 3000 BCE. This site is perhaps unique in possessing ancient rock art combined with local traditional knowledge of the meaning of the rock art. The rock art includes a cluster of seven star-like designs (see Fig 5) said by Elders to represent the Seven Sisters. As in other Australian Aboriginal stories, the Seven Sisters are said to be chased by an evil man with a big penis. In some versions associated with Marra Wonga, the oldest sister is raped by the man. However, the engravings of the Seven Sisters unfortunately do not appear to be an accurate representation of the stars of the Pleiades, and so may be symbolic rather than literal.

A very similar story, summarised in Section 1, is associated with the painted figures in Walinynga cave

doi: https://doi.org/10.52526/25792776-26.73.1-140

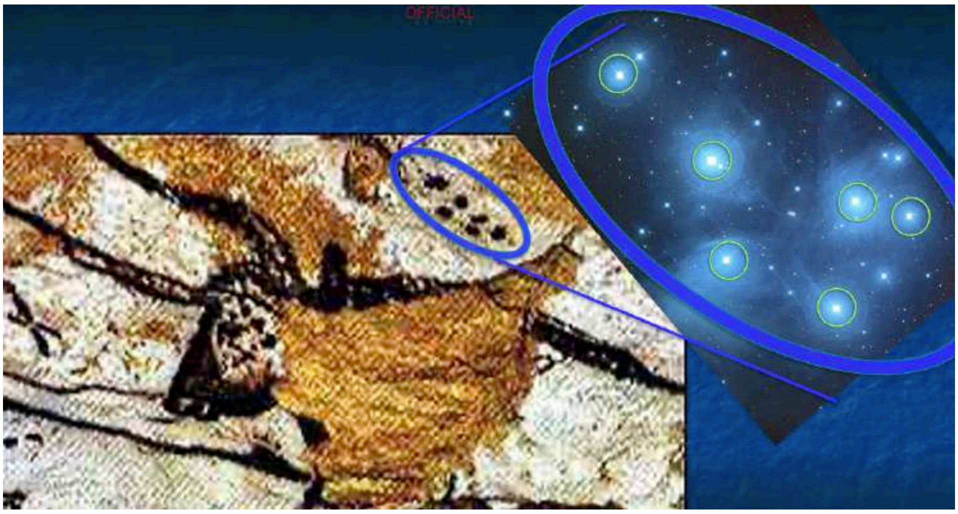

Figure 4. A cave painting from Lascaux, France, dated to about 20,000 BCE, which is controversially claimed to show the Pleiades above the shoulder of Taurus (Rappenglück, 1997). The inset shows the actual image of the Pleiades, revealing a strong similarity to the positions of the painted dots.

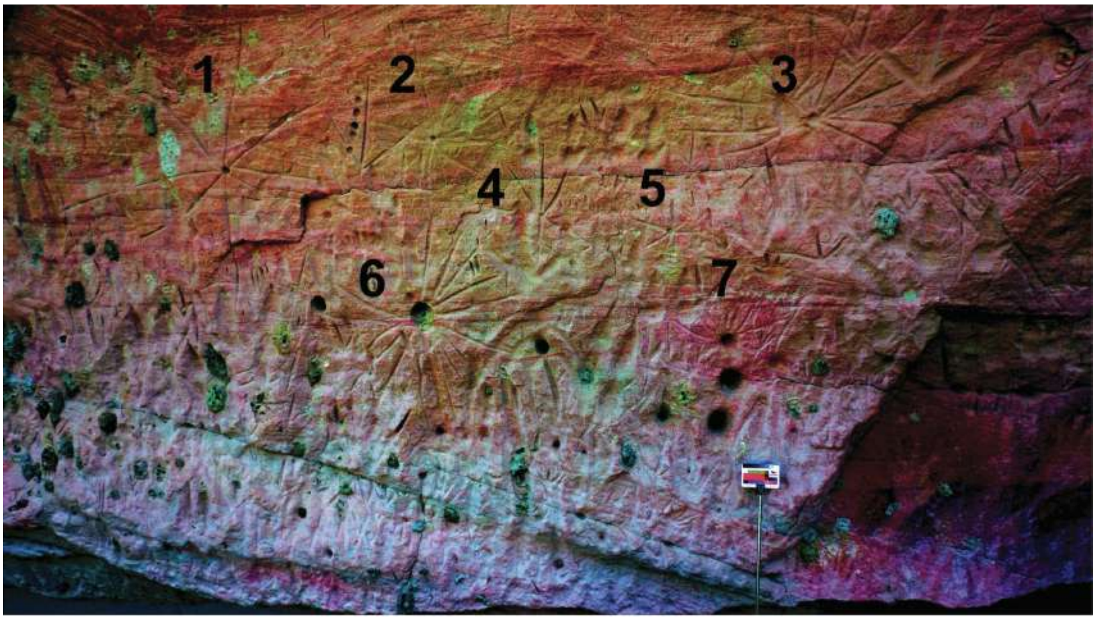

Figure 5. The engraving of the Seven Sisters from Marrawonga, Australia, reproduced with permission from Taçon et al. (2022).

doi: https://doi.org/10.52526/25792776-26.73.1-140

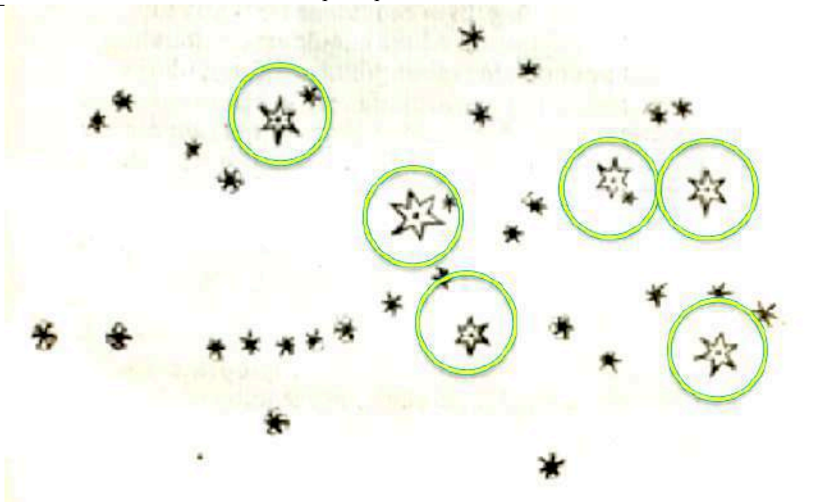

Figure 6. Galileo's diagram of the Pleiades, from Galilei (1610). He shows the six naked-eye stars as large stars (encircled here for clarity), and shows fainter stars, visible only with a telescope, as smaller stars. Note that he does not include Pleione as a naked-eye star.

in South Australia. These show the Seven Sisters as part of the "Seven Sisters songline" which is focussed this cave. These paintings have been dated to before 1000 BCE (but may be much older), and, according to local oral tradition, show the Sisters from the Pleiades cluster, but they do not show any representation of the Pleiades cluster itself.

3. How many stars in the Seven Sisters?

Classical Greek mythology says that the Pleiades were the seven daughters of Atlas and Pleione, and so a purist might argue that the stars Atlas and Pleione (see Fig. 1) should not be included in the Pleiades.

However, we may be guided by Galileo, who **did** include them (see Fig. 6), and said "I have depicted the six stars of the ... Pleiades. I say six intentionally, since the seventh is scarcely ever visible." (Galilei, 1610). Like Galileo, most modern authors include Atlas and Pleione in the Pleiades (e.g. Burnham, 1978). Also like Galileo, most people with good eyesight, in a dark sky, see only six stars (Kyselka, 1993). The first documented mention of the Seven Sisters only having six stars goes back to the third century BCE, when the Greek poet Aratus of Soli named the Seven Sisters but then reported that "only six are visible to the eyes" (Krupp, 1991). It seems that many traditions regard the cluster as having seven stars, but acknowledge that only six are normally visible.

Stories from around the world explain that you can't see the seventh star, which is sometimes called "the lost Pleiad", and then have a story to explain why the seventh is invisible. For example, Greek mythology recounts how one of the sisters, Merope, fell in love with a mortal and her shame caused her to fade from sight (Sparavigna, 2008). Many Australian Aboriginal stories say that the seventh star is missing because one of the sisters has died, is hiding, or has been abducted (Fuller et al., 2014, Kyselka, 1993). There are many similar stories from around the world, such as that from the Onondaga Iroquois (Krupp, 1991) in which one of the stars sang during their ascent to the sky and thus became fainter.

These stories suggest that at some time there really were seven easily visible stars, one of which is now missing. In the words of Hertzog (1987), "the combined testimony of numerous societies, spanning continents and millennia, [militate] for a seventh easily visible ... Pleiad which subsequently dimmed".

So what happened to the seventh star? Possible explanations include:

- Many of the Pleiades are B stars, which are often variable. The long-term variability of B stars is poorly understood, and it is possible that one of the faint stars in the Plaeiades was much brighter in the past. However, there are no data to support this hypothesis.

- It is also possible that one of the stars exploded in a supernova, but there is no evidence for a supernova remnant in the Pleiades.

doi: https://doi.org/10.52526/25792776-26.73.1-140

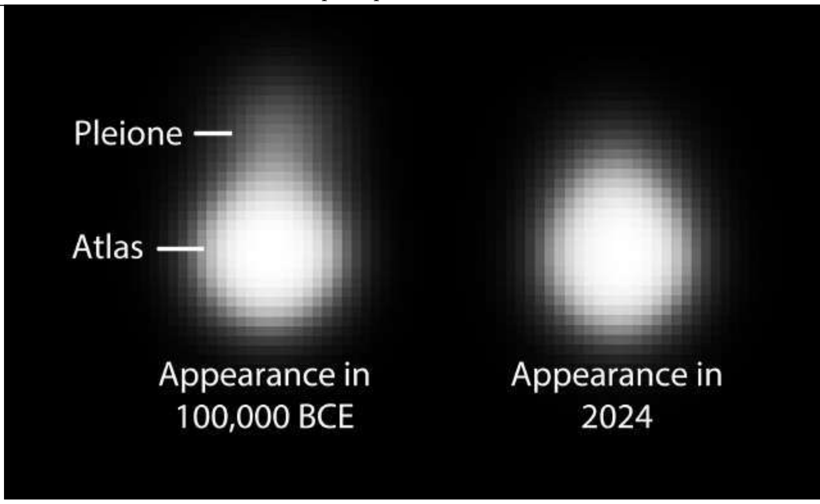

Figure 7. The appearance of Pleione and Atlas in 100,000 BCE and now, based on Norris & Norris (2021) but updated to use more recent astrometric data from Gaia (Gaia Collaboration et al., 2023).

- We have previously noted (Norris & Norris, 2021) that Pleione, despite being magnitude 5.1, is currently invisible to most human eyes because of its proximity to Atlas. For example, Galileo (Galilei, 1610) did not list it as a naked-eye star, although he could see it with his telescope. However, Norris & Norris (2021) pointed out that, because of its proper motion, Pleione was slightly further away from Atlas, and thus visible to most humans, 100,000 years ago, so may have been the lost Pleiad (see Figure 7). But this implies that this story is 100,000 years old, making it by far the oldest known story. Nevertheless, this hypothesis has some supporting evidence, discussed in Section 5.

4. Why are the Greek and Australian Stories so similar?

I have shown above that there is a strong similarity between the stories about the Seven Sisters from around the world. It is particularly instructive to consider the Greek and Australian stories because of the lack of cultural contact between these two societies since the arrival of the first humans in Australia, and so little chance of cultural diffusion. Here I consider possible reasons for the strong similarity between the Greek and Australian stories.

4.1. Cultural Diffusion

The Australian Aboriginal people arrived in Australia at least 65,000 years ago (Clarkson et al., 2017), after which there was then virtually no cultural contact with the west until (a) trading by the Yolngu (Northern Australia) people with Macassan (Indonesian) Trepang collectors from about 1750 onwards (Wesley et al., 2014), (b) the invasion of Australia by the British in 1788. Could either of these be the origin of the Aboriginal Seven Sisters stories? It seems unlikely because

- The Seven Sisters stories are found throughout Australia, with a level of uniformity that suggests an ancient origin. We may compare those with the Christianity stories introduced to Aboriginal people by the British from 1788 onwards, which are not widely diffused but are mainly found near towns and missions.

- The paintings and engravings associated with the Seven Sisters stories at Marra Wonga and Walinynga appear to be thousands of years old.

- stories about other constellations (e.g. Scorpius, Crux) vary widely from group to group. If cultural diffusion across Australia were a rapid process, then it might be expected that other stories would also be uniform.

I conclude that the Aboriginal Seven Sisters stories are very old, and probably predate both the Indonesian and the British influences.

doi: https://doi.org/10.52526/25792776-26.73.1-140

4.2. Independent Invention

Could it be that the Greeks and Australians independently came up with the same story? It might be argued, for example, that the beauty of the Pleiades cluster triggers all humans to regard it as "feminine", whilst the majesty of the Orion constellation triggers all humans to regard it as "masculine". However, the details of the story are very specific, and both Greek and Australian versions contain the following elements.

- they both identify the Pleiades as a group of seven young girls, even though only six stars are normally visible
- they both identify Orion as male,
- they both say that Orion is chasing and attempting to rape one of the girls in the Pleiades,
- they both say that only six of the seven stars are normally visible, and have a story to explain the invisibility of the seventh.

It is difficult to imagine different people in different continents independently contriving stories with these same details.

I therefore conclude the stories most likely have a common origin. As the last cultural contact between the Greeks and Aboriginal Australians was when they left Africa before 65,000 BCE, that suggests that the story is at least that old, and perhaps came out of Africa with the mass migrations.

5. Phylogenetic analysis

Evolutionary biologists developed a technique called phylogenetic analysis, which traces the relationship between species by tracking changes in genes. Anthropologists have applied this technique to different versions of myths from around the world, tracing the transmission of stories from culture to culture, by tracking changes in the elements of the stories (called "motifs").

Julien d'Huy and Yuri Berezkin published a series of papers (e.g. D'Huy & Berzkin, 2017) in which they use this technique to explore the Seven Sisters myths.

They first built a database of about 55,000 myths gathered from about 1,500 ethnic groups from around the world, from which they selected the Seven Sisters stories. They identified 21 different motifs that appear in the stories, such as the Pleiades being a group of girls or women, or the Pleiades being birds, or Orion being male, or Orion chasing the women. They then built phylogenetic trees showing which myths might share a common heritage, and the age of the divergences. This enabled them to trace the evolution of the Seven Sisters stories.

Their analysis showed several of the most common motifs (e.g. the story includes both the Pleiades and Orion, the Seven Sisters are a group of girls or women, and Orion has the opposite gender) probably originated in Africa and were spread across the world through human migration. Using this technique (and unaware of our work), d'Huy and Berezkin had independently reached a similar conclusion to that of Section 4, using a completely independent technique. However, their database is necessarily incomplete, and so further work is planned to extend their analysis.

6. Relationship to the region around Armenia

To test the hypothesis that the Seven Sisters story dates back to the early human migrations, it is important to search for evidence of early traces of the story in other cultures, and also search for other versions of the myth to extend the phylogenetic analysis.

The region surrounding Armenia is extremely important in the study of ancient astronomy, as it lies immediately to the north of Mesopotamia, where our modern constellations are thought to have originated around 3000 BCE (e.g. Horowitz, 2015a,b, and references therein), from where they spread to Europe and elsewhere (Jones, 2015). By 1200 BCE the Pleiades (or "mulMUL") are referred to as the "seven gods". But Armenia is also connected to Europe and the much later astronomical traditions associated with Greek and Roman mythology, and so is an important bridge for understanding the evolution of these stories.

Orion (or *Hayk* in Armenian) is an extremely important constellation in Armenia, and was once the defining point of the Armenian calendar (Broutian, 2017). Similarly, the Pleiades (known as "Bazmats'tegh"

doi: https://doi.org/10.52526/25792776-26.73.1-140

Figure 8. The seven carved birds at the base of Pillar 18 at Göbekli Tepe, dated to about 8000 - 9500 BCE and interpreted by Malkhasyan (2025) as representing the Pleiades, which are traditionallyy assocaited with the winter months in Armenia. The shadow is the noon shadow of Pillar 19 at the winter solstice. Reproduced with permission from Malkhasyan (2025).

in mediaeval Aremian, or "Boylke" in modern Armenian) were also important. There are many (perhaps hundreds) of Armenian folk tales about Orion and the Pleiades, in some of which the Pleiades are the seven daughters, or wives, of Orion, and are chased by him, similar to the Greek and Australian stories (H. Malkhasyan, personal communication). In some cases, the seven stars are associated with seven birds that transform into girls. However, details of these are not yet available and will not be discussed further here.

In the rest of this section, I discuss sites in and around Armenia for which evidence has been claimed of ancient astronomical observations of the Pleiades.

6.1. Göbekli Tepe

Göbekli Tepe, also known as Portasar, in southeastern Turkey, is the oldest known monumental structure in the world, with dates from 9500 to 8000 BCE (Steadman & McMahon, 2011). It features large T-shaped limestone megaliths decorated with intricate animal reliefs. Several authors have argued that some of the megaliths at Göbekli Tepe are aligned with stars or the Sun (e.g. Coombs, 2023, De Lorenzis & Orofino, 2015, Malkhasyan, 2024). Controversially, Collins (2015), Sweatman & Tsikritsis (2017), Vahradyan & Vahradyan (2010) have claimed that some of the carved figures are depictions of constellations, significantly predating the much later Mesopotamian representations of the constellations.

Pillar 18 at Göbekli Tepe shows seven carved figures of birds and Malkhasyan (2025) argues that these represent the seven stars of the Pleiades, and also the seven lunar months of winter. These seven birds are illuminated by the Sun at noon each day, except during the first month of winter when the shadow of pillar 19 obscures one of the birds, as shown in Figure 8, corresponding to the one month interval in 9500 BCE between the winter solstice, and the heliacal rising of the Pleiades.

6.2. Nabta Playa

Nabta Playa, in Egypt's Nubian Desert, is dated to $\sim$ 6000 BCE. and is widely accepted as the world's second oldest known astronomical observatory after Warren Field in the UK (Gaffney et al., 2013). It is claimed (Malville et al., 2008) that the megalithic structures at Nabta Playa indicate not only calendrical positions of the Sun, but also bright stars such as Sirius and Orion's belt.

Again, these predate the traditionally assumed Mesopotamian origin of the constellations, although in this case the alignments are to individual stars, with no suggestion of a representation of constellations.

doi: https://doi.org/10.52526/25792776-26.73.1-140

6.3. Metsamor

Metsamor is an archaeological site in the Armavir province of Armenia. It includes structures dating from 4000 BCE through to medieval times, including several megaliths. Malkhasyan (2024) and Broutian (2017) argue that a petroglyph on the "small hill" platform at Metsamor resembles both the appearance of the Pleiades at its heliacal rising, and the Sumerian cuneiform symbol for the Pleiades. Broutian (2017) also points out that the major axis of the petroglyph points towards the azimuth of the rising Pleiades in about 9000 BC, although this is much earlier than the dates obtained from archaeological evidence.

6.4. Carahunge

The Syunik province in south-east Armenia contains many archaeological sites, including megalithic monuments and thousands of petroglyphs. Particularly important is the site known as Carahunge, or Zorats Karer, which may have served as an astronomical observatory (Belmonte, 2015, González-Garcia, 2015, Herouni, 2004, Simonia & Jijelava, 2015) and has been called the "Armenian Stonehenge" (Herouni, 2004). This site, thought to date from the Bronze Age, consists of more than 200 massive basalt stones, many featuring precisely drilled holes, some of which have been claimed to represent astronomical alignments, although this has been disputed (González-Garcia, 2015). Malkhasyan (2024) has also noted that the Pleiades may have been observed from this site.

7. Conclusion

The Seven Sisters stories associated with the Pleiades cluster are widespread across the world. While many variations exist, a common version is that the Pleiades represents seven girls who are being chased by Orion, who intends to rape one of them. Although called the Seven Sisters, most people see only six stars in the Pleiades, and this is explained in the stories in terms of one girl being captured, or in hiding, or otherwise hidden. This paper has supported the hypotheses that

- based on the similarity between Greek and Australian versions, which have been culturally disconnected since at least 65000 BCE, this story is very old, perhaps dating back to the mass migrations out of Africa, and
- that at that time, because of proper motion, the Pleiades did indeed appear to most human eyes as seven stars.

To test these hypotheses, we need to collect data on early myths and representations from around the world. The region around Armenia appears to be fertile ground for this search, but so far only circumstantial evidence has been found.

Acknowledgements

I thank Hayk Malkhasyan for his advice and help in hunting down Armenian mythology and appropriate references.

References

Al-Sufi A. A.-R., 964, The Book of Fixed Stars

Allen R. H., 1899, Star-names and their meanings. Leipzig: G.E.Stechert

Avilin T., 1998, Folklore, 72, 141

Belmonte J. A., 2015, in Ruggles C., ed., , In Ruggles, Clive L.N. (ed.). Handbook of Archaeoastronomy and Ethnoastronomy.. New York, NY: Springer, pp 133–145, doi:10.1007/978-1-4614-6141-8˙140

Broutian G., 2017, Bazmavep, the Journal of Armenian Studies, 1-2, 37

Burnham Jr. R., 1978, Burnham's Celestial Handbook: An Observer's Guide to the Universe Beyond the Solar System, in three volumes.. New York: Dover

Clarkson C., Jacobs Z., Marwick B., et al., 2017, Nature, 547, 306

Collins A., 2015, Göbekli Tepe: Genesis of the gods. The temple of the watchers and the discovery of Eden. Rochester: Bear and Co.

Coombs A., 2023, Journal of Skyscape Archaeology, 9, 32

Cunningham D., 2011, Midnight Science, 4

D'Huy J., Berzkin Y., 2017, Retrospective Methods Newsletter, 12-13, 100

De Lorenzis A., Orofino V., 2015, Archaeological Discovery, 3, 40

Dempsey F., 2009, J. R. Astron. Soc. Can. , 103, 233

Fuller R. S., Anderson M. G., Norris R. P., Trudgett M., 2014, Journal of Astronomical History and Heritage, 17, 171

Gaffney V., et al., 2013, Internet Archaeology, 34

Gaia Collaboration et al., 2023, Astron. Astrophys. , 674, A1

Galilei G., 1610, Siderius Nuncius

González-Garcia A. C., 2015, in Ruggles C., ed., , In Ruggles, Clive L.N. (ed.). Handbook of Archaeoastronomy and Ethnoastronomy.. New York, NY: Springer, p. 1453–1460, doi:10.1007/978-1-4614-6141-8˙140

Herouni P., 2004, Armenians and Old Armenia. Yerevan

Hertzog K. P., 1987, Quarterly Journal of the Royal Astronomical Society, 28, 27

Homer -850, The Iliad

Horowitz W., 2015a, in Ruggles C., ed., , In Ruggles, Clive L.N. (ed.). Handbook of Archaeoastronomy and Ethnoastronomy.. New York, NY: Springer, pp 1823–1827, doi:10.1007/978-1-4614-6141-8˙140

Horowitz W., 2015b, in Ruggles C., ed., , In Ruggles, Clive L.N. (ed.). Handbook of Archaeoastronomy and Ethnoastronomy.. New York, NY: Springer, pp 1829–1833, doi:10.1007/978-1-4614-6141-8˙140

Johnson D., 2011, in Ruggles C. L. N., ed., IAU Symposium Vol. 278, Archaeoastronomy and Ethnoastronomy: Building Bridges between Cultures.. pp 291–297, doi:10.1017/S1743921311012725

Jones A., 2015, in Ruggles C., ed., , In Ruggles, Clive L.N. (ed.). Handbook of Archaeoastronomy and Ethnoastronomy.. New York, NY: Springer, pp 1877–1881, doi:10.1007/978-1-4614-6141-8˙140

Kelsey-Museum 2005, The Vorotan Project, Armenia: 2005, https://web.archive.org/web/20131109235152/http://www.lsa.umich.edu/kelsey/fieldwork/pastfieldwork/thevorotanprojectarmenia2005_ci

Krupp E., 1991, Griffith Observer, 55, 1

Krupp E. C., 1994, Echoes of the ancient skies. The astronomy of lost civilizations.. New York: Dover

Kyselka W., 1993, Hawaiian J. History, 27, 174

Malkhasyan H., 2024, Communications of BAO, 71, 185

Malkhasyan H., 2025, Communications of BAO, 72, 313

Malville J. M., Schild R., Wendorf F., Brenmer R., 2008, in Holbrook J. C., Urama J. O., Medupe R. T., eds, Astrophysics and Space Science Proceedings Vol. 6, African Cultural Astronomy. p. 131, doi:10.1007/978-1-4020-6639-9˙11

Massola A., 1968, Bunjil's Cave. Melbourne: Lansdowne Press

Mountford C. P., 1976, Nomads of the Australian Desert. Adelaide: Rigby

Norris R. P., 2016, , 33, e039

Norris R. P., Norris C. M., 2009, Emu Dreaming: An Introduction to Australian Aboriginal Astronomy. Emu Dreaming Publications

Norris R. P., Norris B. R. M., 2021, in Boutsikas E., McCluskey S. C., Steele J., eds, , Advancing Cultural Astronomy; Studies In Honour of Clive Ruggles. pp 223–235, doi:10.1007/978-3-030-64606-6˙11

Pascoe B., Norris R., 2026, Big Sky: When the Emu left the Earth. Broome: Magabala Press

Pasztor E., 2015, in Ruggles C., ed., , In Ruggles, Clive L.N. (ed.). Handbook of Archaeoastronomy and Ethnoastronomy.. New York, NY: Springer, pp 1350–1356, doi:10.1007/978-1-4614-6141-8˙140

Ptolemy C., 150, The Almagest

Rappenglück M., 1997, Astronomy and Culture, 217

Rogers J., 1998, J. British Astronomical Association, 108, 9

Simonia I., Jijelava B., 2015, in Ruggles C., ed., , In Ruggles, Clive L.N. (ed.). Handbook of Archaeoastronomy and Ethnoastronomy.. New York, NY: Springer, pp 1443–1450, doi:10.1007/978-1-4614-6141-8˙140

Sparavigna A., 2008, arXiv e-prints, p. arXiv:0810.1592

Stauffer J. R., Schultz G., Kirkpatrick J. D., 1998, Astrophys. J. Lett. , 499, L199

Steadman S., McMahon G., 2011, The Oxford Handbook of Ancient Anatolia: (10,000-323 BCE). ERA Collection, OUP USA, https://books.google.com.au/books?id=TY3t4y_L5SQC

Sweatman M., Tsikritsis D., 2017, Mediterranean Archaeology and Archaeometry, 17, 233–250

Taçon P. S. C., Thompson S., Greenwood K., Jalandoni A., Williams M., Kottermair M., 2022, Australian Archaeology, 88, 159

Ushomirsky G., Matzner C. D., Brown E. F., Bildsten L., Hilliard V. G., Schroeder P. C., 1998, Astrophys. J. , 497, 253

Vahradyan V., Vahradyan M., 2010, Bazmavep, the Journal of Armenian Studies, 1-2, 161

Verderame L., 2016, Mediterranean Archaeology and Archaeometry, 16, 109

Wesley D., Jones T., O'Connor S., Fenner J., Dickinson W., 2014, Aust. Arch., 79, 14

White R. E., Bally J., 1993, Astrophys. J. , 409, 234

Russian Astronomical Sites on the World Heritage List

O.B. Dluzhneskaya*[1] and I.V. Kuznetsova†[2]

[1]Institute of Astronomy of the Russian Academy of Sciences, Moscow, Russia
[2]Sternber Astronomical Institute of Moscow State University, Moscow, Russia

Abstract

The UNESCO World Heritage List includes natural or human-made sites that have cultural, historical, or ecological significance, as determined by UNESCO experts. This article focuses on three sites from the Russian UNESCO List that have scientific significance and are related to astronomy and astronomical heritage.

Keywords: *Astronomical Heritage, Pulkovo Astronomical Observatory, Struve Geodetic Arc, Observatories of Kazan State University*

1. Introduction

There are 33 UNESCO World Heritage sites in the Russian Federation, which is 2.6% of the total number. It is important for Russia to take measures to expand the geography and diversity of the nominated sites, focusing not only on popular landscape and mixed natural and cultural sites but also on technological and scientific-cultural nominations.

To develop and refine the criteria for selecting objects for the UNESCO World Heritage List, scientific and practical conferences and other events are regularly held in countries participating in the Convention on the Protection of the World Cultural Heritage. For example, at the international conference "Astronomy and World Heritage: Across Time and Continents" as part of the "AstroKazan-2009" congress (Kazan, August 20-23, 2009), the conference resolution included a proposal to create a new category, "Space Heritage", as part of the UNESCO Thematic Initiative "Astronomy and World Heritage" (Dluzhnevskaya (2021). It was also proposed to include Space Technology as an important segment of the Astronomy World Heritage (Marov (2016).)

Currently, three objects on the Russian UNESCO list of scientific importance are related to astronomy and astronomical heritage: the Pulkovo Observatory, the Struve Geodetic Arc, and the Observatories of Kazan Federal University (the Kazan City Astronomical Observatory and the V. P. Engelhardt Astronomical Observatory).

2. The Pulkovo Observatory

The Pulkovo Observatory is an astronomical observatory of the Russian Academy of Sciences that conducts research in the fields of astronomy and geophysics. The Pulkovo Observatory was founded on August 7 (19), 1839, by decree of Emperor Nicholas I. The observatory is located in Saint Petersburg, 19 kilometers south of the city center, on the Pulkovo Heights.

The observatory's scientific activities cover almost all priority areas of fundamental research in modern astronomy: astrometry, celestial mechanics, astrophysics, stellar astronomy, the Sun and solar-terrestrial connections, extragalactic astronomy, instruments and methods of astronomical observations, and more. The observatory offers regular guided tours.

The Astronomical Museum of the Pulkovo Observatory is located in the Round Hall of the main building. The large Ertel–Struve vertical circle, which was used to determine the declinations of stars and planets using

*olgad@inasan.ru, Corresponding author
†irinakuznetsova-64@mail.ru

doi: https://doi.org/10.52526/25792776-26.73.1-151

Figure 1. D. Gobert. Observatory on Pulkovskaya Hill near St. Petersburg. 1840s. (Engraving)

the absolute method (now part of the collection of the Astronomical Museum of the Pulkovo Observatory), is also on display. The museum houses over 20,000 exhibits related to science, technology, and local history. It also features historical astronomical instruments.

The center of the Round Hall of the Pulkovo Observatory is the initial zero point of Russia's triangulation. The Pulkovo meridian, which passes through this center at $30°19'34''$ east of Greenwich,was the reference point on all old geographical maps of Russia.

Since 1990, the observatory has been part of the UNESCO-protected site "Historical Center of Saint Petersburg and related monument complexes" [Historic Center of Saint Petersburg and Related Groups of Monuments — UNESCO World Heritage Center], although geographically it is located outside the city. By Decree of the President of the Russian Federation № 275 dated April 2, 1997, the Pulkovo Observatory was included in the State Register of Especially Valuable Cultural Heritage Sites of the Peoples of the Russian Federation [New Law of the Russian Federation, (1997), The Collection of Laws of the Russian Federation, (1997)]. The object of cultural heritage of Russia of federal significance is registered as reg. № 781520299100006 (EGRON), object № 7810327000.

From the history of the Pulkovo Observatory: The first director of the Pulkovo Observatory was the outstanding scientist and astronomer-academician Vasily Yakovlevich (Friedrich Georg Wilhelm) Struve.

Vasily Yakovlevich (Friedrich Georg Wilhelm) Struve was born on April 15 (New Style), 1793, in the city of Altona, near Hamburg, in the large family of a gymnasium director.

At the age of 15, he entered the University of Dorpat (Tartu) to study philology under the influence of his father and older brother. Even then, the young man felt that his true calling was in another field, and he began attending lectures on astronomy and physics. After graduating from the university, he declined a position as a teacher of literature to pursue his passion for astronomy at the university's observatory. In 1818, he became the director of the Dorpat Observatory. It was here that Struve began his research on binary stars. In total, during his lifetime, he studied 12,000 stars and established binarity of 2,500 of them. Before Struve, no more than 500 such stars were known! His star catalogues have won worldwide recognition and have been awarded medals by the Royal Society of London. In addition, he was able to determine the distance to the Vega using the trigonometric parallax method, he proved that the density of stars increases towards the main plane of the Milky Way; he presented arguments the presence about interstellar extinction.

Since 1833, V.J.Struve has been an active participant in the construction of the Pulkovo Observatory,

doi: https://doi.org/10.52526/25792776-26.73.1-151

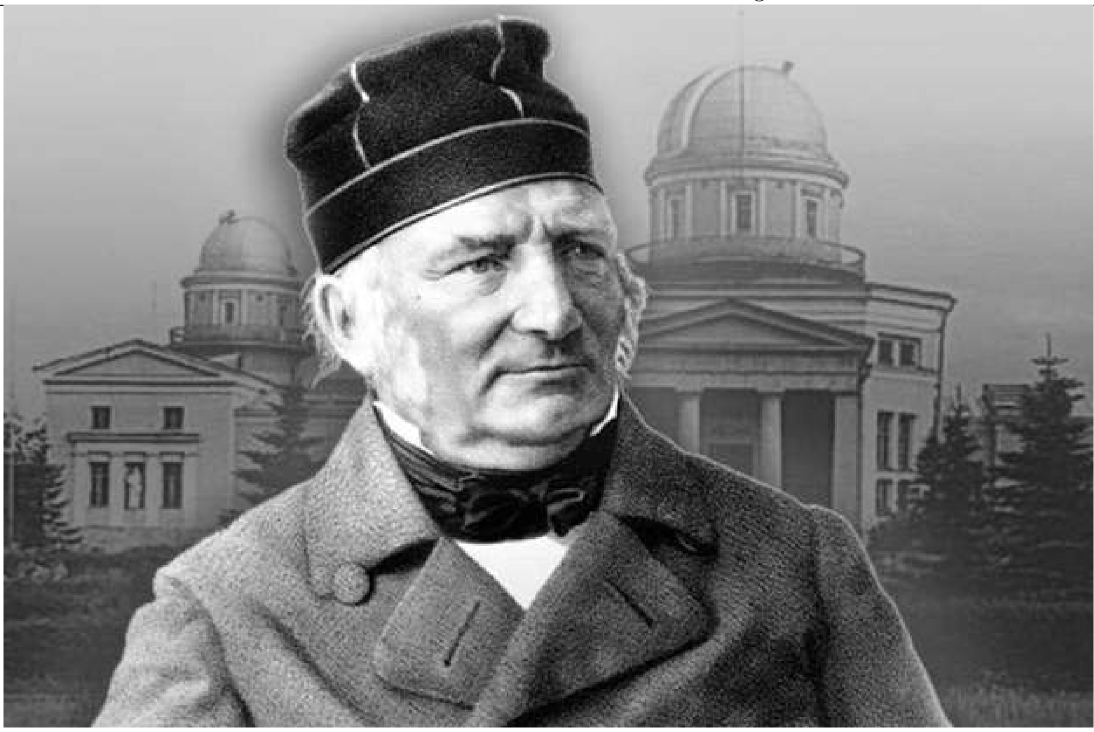

Figure 2. Portrait of V.Ya. Struve. On the background is the Pulkovo Observatory.

which was built under the supervision of architect Alexander Pavlovich Bryullov, brother of the famous artist. While engaged in scientific work, Struve also paid much attention to the technical equipment of the observatory. Thanks to his efforts, the Pulkovo Observatory was equipped with advanced instruments (including, at that time, the world's largest refractor with a 38-centimeter lens; (Litvinova & Pavlenkov (1893).

In 1857, when Vasily Yakovlevich's health began to fail, his eldest son Otto assisted him in his work, and later became the head of the observatory. In the autumn of 1863, V. I. Struve celebrated the 50th anniversary of his scientific career, and in August 1864, he celebrated the 25th anniversary of his beloved creation, the Pulkovo Observatory. These were the last significant events in his life. On November 23, 1864, the great scientist passed away. For almost a quarter of a century, Struve was director of the Pulkovo Observatory, and under his leadership it became, in the words of American astronomer Benjamin Gould, "the astronomical capital of the world". And the French physicist Biot, talking about the Pulkovo Observatory, said that "Russia has a scientific monument, which is the highest in the world". Outstanding scientists worked here, the most accurate observations were carried out, and star catalogs were compiled. In 1941-1944, the observatory was located on the front line and was almost completely destroyed. Many valuable instruments were destroyed, and a unique library with rare astronomy books was burned down. After the war, the Pulkovo Observatory was rebuilt from scratch, and a new complex of buildings was constructed in 1954.

The architectural ensemble of the Pulkovo Observatory is a complex of scientific and administrative buildings united by a common design. The main building is located exactly along the Pulkovo meridian and is oriented according to the cardinal directions.

By Decree of the President of the Russian Federation No. 275 dated April 2, 1997, the Pulkovo Observatory was included in the State Register of Particularly Valuable Cultural Heritage Sites of the Russian Federation.

2.1. Pulkovo meridian

The Pulkovo Observatory was originally conceived not only as a scientific center, but also as the main geodetic reference point of the Russian Empire. A conventional meridian was drawn through its central pavilion, which became the starting point for longitude on all Russian maps, topographic surveys, and even for marking railway tracks. The Pulkovo Meridian is an imaginary line that extends from the North Pole to the South Pole, with coordinates of $30°19'34''$ East longitude from Greenwich. Visually, the meridian "begins" in the center of the round hall of the Pulkovo Astronomical Observatory and "continues" on the

doi: https://doi.org/10.52526/25792776-26.73.1-151

Meridian Path of Pulkovo Hill. The spire of the Peter and Paul Cathedral rises very close to the meridian line.

Figure 3. The Round Hall of the observatory's astronomical museum, through the middle of which runs the Pulkovo meridian.

Unlike Greenwich, which was already gaining international weight at the time, the Pulkovo Meridian was focused on the internal needs of a giant country, representing an attempt to create its own sovereign coordinate system. The scientific significance of the meridian was immense. It served as the foundation for the Russian system of absolute longitudes and was used as a reference point for the famous "arc measurement of the meridian" from the Danube to the Arctic Ocean, as part of Struve's ambitious project to refine the shape of the Earth. Pulkovo astronomers determined coordinates of stars and time with incredible precision for their time, and they also conducted geodetic measurements that allowed them to create the world's best military topographic maps.

After the 1884 international conference that established Greenwich as the world's zero longitude, Russia, although it did not immediately sign the agreement, began a slow process of adopting the unified standard. However, in practical geodesy and cartography, the Pulkovo meridian continued to dominate till the 1920s. In 1919, Soviet Russia, in an effort to internationalize, officially adopted the Greenwich system and world time zones.

3. The Struve Geodetic Arc: 2,820 km from Norway to the Black Sea

In 1816, Struve was asked to make a topographic map of the Livonia province. This applied work gave rise to the idea of grandiose research in him. For many years, he supervised the measurement of the meridian arc over a vast area from the Danube to the Arctic Ocean, with a total length of more than 2,800 km. The measurement results provided valuable knowledge about the parameters of the Earth, its shape and size, as well as materials for making accurate maps of Russia. **Today, this arc is named after the astronomer Struve.**

In 1617, the Dutch astronomer Willebrord Snellius developed a triangulation method that remained the standard for over 300 years. If you take three clearly visible points that form a triangle on the ground and measure one side and two angles (although in practice, all three angles are always checked), you can calculate the lengths of the other sides. And if you form a chain of triangles, each of which shares one side with the previous one, the task reduces to measuring the angles sequentially and accurately measuring the base of one reference side, which can be relatively small for ease of accurate measurements.

Snellius built a quadrant to measure angles between vertices. The device was a quarter of a circle with

doi: https://doi.org/10.52526/25792776-26.73.1-151

two rotating tubes aimed at two high objects. A scale with degree divisions was located between the tubes.

In 1669-1670, Jean Picard used the triangulation method for the first high-precision measurement of the Paris meridian. To achieve this, he modified the quadrant by adding a telescopic sight with an eyepiece equipped with two mutually perpendicular threads, a micrometric screw, and a gradation with a quarter-minute step. As a result, Picard achieved a relative measurement error of approximately 0.44%. It turned out that the length of a meridian arc of 1° is 110.6 km at the equator, 111.3 km near Paris, and 111.9 km near the **Arctic Circle**.

A single, long-range, and continuous measurement system based on a common methodology was required to radically improve accuracy. This opportunity existed in the Russian Empire, which stretched thousands of kilometers from north to south and allowed to construct a long chain of triangulation points within a single state and under a unified scientific leadership.

3.1. The northern part of the arc

Interest in the degree measurements of the meridian was supported not only by academic science, but also by the military department. This factor played an important role in the further development of the project, although its influence was not immediately noticeable.

By the early 1810s, Vasily Yakovlevich Struve (real name Friedrich Georg Wilhelm), an astronomer and director of the Dorpat Observatory, was already actively engaged in the task of measuring the meridian's degrees. Analyzing the geography of the Russian Empire and the accumulated data, he arrived at several key conclusions. Firstly, the meridian passing through the Dorpat Observatory extended over 20° in latitude across the western provinces of the empire. Later, the actual length of the measured arc was $25°20'$, which is approximately one-fourteenth of the Earth's circumference. Moreover, the route did not cross major maritime areas, allowing for a continuous chain of triangulation points with minimal restrictions.

Some of the triangulation points were metal signal rods securely fixed on the roofs of buildings. Others were marked by stone pyramids, individual protruding boulders, or light wooden towers made of logs.

Each point was selected based on a variety of factors, including good mutual visibility of several landmarks, ease of observation, stability of the base, and minimal deviation from the meridian line.

In 1822-1823, Vasily Yakovlevich Struve and his colleagues conducted dozens of measurements. The most advanced universal geodetic instruments designed by Reichenbach were used for angular observations. These instruments allowed not only to measure horizontal angles, but also to determine declinations of celestial bodies and calculate the latitude at each observation point with high accuracy.

After receiving unsatisfactory results over and over again, Vasily Yakovlevich came up with a method of repeated measurements to identify systematic errors.

To measure the base distances, he designed an original device: two measuring rods, each two fathoms long, with bubble levels. These rods were placed on sawhorses in a very precise manner to measure the distance between two triangulation points. It is worth noting that the entire Struve line consists of 10 bases, each approximately 10-12 kilometers long

The project to extend the arc through Finland was approved personally by Nicholas I, who ordered that three thousand silver rubles be allocated for the work each year. By 1844, this stage had been completed, and Struve traveled to Stockholm to negotiate with King Oscar I about continuing the measurements in Sweden and Norway.

The original plan was to connect the new arc to the existing triangulation chain laid out by Jöns Swahnberg in 1801-1803. However, a detailed reconnaissance of the area conducted jointly by Swedish surveyors and specialists from the Pulkovo Observatory revealed that the old points did not meet the required accuracy standards.

As a result, it was decided to build a new triangulation network from scratch, with only the general direction of the route remaining unchanged. The Swedish side agreed to finance a significant portion of the work. Over the next ten years, the measurements were conducted in extremely challenging conditions, with strong winds, rough terrain, significant elevation changes, and harsh weather making the expeditions difficult. Despite these obstacles, the Scandinavian section of the arc was successfully completed by 1855.

After the work was completed in the north in 1855, the entire Struve arc was a single system with the following characteristics:

- 265 triangulation points;
- 258 triangles with a common side;

doi: https://doi.org/10.52526/25792776-26.73.1-151

- 13 main points equipped with astronomical stations for accurate determination of latitude.

The total length of the arc was about 2820 km, or 25.2° of the meridian arc, making it the longest triangulation chain in the history of geodesy.

In the following years, Vasily Yakovlevich Struve and Osip Khodzko conducted repeated control measurements using the most advanced instruments available at the time. These checks confirmed the high accuracy of the initial calculations and solidified the scientific value of the project.

Figure 4. A map showing the entire length of the Struve Arc.

3.2. How the Struve Arc influenced science

Triangulation measurements allowed:

- To create the most detailed topographic maps of the western part of the Russian Empire with an error of only 3.5 cm per kilometer (as later revealed by modern measurements).
- Correlate these data with those obtained during the “Great Trigonometric Study”. Thanks to this, it was possible to confirm that our Earth has a more complex geoid shape and to estimate its parameters even more accurately.

Of the 265 triangulation points, only 34 have survived to the present day. Of these, only two are located in Russia: “Myakipiallus” and “Point Z”. The remaining points are located in ten other modern countries: Norway, Sweden, Finland, Estonia, Latvia, Lithuania, Belarus, Moldova, and Ukraine. It is worth noting that eight of these points were previously part of the Russian Empire.

In 1993, at the initiative of Finland, the remaining sites were designated as UNESCO World Heritage Sites. Two sites have been preserved in Russia.

The Struve Geodetic Arc was inscribed on the UNESCO World Heritage List in 14–15 July 2005 at the 29th session of the World Heritage Committee in **Durban**, South Africa.

doi: https://doi.org/10.52526/25792776-26.73.1-151

4. Observatories of Kazan Federal University (KFU)

Two astronomical observatories of Kazan Federal University (KFU) were included in the UNESCO World Heritage List in Russia in 2023. The decision was made on September 18 at the 45th session of the UNESCO World Heritage Committee.

4.1. Observatories of Kazan University

Astronomical Observatory of Kazan University is a Russian astronomical observatory located in the city of Kazan at an altitude of 75 meters above sea level. It is affiliated with the Department of Astronomy of Kazan University. The Department of Astronomy of the Imperial Kazan University was founded in 1810 by Joseph Johann Litrow. On November 11, 1814, observations began at a small observatory (temporary construction) above a stone gatehouse in the university botanical garden. At the time, it was the easternmost observatory in Europe.

In 1822 the observatory was temporarily placed in a wooden gallery (part of I. M. Simonov's apartment). In 1827 the university yard was chosen as the permanent place of the observatory, and in 1833 the construction of the observatory building began. In 1835 a 23-cm (9-inch) refractor was ordered from Fraunhofer's workshop.

In 1837 the permanent observatory building was completed, and in June of that year the first observations were made in it. In 1838, a 9-inch refractor was installed in the main movable dome. The official date of birth of the University Astronomical Observatory was April 13, 1838, when permanent observations (on the Vienna Meridian Circle) began in the new observatory building

On February 23, 1885, a time service was established: a clock showing the exact Kazan mean time was exhibited in the window of the department

4.2. V.P. Engelhardt Astronomical Observatory

The V.P. Engelhardt Astronomical Observatory of Kazan State University (AOE) is a Russian astronomical observatory located 20 km west of Kazan in the village of Oktyabrsky in the Zelenodolsky District of Tatarstan, at an altitude of 92 meters above sea level. The reason for establishing the observatory was the inconvenience of observation in the city center due to strong light pollution.

The observatory arose from the friendship of two astronomers. It's worth telling more about these remarkable men. The first of them was Dmitry Ivanovich Dubyago (1849–1918), who founded the observatory and became its first director. D.I. Dubyago was a professor of astronomy at Kazan University. He was born in the Mogilev province. After receiving his initial education at the Gatchina Institute, he entered the Physics and Mathematics Department of St. Petersburg University.

After graduating with a PhD, he was retained at the university to prepare for a professorship. In 1873, Dubyago was appointed to the Pulkovo Observatory, where he initially worked as a out of staff astronomer before becoming an adjunct-astronomer. From 1881 to 1884, he lectured at Saint Petersburg University as a private lecturer. In 1884, he was appointed a professor. Dubyago was appointed a full professor and director of the observatory in Kazan. His dissertations are "A Study of the Orbit of Neptune's Satellite" (1878) and "The Theory of the Motion of the Planet Diana" (1880). For his work, he was awarded the title of Doctor of Astronomy and Geodesy by the St. Petersburg Academy of Sciences (Department of Astronomy & Kazan State University (2026).

The second is Vasily Pavlovich Engelhardt (1828–1915). A member of the well-known Engelhardt noble family, Vasily Pavlovich is the grand-nephew of Prince Grigory Potemkin-Tavrichesky. The illustrious prince bequeathed his fortune to his nephew, Engelhardt's grandfather.

After graduating from the St. Petersburg School of Jurisprudence in 1847, V.P. Engelhardt served in the 1st and 5th Departments of the Governing Senate. In 1853, he retired and devoted himself to astronomy.

In 1875, he settled in Dresden, where he built the Great Observatory with his own funds in 1879, where he worked alone without assistants until 1897. Engelhardt's main research focused on comets, asteroids, nebulae, and star clusters. From 1879 to 1894, he observed 50 comets and 70 asteroids. From 1883, he studied nebulae and star clusters, compiling a catalog of more than 400 nebulae. Starting in 1886, he observed 829 stars from the Bradley catalog to detect their companion stars.

D.I. Dubyago and V.P. Engelgardt met and became friends by correspondence — they both studied the asteroid Diana.

doi: https://doi.org/10.52526/25792776-26.73.1-151

In 1897, due to his advanced age and illness, V.P. Engelhardt ceased his practical observations and, in his will, donated all his unique astronomical equipment from his private observatory in Dresden to Kazan University, as well as funds for the development of the observatory. Among the treasures were a 12-inch Grubb refractor, a meridian circle, a heliometer, comet finders, precise clocks, and a rich library. A capital of 50 thousand rubles in securities was also bequeathed.

On July 21, 1899, Dmitry Ivanovich Dubyago was appointed Rector of the Imperial Kazan University, which contributed to the positive decision to build a second observatory near Kazan. Emperor Nicholas II issued a decree allocating funds and land for the construction. The construction of the observatory began on March 7, 1899. On September 21, 1901, the suburban astronomical observatory of Kazan University was inaugurated.

In 1903, the Observatory was officially named the Engelhardt Observatory, and it still bears this name today.

Figure 5. The V.P. Engelhardt Observatory at the beginning of the 20th century.

Until the end of his life, Engelhardt was actively involved in both the construction and the operation of the new observatory.

On September 21, 2014, another significant event took place. With the support of the Russian and Tatar authorities, the Kazan Federal University, with the active participation of KFU employees and with the help of colleagues from Germany, the ceremony of reburial of the ashes of V.P. Engelhardt in the crypt under the Southern Meridian Mark — the tomb of the Astronomical Observatory of KFU, where Vasily Pavlovich's friend and associate, Professor Dmitry Ivanovich Dubyago, was previously buried.

The Engelhardt Astronomical Observatory houses a variety of modern telescopes from different eras, including the zenith telescope, the Heide astrograph, the Maxetov meniscus telescope, the AFR astrograph, the AZT-14 telescope with a modified CPOM detector, and others.

The observatory took part in the creation of a fundamental coordinate system, providing 14 high-precision star catalogs; solar monitoring of solar-terrestrial interactions; optical and radio observations of meteors; research on comets, the Moon, and asteroids. Relativistic astrophysics is being developed here; optical observations of Earth's satellites are being conducted.

Currently, the Observatory is a complex of buildings: a two-storey building in the classical style is adjacent to the main building with an astronomical tower and a meridian circle pavilion. In the early 20th century, it housed apartments for employees.

By the time the observatory was included in the World Heritage List, it had not only retained its architectural integrity, but also its original research and educational function. The observatory is home to a planetarium. The planetarium was opened on June 23, 2013. In 2016, the planetarium was named after Alexei Leonov, a two-time Hero of the Soviet Union who made the first spacewalk in history. The idea came up during Leonov's participation in the International School of Space Science, which was held at KFU in August 2016.

The V.P. Engelhardt Astronomical Observatory is a territory, buildings, and scientific site that is organically connected to the surrounding landscape and forms a single ensemble. Seven of the Astronomical

doi: https://doi.org/10.52526/25792776-26.73.1-151

Observatory's facilities have been included in the State Register of Immovable Urban Planning and Architectural Monuments

Conclusion

The article focuses on the history of three astronomical sites that have been included in the UNESCO World Heritage List. Each site has its own unique history, beauty, and scientific significance. As part of the UNESCO Astronomy and World Heritage Thematic Initiative, which was established in 2004, criteria were developed for the inclusion of "Astronomical and Archaeoastronomical Sites" in the World Heritage List. It was proposed to create a new category "Space Heritage", which should include "Space Technology Heritage" (Marov (2016). It is very important for Russia to continue working on the inclusion of various objects related to astronomy, archaeoastronomy, or the history of space exploration in the list of World Heritage candidates. to preserve the historical, cultural, and scientific-technological values of humanity.

Acknowledgements

The study was conducted under the state assignment of Russian Academy of Sciences (1st author) and of Lomonosov Moscow State University (2nd author). The authors also thank Professor N.N. Samus for carefully reading the article and a number of valuable comments.

References

Department of Astronomy Kazan State University 2026, The role of D.I. Dubyago in the history of the Kazan Observatory, https://kpfu.ru/physics/struktura/kafedry/otdelenie-astrofiziki-i-kosmicheskoj-geodezii/httpskpfurumain-pagep-sub5769p-view1/200-let-kazanskoj-astronomii-5

Dluzhnevskaya O. B., 2021, Heritage and Modern Times, 4, 177

Litvinova E. F., Pavlenkov F. F., 1893, V. Ya. Struve, his life and scientific work : a biographical essay. Printing house of Yu. N. Erlich, Sankt-Peterburg

Marov M. Y., 2016, Space Technology World Heritage: Basic Concept. Kazan Federal University, Kazan, pp 253–263

New Law of the Russian Federation, 1997, Rossijskaya gazeta, April 7

The Collection of Laws of the Russian Federation, 1997, April 7, 1997, № 14, Article 1606

doi: https://doi.org/10.52526/25792776-26.73.1-151

Ancient Astronomical Heritage of Iran: A Linguistic and Cultural Perspective

Saeed Jafari*[1,2,3,4]

[1]International Decade of Indigenous Languages (IDIL 2022–2032), UNESCO
[2]World Space Week Association
[3]Department of Linguistics, University of Kurdistan, Sanandaj, Iran
[4]Commission C5 Cultural Astronomy, International Astronomical Union

Abstract

Language is central to the survival of Iran's astronomical heritage, yet scholarship often treats celestial names, literary imagery, calendrical terms, and ritual symbols as separate evidence. This review examines how Iranian engagements with the sky were preserved and transmitted through language and symbol. It brings together scholarship on Avestan, Middle Persian, New Persian, selected Iranian languages, Persian literature, calendrical traditions, festivals, and astronomical knowledge. The discussion compares established studies from two perspectives, linguistic evidence and culturally situated signification. A diachronic linguistic-semiotic approach traces lexical retention and semantic reanalysis, metaphorical conceptualisation, and calendrical-symbolic representation. Terms including Tištrya, Haftōrang, Parvīn, Bahrām, and Nāhīd illustrate the interaction of celestial reference with ritual authority and moral association. Solar and lunar imagery extends those associations into descriptions of beauty, sovereignty, fortune, and character. Month names and festivals place meanings within recurrent social time, although direct equations between ancient observances and modern equinoxes or solstices require historical caution. Iranian astronomical heritage emerges as a changing archive whose continuity depends on reinterpretation, translation, and use across periods.

Keywords: *Persian; Iranian languages; cultural astronomy; celestial lexicon; symbol; metaphor*

1. Introduction: Astronomy, Language and Cultural Memory in Iran

Studies of Iran's astronomical heritage are dispersed across philology, religious history, literary criticism, art history, and the history of science, and this disciplinary division often obscures the relations among words, images, calendrical names, and recurring practices. The present article synthesises established scholarship and offers no new empirical study. Its narrower purpose is to ask what existing research permits us to say about the preservation and reinterpretation of celestial knowledge from two perspectives, language and culturally situated symbolism. Holbrook places the sky among the knowledge domains that linguistic fieldwork should document, including naming, timekeeping, and navigation, and Holton shows that assumed translation equivalence or weak control of linguistic detail can produce misleading accounts of another community's sky (Holbrook, 2011, Holton, 2016). These cautions remain useful for historical materials, even though the evidence considered here comes mainly from texts, lexicons, visual studies, and earlier scholarship instead of interviews with living speakers. A social-semiotic perspective further treats words, images, rituals, and calendars as resources through which communities organise meaning, and astronomy literacy accordingly includes the cultural conditions under which celestial objects become noticeable, nameable, and memorable (Kelley & Milone, 2011, Kress & van Leeuwen, 2006, North, 2008, Retrê et al., 2019, Ruggles, 2015, Salimpour & Fitzgerald, 2024).

The article adopts a diachronic linguistic-semiotic approach and follows three connected processes, lexical retention with semantic reanalysis, metaphorical conceptualisation, and calendrical-symbolic representation. These formulations correspond to established accounts of meaning change, contextual inference, and culturally distributed conceptualisation, and they state the comparison being made across periods without presenting it as a new formal model (Durkin, 2009, Geeraerts, 2010, Kövecses, 2010, Lakoff & Johnson,

*saeed.jafari@spacegeneration.org

doi: https://doi.org/10.52526/25792776-26.73.1-160

1980, Sharifian, 2017, Traugott & Dasher, 2002). López's discussion of symbols in cultural astronomy adds an important restriction. The term *symbol* should not serve as a loose synonym for every image or celestial motif; symbolic meaning depends on socially established interpretive relations and requires distinction from iconic or indexical signs (López, 2024). This is especially important for ancient material, where the relevant interpreters are absent and claims about meaning remain inferential. Astronomical motifs in prehistoric and Achaemenid art confirm that celestial signs circulated visually, but the images alone leave many semantic values unresolved (Mobini & Marnani, 2019, Root, 1979). Linguistic evidence can narrow those interpretations, though it rarely settles them by itself.

2. Naming the Iranian Sky: A Diachronic Study of Celestial Terms

2.1. Iranian Names of Stars and Constellations

Celestial nomenclature raises a basic interpretive problem because an inherited name may preserve an observation, a mythic relation, or a scholarly identification established in a later period. Iranian evidence frequently contains all three in different proportions. Avestan Tištrya, conventionally identified with Sirius, designates a conspicuous star and a rain-bringing yazata whose conflict with drought places stellar observation within an ecological and ritual account (Boyce, 1975, Malandra, 1983, Panaino, 1990). Haptōiringa, continued by Persian Haftōrang, and the Pleiades name continued as Parvīn show comparable lexical depth. Their significance lies less in proving a fixed ancient "constellation system" than in showing that stellar groupings entered language as culturally ranked units. Lexicography records denotation; surrounding texts disclose agency, seasonality, and omen value (Anklesaria, 1956, Bartholomae, 1904, MacKenzie, 1971).

The distinction also bears on modern naming practice. The IAU Working Group on Star Names maintains the official IAU Catalogue of Star Names, standardising names for scientific use while documenting the etymological, historical, and cultural backgrounds of both adopted and alternative names (Hoffmann et al., 2025). Historical Iranian star terminology, however, does not always correspond one-to-one with the individual stars and naming conventions of a modern catalogue.

2.2. Planetary Names and Their Cultural Associations

Planetary vocabulary reveals similar layering more sharply because Iranian and Arabic names remained in active contact. Middle Persian and New Persian sources preserve Kēwān for Saturn, Bahrām for Mars, Nāhīd or Anāhīd for Venus, Tīr for Mercury, and Māh for the Moon. Arabic forms including Zuḥal, Mirrīkh, Zuhra, and Úṭārid later entered technical and literary registers. Their coexistence allowed writers to choose among inherited religious associations, astrological convention, metre, and audience
(MacKenzie, 1971, Matras, 2009, Schmitt, 1989, Thomason & Kaufman, 1988, Windfuhr, 2009).

The semantic associations also complicate a modern separation of astronomy from astrology. Bahrām joins Mars to a divine name of victory; Nāhīd links Venus with the Iranian reception of Anāhitā; Kēwān becomes a figure of remoteness, slowness, and misfortune in later poetic convention. Such values arose through inherited theology, Hellenistic planetary schemes, and Persian literary use as much as through naked-eye observation (Boyce, 1982, Boyce & Grenet, 1991, de Jong, 1997). The lexicon therefore records negotiated classification and preserves traces of periods in which celestial bodies could be treated as agents, powers, and signs alongside their observational identities.

3. Celestial Imagery and the Human Condition in Persian Literature

3.1. The Sun and Moon as Metaphors of Beauty and Sovereignty

Calling a face māh-rūy, "moon-faced," intensifies beauty and also places the beloved within a scale of visibility, distance, periodic absence, and collective attention. Solar imagery performs a related operation for power. Expressions such as the "sun of kingship" or the rising of a ruler's fortune convert political rank into radiance and centrality. Court poetry used these mappings because sovereignty required language capable of presenting hierarchy as part of the cosmic order (Bürgel, 1988, Meisami, 1987, Schimmel, 1992). The metaphor performs evaluation and places the praised figure within a hierarchy of radiance and rank.

The same celestial imagery also supplies limits. A moon wanes and a sun may be veiled or eclipsed. Persian poets use that instability to describe separation, disgrace, ageing, and reversal of fortune. Celestial

doi: https://doi.org/10.52526/25792776-26.73.1-160

comparison, therefore, carries tension between splendor and mutability, which helps explain its durability across panegyric, romance, and lyric verse. The image can legitimise a ruler in one context and expose human dependence on time in another (Davidson, 1994, Davis, 2006, Rypka, 1968). Treating each simile as an isolated decoration misses the evaluative argument carried by the larger pattern.

3.2. Planets, Constellations and the Poetic Construction of Character

Niẓāmī́s Haft Paykar offers the clearest case of celestial classification becoming narrative structure. The seven domes, planetary weekdays, colours, and princesses organise Bahrām Gūr's movement through distinct ethical and affective environments. Astronomy regulates sequence and makes character legible through a cosmological itinerary (Chelkowski, 1975, Meisami, 1995). The poem adapts Persian, Arabic, and Hellenic associations instead of reproducing one technical system unchanged, and patterned difference becomes part of Bahrām's education.

Elsewhere, planetary names and attributes function as culturally shared symbolic shorthand. A single name can activate a cluster of conventional associations accumulated across astronomical, astrological, and literary traditions: Saturn may suggest severity, delay, or distance; Mars may cue aggression; and Venus may evoke music or desire. Such associations allow a poet to sketch temperament, rank, or fate without extended exposition (Meisami, 1987, Schimmel, 1992). Yet their significance remains open to revision within a poem. Anvarī and Khāqānī, for example, could intensify praise by reversing an expected planetary value or by presenting the heavens as subordinate to the patron. This usage presupposes shared cultural literacy, but it is also shaped by genre and rhetorical purpose; celestial symbolism never operates as a fixed psychological taxonomy.

4. Conceptual Metaphors of the Sky in Persian and Iranian Languages

Persian sky expressions form recurrent conceptual patterns. Čarx and falak, the wheel and the sphere, commonly frame fate through rotation; height and brightness frame rank, and sunrise can frame accession or renewed fortune. These mappings draw on embodied perception, yet their conventional meanings developed within Iranian literary and cosmological histories (Kövecses, 2010, Lakoff & Johnson, 1980, Sharifian, 2017). A single observed pattern can be construed differently across genres. The regular rotation of the heavens may index cosmic order in astronomical prose, yet personified falak can signify capricious fate in poetry. Conceptual structure therefore provides possibilities for interpretation without fixing one cultural judgment.

Lexical history makes this variation visible. Semantic change often proceeds through repeated contextual inference, and language contact introduces near-synonyms that divide by register or genre (Durkin, 2009, Geeraerts, 2010, Traugott & Dasher, 2002). Persian āsmān, sepehr, falak, and gardūn can all refer to the sky or heavens, but their collocational patterns differ. Falak and gardūn readily personify the machinery of fate; āsmān remains broader and less marked. Lexical selection thus identifies a relevant model of the sky, whether visible expanse, rotating mechanism, moral power, or elevated domain.

4.1. A Comparative Perspective across Iranian Languages

Comparison beyond Persian is necessary, although the evidence is uneven. Old and Middle Iranian sources preserve distinct celestial lexemes, and Eastern Middle Iranian materials show astronomical vocabulary circulating through Sogdian and Khotanese scholarly environments (Bailey, 1979, Kent, 1953, Sims-Williams, 1989). Across modern Iranian languages, solar terms often extend into meanings of day or daylight. Persian rūz, Kurdish roj, and Balochi rōč belong to a broader Iranian pattern in which light structures daily time. Their individual histories differ, so surface resemblance alone offers insufficient evidence for a shared metaphor without phonological and textual comparison (Schmitt, 1989, Windfuhr, 2009).

In this article, Persian carries particular evidential weight because its written record is extensive, continuous across many periods, and geographically influential in Iranian-speaking and Persianate regions. That prominence should not be converted into a claim of linguistic uniformity. Sogdian day names involving Mihr or the Moon, Khotanese Buddhist astronomical vocabulary, and regionally distributed Iranian forms reveal other routes between celestial observation and social time (Bailey, 1979, Sims-Williams, 1989, Windfuhr, 2009). The comparative record therefore changes the interpretation of continuity itself. Persian preserves one exceptionally visible trajectory, but inherited forms, loans, semantic extensions, and calendrical terms developed differently in other Iranian languages. Treating the Persian corpus as the whole record would

doi: https://doi.org/10.52526/25792776-26.73.1-160

hide that variation; treating it as one influential archive makes comparison possible and keeps the argument proportionate to the evidence.

5. Astronomical Time in Iranian Language and Culture

5.1. The Linguistic Heritage of Iranian Month Names

Iranian month names preserve a compact religious lexicon inside the civil calendar. Farvardīn recalls the fravašis; Ordībehešt continues Avestan Aša Vahišta; Khordād and Amordād derive from Haurvatāt and Amrtāt; Mehr continues Miθra; Ābān and Āzar retain associations with water and fire. In current usage, these forms function as ordinary calendrical labels. Their etymologies nevertheless keep earlier sacred categories available for reinterpretation in festivals, personal names, and public discourse (Bartholomae, 1904, Boyce, 1975, MacKenzie, 1971).

Lexical retention implies neither universal awareness of the former theological concept nor an unchanged calendrical structure. Iranian calendrical history includes reform, intercalation problems, regional variation, and changes of epoch (al-Bīrūnī, 1879, Boyce, 1970, de Blois, 1996, Taqizadeh, 1938). The month names survived through repeated institutionalisation in new systems, a process better understood as retention accompanied by recontextualisation. The older lexicon remained usable in administration, ritual memory, and national time, with different meanings becoming salient in each setting.

5.2. Nowruz and the Vernal Equinox

Nowruz brings the article's main processes into one case. Its name, "new day," is transparent in Persian; its calendrical position is tied to the vernal equinox, and its observance renews social relations through recurrent acts. The Solar Hijri calendar maintains close alignment with the tropical year by determining the year's opening around the equinoctial transition, although its legal and computational formulation belongs to modern calendrical history and differs from ancient practice (de Blois, 1996, Reingold & Dershowitz, 2018). Al-Bīrūnī's discussion already shows Iranian chronological traditions being compared, corrected, and debated by learned observers (al-Bīrūnī, 1879).

Nowruz turns an astronomical boundary into a named public event that can be anticipated, measured, narrated, and performed. Salimpour and Fitzgerald treat culturally embedded events as representations through which astronomical concepts become socially intelligible (Salimpour & Fitzgerald, 2024). The Iranian case also shows that ritual practice gives the equinox consequences in domestic time, state calendars, and collective memory. Language identifies the threshold, and recurrence converts that designation into a social fact. This relation is historically strong, though every element of present practice need not derive from the same period.

6. Astronomical Phenomena, Ritual Time and Cultural Memory

6.1. Equinoxes, Solstices and the Organization of Ritual Time

Popular accounts sometimes assign every Iranian festival a direct and timeless relation to an equinox or solstice. Historical calendars make that scheme difficult to sustain. A 365-day year without regular intercalation drifts against the seasons, so the date of a feast and a solar event associated with it may separate over centuries (Bickerman, 1980, Boyce, 1970, Taqizadeh, 1938). Relations between ritual and astronomy therefore require reconstruction for specific periods, based on calendrical history and evidence for actual observance.

Seasonal thresholds nevertheless remained culturally powerful because changes in daylight, temperature, agriculture, and celestial visibility were repeatedly interpreted through named periods. Yaldā and the forty-day čella cycle show that long winter nights could be organised as social time, even though their terminology and customs have complex histories. Equinoxes and solstices supplied observable constraints; communities added segmentation, narrative, and ritual emphasis. Cultural memory depended on repeated adjustment as calendrical positions and ritual meanings changed.

doi: https://doi.org/10.52526/25792776-26.73.1-160

6.2. Tīrgān, Mehrgān and the Celestial Dimensions of Iranian Festivals

Tīrgān demonstrates the value of linguistic evidence. The name Tīr continues Tištrya, the stellar divinity associated with Sirius, rain, and the defeat of drought. Water-related customs in later celebrations become more intelligible when placed beside that semantic history (Boyce, 1975, Panaino, 1990). Assigning the festival a fixed summer-solstice position for every period exceeds the evidence. Calendar drift and regional practice complicate that equation. A stronger claim concerns continuity of association, since a star-name and month-name kept rain, heat, and seasonal relief within the festival's interpretive field.

Mehrgān, held on the day Mehr in the month Mehr, similarly joins a calendrical name with Miθra's inherited semantic domain and autumnal social practice. In later Iranian history it acquired royal, harvest, and communal meanings that arose through more than one historical route (Boyce, 1982, Boyce & Grenet, 1991, Daryaee, 2009). Together, Tīrgān and Mehrgān show calendrical-symbolic representation in practice. Celestial or seasonal knowledge persists when a name coordinates recurring action, even as the action and its explanations change. The evidence supports transformed continuity, with each period selecting and reorganising parts of an inherited field.

7. Language Contact and the Transmission of Astronomical Knowledge

7.1. Translation, Borrowing and the Formation of a Persian Astronomical Lexicon

The Persian astronomical lexicon developed through sustained multilingual exchange. Achaemenid rule placed Iranian elites in direct contact with Mesopotamian scholarly traditions, and later Sasanian and early Islamic environments brought Greek, Indian, Syriac, and Arabic materials into new compilations (Pingree, 1963, 1973, Sezgin, 1978, Steele, 2012). Translation altered categories as well as terminology. A borrowed word could enter beside an Iranian equivalent, narrow its meaning, or become the preferred form in technical prose.

The Abbasid translation movement accelerated this process, and Persianate scholars participated actively in it (Gutas, 1998, Sabra, 1987). Arabic became the principal language of much advanced astronomy, whereas Persian retained older celestial names and later expanded as a medium of scientific exposition. Astronomical tables, instrument traditions, and planetary models circulated through institutions from Baghdad to Marāgha (Kennedy, 1956, King, 2004, Ragep, 1993, Sayılı, 1960). The Marāgha tradition is especially important because it joined observation, mathematical criticism, and teaching within a network crossing linguistic boundaries (Morrison, 2007, Ragep & Ragep, 1996, Saliba, 1994).

The outcome was a stratified lexicon. Persian setāra, māh, Mehr, and Nāhīd coexisted with Arabic kawkab, qamar, šams, and Zuhra; Greek-derived technical concepts arrived largely through Arabic, and Indian parameters entered astronomical tables through translation and recalculation. Language contact thus became a mechanism of continuity, enabling the incorporation of new models alongside inherited categories (Brentjes, 2016, Dallal, 2010, Matras, 2009). Its ancient components remain visible through this uneven layering; mixture itself forms the historical record.

References

Anklesaria B. T., 1956, Zand-Akasih: Iranian or Greater Bundahishn. Rahnumae Mazdayasnan Sabha, Bombay

Bailey H. W., 1979, Dictionary of Khotan Saka. Cambridge University Press, Cambridge

Bartholomae C., 1904, Altiranisches Wörterbuch. Trübner, Strasbourg

Bickerman E. J., 1980, Chronology of the Ancient World, 2nd edn. Thames and Hudson, London

al-Bīrūnī A. R., 1879, The Chronology of Ancient Nations, translated by C. E. Sachau. W. H. Allen, London

Boyce M., 1970, Bulletin of the School of Oriental and African Studies, 33, 513

Boyce M., 1975, A History of Zoroastrianism, Vol. 1. Brill, Leiden

Boyce M., 1982, A History of Zoroastrianism, Vol. 2. Brill, Leiden

Boyce M., Grenet F., 1991, A History of Zoroastrianism, Vol. 3. Brill, Leiden

Brentjes S., 2016, Teaching and Learning the Sciences in Islamicate Societies, 800–1700. Brepols, Turnhout

Bürgel J. C., 1988, The Feather of Simurgh: The "Licit Magic" of the Arts in Medieval Islam. New York University Press, New York

doi: https://doi.org/10.52526/25792776-26.73.1-160

Chelkowski P. J., 1975, Mirror of the Invisible World: Tales from the Khamseh of Nizami. Metropolitan Museum of Art, New York

Dallal A., 2010, Islam, Science, and the Challenge of History. Yale University Press, New Haven

Daryaee T., 2009, Sasanian Persia: The Rise and Fall of an Empire. I.B. Tauris, London

Davidson O. M., 1994, Poet and Hero in the Persian Book of Kings. Cornell University Press, Ithaca

Davis D., 2006, Epic and Sedition: The Case of Ferdowsi's Shahnameh. Mage, Washington, DC

de Blois F., 1996, Iran, 34, 39

de Jong A., 1997, Traditions of the Magi: Zoroastrianism in Greek and Latin Literature. Brill, Leiden

Durkin P., 2009, The Oxford Guide to Etymology. Oxford University Press, Oxford

Geeraerts D., 2010, Theories of Lexical Semantics. Oxford University Press, Oxford

Gutas D., 1998, Greek Thought, Arabic Culture. Routledge, London

Hoffmann S. M., Vickers D., Mamajek E., Adams D., et al., 2025, preprint

Holbrook J., 2011, in Thieberger N., ed., The Oxford Handbook of Linguistic Fieldwork. Oxford University Press, Oxford, pp 345–367

Holton G., 2016, in Schleigh S., ed., Introduction to Cultural Archeoastronomy Across the Pacific Basin. East Carolina University, Greenville

Kelley D. H., Milone E. F., 2011, Exploring Ancient Skies, 2nd edn. Springer, New York

Kennedy E. S., 1956, Transactions of the American Philosophical Society, 46, 123

Kent R. G., 1953, Old Persian: Grammar, Texts, Lexicon, 2nd edn. American Oriental Society, New Haven

King D. A., 2004, In Synchrony with the Heavens, 2 vols. Brill, Leiden

Kövecses Z., 2010, Metaphor: A Practical Introduction, 2nd edn. Oxford University Press, Oxford

Kress G., van Leeuwen T., 2006, Reading Images: The Grammar of Visual Design, 2nd edn. Routledge, London

Kunitzsch P., Smart T., 2006, A Dictionary of Modern Star Names, 2nd edn. Sky Publishing, Cambridge, MA

Lakoff G., Johnson M., 1980, Metaphors We Live By. University of Chicago Press, Chicago

López A. M., 2024, in Frîncu M., ed., Proceedings of the 29th Conference of the European Society for Astronomy in Culture, Timişoara 2022. Editura Universităţii de Vest, Timişoara, pp 151–168

MacKenzie D. N., 1971, A Concise Pahlavi Dictionary. Oxford University Press, London

Malandra W. W., 1983, An Introduction to Ancient Iranian Religion. University of Minnesota Press, Minneapolis

Matras Y., 2009, Language Contact. Cambridge University Press, Cambridge

Meisami J. S., 1987, Medieval Persian Court Poetry. Princeton University Press, Princeton

Meisami J. S., 1995, Niẓāmī, The Haft Paykar: A Medieval Persian Romance, translated by J. S. Meisami. Oxford University Press, Oxford

Mobini M., Marnani P. R., 2019, Journal of Art Faculty, Shahid Chamran University of Ahvaz, 8, 54

Morrison R. G., 2007, Islam and Science: The Intellectual Career of Niẓām al-Dīn al-Nīsābūrī. Routledge, London

North J., 2008, Cosmos: An Illustrated History of Astronomy and Cosmology. University of Chicago Press, Chicago

Palmer G. B., 1996, Toward a Theory of Cultural Linguistics. University of Texas Press, Austin

Panaino A., 1990, Tištrya, Part I: The Avestan Hymn to Sirius. Istituto Italiano per il Medio ed Estremo Oriente, Rome

Pingree D., 1963, Isis, 54, 229

Pingree D., 1973, Journal of the American Oriental Society, 93, 32

Ragep F. J., 1993, Naṣīr al-Dīn al-Ṭūsī's Memoir on Astronomy. Springer, New York

Ragep F. J., Ragep S. P., eds, 1996, Tradition, Transmission, Transformation. Brill, Leiden

Reingold E. M., Dershowitz N., 2018, Calendrical Calculations: The Ultimate Edition. Cambridge University Press, Cambridge

Retrê J., Russo P., Lee H., Penteado E., et al., 2019, Big Ideas in Astronomy: A Proposed Definition of Astronomy Literacy, International Astronomical Union Commission C1

Root M. C., 1979, The King and Kingship in Achaemenid Art. Brill, Leiden

Ruggles C. L. N., ed. 2015, Handbook of Archaeoastronomy and Ethnoastronomy. Springer, New York

Rypka J., 1968, History of Iranian Literature. Reidel, Dordrecht

doi: https://doi.org/10.52526/25792776-26.73.1-160

Sabra A. I., 1987, History of Science, 25, 223

Saliba G., 1994, A History of Arabic Astronomy. New York University Press, New York

Salimpour S., Fitzgerald M. T., 2024, Science & Education, 33, 405

Sayılı A., 1960, The Observatory in Islam. Turkish Historical Society, Ankara

Schimmel A., 1992, A Two-Colored Brocade: The Imagery of Persian Poetry. University of North Carolina Press, Chapel Hill

Schmitt R., ed. 1989, Compendium Linguarum Iranicarum. Reichert, Wiesbaden

Sezgin F., 1978, Geschichte des arabischen Schrifttums, Vol. 6. Brill, Leiden

Sharifian F., 2017, Cultural Linguistics: Cultural Conceptualisations and Language. John Benjamins, Amsterdam

Sims-Williams N., 1989, in Schmitt R., ed., Compendium Linguarum Iranicarum. Reichert, Wiesbaden, pp 165–172

Steele J. M., 2012, A Brief Introduction to Astronomy in the Middle East. Saqi, London

Taqizadeh S. H., 1938, Old Iranian Calendars. Royal Asiatic Society, London

Thomason S. G., Kaufman T., 1988, Language Contact, Creolization, and Genetic Linguistics. University of California Press, Berkeley

Traugott E. C., Dasher R. B., 2002, Regularity in Semantic Change. Cambridge University Press, Cambridge

Windfuhr G., ed. 2009, The Iranian Languages. Routledge, London

doi: https://doi.org/10.52526/25792776-26.73.1-160

The Name of Pavel Petrovich Parenago in Science as a Part of Astronomical Heritage

I.V. Kuznetsova*

Sternber Astronomical Institute of Moscow State University, Moscow, Russia

Abstract

Astronomical heritage is a broad concept. It mainly includes objects related to astronomical observations, as well as places that contain evidence of traditional astronomical beliefs among local communities. Additionally, it now includes astronomical photographic plates that are being digitized to preserve their images. This article proposes a perspective on scientific phenomena named after Pavel Petrovich Parenago, a remarkable Russian astronomer, as part of the astronomical heritage.

Keywords: ~~*astronomical heritage, stellar astronomy, Parenago paradox, Parenago formula, Parenago effect, Parenago ratio.*~~

The name of Pavel Petrovich Parenago, one of the founders of the Moscow School of Stellar Astronomy, which still actively working and continues the traditions laid down by the master both in Moscow and in other astronomical centers, named by many scientific phenomena. This name is now part of the astronomical heritage Pavel Petrovich Parenago wrote the world's first textbook on stellar astronomy. He is the author of the term "Stellar Astronomy" (Efremov (2006)). This alone makes his name a part of the Astronomical Heritage. In addition to the term itself, he developed the course in detail and taught this course at Moscow University since 1934. The course is still relevant under the name "Galactic astronomy".

How often do scientists' names remain in science? It turns out that this doesn't happen very often. Sometimes, names appear and then disappear unnoticed. Relationships and formulas are refined, theorems are generalized, and new names emerge. This work is dedicated to the question of how many scientific phenomena are called by the name of Pavel Petrovich Parenago, one of the founders of the Moscow school of stellar astronomy. There are several "Parenago paradoxes, Parenago plans, and formulas and relations named after him".

Parenago does not seem to be a Russian surname. Pavel Petrovich Parenago himself, with humor, explained the origin of his surname by saying that one of his ancestors had the nickname "Parenoy" and the next was already the son of "Parenoy", in the old way "son of P*A*renag*o*", and then the stress shifted to the end, and became "Paren*A*go".

The ancestors of the Parenago family served the Russian throne as nobles and received estates from the tsar in 1615 and in subsequent years. This is confirmed by a certificate from the Department of Estates and a copy of a resolution from the Voronezh Noble Assembly, which included the Parenago family in the 6th part of the old nobility (Russian State Historical Archive (1857)). The Parenago family coat of arms was very picturesque: it depicted a goose sitting on the grass with its head facing to the right on a blue field. The shield was topped with a noble helmet and a crown with ostrich feathers. The shield was edged with a blue border and a silver border (see figure 1).

My hero's biography is typical for a scientist. He was born on March 7 (20), 1906, in the family of a doctor in Ekaterinodar, now Krasnodar. The date of birth is also given in the old style, as the Julian calendar was used in Russia until 1917. Since 1912, the family has been living in Moscow. At school, the boy was interested in chemistry and astronomy. Already in 1919, he began astronomical observations using binoculars and a spyglass. In 1921, he joined the Moscow Society of Astronsfomy Lovers. Pavel became involved in the study of variable stars and mastered photometric methods. This interest defined the activities of the young observer for many years. In 1922, he enrolled in two faculties of Moscow State University: the Faculty of Chemistry and the Faculty of Physics and Mathematics.

*irinakuznetsova-64@mail.ru

doi: https://doi.org/10.52526/25792776-26.73.1-167

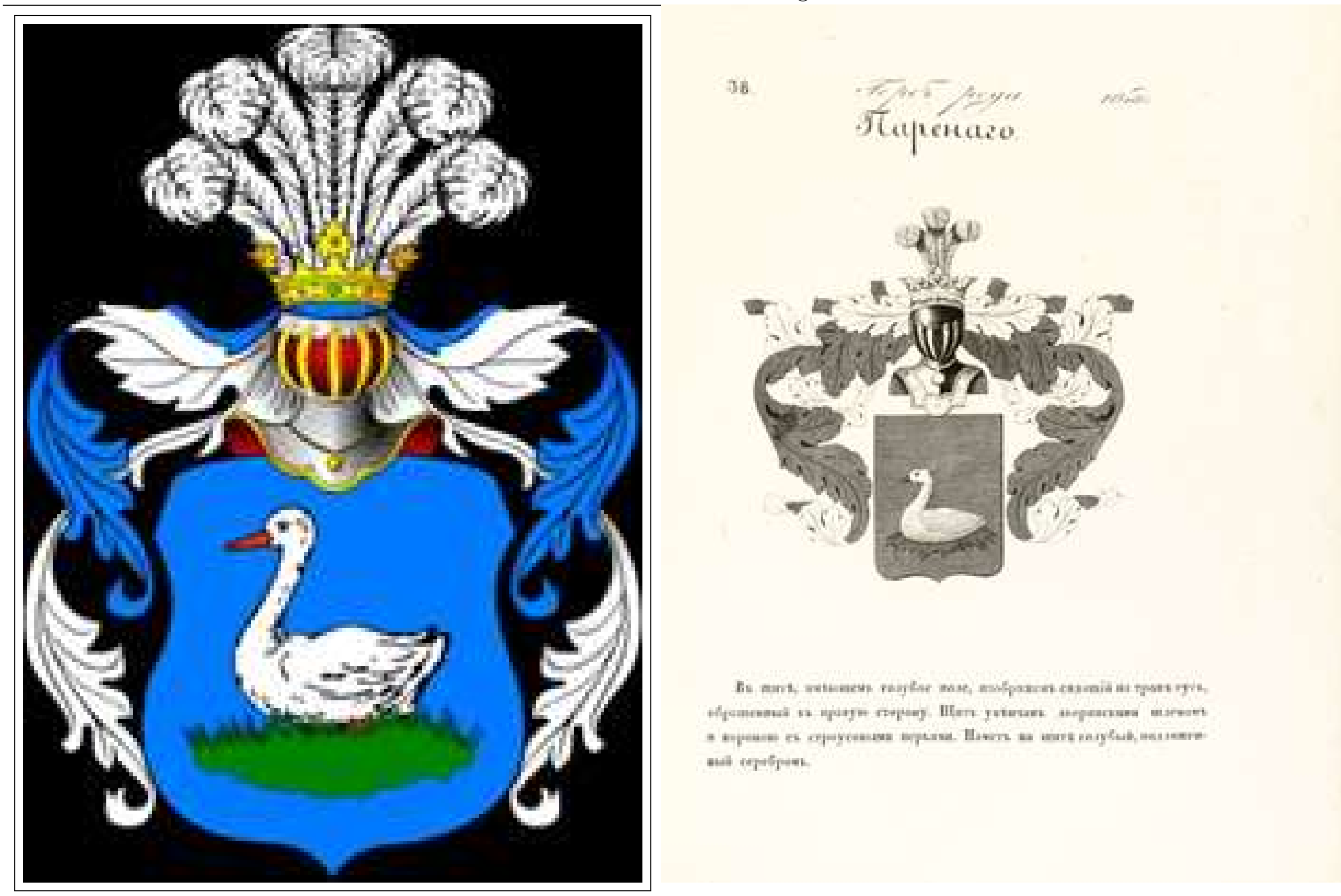

Figure 1. The coat of arms of the Parenago family.

At the same time, he began systematically observing variable stars. However, it became too difficult for him to study in two different faculties simultaneously. As a result, he had to leave the chemistry department. It is worth noting that his future family continued to share a common interest in chemistry. His son, Oleg Pavlovich Parenago, is a renowned Russian chemist and winner of the N.D. Zelinsky Prize, while his granddaughter, Olga Olegovna Parenago, is actively engaged in chemical research, just like her father. Let's go back to the stars.

From 1927 to 1931, Pavel Petrovich worked at the Krasnopresnenskaya Observatory, where he photographed the sky using an equatorial camera. He studied the images and made several tens of thousands of brightness estimates for nearly a thousand poorly studied or unstudied variable stars. In total, Pavel Petrovich studied at the university for seven years, in parallel with his work. In 1925, he became a researcher at the State Astrophysical Institute, and in 1927, he joined the Astronomical and Geodetic Institute at Moscow State University. As is well known, the merger of these two institutes with the Moscow State University's astronomical observatory led to the establishment of the Sternberg State Astronomical Institute at Moscow State University in 1931, and in 1932, P.P. became a senior researcher at the Sternberg Institute. At the time, the institute had a truly stellar team of researchers studying variable stars. Blazhko, Kukarkin, Zverev, Kulikovsky, and others. Even then, the surname Parenago became well-known in the astronomical scientific community.

After graduating from university in 1929, during the summer holidays, he began working with the archive of photographic plates at the Simeiz Observatory. It was during this time that he realized that personal observations alone were not sufficient for serious research. In our country, Parenago was a pioneer in the use of mass photographic heritage on glass plates. Since then, the use of glass libraries has become widespread. In his spare time at the Simeiz Observatory, he read all the major astronomical journals published after 1900, and his excellent memory made this reading very useful.

In 1932, according to the "Parenago Plan", researchers at the Sternberg Institute and the Astronomical Council of the Academy of Sciences organized the **Central Commission for the Study of Variable Stars**. This commission united all research on variable stars conducted in the USSR.

Later, P.P Parenago's activities were quite diverse: research, teaching, organizational, administrative, and publishing activities, work in the USSR and abroad, in the International Astronomical Union, and

doi: https://doi.org/10.52526/25792776-26.73.1-167

other organizations. Since 1934, P.P. has been the first person in our country to give systematic lectures on stellar astronomy. Prior to this, lectures on specific aspects of stellar astronomy were only held occasionally. At that time, stellar astronomy was generally limited to stellar statistics, but P.P. viewed it as a branch of astronomy that was just as important as astrometry, astrophysics, and celestial mechanics, with the primary goal of studying the structure and evolution of stellar systems. Thus, stellar dynamics is an integral part of stellar astronomy, and the most important objects are variable stars, special stars that we usually know much more about than stars of constant luminosity. He considered his greatest achievement in life to be the fact that he contributed to the introduction of this course in all universities with an astronomy department.

In 1934, Parenago and Kukarkin discovered a linear relationship between the amplitude of dwarf star flashes and the logarithm of the time between flashes. Parenago and Kukarkin applied this relationship to the star called Nova T Corona Borealis, T CrB). In 1866 it had only one flash, with an amplitude lower than the amplitudes of Nova Stars and closer to the Repeated Nova ones.

Pavel Petrovich Parenogo and his collaborator Boris Vasilievich Kukarkin took the risk of applying this dependence to T Corona Borealis and predicted its surge 60-100 years after the previous one, i.e. from 1926 to 1966. And it happend in 1946! The Kukarkin-Parenago dependence means that energy accumulates between flashes, and the longer it accumulates, the more powerful the flash becomes. Thus, the variability of Nova, recurrent Nova, and U Geminorum-type stars is associated with their binarity and occurs in the late stages of the evolution of close binary systems.

In 1935, Parenago became a Doctor of Sciences (the second highest scientific degree accepted in Russia) for his significant contribution to science without submitting and defending a doctoral dissertation.

In about 1936, P.P. Parenago and B.V. Kukarkin began thinking about creating a new department of Stellar Astronomy in Moscow University.

Back in the 1920s, Pavel Petrovich came up with the idea of collecting all the known information about all the known stars. When he processed the vast amount of data he had collected, he discovered that the kinematic parameters of early-type (B-F) and late-type (G-M) stars were similar within their respective groups, but there was a gap between them. This phenomenon later became known as the Parenago effect (also referred to as the Parenago gap in foreign literature) (Parenago (1950)). In the late 1920s, Pavel Petrovich spent a lot of time photographing the sky. It is likely that his work with photographic plates inspired him to collect all the known information about all the famous stars. In the early 1930s, Parenago and his team began compiling a database containing information about stars, including their brightness, proper motions, parallaxes, and radial velocities. Did they create several tens of thousands of cards, which formed the basis for the combined catalog of variable stars.

The illustration of the process of collecting stars in the catalogues of P.P. Parenago and B.V. Kukarkin takes us back to the distant times of Ancient Babylon. The stars that moved across the sky as a single group were called "rams", and the wandering planets among them were called "goats" (bibu) these were more intelligent beings who served as guides for herds of sheep.Currently, wall newspapers have not been preserved, but in the past, they were a means of communication, criticism, and education in various groups. The wall newspaper at the Sternberg Astronomical Institute appeared in late 1944. Along with the texts of the newspaper "Vladilena" (named after Vladimir Lenin), it also featured drawings related to current events. The main illustrator was I.S. Shklovsky, who was not only a renowned astrophysicist but also a talented cartoonist with a keen eye for both the scientific and social aspects of the institute's life.

When the card index covered all the variable stars known at that time, B.V. Kukarkin and P.P. Parenago were able to propose, at the first post-war meeting of the Executive Committee of the International Astronomical Union, to continue the work on the systematization and cataloging of variable star data that had previously been carried out by Germany in Moscow. The proposal was accepted, and in 1948, the first edition of the General Catalogue of Variable Stars was published in Moscow.

The Parenago effect was later confirmed on a more representative sample of millions of stars when processing the results of the Hyparchos and Gaia space missions.

Another area of Parenago's research was the study of the structure of our Galaxy. This included not only the star counts that had been conducted before, but also the determination of the gravitational potential of the galaxy and the distribution of its mass. Parenago was the first who calculate the orbit of the Sun in the Galaxy before the Second World War, and in 1945 he studied the oscillations of stars (including the Sun) perpendicular to the Galactic disk.

These studies were followed by analytic research on the gravitational potential of the Galaxy. In this task, Pavel Petrovich considered our Galaxy as a stellar system with axial symmetry that is in statistical equilibrium. In this case, the distribution of stars is expressed through six constants, the integrals of motion,

doi: https://doi.org/10.52526/25792776-26.73.1-167

Figure 2. Drawing by I.S. Shklovsky from the 1947 issue of the Vladilena wall newspaper of the Astronomical Institute.

but only two of them can be found explicitly for the axisymmetric case. The equations describing this system can be solved analytically and provide a good description of the rotation curve in the vicinity of the Sun. While working on this problem, he came up with a result known as the Parenago Paradox: the density of stars far from the center of the Galaxy was negative. Another paradox associated with Parenago's name is that he was the first to question the enormous mass of our Galaxy's core (60 percent) in the Oort model.

In the 1930s, it became clear that there was light extinction in the Galaxy, causing a decrease in the brightness and a change in the colors of stars. This became one of the most important problems in stellar astronomy. Parenago's first work on interstellar extinction was done in the mid-1930s. By 1940, Pavel Petrovich assumed that the absorbing matter was distributed near the Galactic plane in the same way as the stars, i.e., according to the barometric law, with an exponential decrease in density with distance from the Galactic plane. It is often referred to as Parenago's formula, and it has become widely accepted.

A private but very important discovery made in 1950 by P.P. Parenago and A.G. Masevich was the Algol Paradox, sometimes also called the Parenago Paradox (Parenago & Masevich (1951)). According to theory, more massive stars evolve faster. In a binary system, the components are formed simultaneously, so the more massive star should be in a later stage of evolution. However, in the Algol system, the opposite is true: the less massive component has already left the main sequence, while the more massive component is still on it. Is this a paradox? In 1955, American astronomer J. Crawford provided an explanation for this paradox. The state of the binary system was attributed to the transfer of matter between its components. And these are not all the names. There is also the Ogorodnikov-Parenago potential, the Fesenkov-Parenago theorem, which is used in the calculation of stars, and the Kamma-Parenago function, which is used to describe the kinematics of a Galaxy (Kuznetsova & Prokhorov (2024)).

In 1953, P.P. Parenago was elected a corresponding member of the USSR Academy of Sciences, and in the same year, he organized the Commission on Stellar Astronomy under the Astronomical Council of the Academy of Sciences, which he headed until the end of his life. In 1954, P.P. Parenago became the first recipient of the Bredikhin Prize of the USSR Academy of Sciences. In 1955, the fist plan evolved into the 2-nd Parenago Plan which aimed to comprehensively study special regions of the Milky Way, including dark and bright nebulae, star clusters, and associations. The plan included the observation of 40,000 stars down to 13-th magnitude. Several observatories in the USSR joined the effort to implement this plan.

So, there are three Parengo paradoxes in astronomy. In addition to his name in the name of scientific phenomena, Parengo left behind a whole school of followers who continued his work (Vorontsov-Velyaminov et al. (1961)).

P.P. Parenago's printed legacy includes several hundred scientific papers and a number of popular science books (Lavrova (1961)).

It turned out that in 1958 and 1959, Parenago was the most cited author in the USSR, and even in 1965

doi: https://doi.org/10.52526/25792776-26.73.1-167

(five years after his death), he was in third place.

Pavel Petrovich is an outstanding scientist and a wonderful person whose name belongs to the astronomical heritage. The name Parenago is also used for naming space objects .It was given to the asteroid 2484, discovered on October 7, 1928, by the Russian and Soviet astronomer Grigory Neuymin at the Simeiz Observatory, and it was named after P.P. Parenago on June 6, 1982. Additionally, the name Parenago was given to a crater on the far side of the Moon. According to the IAU rules, craters are named after deceased prominent scientists, engineers, and researchers who made significant contributions to their fields, although there are exceptions. Most of the new names were assigned in the 1970s, after the acquisition of images of the far side of the Moon.

In 1975, the ship Pavel Parenago was built in the Soviet Union. The ship was built in Gdansk, Poland. The ship was used by the Latvian Maritime Shipping Company until 2003.

It is impossible to tell the story of such a great person in a short article.

P.P. Parenago died of laryngeal cancer on January 5, 1960. Until the last weeks of his life, he continued to work. His life in astronomy, as a hardworking employee, an enthusiast, and an encyclopedist, is the best example for anyone who understands that without the accumulation of observational data, theory is powerless, and that without attempting to interpret this data based on existing theory, it remains a dead weight. Ultimately, it is the theory that determines which data are necessary at any given time.

We have only touched on the aspects of his work that are directly related to his name. His astronomical heritage is much greater than that. The questions he posed in science are still being refined using modern methods and much more extensive data.

Acknowledgements

The study was conducted under the state assignment of Lomonosov Moscow State University.

References

Efremov Y. N., 2006, Earth and Universe, 3, 57

Kuznetsova I. V., Prokhorov M. E., 2024, Astron. Rep. , 68, 97

Lavrova N. B., 1961, Historical and Astronomical Research, 7, 383

Parenago P. P., 1950, Asron. Zhurn., 27, 150

Parenago P. P., Masevich A. G., 1951, Publ. SAI, 20, 81

Russian State Historical Archive 1857, fond. 1343, inventory. 27, case. 876

Vorontsov-Velyaminov B. A., Kukarkin B. V., Kulikovsky P. G., et al. 1961, Historical and Astronomical Research, 7, 335

doi: https://doi.org/10.52526/25792776-26.73.1-167

Reconsidering the *Bundahishn* through Cultural Astronomy

Shirin Zandian *[1] and Saeed Jafari†[2,3,4,5]

[1]IAU OAE National Astronomy Education Coordinator for Iran, Tehran, Iran
[2]International Decade of Indigenous Languages (IDIL 2022–2032), UNESCO
[3]World Space Week Association
[4]Department of Linguistics, University of Kurdistan, Sananda
[5]IAU Commission C5 Cultural Astronomy, International Astronomical Union

Abstract

The relationship between myth and astronomy began long before telescopes. Celestial change was followed through observation, memory, ritual, and narrative, allowing practical knowledge of seasons and stars to pass across generations. This review examines Zoroastrian cosmology, especially the *Bundahishn*, and considers its use in astronomy education. It brings together cultural astronomy, science education, Iranian myth studies, and research on narrative learning. Henning's analysis shows that the astronomical chapter coordinates inherited Avestan material with pre-Achaemenian conceptions, Babylonian zodiacal knowledge, and elements of Greek astronomy in a single cosmological compilation. The Tishtrya tradition offers a focused example in which seasonal concern, ritual time, and Sirius meet within a memorable account. Comparative evidence further suggests that culturally grounded storytelling can connect astronomical concepts with identity without presenting myth as an empirical model. The article proposes a three-stage teaching framework moving from narrative encounter to observational checking and critical interpretation, with particular relevance to historically informed astronomy literacy among younger learners in Iran today.

Keywords: *Bundahishn; Zoroastrian cosmology; cultural astronomy; science education; storytelling; history of astronomy*

1. Introduction

The history of astronomy begins before instruments, in sustained watching, memory, and the effort to account for changes in the sky. Early cosmologies brought together records of observed events with explanations of their significance and narrative forms through which knowledge could be recalled and transmitted. Although these accounts differ from modern scientific models, their organisation was often closely related to seasonal timing, stellar appearances, and weather patterns of practical importance.

Research in science education shows that learning astronomy involves more than mastering equations or memorising the names of planets since learners approach the sky through prior conceptions shaped by language, culture, and personal experience. These conceptions may support new understanding or interfere with it (Galili, Weizman & Cohen, 2004). Zoroastrian cosmology, especially the account preserved in the *Bundahishn*, is useful in this context as it presents an ordered universe in which celestial structure is closely connected with time, ritual, and moral life.

This article brings together several studies and perspectives from cultural astronomy, comparative myth, Iranian philology, and research on storytelling in science education. Henning's source analysis of chapter 2 provides a distinctive historical point. The astronomical compilation places early Iranian cosmological assumptions beside knowledge of the zodiac and planets acquired through Babylonian contact, and later elements of Greek astronomy such as stellar magnitudes and planetary elongations (Henning, 1942). This layered composition matters for education as it shows astronomical knowledge being selected and coordinated across periods instead of developing within an isolated tradition.

*shzandian@gmail.com, Corresponding author
†saeed.jafari72@gmail.com

doi: https://doi.org/10.52526/25792776-26.73.1-172

2. The *Bundahishn* as a Cosmological Compilation

The *Bundahishn*, usually translated as "Primal Creation," is a major Middle Persian work of Zoroastrian cosmogony and cosmography. Henning (1942) identifies *Zand-agahih* as its more exact title and glosses it as an exposition of information supplied by the Pahlavi version of the Avesta. He treats the work as an original cosmological compilation, whose compiler coordinated dispersed Avestan teachings and drew on several sources. The surviving recensions were transmitted and revised over a long period, so their chapters preserve materials from different historical layers.

The astronomical chapter begins with the creation of the Lights and distinguishes fixed stars, non-fixed stars, the moon, and the sun. It then sets the twelve zodiacal constellations on a sphere formed in the likeness of the year, each sign corresponding to a month and each thirty-degree division to its days (Henning, 1942). The chapter also assigns celestial commanders to the directions. The Great Bear, or Haftoreng, governs the north and is linked through seven tethers to the seven continents, a cosmographic arrangement in which observable star groups acquire administrative and protective functions.

Henning's reading reveals an unusually composite astronomical scheme. Early assumptions about the order and distance of the celestial bodies remain beside the Babylonian ecliptic and zodiac; the planets and later Greek elements, including stellar magnitudes and calculated elongations. The same chapter refers to the zodiacal sphere, lunar mansions, and the sphere of the Unmixable Stars. These technical strata give a more precise basis for studying the *Bundahishn* than broad descriptions of an ordered sky, and they show how the compiler reconciled inherited authority with astronomical materials of different origins and dates.

3. Myth as Encoded Astronomy in Bahar's Reading

In some science classrooms myth is still presented as a discarded stage that rational inquiry had to leave behind. Bahar (1998), drawing on Iranian and Indo-European materials, offers a less rigid account in which myths compress repeated encounters with weather, seasonal change, animals and the sky into forms that can be remembered and taught. Symbolic meaning and measurement remain different forms of knowledge, yet narrative may preserve relationships among events long after the circumstances of the first telling have disappeared. Its evidential value must therefore be assessed case by case.

The Tishtrya cycle provides a strong Iranian example. Tishtrya is associated with Sirius, the brightest star in the night sky, and Yasht 8 recounts his contest with Apaosha, a demon of drought, ending with rain and the release of waters. Read beside the seasonal calendar, the episode connects the return of a conspicuous star with concern over water and expected changes in weather on the Iranian plateau (Krupp, 2003, Panaino, 1995). The climatic correspondence requires caution because stellar visibility, latitude, and historical calendar practices vary; yet, the recurring conjunction of Sirius, ritual time, and rain gives the association a structure that exceeds a casual resemblance.

Panaino (1995) places Tishtrya within the Zoroastrian month-name system and ritual year, where the episode could serve as a cognitive index linking an ecological concern with a celestial marker and then binding both to communal obligation. Bahar's approach helps explain the durability of such an account as several forms of information could be carried together without being treated as identical kinds of knowledge. Henning's translation adds a further detail from the astronomical chapter, where Tishtrya appears as the General of the East and assists the wind, clouds and lightning-fire in bringing down rain (Henning, 1942).

4. Cultural Astronomy, Literacy and Identity

Cultural astronomy approaches the sky as measured experience and interpreted environment. Groups observing similar stars may draw different figures, names and moral associations from them, with those differences shaped by geography, language and social history. Astronomy education gains little when culture is treated as an optional decoration. Salimpour & Fitzgerald (2024) argue that culture can provide a starting point for astronomy learning provided that local knowledge is examined seriously and scientific claims remain open to evidential testing.

Retré et al. (2019) widen astronomy literacy beyond factual knowledge by including astronomy's place in culture, history, civilisation and art alongside its scientific concepts. This formulation is particularly relevant to the *Bundahishn*. A learner who can identify Sirius yet lacks the means to discuss why stars entered calendars, architecture, poetry or ritual has acquired a restricted form of literacy. The cosmological

doi: https://doi.org/10.52526/25792776-26.73.1-172

compilation therefore allows astronomical classification to be studied together with the practices that gave celestial knowledge public meaning and historical durability.

Jaleh Amuzgar gives this cultural argument a specifically Iranian grounding by explaining that people form myths over long periods from their social conditions, beliefs, needs, and surrounding environment, and that these narratives preserve the ways communities understood themselves and their world (Amuzgar, 2014). Reading Iranian myths can therefore become a way of reading the land because mountains, drought, water, seasonal uncertainty, and concepts of order enter the narratives as lived pressures instead of neutral scenery. In astronomy education, a mythic sky should be interpreted in relation to the environment from which its patterns gained urgency.

The aspect of Figueiró et al. (2019) that most closely connects with the present article is reciprocal cultural exchange. The GalileoMobile team worked in November 2016 in the Sete de Setembro Indigenous Land near Cacoal in Rondônia. Activities at Linha 12, Linha 14, and Linha 9 combined storytelling, drawing, shadow puppetry, and sky observation with dialogue about Paiter Suruí knowledge. Interviews and records were returned to the community for educational and cultural use. The Iranian setting differs; yet, the methodological lesson remains relevant. Cultural astronomy materials should be developed with attention to their holders, language, and local purpose instead of being extracted as a colorful introduction to standard content.

5. Storytelling-Based Teaching and Iranian Narrative Forms

Storytelling-based teaching organises a lesson around a narrative problem and then uses guided questions, observation, or other evidence to revise the learner's first interpretation. This approach is relevant to astronomy since many concepts involve scales, movements, and intervals of time that are difficult to experience directly. Narrative supplies a sequence through which those relations can first be imagined and later examined. Salimpour & Fitzgerald's (2022) idea of the "cosmic interaction" is useful here, as learners often encounter questions of origin and time through scientific and cultural resources at the same moment.

Iran also has performative traditions accessible to children and adolescents. Naqqāli uses voice, gesture, and at times painted scrolls to carry epic and religious narratives into public performance. UNESCO identifies it as Iran's oldest dramatic storytelling tradition (UNESCO, 2011). Modern children's theater developed through educators and institutions, including Jabbar Baghcheban, who wrote *Khānom Khazuk* in 1928 as an early Persian play for children, and Kanoon's Theater Center, which later used puppet theater, touring productions, and adolescent acting groups in artistic education (Encyclopaedia Iranica Foundationr, 1991, 2011). These forms allow an episode from the *Bundahishn* to be voiced, staged, and questioned instead of being reduced to a textbook paraphrase.

Persian publishing includes a large body of translated and originally authored books on children's literature, storytelling and narrative writing. Many approach astronomy or space through modern settings and fictional characters. Illustrated retellings from classical Persian literature are also well established, yet narratives comparable to the *Bundahishn* remain largely unadapted as educational stories for children and adolescents. The contest of Tishtrya and Apaosha and the account of Yima's Vara are two recognised ancient examples. Any adaptation should distinguish the source passage from later interpretation and present-day astronomy. Figueiró et al. (2019) offers a practical precedent through activities that join elder-told myths with drawings, shadow puppets, and direct observation. A *Bundahishn*-based lesson could similarly lead into a star chart, seasonal visibility exercise, or short performance whose script is revised after its celestial claims are checked against observation, simulation, or a reliable astronomical source.

6. Toward an Integrated Pedagogical Model

A workable classroom model can proceed through three stages, beginning with narrative entry. A short, source-based version of the Tishtrya episode introduces Sirius, drought, and calendrical expectation in a form that learners can recall. The teacher then identifies the source and explains that the episode belongs to an older cosmology. This framing prevents the account from appearing either as an anonymous folktale or as a disguised scientific explanation.

The second stage involves observational comparison. Learners examine when Sirius is visible at a selected latitude, how heliacal rising is defined, and how differences among calendar systems affect any proposed seasonal connection. A planetarium program or historical sky simulation may support this work, although

doi: https://doi.org/10.52526/25792776-26.73.1-172

a printed horizon diagram can also be sufficient. Agreements and discrepancies both deserve attention as they reveal which observational relations narrative compression preserves and which details it modifies.

The third stage is critical interpretation. Learners consider what the episode organised for its community and what a modern visibility model is designed to explain. They may compare a ritual calendar with an astronomical table or rewrite one scene after checking the sky data, so the difference between a Yasht and a scientific paper becomes visible through their distinct questions and rules of evidence. This stage gives the arts a precise educational role, allowing drawing, theatre and illustrated narrative to externalise a learner's model and make it available for correction, discussion and comparison within an interdisciplinary approach linking science with history and the humanities.

7. Discussion

The *Bundahishn* presents observation and interpretation within a single cosmological compilation, a feature that gives the work educational value and also requires careful handling. If it is presented only as imaginative heritage, its technical distinctions may disappear. If it is treated as a concealed modern textbook, its religious and historical character becomes distorted. A more defensible approach examines what the astronomical chapter classifies, how those classifications are placed within the cosmological scheme, and where modern evidence alters or qualifies them.

Storytelling can change the learner's relation to abstract content by making visible the human reasons for watching the sky. Yet the present article proposes a pedagogical framework and reports no classroom intervention involving Iranian pupils. References to possible learner responses are included as instructional cautions since the argument draws on astronomy education research and comparable cultural programmes rather than student data produced for this review. Particular attention is given to the risk of treating a symbolic account as an empirical model or merging astronomy with astrology through their historical overlap.

Historical accuracy is more than a scholarly preference because simplified or romantic versions of Zoroastrian cosmology can imply that ancient observers were either irrational or secretly modern, and both interpretations misrepresent the sources. Provenance, translation choices, and the limits of astronomical reconstruction should remain visible in teaching materials even when the language is adapted for younger groups. Future development should concentrate on source-based Persian materials prepared with input from historians of religion and astronomy educators. Any pilot use would require clearly documented age groups, teaching settings, and learning aims. Until such work is undertaken, the model proposed here remains a reasoned pedagogical framework rather than an evaluated intervention.

8. Conclusion

The *Bundahishn* can contribute to astronomy education when its celestial classifications are examined together with the cultural work performed by its narratives. The central implication is methodological: begin with a historically sourced episode, test its astronomical relations, and then interpret why those relations mattered within their own society. This sequence avoids romantic equivalence and sterile separation. It also identifies a specific gap in Persian educational publishing, where modern space stories are common, but illustrated and critically framed adaptations of Zoroastrian cosmology remain limited. Developing such material requires philological care, age-appropriate design, and explicit rules of evidence. Henning's analysis makes another requirement clear. The astronomical chapter contains material from different intellectual periods, so educational adaptations must preserve that internal layering instead of presenting the compilation as a single undifferentiated voice.

References

Amuzgar J., 2014, People of every land construct myths and repetition gives them legitimacy. [Persian lecture transcript], Center for the Great Islamic Encyclopedia

Bahar M., 1998, Pajuhesh-i dar asatir-i Iran [Research on Iranian mythology]. (rev. ed.), Agah.

Encyclopaedia Iranica Foundationr 1991, Children vii. Children's literature.. Encyclopaedia Iranica,, 5(4), 417

Encyclopaedia Iranica Foundationr 2011, Kānun-e Parvareš-e Fekri-e Kudakān va Nowjavānān vii.. Visual Arts Training Center, Encyclopaedia Iranica

doi: https://doi.org/10.52526/25792776-26.73.1-172

Figueiró S. P., Germano A. P., Fernades C., et al & GalileoMobile Team 2019, Astronomy across cultures. Reporting experiences on the GalileoMobile education activities in the Paiter Suruı indigenous community. EPJ Web of Conferences, 200, doi.org/10.1051/epjconf/201920002009

Galili I., Weizman A., Cohen A., 2004, The sky as a topic in science education. Science Education. 88(4), 574-593

Henning W. B., 1942, An astronomical chapter of the Bundahishn. Journal of the Royal Asiatic Society of Great Britain and Ireland. Journal of the Royal Asiatic Society of Great Britain and Ireland, 74(3–4), 229–248, doi.org/10.1017/S0035869X00097926

Horowitz W., 2010, Stars, cows, semicircles and domes. Astronomical creation myths and the mathematical universe. W. Horowitz, U. Gabbay, F. Vukosavović (Eds.), A woman of valor. Jerusalem Ancient Near Eastern studies in honor of Joan Goodnick Westenholz (pp. 73–87), CSIC

Krupp E. C., 2003, Echoes of the ancient skies. The astronomy of lost civilizations. Dover Publications.

McLeod A., 2016, Astronomy in the ancient world. Early and modern views on celestial events. Springer, doi.org/10.1007/978-3-319-23600-1

Panaino A. C. D., 1995, Tišstrya, Part II. The Iranian myth of the star Sirius. Serie Orientale Roma, Vol. 68, No. 2, Istituto Italiano per il Medio ed Estremo Oriente

Panaino A. C. D., 2004, Astral characters of kingship in the Sasanian and the Byzantine worlds. In La Persia e Bisanzio. Atti dei Convegni Lincei (Vol. 201, pp. 555–594), Accademia Nazionale dei Lincei

Retré J., Russo P., Lee H., et al. 2019. Big ideas in astronomy: A proposed definition of astronomy literacy. International Astronomical Union Commission C1 Astronomy Education and Development

Salimpour S., Fitzgerald M. T., 2022, The cosmic interaction. A review of the literature on cosmology, religion and the big questions in the context of astronomy education research. Science & Education, 31(3), 819–849, doi.org/10.1007/s11191-021-00250-x

Salimpour S., Fitzgerald M. T., 2024, Astronomy and culture. A social semiotic perspective on the role of culture in astronomy education. Science & Education, 33(2), 405–426, doi.org/10.1007/s11191-022-00389-1

UNESCO 2011, Naqqāli, Iranian dramatic story-telling. Intangible Cultural Heritage in Need of Urgent Safeguarding

doi: https://doi.org/10.52526/25792776-26.73.1-172

Communications of BAO, Vol. 73, Issue 1, 2026, pp. 177-188

Armenian Astrolabes between Appropriation and Agency: Epistemic Recalibration and Material Production

A. Margaryan *

School of Art, Soochow University, Jiangsu, China

Abstract

Despite their presence in museum collections and specialist footnotes, astrolabes bearing Armenian inscriptions or commissioned by Armenian patrons have never been the subject of a systematic, interdisciplinary study. This article addresses that gap through the first integrated analysis of six instruments—held in Oxford, Fez, Doha, Yerevan, and Byurakan—dating from the late ninth to the early eighteenth century. Drawing on object biography, material epistemology, and visual semiotics, the study examines epigraphic layers, rete typologies, and patronage contexts as primary evidence. The instruments are shown to exist on a spectrum: from Islamic devices reinscribed with Armenian alphanumerical notation and vernacular star names to European-type astrolabes produced entirely in Armenian script. In each case, the physical artifact records a deliberate act of adaptation or autonomous commissioning, embedded within trans-Eurasian mercantile and courtly networks. The article thereby reconceptualises these objects not as peripheral curiosities but as material witnesses to a sustained, cross-cultural Armenian practice of astronomical knowledge production and proposes a new, object-centered agenda for their further interdisciplinary study.

Keywords: *astrolabe, Armenian astrolabe, Ghukas Vanandetsi, Amirdovlat Amasiatsi, Armenian diaspora*

1. The Template

The astrolabe (Greek astrolabos, "star-taker") designates a family of analog computational technologies extending from the third century BCE to the present. Earliest forms—large armillary spheres exemplified by Claudius Ptolemy's second-century instrument—evolved into compact devices for astronomical computation and navigation: the planispheric astrolabe; the universal astrolabe (11th-century Toledo, overcoming latitude-sensitivity); the Rojas universal astrolabe (16th-century projection of all celestial spheres onto one plate); the linear astrolabe (rod-based altitude measurement); the spherical astrolabe; and the mariner's astrolabe. The etymology astron (star) and lambanein (to take, calculate) encodes the acquisition and computation of celestial data. Whether suspended in silver for princely collectors or fashioned in wood for a mosque astronomer to determine Mecca's direction and prayer hours, the astrolabe materialized the Ptolemaic cosmos through stereographic projection (Vafea, 2019).

Two historiographical threads must be disentangled: the theoretical development of stereographic projection and its translation into a functional portable object. The mathematical principle of projecting the celestial sphere onto a plane was known to Hellenistic mathematicians such as Hipparchus of Nicaea (2nd century BCE), who may have used it for an anaphoric clock, though this was not a true planispheric astrolabe. Other sources attribute the invention to Apollonius of Perga (3rd century BCE), while the earliest unequivocal treatise is Theon of Alexandria's (4th century CE). Thus, theoretical foundations were laid in Hellenistic Greece, but the fully realized device emerged no later than the 1st century CE, with Theon providing the first unambiguous textual evidence. Physical refinement into a precision instrument with engraved tympans for specific latitudes, an openwork rete depicting fixed stars, and a rotating alidade occurred primarily within the Abbasid caliphate from the 8th century onward. The earliest surviving astrolabe (927-928 CE) is Islamic, testifying to this environment. This tradition inspired Geoffrey Chaucer's 14th-century Treatise on the Astrolabe, one of the earliest English technical works.

The standard planispheric astrolabe comprised a cast or hammered metal frame (brass, iron, copper alloy, or, for ceremonial examples, silver or gold) and five components: the mater (hollowed disk with

*animargaryan@suda.edu.cn

doi: https://doi.org/10.52526/25792776-26.73.1-177

graduated limb); replaceable tympans (plates with stereographic coordinates for specific latitudes); the rete ("net"), an openwork skeletal rotating plate tipped with pointers indicating the brightest stars; the alidade (sighting bar on the reverse face to measure altitude); and the rule for transferring readings. Operational logic reduces to three steps: measure the altitude of the sun or star; align the rete for date and time to read celestial configurations on the tympan; and, through this two-dimensional simulation, solve problems of time, position, and spherical astronomy algorithmically.

Beyond computation, the astrolabe functioned as a symbolic vector of knowledge and authority. Possession or commission signified institutional standing, scientific mastery, and often political legitimacy – authority encoded in brass. Those unable to read the instrument faced epistemic exclusion, so the astrolabe policed the boundaries of science. This dual symbolic function is inscribed on surviving artifacts, which often carry geometric tracery, calligraphic dedications, and multiple engraved names of makers, commissioners, patrons, and later owners. The astrolabe was simultaneously a calculative device, a luxury object, and a palimpsest of social relationships.

Peak production coincided with intensified long-distance trade when technical knowledge traveled alongside commercial goods. On the Silk Road, astrolabes served merchants in determining latitude. In the early modern period, surviving astrolabes multiplied considerably due to commercial expansion, European overseas exploration, and Enlightenment currents valorizing empirical observation. Planispheric astrolabes were not the exclusive product of a single cultural lineage: stereographic projection was independently adapted across regions, from Byzantine ivory to Mughal gilt brass, from Safavid silver to Renaissance paper instruments. Regional variations rendered the astrolabe a genuinely hybrid, multi-national artifact (Borrelli, 2008).

From the standpoint of material epistemology, the astrolabe is a biosocial artifact: its physical form encodes a scientific worldview, while its social life – production, exchange, contested reading, accumulation – reveals how societies construct and deploy understandings of the heavens. This analytical framework is essential for examining instruments connected to Armenian patronage, ownership, or modification.

2. Methodology

This study applies an art-historical and material culture framework to examine the astrolabe as a composite artifact whose visual form, epigraphic layering, patronage contexts, and cross-cultural circulation reveal the epistemic practices of the Armenian diaspora.

The theoretical basis draws from three interconnected approaches: object biography (Kopytoff, 1986), which traces an artifact's trajectory through different regimes of value; material epistemology (Malafouris, 2013), which treats the instrument as an active mediator in knowledge production; and visual semiotics (Panofsky, 1939), which interprets form and ornament as carriers of cultural meaning. These are operationalized through four analytical variables:

1) Visual form and technical architecture – analysis of rete design, tympan latitudes, and scale calibration as visual systems.

2) Epigraphic layering as epistemic intervention – analysis of palimpsest inscriptions, interpreted as visual claims to vernacular operability within Armenian cognitive frameworks.

3) Patronage and socio-historical context – identification of commissioners, makers, and owners within Armenian mercantile-scholarly networks (New Julfa, Ottoman court, Amsterdam). This variable maps the object onto structures of patronage, prestige, and institutional affiliation.

4) Iconographic borrowing and cross-cultural circulation – identification of visual motifs that index non-native scientific traditions, reconstructing the artifact's social life within trans-Eurasian mercantile and diplomatic networks.

3. Literature Review

A systematic review of the existing literature reveals a pronounced scholarly gap: Armenian astrolabes are acknowledged in passing by historians of Islamic instrumentation but have never received a dedicated, systematic study. The earliest and still foundational reference is Tumanyan's (1964) Hay astğagitutyan patmutyun, published in Yerevan. This work first provided photographic documentation and descriptive notes for several astrolabes bearing Armenian inscriptions or attributed to Armenian makers. However, it remains a preliminary survey rather than a definitive reference.

doi: https://doi.org/10.52526/25792776-26.73.1-177

Tumanian's contributions have been consistently cited by preeminent Western historians of Islamic scientific instruments, most notably King (1996a) in his Catalogue of Medieval Astronomical Instruments and in subsequent collaborative publications (King Charette, 2024). On pages 147–148 of the latter, King explicitly states that three Armenian astrolabes are known but have never been properly described in Western scholarship. Similarly, the History of Science Museum in Oxford houses at least two items with Armenian connections, yet the museum's published online catalogue offers only brief technical descriptions without socio-historical contextualization. Thus, despite being recognized as extant objects, these instruments have remained on the periphery of scholarly attention.

A notable exception to this general neglect is Comes's (2005) article "Armenian Alphanumerical Notation on a 14th Century Iranian Astrolabe Found in Fez". Comes identifies that the second set of numerals inscribed on the astrolabe made by Muḥammad ibn Ja'far al-Kirmānī in 1393/94 CE are not Rūmī (Greek-derived) numerals but minuscule Armenian alphanumerical signs. Drawing on the fact that the Armenian alphabet assigned numerical values to its first thirty-six letters, Comes argues that this overwriting was most probably executed in New Julfa (Isfahan). She acknowledges David King for first bringing the astrolabe's photographs to her attention, thereby demonstrating how an Islamic instrument could be physically and linguistically repurposed within an Armenian cognitive framework. Despite its significance, Comes's article remains an isolated contribution; no subsequent study has expanded upon her methodology or applied it to other instruments.

Beyond Comes's article, no dedicated academic study exists. Major reference works – such as King's (2018) The Astrolabe: What It Is & What It Is Not– make no mention of Armenian patronage or ownership. Auction catalogues (Hôtel Drouot, 1997) list Armenian astrolabes without scholarly commentary. The comprehensive Répertoire des facteurs d'astrolabes et de leurs oeuvres en terre d'Islam (Brieux et al., 2021) does include an entry for Ghukas Vanandetsi, but only as a brief inventory entry with no attempt at stylistic or contextual analysis. Situated within a broader review of Armenian archaeoastronomy, the article by Areg Mickaelian and Sona Farmanyan, "Armenian Archaeoastronomy and Astronomy in Culture", provides a reference to the material evidence of medieval Armenian instrumentation. While the article's primary focus is on ancient astronomical practices, celestial iconography, and calendrical systems, it also explicitly acknowledges the existence of medieval scientific instruments, citing the foundational surveys by Tumanian (1958, 1985). In this context, Mickaelian and Farmanyan (2023) draw specific attention to the astrolabe "built by Ghukas Vanandetsi (17th–18th centuries), describing it as a particularly interesting "astronomical-geodetical device." Nonetheless, it remains debatable whether the device was constructed by Vanandetsi himself or for Vanandetsi.

Recent exhibitions, including "In the Parallels of Ancient World: Armenia-Netherlands" (History Museum of Armenia, Yerevan, 2 June – 30 August 2025), displayed Ghukas Vanandetsi's astrolabe as a cross-cultural artifact but did not publish a critical catalogue. Parallel contextual research – such as Galichian's (2025) Cosmographic and Geographic Heritage in the Matenadaran– provides invaluable background on Armenian cartographic and astronomical manuscripts but does not engage directly with the instruments themselves[1].

Outside formal scholarship, Armenian astrolabes have gained visibility on social media platforms and heritage websites. For instance, the PeopleOfAr cultural website posted an image of Ghukas Vanandetsi's astrolabe with the inaccurate description "Armenian Astrolabe 15th century" (PeopleOfAr, 2012). Some online sources also claim that the same astrolabe belonged to Coja Petrus Uscan (also known as Woskan or Voskan, 1680/81–1751), a prominent Armenian merchant and philanthropist in Madras. At present, no documentary evidence supports this attribution (Balayan, 2025)[2].

[1]It elucidates a foundational manuscript context for Armenian astrolabe studies. The research highlights previously unknown scientific treatises, including Manuscript MM-8973, a vellum codex containing astrological and astronomical subjects, multiplication tables, andarchitectural drawings. Folio 001b presents the Zodiac and planets in an unconventional layout, with vertical lines marking the zodiacal months. Folio 013b contains a complex diagram of concentric circles with thirteen radial divisions, linking zodiacal names to planets on their orbits. Crucially, folio 032a is interpreted by the author as a "partial astrolabe, " featuring a meticulous description of the instrument's use, explicitly naming it in Armenian as "sturlap". This codicological evidence confirms that the material astrolabes were supported by a sophisticated and native textual tradition.

[2]On 25 September 2025, Karen Balayan, president of the "Ayas" Marine Research Club and captain of the sailing vessel "Cilicia," delivered a lecture at the History Museum of Armenia in which he stated that one of the astrolabes on display "was made by Ghukas Vanandetsi for Khoja Petros, a merchant and shipowner from Julfa"; however, he did not furnish any documentary or material evidence to support this attribution.

doi: https://doi.org/10.52526/25792776-26.73.1-177

Figure 1. The Khafif Astrolabe. History of Science Museum, Oxford, Inv. 47632. Late 9th century (Museum of the History of Science, Oxford, n. d.)

4. Corpus Analysis: Six Case Studies

4.1. The Khafif Astrolabe

The astrolabe constructed by Khafīf, ghulām (apprentice) of the astronomer 'Alī ibn 'Īsā al- Asturlābī, is the earliest object in this corpus (History of Science Museum, Oxford, Inv. 47632). The names of several of 'Alī ibn 'Īsā's apprentices and of their own apprentices are known, providing an approximate date for this instrument and establishing him as one of the pioneers of astrolabe-making in the early centuries of Islam. 'Alī ibn 'Īsā lived in the mid-9th century in the region approximating to modern Syria, and Khafīf's astrolabe, dated to the late 9th century, is the oldest in the Oxford collection. It is made of brass and was presented by J. A. Billmeir in 1957.

The throne is of the pierced type, made of brass, with an integrated base of brass, a simple squared-cross-section ring of brass, and an omega-type shackle of brass. The mater and limb are of one-piece construction, with a tab used to hold the tympans in place located at the bottom of the instrument, 180° from the throne. The limb carries a degree scale. There are three plates with latitudes ranging from 33°0' to 41°0', a range that the Oxford catalogue notes is appropriate to the region of Syria and, to the north, Armenia. The rete contains 17 stars. The zodiac on the rete is labelled in Arabic: al-amal (Aries), al-Thawr (Taurus), al-Jawzā (Gemini), al-Saraṭān (Cancer), al-Asad (Leo), al-Sunbulah (Virgo), al-Mīzān (Libra), al-'Aqrab (Scorpio), al-Qaws (Sagittarius), al-Jady (Capricorn), al-Dalu (Aquarius), al-Samakah (Pisces). The rete is attached using a pin and wedge; the head of the pin is decorated with radial lines. The back of the instrument contains four scales: altitude, cotangent, shadow square, and dastūr circle. The pointer is single-ended, and its front is engraved with a decorative pattern. The alidade is double-ended, counter-changed, and its front is engraved with the same decorative pattern found on the pointer.

The inclusion of this astrolabe in a study of Armenian scientific instrumentation is justified not by its original manufacture, which is unequivocally Abbasid Syrian, but by the later, demonstrably Armenian modifications that transformed its functionality and cultural identity. As documented by David King and Benik Tumanyan, and confirmed in the Oxford catalogue, the astrolabe features "early additions in Armenian": Armenian numerals, a shadow square recalibrated to a base-12 system with an inscription for "shadow" on the diagonal, and latitude indications in Armenian on two of the three plates (King, 1996b). These are not passive provenance marks (such as a name or date of acquisition) but active, substantive recalibrations that altered the instrument's computational capabilities. The addition of a trigonometric grid and the recalibrated shadow square would have required a practitioner with both the skill to manipulate a precision device and the motivation to integrate it into a local Armenian scientific tradition. This appropriation took place during a period when Armenia, though under Abbasid suzerainty, was reasserting its cultural and political identity. By the late 9th century, the Bagratid dynasty had risen to power, and

doi: https://doi.org/10.52526/25792776-26.73.1-177

in 885 CE, the Caliphate recognised an independent Armenian kingdom. Armenia's position astride the Silk Road facilitated the movement of goods and knowledge between the Abbasid world and the Caucasus. Archaeological evidence, including Abbasid coins and Abbasid ceramics excavated in Armenia (Zohrabyan et al., 2018), confirms the scale of commercial and cultural exchange along these routes.

Figure 2. The rete fragment. History of Science Museum, Oxford, Inv. 48470. Early 10th century (Museum of the History of Science, Oxford, n.d.)

4.2. The rete fragment

The rete fragment documents the cross-cultural circulation of Islamic scientific material and its later adaptation by an Armenian user. Stylistic features – angular Kufic script and dagger-shaped star pointers (a diagnostically early form) – position the object within early 10th-century Syrian manufacture. David A. King, in his unpublished working catalogue (entry 2529; King, 1996b), explicitly attributes the rete to the workshop of Khafīf, apprentice of 'Alī ibn 'Īsā al-Asturlābī (Maddison, 1957, 1976). King's attribution rests on multiple concordances: the script type, the selection of seventeen stars, the presence of dagger pointers on each star, the absence of a star pointer opposite qalb al-'aqrab, and the placement of the rotation tab on the left support of the lower circular bar. He notes that the rete's star positions are more accurate than those on the complete Khafif astrolabe (inv. 47632), suggesting a refinement in the workshop's production chronology. The rete is of the indicator-line (simple) type, with a single tab for rotation – a feature shared with the Khafif instrument. It carries the same seventeen stars as the Khafif astrolabe, each marked with a dagger pointer, and the zodiacal signs are labelled in Arabic (al-amal through al-Samakah). The object was acquired by J. A. Billmeir between 1955 and 1957 and presented to the museum in 1957 (accession number 1957-84/156).

The Oxford rete's scholarly value derives not from its Abbasid provenance but from a deliberate epigraphic intervention: the systematic addition of Armenian translations adjacent to each Arabic star and zodiac name, a linguistic overlay documented by both the museum catalogue and 8 Benik Tumanyan. This operation functionally recalibrated the instrument for an Armenian user, converting a monolingual Islamic artifact into a bilingual interface. Unlike the Khafif astrolabe— where Armenian numerals and latitude inscriptions occupy the back and plates—the rete's Armenian glosses supplement rather than supplant the original Arabic, producing a bilingual palimpsest. This strategy prioritized vernacular accessibility: star and zodiac names, the most frequently consulted elements for time-telling and astrological calculation, were translated to enable use without full Arabic literacy. The rete's isolated survival suggests its continued utility as an instructional tool. Its inclusion as a case study documents Armenian epistemic agency—active re-engineering of foreign instruments, not passive reception.

doi: https://doi.org/10.52526/25792776-26.73.1-177

Figure 3. The astrolabe from the Dār al-Batḥā' in Fez, Morocco. Inventory no. 764; International Instrument Checklist no. 2710. 1393–1394 CE.

4.3. The astrolabe from the Dār al-Batāḥ' in Fez, Morocco Figure

The astrolabe dated 796 H (1393/94 CE) and signed by Muḥammad ibn Ja'far al-Kirmānī, known as Jalal, is now preserved in the Dār al-Batāḥ' in Fez, Morocco. David A. King, in his unpublished working catalogue (part XIVd, pp. 772-774), provides a detailed description of this instrument, noting that its reported diameter is either 135 mm or 122 mm. Although the date 1393/94 CE seems relatively early for the quality of execution, the reading is unequivocal. King characterizes the instrument as "not in the same class as the Copenhagen astrolabe or the Oxford rete and Istanbul plate," being more typical of the productions of al-Kirmānī's grandfather and father. Those other pieces, King observes, "well reflect what a competent craftsman can achieve when he has a generous sponsor and an intellectual milieu conducive to excellence." The Fez astrolabe, by contrast, represents a more modest level of craftsmanship. King further remarks on the instrument's physical condition and subsequent history, noting that he has not seen the instrument in person but came across photographs of the front and back in May 2004. He states that, "one could argue that it has not fared well, neither when it first landed in the Maghrib nor more recently. Centuries ago, some Maghribi craftsman did not like it and tried to fix it up according to his own limited local tradition. In 1990, the astrolabe was intended for an exhibition on the Maghrib at the Musée du Petit Palais in Paris, but none of the astrolabes from Morocco reached Paris, and the catalogue entries are "pathetically inadequate (King, 2005)."

The object's principal scholarly significance, however, lies in its additional markings. When King first examined the additional numbers on the outer scale and the ecliptic scale, he initially hypothesized that they might be al-qalam al-fāsi ("chiffres de Fès"), a numeral system attested in Andalusian, Maghribi, and Spanish Latin sources. As King writes, "What would have been more appropriate for an Iranian astrolabe ending up in Fez?"

However, Rosa Comes of the University of Barcelona demonstrated conclusively that the additional numbers are not "chiffres de Fès" but rather lower-case Armenian alphanumerical notation. The Armenian alphabet, created by Mesrop Mashtots around 400 CE on a Greek model with Syriac influence, assigns numerical values to its first thirty-six letters according to their sequential order. Comes's (2005) analysis shows that on the Fez astrolabe, the Armenian ciphers were added directly on top of the original Eastern Arabic abjad numerals, sometimes overlapping the Arabic figures. On the outer scale, the Armenian notation begins at a distance of 60° anticlockwise from the Arabic graduation, marking every 5° and covering the full 360° (though not every numeral is written). On the ecliptic, the Armenian hand inserted degrees corresponding to each zodiacal division, starting with Capricorn (30° through 360°), a choice that Comes

doi: https://doi.org/10.52526/25792776-26.73.1-177

interprets as intended for the computation of right ascensions. The Armenian notation thus creates an independent, offset 360-degree scale, enabling astronomical calculations without erasing the underlying Arabic data.

The crucial historical question is where and why this numeral overwriting occurred. Comes proposes that the Armenian notation was most probably added in New Julfa, the Armenian mercantile colony established near Isfahan after Shah 'Abbās I the Great deported Armenian merchants and craftsmen from Old Julfa between 1603 and 1605. New Julfa was not merely a commercial entrepôt; it developed into a sophisticated centre of Armenian intellectual, artistic, and technological activity. The colony's merchants controlled a substantial portion of trans-Asian trade in silk, textiles, spices, and precious stones, operating networks that extended from the Levant and Venice to the Indian Ocean and Southeast Asia. This commercial infrastructure simultaneously functioned as a conduit for the circulation of books, manuscripts, scientific instruments, and technical knowledge. The intellectual environment of New Julfa supported diverse scholarly pursuits. The colony maintained schools, a printing press established at the Holy Savior's Monastery in 1638 (McCabe, 1999) – the first printing press in Persia – and scriptoria where manuscripts in Armenian, Persian, and other languages were copied and illuminated. The monks of the monastery, despite never having seen a printing press before, manufactured their own ink and paper and commissioned local Armenian goldsmiths to cast the type. New Julfa Armenians also patronized the production of luxury goods that blended Persian, European, and Armenian stylistic elements: illustrated manuscripts, metalwork, textiles, and, relevantly, scientific instruments. Surviving records document commissions of astrolabes and other precision instruments by wealthy Armenian merchants, some of whom maintained personal libraries containing both Eastern and Western scientific texts. Although no documentary record currently links a specific New Julfa patron to the Fez astrolabe, the cumulative evidence of Armenian agency in modifying imported scientific instruments – seen also in the Khafif astrolabe (Inv. 47632) and the Oxford rete (Inv. 48470) – makes Comes's attribution plausible.

Figure 4. The Amirdovlat' Amasiatsi Astrolabe. Museum of Islamic Art, Doha, Inv. MW.498.2013. 1479 CE.

4.4. The Amirdovlat' Amasiatsi Astrolabe

An astrolabe dated 1479 CE (Armenian calendar 928) and linked to the court of Mehmed II has circulated in scholarly literature largely through auction records and passing references by David A. King (King & Charette, 2024). The Paris Drouot catalogue of 19 December 1997 described the piece as unsigned, with a corrupted maker's name – "Zilmaspout" or "Zilmanfous" – derived from the Arabic shadow-scale terms ill mabsūṭ (horizontal shadow) and ill ma'kūs (vertical shadow). That catalogue also noted plates for latitudes 41° (Istanbul) and 42° (Edirne) and an Armenian inscription "in memory of the medic Amirdovlat." (Hôtel Drouot, 1997) King later observed that Amirdovlat Amasiatsi died in 1496, so an astrolabe dated 1479 would have been produced within his lifetime, presumably for his personal use or as a commemorative instrument. This research definitively identifies that previously elusive astrolabe as the instrument now held by the Museum of Islamic Art in Doha (MW.498.2013). Prior to this identification, the Doha astrolabe was catalogued anonymously as "Turkish," without recognition of its Armenian epigraphy or its connection to the Ottoman court physician. A published account of Armenian cultural heritage specifies that the artifact is crafted from tin and bears a rotating frame engraved with Armenian symbols, letters, star and constellation

doi: https://doi.org/10.52526/25792776-26.73.1-177

names, and circles. The honorific "Amirdovlat' Brzhskapet" (scientific doctor) together with the date "928 Armenian era" (1479 CE) confirms its epigraphic link to Amirdovlat' Amasiatsi. Provenance aligns with the 1997 Paris auction: the same source reports acquisition at that sale by a princess of the Qatari royal family, who can presumably be Sheikha Al-Mayassa bint Hamad bin Khalifa Al Thani – acting for the museum collection, at a price exceeding 200,000 US dollars. In fact, the Doha astrolabe is not an anonymous Turkish object but a precision instrument commissioned or used by an Armenian chief physician serving the Sultan, inscribed in Armenian script and calibrated for Ottoman latitudes.

The attribution to Amirdovlat' Amasiatsi correlates precisely with his known biography and intellectual profile. Born in Amasya around 1420–1425, Amirdovlat' was a polyglot fluent in six languages and served as bzhshkapet (chief physician) to Mehmed II in Constantinople. He authored medical and pharmacological works, notably Angitats Anpet (Useless for Ignoramuses) and the 1474 pharmacognosy Girk' Rhamkakan, which catalogues hundreds of medicinal substances from across Eurasia. His methodology integrated empirical observation with astrological cosmology. The functional link between his textual prescriptions and the astrolabe is established by the instrument's engraved rete and ecliptic, featuring Capricorn and other zodiacal markers – the computational apparatus required for his astrologically governed medicine. Vardanyan's (1999) study documents a definitive example: Amirdovlat"s instruction for harvesting mandrake root demanded that Mars occupy the twenty-fourth degree of Aries or Capricorn, with the Moon in conjunction within the same zodiacal house, on a Tuesday after sunrise. The astrolabe's capacity to compute planetary longitudes for any moment would have been essential for such determinations. Amirdovlat"s empirical reach extended far beyond local Armenian flora to a global geography of medicinal substances, mapping contemporary Eurasian exchange networks. His compendium synthesizes knowledge from classical (Greco-Roman), Eastern (Arabic, Persian), and oral sources (travelers, merchants) across Armenia, Anatolia, the Balkans, Iran, the Iberian Peninsula, North Africa, Arabia, India, Central Asia, China, and the Mediterranean and Black Sea littorals – an encyclopedic awareness facilitated by long-distance trade circuits. His pharmacognosy and his possession of a precision astrolabe are thus interrelated facets of a single diasporic socio-intellectual system: the same mercantile networks that supplied exotic substances also provided capital, cosmopolitan connections, and technological access enabling the commissioning and use of such instruments.

Figure 5. The Ghukas Vanandetsi Astrolabe. History Museum of Armenia. Late 17th–early 18th century.

4.5. The Ghukas Vanandetsi Astrolabe

The copper astrolabe produced under the auspices of Ghukas (Luca) Vanandetsi (also known as Gukas Vanandetsi or Gukas Nurijanyan) differs fundamentally from the Islamic-derived instruments discussed in previous case studies because its rete follows a lost medieval Dutch or German prototype, marking a complete departure from Islamic rete typologies (King, 2005). Vanandetsi was not a craftsman himself but a versatile Armenian intellectual—chronicler, translator, philosopher, publisher, and man of culture active during the second half of the 17th century and the first quarter of the 18th century. Born in the village of Vanand (in

doi: https://doi.org/10.52526/25792776-26.73.1-177

present-day Nakhichevan) around the early 1650s, he received his initial education in his native village before continuing his studies from 1679 to 1682 at the Urbana School in Rome. This Roman education exposed him to the latest European intellectual currents, including cartography and scientific instrument design. In 1690, he joined his compatriot, the printer Matteos Vanandetsi, in Amsterdam and actively participated in the work of the Armenian printing house, becoming a central figure in the Armenian press (Nahapetyan & Aleksanyan, 2021).

His published oeuvre included the first Armenian world map, Amatarats Ashkharatsuits (1695), and a practical mercantile manual entitled Gandz ch‘ap‘voy, kshrroy, t‘uots‘ yev dramits‘ bolor ashkharhi (A Treasure Trove of Measures, Weights, Numbers and Currencies from Around the World, Yemsterdem [Amsterdam], 1699; known in English as the Treasury of Measures, Weights, Numerations and Currency From All Over the World). This manual, containing conversion tables, accountancy exercises, silk standards, and ethnographic observations, catered directly to the globally dispersed Armenian merchant class. His scholarly profile, honed in Rome and exercised in Amsterdam, made him a conduit for European scientific knowledge, which he then adapted for his diasporic audience.

We presume that the astrolabe itself was executed by specialised Dutch artisans whom Vanandetsi commissioned. Unlike the earlier astrolabes in this corpus, where Armenian script appeared selectively alongside Arabic or Persian originals, the Ghukas Vanandetsi astrolabe is inscribed entirely in Armenian – from the graduated scales to the rete pointers and the dedicatorial formula – a linguistic completeness that signals a deliberate shift from passive appropriation to confident vernacular ownership, transforming the instrument into an autonomous Armenian epistemic artifact rather than a modified import. Amsterdam at that time possessed a dense network of such professionals, including the Blaeu firm (Keuning, 1973), which produced precision quadrants and globes, and wood-engravers like Christoffel van Sichem the Younger, who supplied approximately 150 illustrations for the Psalter printed by Ghukas Vanandetsi in 1714–1715. The core Armenian identity of the object, however, is explicitly asserted by the inscription engraved on its frontal part (Ghuk Vananden, i.e., Ghukas Vanandetsi). The most revealing evidence of Vanandetsi's broader astronomical and epistemological ambitions, however, is not the astrolabe alone but the frontispiece of his 1699 Treasury. The engraving shows a pair of serpentine dragons supporting an armillary sphere – an iconography that cannot be explained by Western armillary traditions. In contemporary European depictions, the armillary sphere was a compact, portable demonstrative device resting on a plain tripod or a simple stand. By contrast, the Chinese armillary sphere (Hunyi) was conceived as a monumental, fixed observatory instrument, and from at least the Ming Dynasty (1368–1644) (Sun, 2015), its most distinctive structural feature was the use of sculpted dragons as load-bearing supports. This tradition was codified in the instruments installed at the Beijing Ancient Observatory and was reproduced in Jesuit treatises and printed engravings that circulated in Europe. Therefore, the dragon-supported armillary sphere on Vanandetsi's frontispiece is not a vague piece of chinoiserie; it is a precise, technically informed citation of Chinese imperial astronomical material culture (Smith, 1998).

Figure 6. The Gevorg Vanandetsi Astrolabe. Byurakan Astrophysical Observatory. Early 18th century.

doi: https://doi.org/10.52526/25792776-26.73.1-177

4.6. The Gevorg Vanandetsi Astrolabe

A distinct astrolabe preserved at the Byurakan Astrophysical Observatory in Armenia is entirely inscribed in Armenian – from its numerals (using Armenian alphabetic notation) to its dedicatory formula and all operational labels. The instrument bears the unequivocal inscription ("For the Enjoyment of Gevorg Vanandetsi"), naming an owner different from the Ghukas Vanandetsi astrolabe held in the History Museum of Yerevan. David A. King catalogued this piece as item #3800 in his working inventory, identifying it as an 18th-century Dutch construction whose rete is unrelated to contemporary Islamic patterns and derives from a lost medieval exemplar from the Low Countries (King, 2005). King noted that the numeral scales are executed entirely in Armenian alphabetic notation, a feature unique among known astrolabes, and recorded that photographs of the instrument are preserved in the Ernst Zinner Archives at the Institute for the History of Science in Frankfurt am Main. Although King misattributed this astrolabe to Ghukas Vanandetsi, the inscription explicitly names Gevorg Vanandetsi, a hitherto less documented member of the same family. The palaeographic style of the Armenian script – the letter forms, spacing, and engraving technique – is identical to that on the Ghukas Vanandetsi astrolabe, indicating that both instruments were produced within the same workshop or by the same letter-cutting tradition, likely commissioned through the Vanandetsi family's extensive network in Amsterdam (Merian, 2022). The Vanandetsi family constituted a multi-generational intellectual and commercial dynasty: Tovma Vanandetsi (1617-1708), a bishop and publisher, operated one of the most active Armenian printing houses in Amsterdam; Ghukas Vanandetsi and Gevorg Vanandetsi were later representatives of the same lineage, combining printing, map-making, and the commissioning of precision astronomical instruments. The existence of two separate astrolabes – one named for Ghukas, the other for Gevorg – both entirely in Armenian and both based on Dutch prototypes, demonstrates that this engagement with European instrument-making was not an isolated individual effort but a deliberate, multi-generational family enterprise. Nonetheless, as no specific information survives concerning Gevorg Vanandetsi's life and oeuvre, it remains impossible to determine which astrolabe served as the prototype or primary source for the production of another.

5. Conclusion

The present study established that Armenian engagement with astrolabes constituted a systematic, polycentric practice rather than an accidental accumulation of objects. This practice emerged as a logical extension of a broader epistemic tradition in which astronomical knowledge was continuously interpreted across textual, visual, and material registers, enabling the simultaneous assimilation of Eastern and Western scientific systems. Islamic instruments were not merely adopted but recalibrated through vernacular epigraphic intervention, while Europeanderived retes were commissioned with exclusively Armenian inscriptions, demonstrating a deliberate oscillation between appropriation and autonomous production. Such dual competency was sustained by mercantile patronage and courtly networks. The research rectifies several historiographic inaccuracies: the Doha astrolabe is reattributed from an anonymous "Turkish" classification to Amirdovlat'; the instruments of Ghukas and Gevorg Vanandetsi are disentangled after prolonged conflation; and Rosa Comes's identification of Armenian alphanumerical notation on the Fez astrolabe is brought into Armenological discourse. Future inquiry requires in-situ analysis and interdisciplinary publication co-authored with astronomers, advancing these artifacts from peripheral notices to a central position in the global history of science.

References

Baghdiantz McCabe, Ina. 1999, The Shah's Silk for Europe's Silver: The Eurasian Trade of the Julfa Armenians in Safavid Iran and India (1530–1750). University of Pennsylvania Armenian Texts and Studies, no. 15. Atlanta: Scholars Press.

Balayan, K. 2025, https://historymuseum.am/en/event-item/captain-karen-balayan-onarmenian\-navigation/

Borrelli, A. 2008, Aspects of the Astrolabe: 'Architectonica Ratio' in Tenth- and Eleventh-Century Europe. Sudhoffs Archiv, Beihefte 57. Stuttgart: Franz Steiner Verlag, p. 125.

Brieux A., Halff B., Maddison F., et al. 2021, Répertoire des facteurs d'astrolabes et de leurs oeuvres en terre d'Islam, 2 vols. Volume 1 (Texte). Turnhout, Belgium: Brepols, pp. 472–474.

doi: https://doi.org/10.52526/25792776-26.73.1-177

Comes, R. 2005, “Armenian Alphanumerical Notation on a 14th Century Iranian Astrolabe Found in Fez,” Suhayl 5: 243–251.

Galichian, R. 2025, Cosmographic & Geographic Heritage in the Matenadaran. Yerevan: Matenadaran.

Hôtel Drouot. 1997, Catalogue des objets d’art, faïences italiennes, bronzes, cuivres, étains, armes, bois sculptés, instruments de mathématiques, compas, règles, cadrans solaires, astrolabes, sphères, lunettes, microscopes, etc., outils, meubles, tableaux, étoffes, etc. principalement du XVIe siècle : composant la collection de feu M. Rousell, dont la vente aura lieu à Paris Hôtel Drouot, le vendredi 19 décembre 1997. Paris: Hôtel Drouot.

Keuning, J. 1973. Willem Jansz. Blaeu: A Biography and History of His Work as a Cartographer and Publisher. Amsterdam: Theatrum Orbis Terrarum.

King, D. A. 1996a, A Catalogue of Medieval Astronomical Instruments. Frankfurt: Institut für Geschichte der Arabisch-Islamischen Wissenschaften an der Johann Wolfgang Goethe-Universität.

King, D. A. 2005, In Synchrony with the Heavens: Studies in Astronomical Timekeeping and Instrumentation in Medieval Islamic Civilization, vol. 2, Instruments of Mass Calculation (Studies XXVIII), Islamic Philosophy, Theology and Science: Texts and Studies, vol. 55. Leiden and Boston: Brill, part XIVd.

King, D. A. 2018, The Astrolabe: What It Is & What It Is Not (unpublished research supplement). Available at Academia.edu:
https://www.academia.edu/37613545/KING_The_Astrolabe_18_10_2018_pdf

King, D. A. and Charette F. 2024, “A Universal Sundial Made for Sultan Mehmet II, in the Context of Astronomical Instrumentation in Late-15th Century Istanbul,” Suhayl 21.

King, David A. 1996b, A Catalogue of Medieval Astronomical Instruments, Parts 1.1-2.3: Islamic Astrolabes (to ca. 1550) with Additional ‘Old-Style’ Astrolabes (to ca. 1800). October 1996 version. Typescript.

Kopytoff, I. 1986, “The Cultural Biography of Things: Commoditization as Process,” in The Social Life of Things: Commodities in Cultural Perspective, ed. Arjun Appadurai. Cambridge: Cambridge University Press.

Maddison, F. R. 1957, A Supplement to a Catalogue of Scientific Instruments in the Collection of J. A. Billmeir, Esq., C.B.E. Oxford: Partridge & Sons, p. 18 (no. 156).

Maddison, F. R. 1976, Science and Technology in the Service of Mankind: An Exhibition of Scientific Instruments from the Middle Ages to the 20th Century. London: Science Museum, p. 99.

Malafouris, L. 2013, How Things Shape the Mind: A Theory of Material Engagement. Cambridge, MA: MIT Press.

Merian, S. L. 2022. ”4 The Dissemination of Western European Prints Eastward: The Armenian Case.” In Prints as Agents of Global Exchange: 1500-1800, ed. Heather Madar. Amsterdam: Amsterdam University Press, p.127-158.

Mickaelian, A. M., and Farmanyan S. V. 2023, “Armenian Archaeoastronomy and Astronomy in Culture,” Mediterranean Archaeology and Archaeometry 16, no. 4: 385–395, p. 387.

Museum of the History of Science, Oxford, ”Astrolabe made by Khafīf, apprentice of ’Alī ibn ’Īsā, late 9th century,” Astrolabe Catalogue, accessed April 27th, 2026,
https://www.mhs.ox.ac.uk/astrolabe/catalogue/browseReport/Astrolabe_ID%3d[ID].html

Museum of the History of Science, Oxford. 2026, Rete Fragment (Inv. 48470). Astrolabe Catalogue http://www.mhs.ox.ac.uk/astrolabe/catalogue/browseReport/Astrolabe_ID=147.html

Nahapetyan, A. A., and Aleksanyan A. V. 2021, “Vanandets’u ‘Hamatarats Ashkharhatsuyts” ev dṛa patmakan dṛ” (Vanandetsi’s ’Universal World Map’ and Its Historical Role), Gitakan teġekagir (Scientific Proceedings) of M. Nalbandyan State University of Shirak, no. 2021.2a: 100–106.

Panofsky, E. 1939, Studies in Iconology: Humanistic Themes in the Art of the Renaissance. New York: Oxford University Press.

PeopleOfAr, 2012, Armenian Astrolabe 15th century, December 13, 2012, https://www.peopleofar.com/2012/12/13/armenian-astrolabe/

Smith, D. W. 1998. ”International Symposium on Astronomical Exchange Between China and Other Countries: A Report.” International Planetarium Society.
https://www.ipsplanetarium.org/page/a_smith1998

doi: https://doi.org/10.52526/25792776-26.73.1-177

Sun, X. 2015. "Chinese Armillary Spheres." In Handbook of Archaeoastronomy and Ethnoastronomy, edited by Clive L. N. Ruggles, 2135–2142. New York: Springer.

Tumanian, B. E. 1958, Newly-Found Armenian Astronomical Device. Yerevan: Haypethrat, 31 p. (in Armenian).

Tumanian, B. E. 1985, History of Armenian Astronomy. Yerevan: Publishing House of Yerevan State University, 286 p. (in Armenian).

Tumanian, B. E.1964, Hay astğagitut'yan patmut'yun [History of Armenian Astronomy]. Vol. 1. Yerevan: Publishing House of the Armenian Academy of Sciences.

Vafea, F. 2019, "From the Celestial Globe to the Astrolabe: Transferring Celestial Motion onto the Plane of the Astrolabe," in Josefina Rodríguez-Arribas, Charles Burnett, Silke Ackermann, and Ryan Szpiech (eds.), Astrolabes in Medieval Cultures. Leiden and Boston: Brill, pp. 125– 148, https://doi.org/10.1163/9789004387867_004

Vardanyan, S., and Amasiatsi A. 1999, A Fifteenth-Century Armenian Natural Historian and Physician, trans. Michael Yoshpa, ed. Ara Der Marderosian. Delmar, NY: Caravan Books, 39.

Zohrabyan, A., Gasparyan B., and Dan R. 2018, "A Sasanian Coin of Khosrow I and an Abbasid Coin of Al-Manṣur from the Areni-1 Cave, Armenia, " ARAMAZD: Armenian Journal of Near Eastern Studies 12, no. 2: 182–87.

Astronomical Heritage Related Educational and Outreach Activities in Armenia

L. Darbinyan [*], A. Mickaelian[†] and S. Farmanyan[‡]

V. Ambartsumian Byurakan Astrophysical Observatory, Byurakan, Armenia

Abstract

Astronomical heritage represents an important component of scientific and cultural identity, preserving the achievements, instruments, archives, and intellectual legacy of astronomy. In Armenia, the Byurakan Astrophysical Observatory (BAO) plays a central role in safeguarding this heritage while actively integrating it into modern educational and outreach initiatives. This article presents key educational and outreach activities related to astronomical heritage in Armenia, highlighting programs designed to promote astronomy education, engage the public, and inspire new generations of scientists. Initiatives such as the "From School to Space" lecture series, the Byurakan Science Camp, teacher training workshops, astrojournalism and astrophotography competitions, and digital outreach programs demonstrate how BAO connects historical scientific achievements with contemporary educational practices. Through these initiatives, the observatory continues to strengthen astronomy education, promote scientific communication, and foster international collaboration while preserving Armenia's rich astronomical heritage.

Keywords: *outreach, journalism, astronomy education, scientific literacy.*

1. Introduction

Astronomical heritage encompasses not only historic observatories, instruments, and scientific archives, but also the intellectual traditions and educational efforts that sustain astronomy across generations. Armenia possesses a remarkable astronomical legacy, closely associated with the work of prominent scientists such as Viktor Ambartsumian, founder of the Byurakan Astrophysical Observatory.

The Byurakan Astrophysical Observatory (BAO) has long served as one of the leading scientific institutions in the region, contributing significantly to astrophysical research and international scientific collaboration. At the same time, BAO plays a vital role in promoting astronomy education and public engagement. The observatory's mission therefore includes a dual responsibility: conducting scientific research while actively preserving and promoting astronomical heritage through educational and outreach activities.

This article presents several major initiatives that illustrate how astronomical heritage in Armenia is preserved, communicated, and transformed into a dynamic educational resource.

List of Astronomical Heritage in Armenia

- Calendars: in Matenadaran manuscripts, etc.
- Rock Art
- Ancient Observatories: Zorats Karer, Metzamor, etc.
- Ancient and Medieval astronomy-related records: Tigranes the Great coin, SN 1054, etc.
- Medieval sky maps
- Astronomical Instruments: astrolabe, etc.

[*]lilit.darbinyan7@gmail.com, Corresponding author
[†]aregmick@yahoo.com
[‡]sona.farmanyan@mail.ru

doi: https://doi.org/10.52526/25792776-26.73.1-189

- BAO as astronomical and cultural heritage
- Scientific (Astro) Tourism sites
- BAO Plate Archive; 37,500 photographic plates
- Markarian Survey as UNESCO “Memory of the World” Documentary Heritage
- Viktor Ambartsumian House-Museum
- Museum of History of the Armenian Astronomy

2. Institutional Framework for Astronomy Outreach

Educational and outreach activities related to astronomical heritage in Armenia are coordinated through collaboration between several institutions.

The Byurakan Astrophysical Observatory hosts the International Astronomical Union (IAU) South-West and Central Asia Regional Office of Astronomy for Development (SWCA ROAD), which supports regional astronomy education and public engagement programs. These initiatives aim to strengthen astronomy development across neighboring countries and promote international scientific cooperation.

Another key organization is the Armenian Astronomical Society (ArAS), founded in 1999 by members of the Armenian astronomical community. The society works to promote astronomical research, education, and outreach within Armenia while fostering connections with astronomers worldwide. Through publications, conferences, and community initiatives, ArAS plays an important role in strengthening the national astronomy network.

Figure 1. ARAS logo

3. Educational Programs and Outreach Initiatives

3.1. The “From School to Space” Lecture Series

One of the most impactful outreach initiatives is the **“From School to Space”** lecture series, launched in 2012. The program was developed partly in response to the absence of astronomy in Armenia’s school curriculum.

Scientists and educators travel to schools across the country—including remote and rural regions—to present lectures, demonstrate telescopes, and introduce students to astronomical discoveries. Over more than a decade, the program has reached thousands of students and provided many young people with their first direct exposure to modern astronomy (Figure 2).

doi: https://doi.org/10.52526/25792776-26.73.1-189

Figure 2. From School to Space.

3.2. Byurakan Science Camp

The Byurakan Science Camp, launched in 2014, is designed for schoolchildren aged 11–14. The program provides participants with a week-long immersive experience at the observatory.

Students take part in hands-on experiments, workshops, and observational activities guided by professional astronomers. Evening stargazing sessions allow participants to observe celestial objects directly through telescopes, while excursions integrate scientific learning with Armenia's cultural and natural heritage.

The camp has become one of BAO's most successful educational initiatives, creating an inspiring environment that encourages young people to explore science and research careers (figure 3).

3.3. Teacher Training Programs

Recognizing the crucial role of educators in science communication, BAO launched teacher training workshops in 2024. These programs aim to strengthen astronomy education in Armenian schools by providing teachers with modern teaching methods and updated scientific knowledge. The workshops combine theoretical lectures with practical activities such as astronomical observations, field visits, and problem-solving exercises. By empowering teachers with new educational tools, the program indirectly reaches thousands of

doi: https://doi.org/10.52526/25792776-26.73.1-189

Figure 3. Byurakan Science Camp.

students throughout the country (Figure 4).

4. Educational Resources and Scientific Communication

4.1. The Astronomical Dictionary

One of BAO's important educational tools is the Astronomical Dictionary, a trilingual resource available in Armenian, English, and Russian. The dictionary includes astronomical terminology, object names, and star names, helping students, educators, and the general public navigate the complex vocabulary of astronomy.

This resource plays an essential role in supporting astronomy education by providing accurate and standardized terminology accessible to a broad audience.

4.2. ArAS Electronic Newsletter

The ArAS Electronic Newsletter serves as an important platform for scientific communication within the Armenian astronomical community. Published regularly by the Armenian Astronomical Society, the newsletter disseminates information about scientific achievements, conferences, educational initiatives, and astronomy-related events.

By connecting researchers, educators, and enthusiasts both nationally and internationally, the newsletter strengthens collaboration and ensures that developments in Armenian astronomy remain visible within the global scientific community (Figure 5).

doi: https://doi.org/10.52526/25792776-26.73.1-189

Figure 4. Teacher Training Programs

5. Science Communication and Public Engagement

5.1. Astrojournalism Competition

The Astrojournalism Competition was created to bridge the gap between science and society. The initiative encourages journalists and science communicators to present astronomical topics in accessible language for the general public.

Through this competition, participants develop skills in scientific communication while promoting public understanding of astronomy and highlighting local scientific achievements.

5.2. Astrophotography Competition

The Astrophotography Competition combines scientific observation with artistic creativity. By capturing images of celestial objects and astronomical phenomena, participants contribute to public appreciation of the beauty of the Universe. Such visual representations often communicate complex scientific ideas more effectively than written descriptions, making astrophotography an important tool for science outreach (Figure 6).

doi: https://doi.org/10.52526/25792776-26.73.1-189

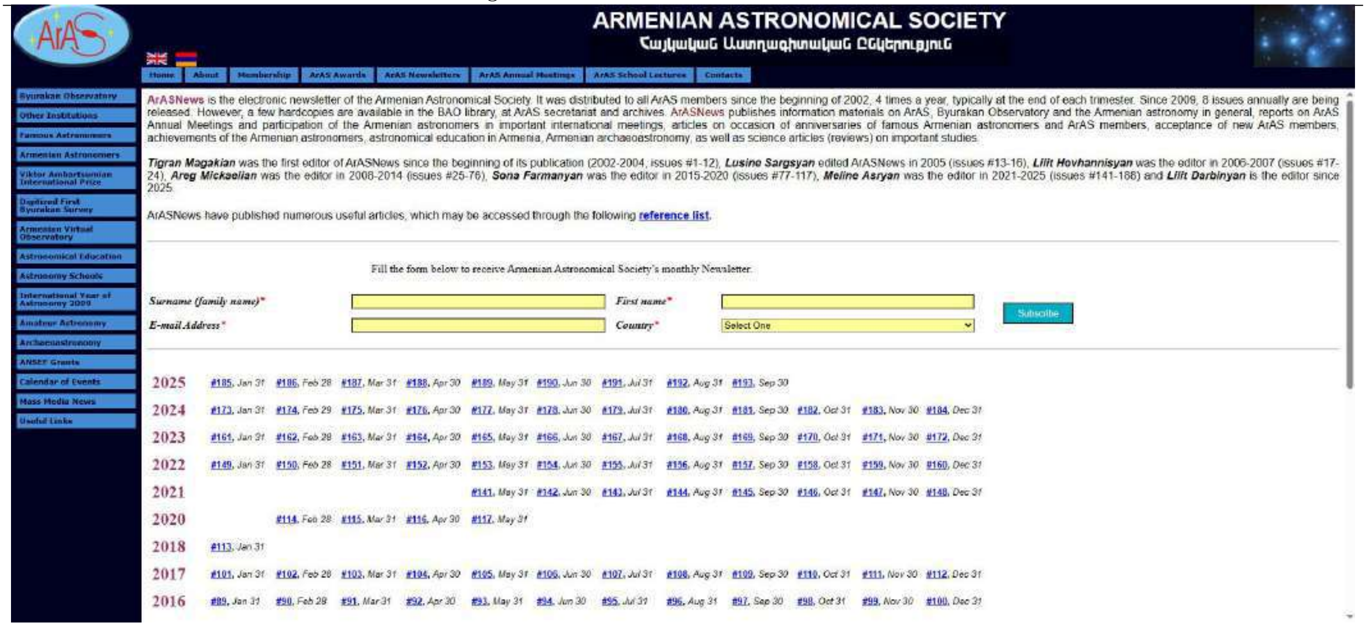

Figure 5. ArAS Electronic Newsletter

Figure 6. Byurakan Astrophysical Observatory and Mount Ararat.

6. Astrotourism and Digital Outreach

The Byurakan Astrophysical Observatory has also become one of Armenia's most significant astrotourism destinations. Each year, thousands of visitors—including students, tourists, and astronomy enthusiasts—visit the observatory to explore its telescopes, scientific history, and unique astronomical environment.

doi: https://doi.org/10.52526/25792776-26.73.1-189

In addition, BAO actively uses social media platforms such as Facebook and Instagram to share astronomy news, educational materials, and updates about observatory activities. Digital outreach allows the institution to reach global audiences and engage individuals who cannot visit the observatory in person.

7. Conclusion

Astronomical heritage in Armenia represents a valuable intersection of scientific history, cultural identity, and educational development. Through the initiatives of the Byurakan Astrophysical Observatory and the Armenian Astronomical Society, this heritage is actively preserved and transmitted to new generations.

Programs such as science camps, teacher training workshops, lecture series, and science communication competitions demonstrate how historical scientific achievements can be transformed into dynamic educational experiences. By combining tradition with innovation, Armenia continues to strengthen astronomy education and inspire curiosity about the Universe.

The experience of BAO illustrates how scientific institutions can successfully integrate research, heritage preservation, and public engagement to build a sustainable future for astronomy education.

References

Asryan M. A., Farmanyan S. V., Mickaelian A. M., 2020, Communications of the Byurakan Astrophysical Observatory, 67, 119

Baleyan G. D., Farmanyan S. V., Davtyan A. K., Mickaelian A. M., 2024, Communications of the Byurakan Astrophysical Observatory, 71, 162

Darbinyan L., Mickaelian A., Farmanyan S., 2025, Communications of the Byurakan Astrophysical Observatory, 72, 131

Farmanyan S. V., Mickaelian A. M., 2015, in Relation of Astronomy to other Sciences, Culture and Society. pp 223–231

Farmanyan S. V., Mickaelian A. M., 2018, Communications of the Byurakan Astrophysical Observatory, 65, 155

Farmanyan S. V., Mickaelian A. M., 2019, in Farmanyan S. V., Mickaelian A. M., McKim Malville J., Bagheri M., eds, Astronomical Society of the Pacific Conference Series Vol. 520, Astronomical Heritage of the Middle East. p. 253

Farmanyan S. V., Mickaelian A. M., McKim Malville J., Bagheri M., eds, 2019a, Astronomical Heritage of the Middle East. Astronomical Society of the Pacific Conference Series Vol. 520

Farmanyan S. V., Harutyunyan V. L., Mikayelyan G. A., Mickaelian A. M., 2019b, in Farmanyan S. V., Mickaelian A. M., McKim Malville J., Bagheri M., eds, Astronomical Society of the Pacific Conference Series Vol. 520, Astronomical Heritage of the Middle East. p. 259

Farmanyan S. V., Mikayelyan G. A., Mickaelian A. M., 2024, Communications of the Byurakan Astrophysical Observatory, 71, 169

Mickaelian A., 2015, Highlights of Astronomy, 16, 565

Mickaelian A. M., Farmanyan S. V., Mikayelyan G. A., Mikayelyan A. A., 2016, in Farmanyan S. V., Suvaryan Y. M., Mickaelian A. M. E. ., eds, Cultural Astronomy in the Armenian Highland. pp 203–209

Mickaelian A. M., Farmanyan S. V., Mikayelyan G. A., 2020, Communications of the Byurakan Astrophysical Observatory, 67, 133

Mickaelian A. M., Sargsyan L. A., Mikayelyan G. A., Gigoyan K. S., Nesci R., Rossi C., 2021a, Communications of the Byurakan Astrophysical Observatory, 68, 390

Mickaelian A. M., Farmanyan S. V., Mikayelyan G. A., 2021b, Communications of the Byurakan Astrophysical Observatory, 68, 400

Mickaelian A. M., Farmanyan S. V., Mikayelyan G. A., 2024, Communications of the Byurakan Astrophysical Observatory, 71, 331

doi: https://doi.org/10.52526/25792776-26.73.1-189

Massive Early Seeds as a Phenomenological Framework for the Origin of High-Redshift Supermassive Black Holes

Vasily N. Bruilo *

Minsk, Belarus ORCID: 0009-0006-0085-4155

Abstract

Supermassive black holes (SMBHs) with masses of 10^8–10^9 $M_\odot$ are observed at redshifts z > 7– 10, corresponding to cosmic times less than 700 Myr after the Big Bang within ΛCDM cosmology. Recent JWST discoveries, including Little Red Dots (LRDs), compact galaxies hosting overmassive SMBHs, and dust-obscured AGN (e.g., CAPERS-LRD-z9 at z ≃ 9.3), challenge light-seed models that rely solely on Eddington-limited accretion from stellar-mass remnants (Kocevski et al., 2025, Maiolino et al., 2024, Rusakov et al., 2026).

While heavy-seed scenarios such as direct collapse partially alleviate growth timescale issues, they often require finely tuned initial conditions or episodic super-Eddington accretion to match the observed abundance and mass distribution of high-z SMBHs.

Unlike existing heavy-seed models, this work proposes a phenomenological framework in which massive early seeds ($M_{seed} \geq 10^5$–$10^6\, M_\odot$) are treated as an effective macroscopic population constrained by observations, without invoking a single specific formation channel. Forming preferentially in highly biased overdense environments at $z \geq 15$, these seeds act as gravitational centers that accelerate galaxy and quasar assembly, reducing the required growth from ≃18–20 e-folds to ≥10 while remaining consistent with realistic duty cycles and feedback physics. The model naturally explains the elevated M_{BH}/M_* ratios observed in compact high-redshift systems without extreme dust obscuration or feedback fine-tuning.

We outline viable parameter ranges and present multiple independent observational tests, including an enhanced central SMBH occupation fraction in compact galaxies (testable with JWST programs such as GLIMPSE and PRIMER), relic intermediate-mass black hole populations, and elevated early merger rates detectable by LISA Consortium (2025). The framework is fully consistent with ΛCDM cosmology and does not modify global cosmological observables. It can be decisively tested or falsified with ongoing JWST deep fields, ngEHT observations, and future gravitational-wave measurements. In particular, the absence of an enhanced SMBH occupation fraction in the most compact high-redshift galaxies would directly falsify the model.

Keywords: *supermassive black holes, high-redshift galaxies, JWST, direct collapse, gravitational waves, LISA*

1. Introduction

Supermassive black holes (SMBHs), with masses ranging from 10^6 to 10^{10} $M_\odot$, reside at the centers of massive galaxies and play a fundamental role in their evolution through feedback processes such as outflows, jets, and radiative heating (Fabian et al., 2012, Kormendy & Ho, 2013). Understanding their origin remains one of the central challenges in modern astrophysics, particularly given the rapid assembly of billion-solar-mass SMBHs within the first billion years after the Big Bang (z > 6–10).

Recent observations from the James Webb Space Telescope (JWST) have significantly sharpened this problem by revealing a growing population of SMBHs at z > 7, many of which appear overmassive relative to their host galaxies (M_{BH}/M^* significantly exceeding local scaling relations). Notable examples include dust-obscured active galactic nuclei (AGN) in compact systems known as Little Red Dots (LRDs), as well

*labtest940@gmail.com

doi: https://doi.org/10.52526/25792776-26.73.1-196

as broad-line sources such as CAPERS-LRD-z9 at z $\simeq$ 9.3 and the Virgil galaxy at a cosmic age of ~800 Myr (Kocevski et al., 2025, Maiolino et al., 2024, Naidu et al., 2025, Rusakov et al., 2026, Taylor et al., 2025). These findings suggest that SMBH seeds must have formed early and grown efficiently under extreme conditions, placing strong constraints on theoretical models.

Standard formation scenarios include: (i) growth from light stellar-remnant seeds ($\sim$ 10–100 $M_\odot$) via prolonged Eddington or super-Eddington accretion (Madau & Rees, 2001, Volonteri, 2010), (ii) direct collapse of pristine gas clouds into heavy seeds ($\sim 10^4$–$10^6 M_\odot$) under intense Lyman–Werner radiation (Bromm & Loeb, 2003, Inayoshi et al., 2020) (iii) runaway stellar mergers in dense nuclear clusters (Portegies Zwart et al., 2023), (iv) primordial black holes formed from early density fluctuations (Carr et al., 2021), and (v) more speculative mechanisms involving dark matter or other new physics.

Each of these scenarios encounters difficulties when confronted with recent JWST data. Light-seed models typically require sustained high accretion rates and large duty cycles, while heavy-seed formation channels often rely on rare environmental conditions that may not reproduce the observed abundance (De Graaff et al., 2025, Latif et al., 2022). Primordial black hole scenarios are additionally constrained by limits from the cosmic microwave background, microlensing, and evaporation (Inayoshi et al., 2020, Ziparo et al., 2025).

In this work, we propose a phenomenological framework in which massive early seeds ($M_{seed} \geq 10^5$–10^6 $M_\odot$) form preferentially in highly biased overdense regions at z > 15. These seeds act as early gravitational centers that accelerate the hierarchical assembly of galaxies and quasars, naturally accounting for elevated M_BH/M* ratios without invoking extreme accretion histories or finely tuned feedback.

We review the limitations of standard models in Section 2, derive physical constraints and parameter ranges for the proposed framework in Section 5, and outline testable observational signatures using current JWST surveys (e.g., GLIMPSE, PRIMER), next-generation interferometry (ngEHT), and the future LISA mission (Sections 6–7). This framework provides a consistent and testable pathway to reconcile early SMBH observations with theoretical growth limits.

Throughout this work, “massive early seeds” refers to black holes with initial masses $\geq 10^5$–$10^6\, M_\odot$ formed at very early cosmic epochs (z > 15) in rare and extreme environments. Their origin may involve enhanced gas collapse, rapid protostellar mergers, or the collapse of dense protocluster structures under metal-poor conditions. Rather than assuming a single formation channel, we treat these seeds as an effective initial condition compatible with a range of processes within standard cosmology.

2. Review of Standard Formation Scenarios for Supermassive Black Holes

We briefly review the principal proposed mechanisms for supermassive black hole (SMBH) seed formation at high redshifts, highlighting their strengths and key limitations, particularly in light of recent JWST discoveries of overmassive SMBHs in compact systems at z > 7.

2.1. Light Seeds from Stellar Remnants

The standard scenario assumes that SMBHs grow from stellar-mass seeds ($\sim$ 10–100 $M_\odot$) formed in the first Population III stars via core collapse or pair-instability supernovae. Subsequent growth occurs through Eddington-limited or super-Eddington accretion (Madau & Rees, 2001, Volonteri, 2010).

The mass growth under Eddington-limited accretion follows the exponential form:

$$M(t) = M_0 exp[(1{-}\epsilon)/\epsilon \times t/t\_Edd], \tag{1}$$

where M_0 is the initial seed mass, $\epsilon \simeq 0.1$ is the radiative efficiency and $t_{Edd} \simeq 45$ Myr is the Salpeter timescale (Inayoshi et al., 2020, Salpeter, 1964).

Even under ideal conditions, this corresponds to a mass growth timescale of $\simeq$ 0.45 Gyr for 10 e-foldings, leaving little room for interruptions in the accretion history. Reaching 10^9 $M_\odot$ from $\sim 100\, M_\odot$ in less than 700 Myr remains challenging under realistic early-Universe conditions due to strong feedback, rapid gas depletion, and low average accretion rates (Johnson & Bromm, 2007). JWST observations of overmassive SMBHs in compact systems (e.g., LRDs with $M_{BH}/M*$ significantly exceeding local scaling relations) further strain this model, requiring extreme and potentially difficult-to-sustain assumptions about prolonged super-Eddington phases (Kocevski et al., 2025, Maiolino et al., 2024).

doi: https://doi.org/10.52526/25792776-26.73.1-196

2.2. Direct Collapse Black Holes (Heavy Seeds)

In metal-poor, pristine gas clouds exposed to intense Lyman-Werner UV flux from nearby star-forming regions, gas can cool nearly isothermally and collapse directly into $\sim 10^4$–$10^6\,M_\odot$ seeds, bypassing the need for prolonged super-Eddington growth (Bromm & Loeb, 2003, Inayoshi et al., 2020).

Recent JWST candidates include compact objects in merging systems and LRDs interpreted as possible direct-collapse remnants (Rusakov et al., 2026, Taylor et al., 2025). However, the required conditions — pristine gas and a strong, sustained UV background — are extremely rare. Detailed simulations and abundance estimates indicate that direct collapse may struggle to reproduce the observed number density of high-z SMBHs and quasars without fine-tuning (De Graaff et al., 2025, Latif et al., 2022).

2.3. Runaway Collapses in Dense Stellar Clusters

Dense nuclear star clusters can undergo runaway mergers driven by dynamical friction and stellar collisions, potentially producing intermediate-mass black hole seeds ($\sim 10^2$–$10^4\,M_\odot$) (Portegies Zwart et al., 2023, Vergara et al., 2025).

While efficient in dense environments, this channel faces uncertainties at z > 15 due to limited protocluster assembly timescales and early metal enrichment. JWST has not yet provided clear evidence for a widespread population of IMBHs in high-redshift systems, and the mechanism is not expected to dominate under current constraints.

2.4. Primordial Black Holes (PBHs)

PBHs could form from high-density fluctuations in the early Universe, with masses potentially spanning $10^{-16}M_\odot$ to $10^5M_\odot$ (Carr et al., 2021, Ziparo et al., 2025).

Strong observational constraints severely limit their contribution:

- CMB anisotropies and μ-distortions exclude significant PBH fractions in the 10–100 $M_\odot$ range (Inomata et al., 2021, Planck Collaboration et al., 2020).
- Lensing (HSC, OGLE) and microlensing surveys constrain f_PBH < 0.01–0.1 in relevant mass ranges.
- Hawking evaporation excludes PBHs with masses below $\sim 10^{15}$ g.

Although PBHs could seed some high-z SMBHs, current bounds make them unlikely to dominate the observed population without extreme fine-tuning, although they remain an active area of theoretical investigation (Carr et al., 2021, Green & Kavanagh, 2021).

2.5. Alternative and Speculative Scenarios

Models involving self-interacting dark matter, axion miniclusters, or other speculative physics remain poorly constrained and lack robust observational support (no confirmed signatures in CMB, GW, or JWST data).

2.6. Summary

Taken together, these limitations suggest that no single standard formation scenario appears to simultaneously reproduce the observed abundance, masses, and early appearance of SMBHs revealed by JWST without invoking rare environmental conditions, prolonged super-Eddington growth, or additional physics. Light-seed models primarily struggle with growth timescales and duty cycles, heavy-seed mechanisms (direct collapse, runaway mergers) are limited by environmental rarity, and PBH scenarios are tightly constrained by multiple independent observations. These limitations motivate the exploration of complementary or extended seeding pathways that relax growth constraints while remaining fully consistent with ΛCDM cosmology. The phenomenological massive early seed framework introduced here provides such a pathway, treating massive seeds ($M_{seed} \geq 10^5$–$10^6M_\odot$) as an effective initial condition in biased overdense regions at z > 15.

doi: https://doi.org/10.52526/25792776-26.73.1-196

Table 1. Comparison of Standard SMBH Seed Formation Scenarios

Scenario	Seed Mass	Advantages	Key Limitations
Light seeds	10–100 $M_\odot$	Common formation in Pop III stars	Slow growth, requires extreme duty cycles
Direct collapse	10^4–10^6 $M_\odot$	Large initial seeds, bypasses Eddington limit	Extremely rare conditions
Cluster mergers	10^2–10^4 $M_\odot$	Dynamical channel in dense clusters	Limited efficiency at $z > 15$
PBHs	Broad range	Early formation	Strong observational constraints (CMB, lensing,evaporation)

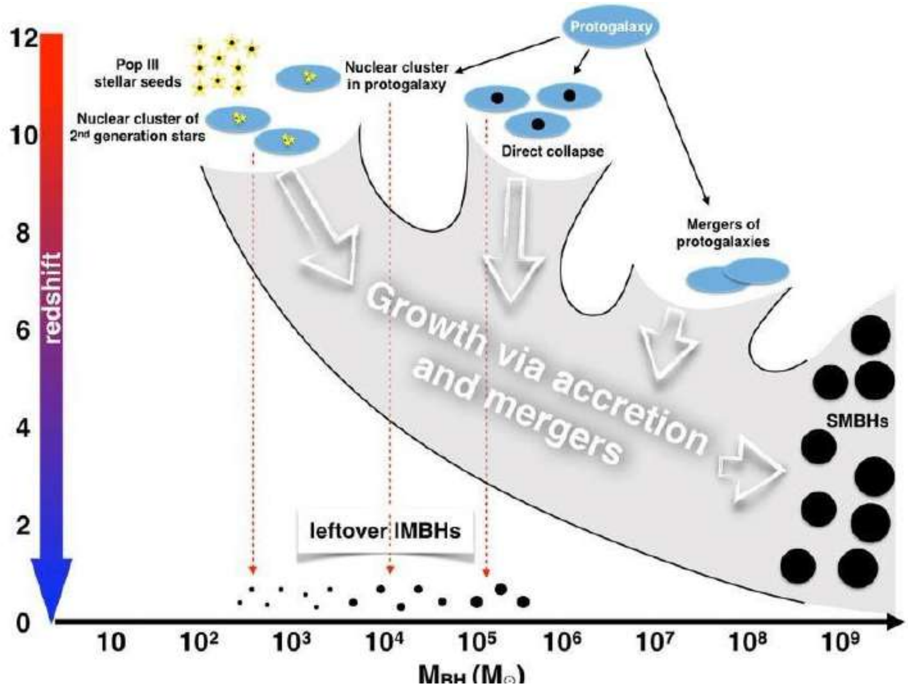

Figure 1. Schematic overview of standard SMBH seed formation and growth pathways from $z \geq 12$ to the present. The diagram illustrates the main channels (Pop III stellar seeds, direct collapse, nuclear cluster mergers, Lyman-Werner radiation effects) and their temporal evolution.

3. Constraints on Growth

Black hole growth is limited by the Eddington accretion rate, governed by the Salpeter equation 1. For light seeds with initial masses of order 10–100 $M_\odot$, reaching the observed SMBH masses of 10^8–10^9 $M_\odot$ at $z > 7$ (corresponding to cosmic times $t \lesssim 700$ Myr) requires approximately 18–20 e-folding growth phases. For example, growing from 10 $M_\odot$ to 10^9 $M_\odot$ demands $\ln(10^8) \simeq 18.42$ e-folds, equivalent to roughly 9–10 e-folding times ($\simeq$ 405–450 Myr for $\epsilon \simeq 0.1$) of near-continuous Eddington or super-Eddington accretion. This corresponds to an effective duty cycle approaching unity ($f_{duty} \geq 0.8$–1), which is difficult to sustain under realistic early-Universe conditions due to strong radiative feedback and limited gas supply (Pacucci et al., 2023, Volonteri, 2010). See Figure 2 for a direct comparison of growth curves for light and heavy seeds.

Black hole mergers can supplement mass growth, but gravitational wave energy losses typically remove 5–10% of the total system mass per merger (Abbott et al., 2016, Baker et al., 2006). While hierarchical mergers contribute to the final mass budget, they are insufficient to fully bridge the gap for stellar-mass seeds without prolonged super-Eddington phases — which remain observationally rare and theoretically constrained at high redshift due to feedback-driven outflows (Inayoshi et al., 2020, Wang et al., 2021).

Adopting heavy initial seeds with masses $M_{seed} \geq 10^5$–$10^6 M_\odot$ (as proposed in this work) dramatically alleviates these constraints. Starting from $M_0 = 10^5 M_\odot$, reaching 10^9 requires only ∼9.21 e-folds ($\ln(10^4) \simeq 9.21$), equivalent to roughly 4–5 e-folding times ($\simeq$ 180–225 Myr) at $\epsilon = 0.1$. This timescale is comfortably accommodated within the available ∼700 Myr (∼15 e-folding times), even when allowing for intermittent

doi: https://doi.org/10.52526/25792776-26.73.1-196

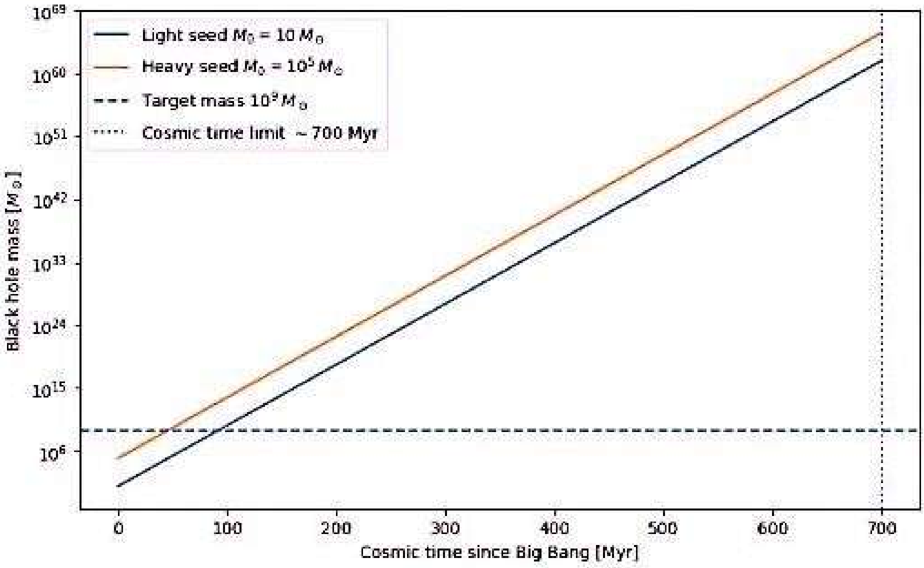

Figure 2. Eddington-limited growth curves for light seeds ($M_0 = 10M_\odot$) and heavy seeds ($M_0 = 10^5 M_\odot$) as a function of time since the Big Bang. The horizontal dashed line indicates the available cosmic time at z $\simeq$ 7 ($\sim$ 700 Myr). Heavy seeds reach $10^9\ M_\odot$ well within the limit, while light seeds require prolonged and potentially difficult-to-sustain accretion histories.

accretion and feedback effects. This effectively relaxes the growth-time tension inherent to light-seed models.

Hawking evaporation has negligible impact on such objects. The evaporation timescale is given by:

$$t_{evap} \simeq 5120\pi G^2 M^3/(\hbar c^4), \tag{2}$$

which exceeds the current age of the Universe by many orders of magnitude. For example, a black hole with $M \simeq 10^5\ M_\odot$ has an evaporation timescale $t_{evap} \geq 10^{90}$ yr. Consequently, heavy early seeds remain stable and can serve as dynamically significant gravitational centers throughout cosmic history.

These growth constraints are particularly relevant for the compact, overmassive systems revealed by JWST, such as Little Red Dots (LRDs), where elevated M_{BH}/M_* ratios suggest rapid and efficient black hole assembly in biased environments (Maiolino et al., 2024, Rusakov et al., 2026, Taylor et al., 2025). Our model of massive early seeds naturally explains these observations by reducing the required accretion duty cycle and enabling early seeding in overdense regions.

4. The Massive Early Seed Hypothesis

We propose a phenomenological scenario in which heavy black hole seeds with initial masses $M_{seed} \geq 10^5$–$10^6 M_\odot$ form preferentially in extremely overdense environments at redshifts z $\geq$ 15. These environments correspond to the high-δ tails of the primordial density field — strongly biased regions where the local overdensity δ exceeds typical collapse thresholds, corresponding to rare high-δ fluctuations (3σ peaks; Bromm & Loeb, 2003, Inomata et al., 2021, Lodato & Natarajan, 2006).

Several physical pathways may plausibly contribute to the formation of such seeds. One possibility is enhanced direct collapse in atomic-cooling halos where molecular hydrogen cooling is suppressed by strong Lyman–Werner radiation fields produced by nearby star-forming regions (Inayoshi et al., 2020, Latif et al., 2022). Another pathway involves dynamical processes in dense proto-clusters or mini-halos, where runaway stellar collisions or gas fragmentation can produce intermediate-mass black hole seeds that subsequently merge rapidly (Freitag & et al., 2006, Portegies Zwart et al., 2023).

In this framework, the resulting heavy seeds act as dominant gravitational centers that accelerate gas infall and baryonic collapse on timescales comparable to or shorter than the effective baryonic collapse time within the surrounding dark matter halo. As a consequence, the growth of the black hole becomes less dependent on prolonged super-Eddington accretion phases, which are energetically demanding and observationally constrained in the high-redshift Universe (Pacucci et al., 2023, Wang et al., 2021). Importantly, the model remains agnostic regarding the precise microphysical mechanism responsible for seed formation

doi: https://doi.org/10.52526/25792776-26.73.1-196

and instead focuses on the macroscopic dynamical consequences. In this picture, massive seeds serve as preferred centers for early galaxy and quasar assembly.

Quantitatively, a seed with mass $M_{seed} \simeq 10^5 M_\odot$ embedded within a halo of virial mass $M_{halo} \simeq 10^8$–$10^9 M_\odot$ at redshifts z ≃ 15–20 can significantly shorten the gas-collapse timescale compared with models in which collapse is driven solely by the halo potential. In such systems, the enhanced gravitational potential near the seed can drive efficient early gas accretion. Order-of-magnitude estimates based on Bondi–Hoyle-like accretion in dense environments suggest that the initial growth phase can proceed at near-Eddington rates for approximately 100–200 Myr without requiring sustained super-Eddington accretion (see also Section 3).

This scenario is fully consistent with the standard ΛCDM cosmological framework and does not require modifications to fundamental physics or exotic mechanisms. Instead, it shifts the emphasis toward rare initial conditions and environmental bias as key drivers of early SMBH formation. It complements existing seed formation channels — including light Population III remnants, direct collapse black holes, and primordial black holes — by providing a pathway for rapid early supermassive black hole growth in the rarest overdense regions of the early Universe. In this way, the model naturally explains the elevated black hole–to–stellar mass ratios observed in compact high-redshift systems discovered by JWST, including the class of objects known as Little Red Dots (Maiolino et al., 2024, Rusakov et al., 2026, Taylor et al., 2025).

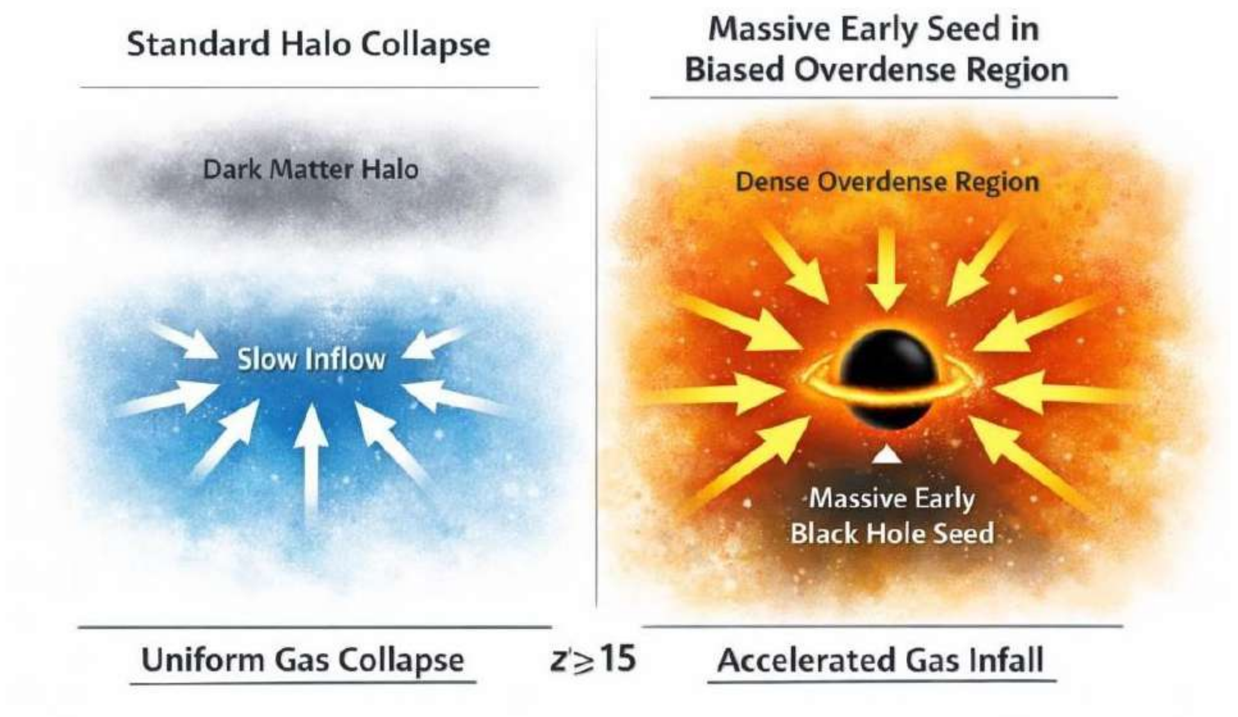

Figure 3. Schematic illustration of a massive early seed embedded in a biased overdense region at z ≥ 15, illustrating accelerated gas infall toward the seed compared with a uniform halo collapse scenario. The diagram highlights how extreme overdensity can facilitate rapid baryonic collapse and reduce the required accretion duty cycle for early supermassive black hole growth.

5. Model Constraints and Parameter Estimates

Any viable model for the formation of supermassive black holes must remain consistent with existing observational data and with the standard cosmological framework. In this section, we outline the principal physical constraints and characteristic parameter ranges of the proposed massive early seed model.

5.1. Seed Mass Scale

Observations of high-redshift quasars reveal black holes with masses $MBH \simeq 10^8$–$10^9 M_\odot$ at redshifts z > 7, corresponding to cosmic ages of less than 700 Myr (e.g. Bañados et al., 2018, Mortlock et al., 2011). Explaining the existence of such massive objects within this limited time window places strong constraints on the initial mass of black hole seeds.

doi: https://doi.org/10.52526/25792776-26.73.1-196

In the proposed framework, the initial seed masses are assumed to lie well above the stellar-mass regime. A conservative lower bound for massive early seeds is $M_{seed} \geq 10^5$–$10^6 M_\odot$. Such masses significantly reduce the number of required e-folding times needed to reach the observed quasar masses under Eddington-limited accretion. Consequently, the model alleviates the need for prolonged super-Eddington growth phases, which are limited by radiative feedback and gas supply (Maiolino et al., 2024, Pacucci et al., 2023). Observations of compact JWST sources such as Little Red Dots at z $\simeq$ 8–10 suggest seed masses above $\sim 10^4 M_\odot$ to explain their rapid assembly (Rusakov et al., 2026, Taylor et al., 2025). Upper bounds are expected to be comparable to the characteristic collapse mass scale in metal-free atomic-cooling halos ($\sim 10^6$ Bromm & Loeb, 2003).

5.2. Growth-Time Constraints

The mass growth of a black hole accreting at the Eddington limit (see Eq. 2). Starting from stellar-mass seeds ($M_0 \simeq 10 M_\odot$), reaching $10^9 M_\odot$ within 700 Myr requires nearly continuous accretion at or above the Eddington limit, corresponding to roughly 18–20 e-foldings with duty cycles approaching unity. Such a scenario is difficult to reconcile with observational indications of intermittent AGN activity in the early Universe (Wang et al., 2021). In contrast, seeds with initial masses $M_0 \simeq 10^6 M_\odot$ require substantially fewer e-folding times ($\sim$ 7–9), making the observed early SMBHs achievable within standard accretion scenarios even with moderate duty cycles ($\sim$ 0.1–0.5) (Volonteri, 2010).

Higher radiative efficiencies ($\epsilon \geq 0.15$), expected for rapidly spinning black holes, would further increase the growth timescale under Eddington-limited accretion. Since the e-folding time scales as $\epsilon/(1-\epsilon)$, even moderate increases in spin can significantly slow mass growth. This further strengthens the argument that massive initial seeds may be required to reproduce the observed high-redshift SMBH population within the available cosmic time.

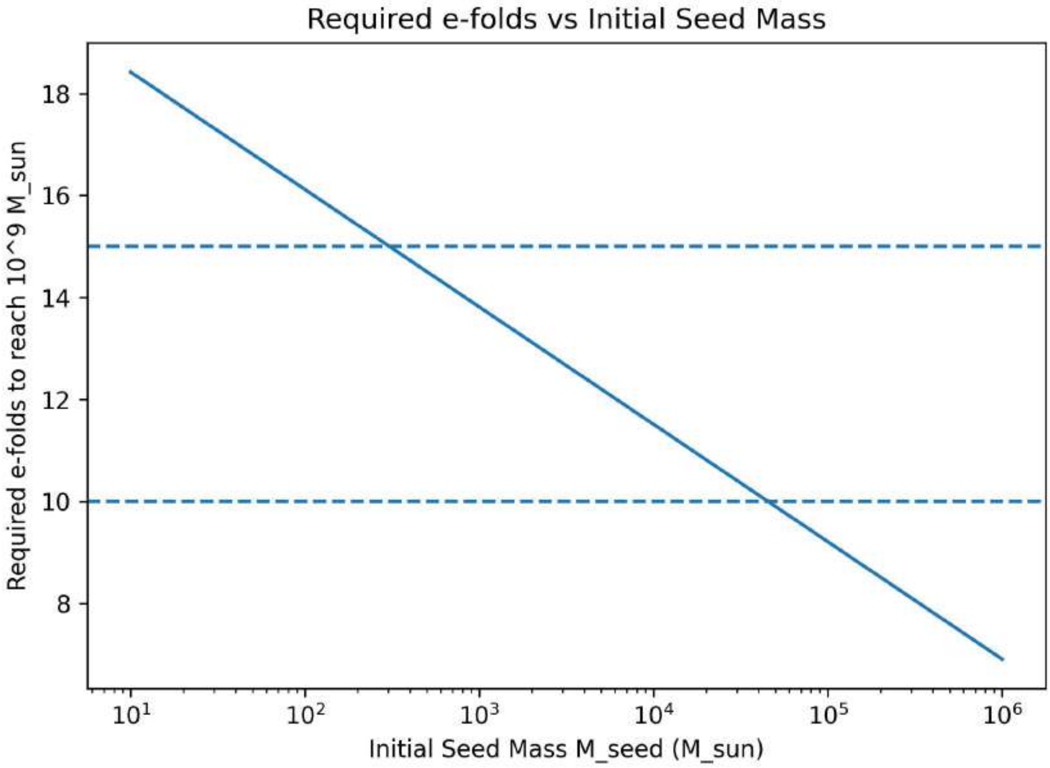

Figure 4. Required number of e-foldings to reach $10^9 M_\odot$ under Eddington-limited accretion as a function of the initial seed mass, $M_{\rm seed}$. The horizontal dashed line indicates the maximum of approximately 14–15 e-foldings available within $\sim$ 700 Myr. Seeds with $M_{\rm seed} \geq 10^5 M_\odot$ easily satisfy this constraint, whereas light seeds require an unphysically large number of e-foldings.

doi: https://doi.org/10.52526/25792776-26.73.1-196

5.3. Stability and Survival

Black holes with masses exceeding $\sim\ 10^5 M_\odot$ are effectively stable over cosmological timescales. The Hawking evaporation time, given by Eg. 2, greatly exceeds the age of the Universe ($\sim 10^{10}$ yr) for massive seeds and supermassive black holes (Hawking & Ellis, 1975). Consequently, once formed, massive early seeds can persist throughout cosmic history and remain dynamically relevant during the earliest stages of galaxy formation.

5.4. Number Density and Environmental Constraints

The observed comoving number density of luminous quasars at high redshift is relatively low $\sim 10^{-6}$–$10^{-7} Mpc^{-3}$ at z > 6 (e.g., Shen, 2020, Willott et al., 2010) . Massive early seeds must therefore represent a rare population rather than a ubiquitous component of the early Universe.

The model therefore requires: (i) a low initial number density of massive seeds ($n_{seed} \leq 10^{-4}$–$10^{-5} Mpc^{-3}$) to avoid the overproduction of SMBHs, (ii) preferential formation in highly biased overdense regions (bias parameter b ≥3–5, corresponding to rare peaks in the primordial density field), and (iii) association with the most massive early dark matter halos ($M_{halo} \simeq 10^9$–10^{10} $M_\odot$ at z ≃ 15–20). These conditions remain compatible with constraints from large-scale structure formation, including halo mass functions derived from cosmological N-body simulations (e.g., Jenkins et al., 2001, Reed et al., 2007).

5.5. Consistency with Standard Cosmology

The massive early seed model does not modify the global expansion history of the Universe and remains fully compatible with the ΛCDM cosmological framework. The seeds act only as localized gravitational centers and do not contribute significantly to the total matter density of the Universe. Even at peak abundance, their contribution to Ω_m is negligible ($< 10^{-5}$).

Any observable deviations from standard cosmological predictions would therefore appear primarily at small scales and high redshifts, affecting the earliest stages of galaxy and quasar formation. Current constraints from the cosmic microwave background and large-scale structure surveys do not exclude this scenario, as it operates within the allowed parameter space for rare seed formation in the early Universe.

Table 2. Summary of parameter ranges for the massive early seed model

Parameter	Range	Justification / Observational Constraint
Seed mass (M_{seed})	10^5–$10^6 M_\odot$	Lower bound from growth constraints (Sec. 3); upper from Jeans mass in metal-free halos (Bromm & Loeb, 2003)
Formation redshift (z_{form})	z > 15	Early biased regions; compatible with reionization timelines (Planck Collaboration et al., 2020)
Number density (n_{seed})	$< 10^{-4}$–$10^{-5}\ Mpc^{-3}$	Matches quasar luminosity function at z > 6; avoids overproduction (Shen, 2020, Willott et al., 2010)
Bias parameter (b)	3-5	Rare peaks ($\sigma > 3$); from Gaussian field statistics (Jenkins et al., 2001)
Halo mass at formation	10^9–$10^{10}\ M_\odot$	Most massive early halos; from N-body simulations (Reed et al., 2007)

6. Observational Implications and Testability of the Model

The proposed model of massive early seeds generates several robust and independently testable observational signatures that can be probed with current and upcoming astronomical facilities. These predictions differentiate the scenario from standard light-seed and direct-collapse models and provide clear pathways for empirical verification. A key strength of the massive early seed framework is that it produces multiple independent and quantitatively testable predictions across both electromagnetic and gravitational-wave observations.

doi: https://doi.org/10.52526/25792776-26.73.1-196

One of the most distinctive predictions of the model is the combination of a relatively high black hole occupation fraction in early galaxies together with elevated merger rates at very high redshift — a combination that is difficult to reproduce simultaneously in conventional seeding scenarios.

Enhanced fraction of compact galaxies hosting central black holes. The model predicts a significantly higher incidence (≃30–50%) of central black holes in compact high-redshift galaxies compared with uniform light-seed models, which typically predict occupation fractions below ∼10%. This prediction can be tested using deep-field observations from the James Webb Space Telescope, including surveys such as GLIMPSE, PRIMER, and COSMOS-Web, which are already identifying large samples of compact galaxies at z > 7 (Maiolino et al., 2024, Taylor et al., 2025). Detection of black hole signatures — such as broad emission lines or X-ray counterparts — in a substantial fraction of these systems would strongly support the proposed scenario.

Reduced duration and duty cycle of super-Eddington accretion phases. Because massive seeds require only approximately 4–5 e-foldings of Eddington growth (Sec. 3), the model predicts shorter or more intermittent super-Eddington accretion episodes with duty cycles of roughly 0.1–0.5. Observationally, this should manifest as lower average Eddington ratios or weaker large-scale outflow signatures in high-redshift active galactic nuclei compared with predictions from light-seed growth models. Spectroscopic observations of compact sources such as Little Red Dots using JWST NIRSpec and MIRI instruments can constrain these accretion properties (Pacucci et al., 2023, Rusakov et al., 2026, Wang et al., 2021).

Relic population of intermediate-mass black holes. The model naturally predicts a population of relic intermediate-mass black holes (IMBHs) with masses of approximately 10^3–$10^5\,M_\odot$that fail to grow efficiently due to limited gas supply or strong feedback. Such objects could appear as off-nuclear compact sources in dwarf galaxies or ultra-compact stellar systems. The detection of these relic IMBHs through dynamical mass measurements with JWST or future extremely large telescopes would support the model, while stringent upper limits on their abundance would constrain the seed mass function.

Elevated early merger rates and gravitational-wave background. Rapid hierarchical assembly in the early Universe implies enhanced black hole merger rates at redshifts z > 10. This should generate a distinct stochastic gravitational-wave background in the millihertz frequency band accessible to the future Laser Interferometer Space Antenna mission. Characteristic amplitudes of $\Omega_{GW} \simeq 10^{-11}$–$10^{-10}$ are expected for merger-driven scenarios involving massive early seeds (Klein, 2024, LISA Consortium, 2025). Detection of a stronger-than-expected high-redshift signal would provide strong support for the model.

Overmassive black hole–to–stellar mass ratios. The massive early seed framework naturally explains the elevated black hole–to–stellar mass ratios observed in compact high-redshift systems. Ratios of $M_{BH}/M_* \geq 10^{-3}$–10^{-2} inferred in Little Red Dot galaxies can arise without invoking extreme dust obscuration or finely tuned feedback processes (Maiolino et al., 2024, Taylor et al., 2025). Future JWST imaging and spectroscopic surveys of larger LRD samples can test whether these ratios correlate with galaxy compactness and local overdensity — a key prediction of the model.

Falsifiability of the scenario. The massive early seed model is directly falsifiable through several observational tests. In particular, the model would be strongly disfavored if: • JWST surveys detect central black holes in fewer than ∼30% of compact high-redshift galaxies. • The LISA mission measures a gravitational-wave background fully consistent with predictions from light-seed scenarios without evidence for enhanced early merger activity. • Observational searches fail to identify relic populations of intermediate-mass black holes in dwarf galaxies or compact stellar systems.

Such null results would significantly constrain or potentially rule out the massive early seed formation scenario.

7. Discussion and Conclusions

The massive early seed model provides a physically motivated, self-consistent, and observationally testable framework that complements existing scenarios of supermassive black hole (SMBH) formation, such as light Population III remnants, direct collapse, and prolonged super-Eddington accretion. By positing heavy seeds ($M_{seed} \geq 10^5$–$10^6\,M_\odot$) forming preferentially in strongly biased, overdense environments at z ≥ 15, the model naturally alleviates the severe timing tension revealed by JWST observations of over-massive black holes in compact systems at z > 7 (Maiolino et al., 2024, Rusakov et al., 2026, Taylor et al., 2025). It requires no invocation of new fundamental physics, relying solely on plausible variations in the initial conditions of the early Universe — specifically, the rare high-σ peaks of the density field where

doi: https://doi.org/10.52526/25792776-26.73.1-196

Table 3. Summary of quantitative observational tests distinguishing the massive early seed scenario from standard seeding models

Prediction	**Observable Signature**	**Instrument**	**Expected Signal**	**Falsification Condition**
Enhanced BH fraction in compact galaxies	Central BH signatures in LRDs	JWST (GLIMPSE/ (GLIMPSE/PRIMER)	>30–50%	< 10%
Reduced super-Eddington phases	Lower Eddington ratios, weaker outflows	JWST NIRSpec / MIRI Duty cycle	Persistent high duty cycles	occupation <10% fraction
Relic IMBH population	Off-nuclear compact sources	JWST / ELT	10^3–10^5 $M_\odot$ BHs	No detectable population
Elevated merger rates	Stochastic GW background	LISA	$\Omega_{GW} \sim 10^{-11}$–$10^{-10}$	Standard light-seed amplitude
Over-massive ratios	$\mathrm{M}_{BH}/M_* > 10^{-3}$–$10^{-2}$	JWST NIRCam	Correlation with compactness	No correlation

atomic-cooling halos and rapid collapse can occur under intense Lyman-Werner backgrounds or proto-cluster dynamics (Inayoshi et al., 2020, Latif et al., 2022).

Compared to light-seed models, the scenario dramatically reduces the required number of e-folding growth phases (Section 3), lowering the growth burden from ∼18–20 e-folds to ≤10 for seed masses ≥ $10^5\ M_\odot$. This allows observed SMBH masses to be reached with realistic duty cycles and without extreme fine-tuning of feedback or accretion physics. Relative to standard direct-collapse models, it broadens the viable parameter space by relaxing the need for perfectly tuned pristine environments, instead emphasizing preferential formation in the most overdense regions. The model remains fully consistent with ΔCDM cosmology (Section 5.5 and does not contribute significantly to the matter budget or large-scale structure.

A key strength of the massive early seed scenario lies in its predictive power and falsifiability (Section 6). Multiple independent observational signatures — enhanced BH fractions in compact galaxies, reduced super-Eddington phases, relic intermediate-mass black holes, elevated merger rates, and overmassive M_{BH}/M_* ratios — can be probed with existing JWST data and will be decisively tested by future ultra-deep surveys (GLIMPSE, PRIMER, COSMOS-Web), next-generation radio interferometry (ngEHT), and the LISA gravitational-wave mission (launch ∼2035). These facilities will provide decisive constraints and potentially resolve one of the most pressing puzzles of the high-redshift Universe: the rapid emergence of supermassive black holes.

The main uncertainty of the model lies in the poorly constrained abundance of high-σ peaks at $z > 15$, which future surveys and cosmological simulations will clarify. If confirmed, the scenario would highlight the critical role of rare, biased environments in shaping the first quasars and massive galaxies, implying that the earliest stages of galaxy formation were governed primarily by rare initial conditions rather than by average cosmological evolution.

In conclusion, the massive early seed model offers a simple yet powerful framework that reconciles JWST's surprising discoveries with theoretical expectations while remaining firmly rooted in established physics. Future observations will ultimately determine whether this scenario or an alternative mechanism best describes the dawn of supermassive black holes in the early Universe. Regardless of the outcome, the massive early seed model highlights the potential role of rare environmental conditions in driving the rapid emergence of the first supermassive black holes, offering a new perspective on early galaxy formation. Further theoretical development and high-resolution cosmological simulations will be essential to quantify the expected abundance of such massive seeds in high-σ regions.

References

Abbott B. P., et al., 2016, Astrophys. J. Suppl. Ser. , 227, 14

Bañados E., Carilli C., Walter F., Momjian E., Decarli R., Farina E. P., Mazzucchelli C., Venemans B. P., 2018, Astrophys. J. Lett. , 861, L14

Baker J. G., Centrella J., Choi D.-I., Koppitz M., van Meter J., 2006, Phys. Rev. D. , 73, 104002

Bromm V., Loeb A., 2003, Astrophys. J. , 596, 34

Carr B., Kohri K., Sendouda Y., Yokoyama J., 2021, Reports on Progress in Physics, 84, 116902

doi: https://doi.org/10.52526/25792776-26.73.1-196

De Graaff A., et al., 2025, arXiv e-prints, p. arXiv:2511.21820

Fabian A. C., et al., 2012, Mon. Not. R. Astron. Soc. , 424, 217

Freitag M., et al. 2006, Astrophys. J. , 649, 640

Green A. M., Kavanagh B. J., 2021, Journal of Cosmology and Astroparticle Physics, 2021, 009

Hawking S. W., Ellis G. F. R., 1975, The Large Scale Structure of Space-Time

Inayoshi K., Visbal E., Haiman Z., 2020, Ann. Rev. Astron. Astrophys. , 58, 27

Inomata K., McDonough E., Hu W., 2021, Phys. Rev. D. , 104, 123553

Jenkins A., Frenk C. S., White S. D. M., Colberg J. M., Cole S., Evrard A. E., Couchman H. M. P., Yoshida N., 2001, Mon. Not. R. Astron. Soc. , 321, 372

Johnson J. L., Bromm V., 2007, Mon. Not. R. Astron. Soc. , 374, 1557

Klein A., 2024, Astrophys. J. , 965, 123

Kocevski D. D., et al., 2025, Astrophys. J. , 986, 126

Kormendy J., Ho L. C., 2013, Ann. Rev. Astron. Astrophys. , 51, 511

LISA Consortium 2025, Living Rev. Relativ., 28, 1

Latif M. A., Whalen D., Khochfar S., 2022, Mon. Not. R. Astron. Soc. , 511, 1234

Lodato G., Natarajan P., 2006, Mon. Not. R. Astron. Soc. , 371, 1813

Madau P., Rees M. J., 2001, Astrophys. J. Lett. , 551, L27

Maiolino R., et al., 2024, Astron. Astrophys. , 691, A145

Mortlock D. J., et al., 2011, Nature. , 474, 616

Naidu R. P., et al., 2025, arXiv e-prints, p. arXiv:2503.16596

Pacucci F., Nguyen B., Carniani S., Maiolino R., Fan X., 2023, Astrophys. J. , 950, 123

Planck Collaboration et al., 2020, Astron. Astrophys. , 641, A6

Portegies Zwart S. F., et al., 2023, Astrophys. J. , 942, 45

Reed D. S., Bower R., Frenk C. S., Jenkins A., Theuns T., 2007, Mon. Not. R. Astron. Soc. , 374, 2

Rusakov V., et al., 2026, Nature. , submitted

Salpeter E. E., 1964, Astrophys. J. , 140, 796

Shen Y., 2020, Astrophys. J. , 892, 34

Taylor A. J., et al., 2025, Astrophys. J. Lett. , 960, L12

Vergara M. C., et al., 2025, Astron. Astrophys. , 704, A321

Volonteri M., 2010, Astron. Astrophys. Rev. , 18, 279

Wang J.-G., Jiang C., Yuan D., Zou P., 2021, Astrophys. J. , 907, 123

Willott C. J., et al., 2010, Astron. J. , 140, 546

Ziparo F., Gallerani S., Ferrara A., 2025, Journal of Cosmology and Astroparticle Physics, 2025, 040

doi: https://doi.org/10.52526/25792776-26.73.1-196

Communications of BAO, Vol. 73, Issue 1, 2026, pp. 207-219

A Historical-Comparative Analysis of Armenian Parallels to the Principal Night Names of Pre-Eastern Polynesian Lunar Calendars

L.G. Stepanyan *

Brusov State University (BSU), Armenia

Abstract

The subject of this study is the most stable night names of the Pre-Eastern Polynesian lunar calendars, whose etymologies are comparatively reliable, namely **Hiro, Kokore, Hotu,** and **Mutu**. Using the method of historical-comparative linguistics, the semantic and structural features of these night names were examined, and their possible comparative correspondences in Armenian were proposed. During the study, methods of historical-comparative, etymological, and semantic analysis were employed, based on comparative data from Polynesian languages, materials from the POLLEX project, and classical ethnographic sources. The analysis shows that the night names under consideration exhibit interesting formal and semantic parallels with certain lexical strata of Armenian. In some cases, these comparisons contribute to a more precise semantic interpretation of Polynesian night names. In particular, in the case of the **Kokore** series, it is proposed to distinguish two semantic layers corresponding to the phases of the waxing and waning moon: "curvature / curving" and "loss / diminution / disappearance." The aim of the study is to enrich the material basis for investigating possible Armenian-Polynesian linguistic-cultural commonalities and to expand the scope of comparative calendrical studies.

Keywords: *lunar calendar, Polynesian languages, Armenian, etymology, historical-comparative linguistics, cultural astronomy.*

1. Introduction

Lunar calendars are among humanity's oldest chronological systems and have played an important role in the economic, religious, and cultural life of various peoples. Through them, agricultural activities, navigation, fishing, ritual ceremonies, and other domains of time reckoning were organized. Particularly noteworthy are the lunar calendars of the Polynesian peoples, which have preserved detailed lists of lunar night names and provide valuable material for historical-comparative linguistics and cultural astronomy.

Comparative and computational studies of recent decades have shown that Eastern Polynesian lunar calendars preserve a common inherited structure, whose principal elements can be reconstructed back to the Proto-Central/East Polynesian stage, and in some cases to the Proto-Polynesian stage. Particularly stable are the night names **Hiro/Whiro, Tirea, Hotu, Huna, Atua, Rakau, ʻOturu,** and **Mutu**, which occur in geographically distant island traditions and display regular phonetic and semantic correspondences (Blust, 2013, Pawley, 2003, Valério, 2025).

The lunar night names may conventionally be divided into three main layers. The first is the descriptive layer, in which the names reflect the visible phases of the moon (for example, **Huna** "hidden," **Hotu** "to swell," **Mutu** "end"). The second is the mythological layer, in which the night names are associated with deities or cultural heroes (for example, **Hiro**, **Tangaroa, Tāne**). The third consists of structural naming series composed of recurring names and numerical components (for

*orongo9@mail.ru

example, the **Kokore** series). This multilayered system indicates that the Polynesian lunar calendar was not merely a chronological system, but also a symbolic one (Blust, 2019, Pawley, 2003).

In Armenian culture, the Moon has occupied an important place in calendrical and ritual conceptions. In Armenian, the word *lusin* ("moon") denoted not only the celestial body but also a unit of time—the month—which indicates the existence of ancient layers of lunar reckoning (Acharyan, 1926, EDMAL, 1974). Conceptions related to the phases of the moon, preserved in Armenian calendrical, folk, and linguistic-cultural traditions, likewise allow us to assume the presence of ancient elements of an original lunar or lunisolar reckoning system (Alishan, 2021).

In this context, possible typological, etymological, and semantic comparisons between Armenian and Polynesian languages are of particular interest. The present article continues our previous studies in this direction (Stepanyan, n.d., 2004a,b, 2011, 2015, 2018, 2019, 2020, 2022, 2023, 2024, 2025), focusing on those night names whose etymology is the most reliable.

The aim of the article is to examine, with the help of the historical-comparative method, four of the most stable night names of Pre-Eastern Polynesian—**Hiro, Kokore, Hotu, Mutu**—and to propose their possible comparative correspondences in Armenian. The study focuses primarily on etymological and semantic analysis. Structural comparison will be carried out after the comparative examination of the entire lunar calendar.

2. Material and Methods

The principal material of the study consists of the night names of Eastern Polynesian lunar calendars, their variants, and corresponding lexical data (Table 1). Both classical ethnographic sources and modern comparative databases were used, in particular the **POLLEX Online** project (Buck, 1959, Greenhill & Clark, 2011, Henry, 1928, Métraux, 1940, Routledge, 1919).

Table 1. Integrated Analysis of the Night Names

Night Name	**Position in the Calendar**	**Historical-Comparative Etymology**	**Lunar Interpretation**
Hiro, Whiro, Hilo, Iro	1^{st} night of the lunar month	Associated with the meanings "to weave," "to twist," "to spin thread," "to join"	The first thin crescent of the new moon; the beginning of the lunar cycle
Kokore I, Kokore II	Before the full moon (6 nights), after the full moon (5 nights)	*kore* "there is none, absent, empty"	Unnamed, empty, indeterminate nights
Hotu, Ohotu	14^{th}–15^{th} night	Proto-Polynesian **fotu* "to swell, to grow, to become full"	Maximum growth preceding the full moon; swelling, filling
Mutu, Muku, Motu	29^{th}–30^{th} night	Proto-Polynesian **mutu* "to end, to be cut off, to be exhausted"	Disappearance of the moon, end of the cycle

During the study, the following methods were applied:

1) **Historical-comparative method** — for reconstructing the proto-forms of night names in Polynesian languages and identifying possible Armenian correspondences.

2) **Etymological analysis** — for revealing the root structure of words and their possible historical development.

3) **Semantic analysis** — for examining the development of lexical meanings and correlating them with calendrical functions.

4) **Structural comparison** — for studying the internal organization of naming series.

In evaluating the comparative material, priority attention was given not only to formal similarities, but also to regular phonetic correspondences, semantic proximity, and the comparability of calendrical functions, since superficial formal similarities alone are insufficient to establish an etymological connection.

2.1. The Night Name HIRO and Its Armenian Parallels

2.1.1. Position in the Lunar Calendar

The night name **Hiro/Whiro/Hilo/Iro** is among the most widespread and stable names in Eastern Polynesian lunar calendars. It is usually the first night of the lunar month and is associated with the beginning of a new lunar cycle. In Rapa Nui, Tahitian, Marquesan, Māori, and Hawaiian traditions, **Hiro** opens the entire lunar sequence, marking the beginning of a new cycle (Table 1).

2.1.2. Historical-Comparative Etymology

The etymology of the night name **Hiro** has not been conclusively established; however, comparative data from Polynesian languages indicate that it is associated with the semantic field of "to weave," "to twist," "to spin thread," and "to join." In particular, the Māori form **whiro** and the Hawaiian form **hilo** mean "to weave," "to twist," "to braid rope," and "to prepare thread" (Biggs, 1971, Pukui & Elbert, 1986, Tregear, 1891, Williams, 1971).

2.1.3. Lunar Interpretation

Hiro corresponds to the phase of the new moon, when the moon is still almost invisible or is only beginning to become visible. This phase symbolizes beginning, inner concentration, potential, and renewal (Table 1).

2.1.4. Proposed Armenian Parallels

The forms **Hiro / Hilo** exhibit interesting parallels with a number of Armenian words. The first group is associated with the ideas of rotation, twisting, and spiraling:

- **Grabar** *hiṙ* — "turn, circle, coil" (Jahukyan, 2010)
- **Grabar** *hirel* — "to join, to arrange" (Jahukyan, 2010)
- **Grabar** *heṙ* — "arranged together, interwoven" (Acharyan, 1926)

These words are united within the semantic field of "twisting," "arranging," and "connecting," which closely corresponds to the etymological meaning of **Hiro**.

The second group is associated with tools of spinning and weaving:

- **Grabar** *heryun / herun / helun* — "awl, bodkin, weaving tool" (Jahukyan, 2010)
- **Grabar** *her* — "hair (of the head)," sometimes material for weaving (Jahukyan, 2010)
- **Grabar** *ilik / il* — "spinning tool" (Jahukyan, 2010)
- **Grabar** *t'el*, dialectal *t'il* — "thread" (Jahukyan, 2010)

These forms are likewise associated with spinning, weaving, and material construction or creation.

Also noteworthy is the possible comparison of the Hawaiian form **hilo** with the Western Armenian dialectal word *hil*, meaning "light-emitting stone" (DDAL, 2001) This may symbolically be connected with the Moon, although it requires further substantiation[1].

This semantic field allows Hiro to be interpreted not only as a mythological name, as suggested by some Polynesian scholars, but also as a symbolic expression of the structuring of the lunar cycle. In this context, the metaphor of "thread" is natural, since the new moon becomes visible as a delicate line appearing in the dark sky.

Therefore, the night name **Hiro** may be interpreted as:

- the beginning of the lunar cycle,
- the first spiral of time,
- the first thin crescent emerging from darkness.

[1] A more detailed analysis of this issue will be presented in future work.

This interpretation is consistent with Polynesian cosmogonic conceptions, in which the world is often described as a system of interconnected threads, networks, and bonds.

In our view, "thread," "weaving," and "connection" may represent the continuity of time, while **Hiro** represents the first spiral of the lunar cycle.

2.1.5. Phonetic Observations

From a phonetic perspective, the forms **Hiro/Hilo** correspond to the r/l alternation characteristic of Polynesian languages: in Rapa Nui and Marquesan, **r** is often preserved, whereas in Hawaiian, **l** appears in the same position.

This phenomenon has also been observed in Armenian–Polynesian lexical correspondences (Stepanyan, 2015) and is important for evaluating Armenian parallels. Let us consider several examples:

- *Rapan.* ***rava***$_1$ *"skilled, capable" — Grabar* ***lav*** *"good" (labh- "to grasp"),*
- *Rapan.* ***roto***$_2$ *"swamp," "lake" — Grabar* ***lik*** *"lake" (PIE leg-), (t $\longleftrightarrow$ k),*
- *Rapan.* ***ragaraga***$_2$ *(raga-raga) "to float" — Grabar* ***loganal*** *"to bathe in water" (louənā, lou-),* ***loł*** *"the act of swimming,"*
- *Rapan.* ***regorego*** *(rego-rego) "naked" — Grabar* ***lek, lerk, łerk*** *"hairless, naked" (lerg-), etc.*
- *Rapan.* ***ritorito*** *(rito-rito) "white," "bright" — Grabar* ***lurth*** *"pale white mixed with blue," "clear, bright" (PIE lenk-, kleu- (?)),*
- *Rapan.* ***reo***$_1$ *"voice," "sound" — Grabar* ***lur*** *"voice, sound" (k'luro-, k/leu "to hear"), etc.*

Also noticeable is the widespread loss of unstressed final sounds in Armenian parallels (Stepanyan, 2023), as well as certain vocalic alternations encountered here and throughout the study, which have repeatedly been recorded in Polynesian–Armenian comparisons.

- *Rapan.* ***higaa*** *(higa-a) "miserable, pitiable" — Grabar* ***heg, hek', hik'*** *"wretched, poor, pitiable" (peiu-, pe(i)-) (Jahukyan, 2010); Grabar hełg "sluggish, slow-moving" (selk-),*
- *Rapan.* ***viri***$_2$ *"to fall from a height, roll downward" — Grabar* ***ver*** *"up, above" (upper-),*
- *Rapan.* ***kite***$_2$ *"to see, notice," "to know" — Grabar* ***get/git*** *"knowing, learned" (ueid- / uoid- "to see, to know"),*
- *Rapan.* ***kino*** *"bad, evil" — Grabar* ***k'en*** *"enmity, revenge, jealousy" (kuoinā-), etc.*

Intermediate Conclusion

The night name **Hiro** belongs to the oldest and most stable lunar names of Eastern Polynesian tradition. Its core semantic nucleus—"to weave / to twist / to join"—is consistent with the phase of the new moon as a symbol of the beginning of the lunar cycle. The proposed Armenian parallels are centered around the semantic fields of "rotation," "twisting," "weaving," and "thread-making," and provide interesting comparative material for future, more comprehensive studies

2.2. The Night Name KOKORE/KORE and Its Armenian Parallels

2.2.1. Position in the Lunar Calendar

In the Rapa Nui lunar calendar, two successive series of nights are known under the name **Kokore**, located in different parts of the lunar month. The first series occurs in the phase preceding the full moon and includes six nights (**Kokore tahi–ono**: the 5^{th}, 6^{th}, 7^{th}, 8^{th}, 9^{th}, and 10^{th} nights), while the second series, occurring after the full moon, consists of five nights (**Kokore tahi–rima**: the 19^{th}, 20^{th}, 21^{st}, 22^{nd}, and 23^{rd} nights).

The numerical components **(tahi, rua, toru, hā, rima, ono)** mean respectively "one," "two," "three," "four," "five," and "six," indicating that the series are structured according to the principle of sequential numbering (Barthel, 1978, Métraux, 1940).

2.2.2. Historical-Comparative Etymology

The night name **Kokore** is usually compared with the Māori form **korekore** and is regarded as an important component of the common Eastern Polynesian inheritance. In historical-comparative linguistics, it is interpreted as a reduplicated or intensified form of the root **kore**.

In Polynesian languages, **kore** primarily means:
• "there is none,"
• "is absent,"
• "is empty,"
• "is lacking."
On the basis of this semantic foundation, the designation **Kokore** is generally interpreted as a series of "empty," "unnamed," or "undifferentiated" nights in the lunar calendar. In this interpretation, the second component **kore** is associated in Polynesian languages with the meanings "nothing," "absence," and "emptiness" (Barthel (1978), Métraux (1940), Tregear (1891) s.v.*kore*).

2.2.3. Lunar Interpretation

Two principal approaches to **Kokore** are accepted in the literature (Table 1). According to the first approach, the **Kokore** series are simply sequences of numbered nights without separate individual names (Valério, 2024). The second approach is based on the semantics of the root **kore** and suggests that the **Kokore** nights represent "indeterminate," "empty," or "unnamed" phases. However, this interpretation does not fully explain the first **Kokore** series, which occurs before the full moon, that is, during the period of the moon's most active growth. In that phase, the meaning of "absence" or "emptiness" is not convincing; moreover, it contradicts the logic of the meaning "waxing moon."

2.2.4. Proposed Armenian Parallels

In Armenian, the lexical layer based on **kor/kore** represents two distinct but interconnected semantic directions.
A. "To be lost / diminish / disappear"
(which corresponds well to Polynesian meanings)
The first group is associated with the following Armenian words:
• **kor, korel** — "loss, to be lost" (Jahukyan, 2010)
• **korc'nel** — "to lose, to no longer see" (Aghayan, 1976)
• **korč'el** — "to disappear" (Aghayan, 1976)
• **korust** — "loss, disappearance" (Aghayan, 1976)
• **koruk** — "lost" (Aghayan, 1976)
This group is united around the following meanings:
• disappearance,
• diminution,
• loss,
• cessation of existence.
This semantic field corresponds very well to the **Kokore** series following the full moon, when the moon begins to wane, become smaller, and gradually disappear.
B. "Curvature / Inclination / Rounding"
The second group is associated with the following Armenian forms:
• **kor** — "curved, bent" (Jahukyan, 2010)
• **korel** — "to bend, to curve" (Aghayan, 1976)
• **korvel** — "to become bent, to curve"
• **keṙ** — "curved, crooked" (Jahukyan, 2010)
• **klor** — "having the shape of a ring or circle" (Aghayan, 1976)
These words represent another semantic layer:
• to bend,
• to incline,
• to acquire a curved form,
• to become rounded.
This semantic field is especially interesting for the **Kokore** series preceding the full moon, when the lunar disk gradually curves, enlarges, and becomes rounder.

Proposal for a New Interpretation

Based on the Armenian material, it may be assumed that the two segments of the **Kokore** series reflect two different semantic layers.

First: Kokore I Series (Waxing Moon)

In the case of the series preceding the full moon, the semantic field of "to curve/to become rounded" appears more logical. At this phase, the moon:

- grows larger,
- forms a curved shape,
- approaches fullness.

Therefore, this series may be associated not with **kore** = "there is none," but rather with an older or parallel root such as Rapan. **kero** "crooked"/**kekero*-type root meaning "to bend, to acquire a curved form."

Second: Kokore II Series (Waning Moon)

After the full moon, the semantic axis changes. Here, the interpretation **kore** = "to diminish, to disappear" appears more natural, since the moon:

- becomes smaller,
- decreases,
- moves toward the new moon.

In this case, the classical etymology of the root **kore** fully corresponds to its calendrical position (Table 2).

Table 2. Proposed Integrated Analysis of the Night Name Kokore

Night Name	Position in the Calendar	Historical-Comparative Etymology	Lunar Interpretation
Kokore I or **Kekero*	Before the full moon (6 nights)	Possible connection with the root *kero/kor* "to bend"	Curving and rounding of the waxing moon
Kokore II	After the full moon (5 nights)	*kore* "there is none, absent, empty"	Waning moon, diminution, disappearance

2.2.5. Phonetic Observations

Reduplicative structures are widespread in Polynesian languages and have numerous parallels in Armenian (Stepanyan, 2020). Reduplication may express:

- duration,
- multiplicity,
- gradual development.

From this perspective, the form **ko-kore** may have signified not a static state, but a process:

- "to become increasingly curved," or
- "to gradually diminish."

This interpretation corresponds well to the phase-based transformations of the moon.

Intermediate Conclusion

The night name **Kokore** is among the most interesting and structurally complex elements of Eastern Polynesian lunar calendars. According to the classical etymology, it is associated with the root **kore** "there is none, empty"; however, this interpretation is not convincing for the first **Kokore** series associated with the waxing moon.

The Armenian parallels make it possible to distinguish two semantic layers:

- **first series — waxing moon** — "to curve, to take shape, to become rounded"
- **second series — waning moon** — "to diminish, to be lost, to disappear"

This approach makes it possible to regard the **Kokore** series as a system of descriptive names for the opposing phases of lunar growth and decline.

2.3. The Night Name HOTU/OHOTU/HOKU and Its Armenian Parallels

2.3.1. Position in the Lunar Calendar

The night name **Hotu/Ohotu/Hoku** in Eastern Polynesian lunar calendars is usually positioned around the 14^{th}–15^{th} nights of the lunar month, that is, in the phase immediately preceding or reaching the full moon (Table 1). In the Rapa Nui tradition, it is known as the 14^{th} night name, whereas in Tahitian, Marquesan, and Mangarevan systems it corresponds to the phase of the moon's maximum growth. This position indicates that **Hotu** is associated with the ideas of lunar fullness, growth, and maturation.

2.3.2. Historical-Comparative Etymology

The night name **Hotu** is among the most clearly etymologized names in Polynesian. It is usually connected with the Proto-Polynesian root ***fotu**, whose primary meanings are:

- to swell,
- to become large,
- to grow,
- to become full,
- to mature,
- to become fertile.

Data from Tongan, Samoan, Niuean, Māori, and Tahitian show that the semantic nucleus of the word has been preserved almost entirely (Biggs, 1971, Churchward, 1959, Pratt, 1911, Williams, 1971). Therefore, the etymology of the night name **Hotu** has a high degree of reliability.

2.3.3. Lunar Interpretation

The night name **Hotu** corresponds to the phase when the moon approaches its maximum fullness (Table 1). In this context, the metaphorical shift from "to swell" to "to become full" is natural. Here, the moon is represented as a growing, living, maturing being. If the preceding lunar phases describe gradual growth, then **Hotu** expresses the culmination of that growth—the moment immediately preceding full completeness.

Thus, **Hotu** symbolizes:

- fullness,
- maturation,
- fertility,
- abundance.

2.3.4. Proposed Armenian Parallels

In Armenian, possible parallels for **Hotu/Hoku** are primarily concentrated in the semantic fields of growth, fullness, abundance, and fertility.

The following forms are especially noteworthy:

- **hord** — "abundant, overflowing" (Jahukyan, 2010)
- **horj** — "overflowing, abundant flow" (Jahukyan, 2010)
- **huṙt‘i** — "fertile, productive" (Jahukyan, 2010)
- **urd** — "filled" (Malkhasyants, 1944)
- **urdi** — "increases, there is much" (Malkhasyants, 1944)
- **hogn / hoqn** — "many, numerous" (Jahukyan, 2010)

These words express, to varying degrees:

- increase,
- fullness,
- abundance,
- multiplication,
- fertility.

Semantically, they are quite close to the principal meanings of the Polynesian root **hotu**.

2.3.5. Phonetic Observations

In the compared forms, particular attention is drawn to the stable presence of the Armenian **-r-** element, which has likewise been repeatedly recorded in other Polynesian–Armenian comparisons (Stepanyan, 2015). Let us consider several examples:

- *Rapan.* ***ka***$_3$ *"sunrise,"* ***ka***$_5$ *"to burn, ignite" — Grabar* ***kaṙ*** *"burning, the act of burning" (ker-),*
- *Rapan.* ***hu*** *"flame" — Grabar* ***hur*** *"fire" (pur-, peuōr-, pun-),*
- *Rapan.* ***ha*** *"four" — Grabar* ***qaṙ*** *"four" (PIE ketvores-),*
- *Rapan.* ***mouku*** *"green grass, dry grass, plant" — Grabar* ***murk*** *"grain of wheat, roasted grain" (smug-ro-, smeug(h)),*
- *Rapan.* ***mutu***$_1$ *"lip (human)" — Grabar* ***mṙut/mṙut'*** *"snout, mouth, lip" (mu-), etc.*

The following correspondences are also noteworthy:

- Polynesian **t** → Armenian **t/d/t'**
- Polynesian **k** → Armenian **k/q/g/j**

These are important from the perspective of comparative evaluation (Stepanyan, 2020).

- *Rapan.* ***tupu*** *"tree, bud, shoot" — Grabar* ***t'uph*** *"short, low tree," "thick branch, leafy branch" (from the Old Armenian form tupho-) (Aghayan, 1976),*
- *Rapan.* ***turi***$_2$ *"knee, joint" — Grabar* ***t'yur*** *"crooked, bent" (tek-ro) (Jahukyan, 2010),*
- *Rapan.* ***teka*** *"to turn (of a rotation)" — Grabar* ***t'eq****, whence t'eqel "to bend" (tek-),*
- *.* ***tarai***$_1$ *"heavy rain, flood," "sound of water" — Grabar* ***t'or*** *"running like water," "flow, current, dripping, tear" ((s)ter-),*
- *Rapan.* ***terea*** *"rest, calm" — Grabar* ***darel*** *"to stop, remain" (dher-),*
- *Rapan.* ***tanu*** *"to bury" — Grabar* ***damb*** *"burial" (dhmbh-, dembh- "to bury"),*
- *Rapan.* ***ta*** *"that" — Grabar* ***d-*** *second-person demonstrative article,* ***da*** *"that, this" (from the demonstrative root to-),*
- *Rapan.* ***kau***$_1$ *"to go" — Grabar* ***ga-, gal*** *"to come" (uadh- "to walk, to go"),*
- *Rapan.* ***kite***$_2$ *"to see, notice," "to know" — Grabar* ***get*** *"knowledgeable, learned" (ueid- / uoid-),*
- *Rapan.* ***karu*** *"seed, grain" — Grabar* ***gari*** *"barley" (gher-, gharua- (?)), etc.*

Intermediate Conclusion

The night name **Hotu/Ohotu/Hoku** belongs to the group of Polynesian lunar-calendar names with the most reliable etymologies. Its principal semantic nucleus—"to swell, to grow, to become full"—fully corresponds to the phase in which the moon approaches fullness.

The proposed Armenian parallels are centered around the concepts of abundance, growth, fullness, and fertility, and provide valuable material for further historical-comparative studies.

2.4. The Night Name MUTU/MUKU and Its Armenian Parallels

2.4.1. Position in the Lunar Calendar

The night name **Mutu/Muku** in Polynesian lunar calendars is usually positioned at the end of the lunar month, around the 29^{th}–30^{th} nights, and is associated with the phases immediately preceding the new moon (Table 1). In the Rapa Nui tradition, **Mutu** is known as the 30^{th} night name, whereas in a number of other Polynesian systems, the forms **Mutu** and **Muku** denote the final phase of the lunar cycle (Biggs, 1971, Churchward, 1959, Pratt, 1911, Williams, 1971).

Thus, **Mutu/Muku** represents the end of the lunar cycle—the transition toward a new phase.

2.4.2. Historical-Comparative Etymology

In historical-comparative linguistics, the night name **Mutu** is connected with the Proto-Polynesian root ***mutu**, whose primary meanings are:

- to end,
- to finish,
- to cease,
- to be cut off,

• to be exhausted.

Comparative pan-Polynesian data indicate that the original semantic nucleus of the lexeme **mutu** was formed around the notions of “cut-offness” and “completedness,” from which the meanings “end,” “boundary,” and “closed cycle” later developed (Biggs, 1971, Churchward, 1959, Pratt, 1911, Williams, 1971). The form **motu**, attested in certain languages with the meanings “to be cut off,” “to separate,” and “detached part,” later developed toward the meanings “cut-off piece,” “separated section,” and in some cases even “island” (Biggs, 1971, Greenhill & Clark, 2011, Pukui & Elbert, 1986, Williams, 1971).

2.4.3. Lunar Interpretation

From a lunar perspective, **Mutu/Muku** represents the final stage of the lunar cycle, when the visibility of the moon reaches its minimum or disappears completely (Table 1).

At this phase, the moon:
• fades,
• becomes smaller,
• becomes invisible.

Therefore, the night name **Mutu** symbolizes:
• the end of the cycle,
• the exhaustion of old force,
• preparation for a new cycle.

In this sense, **Mutu** is the opposite pole of **Hiro**: if **Hiro** is the beginning, **Mutu** is the end.

2.4.4. Proposed Armenian Parallels

In Armenian, with respect to the **mutu/muku** base, it is possible to distinguish two distinct but interconnected semantic directions. On the basis of phonetic proximity:

A. “To darken / become obscure / fade”

The first group is associated with the following Armenian words:
• **mut‘** — “darkness, state of being without light” (Acharyan, 1926, Jahukyan, 2010)
• **mug** — “dark, dense, thick” (Acharyan, 1926, Jahukyan, 2010)
• **mət‘nel** — “to darken, to lose light” (Aghayan, 1976)

This group is united around the following meanings:
• darkening,
• fading,
• loss of light,
• invisibility.

This semantic field corresponds very well to the calendrical position of **Mutu**, since during the final nights of the lunar month the moon becomes almost or completely invisible, and the sky enters its darkest phase.

On the basis of the semantic root “to cut / to finish” attested in Polynesian languages:

B. “To cut / separate / finish”

The second group is associated with the following Armenian forms:
• Grabar **mort‘** — “cutting, slaughtering” (Jahukyan, 2010)
• Grabar **mort‘el** — “to kill by cutting off the head” (Aghayan, 1976)
• **hatum/bajanum** — “cutting/division; delimitation”

These words represent another semantic layer:
• to be cut off,
• to be separated,
• to end,
• to be delimited.

This semantic field is especially interesting for the forms **Mutu/Motu**, since in Polynesian languages **motu** often means “cut-off part” or “separated section” (cf. Rapa Nui **motu** “to cut, to be cut off, to break"). In lunar terms, this may be understood as the final separation of the old lunar cycle from the new one.

Proposal for a New Interpretation

Based on the Armenian material, it may be assumed that the night name **Mutu/Muku** reflects two complementary semantic layers.

First Layer — Darkening

In the case of **Mutu**, the semantic field "to darken / become obscure" is the most evident. At this phase, the moon:

- fades,
- disappears,
- the sky darkens.

Therefore, **Mutu** may be connected not only with the Proto-Polynesian root ***mutu** "to end," but also with an older figurative designation associated with darkness.

Second Layer — Ending and Separation

At the same time, the semantic axis "to cut / divide / finish" is also preserved in the name **Mutu/Motu**. Here, **Mutu** functions as a boundary marker (cf. Rapan. **mutu** "30^{th} night name," **muku** "boundary post"), which:

- closes the old cycle,
- separates the old from the new,
- prepares the next lunar cycle.

In this case, the classical etymology fully corresponds to the calendrical position.

Thus, the Armenian parallels help interpret the night name **Mutu/Muku** as having a dual-layer structure as well:

- first layer — "to darken, become obscure, fade,"
- second layer — "to end, be cut off, be divided."

This approach makes it possible to view **Mutu** not merely as the end or completion of the lunar cycle, but also as a transitional boundary—from darkness toward a new beginning.

In Armenian, the most convincing parallels for **Mutu/Muku** belong to the semantic field of darkness and obscurity. Semantically, these are comparable with the Polynesian forms **mutu/muku**. Particularly noteworthy is the comparison **Mutu** ⟷ **mut‘**, since the final night of the lunar month is characterized precisely as a moonless, dark night[2].

2.4.5. Phonetic Observations

Regular correspondences are present, particularly the reflex of Proto-Polynesian **t** as Hawaiian **k** (**mutu → muku**, Armenian **mut‘ → mug/muq**), as well as the vowel alternation **u** ⟷ **o (mutu** ⟷ **motu)**.

This alternation has also been recorded in Rapanui–Armenian parallels:

- *Rapan. **ote** "to suck" — Grabar **utel**, dialectal **otel** "to eat" (ōd-),*
- *Rapan. **otea** "a dance performed by eight boys and eight girls" — Grabar **ut‘**, dialectal **ot’** "eight" (ok’tō),*
- *Rapan. **toku, tooku** "my" — Grabar **duq** "you (pl.)", plural of the personal pronoun **du** (to-),*
- *Rapan. **huri**$_2$ "pit, funnel-shaped hole" — Grabar **hor** "well, deep pit" (poro-, por-),*
- *Rapan. **pu**$_1$ "pit," "opening," "well" — Grabar **p‘or** "opening, cavity, hollow place, womb,"*
- *Rapan. **turuturu** "to drip drop by drop (water, liquid)" — Grabar **t‘or** "flow, current, dripping."*

Intermediate Conclusion

The night name **Mutu/Muku** belongs to the group of Polynesian lunar-calendar names with the most reliable etymologies. The principal semantic nucleus of **Mutu/Motu**—"to cut, ending,

[2] A structural parallel exists between this night name and the 30^{th} day-name of the Proto-Armenian calendar, which will be discussed later.

exhaustion, cessation"—and the semantic field of the Armenian word **mort‘el** ("to slaughter, to kill by cutting off the head") fully correspond to the final phase of the lunar cycle.

The proposed comparison with the Armenian words **mut‘/mug** reveals interesting semantic commonalities worthy of further investigation.

3. Results

The present study has shown that the examined night names of the Pre-Eastern Polynesian lunar calendars are etymologically comparable with certain ancient lexical strata of Armenian. The observed parallels are noteworthy for historical-comparative linguistics. The analysis revealed that the most reliable correspondences concern those names associated with lunar phases, the light–darkness opposition, time reckoning, and cyclical natural phenomena (Table 3). The corresponding roots and semantic fields preserved in Armenian often display both phonetic and semantic proximity, which is difficult to explain as mere accidental coincidence.

The analysis conducted through comparison with Armenian parallels makes it possible to construct a model in terms of semantic structure.

Table 3. Proposed Core Semantic Structure of the Pre-Eastern Polynesian Lunar Cycle

Lunar Phase	**Night Name**	**Primary Meaning**	**Main Armenian Parallel**	**Meaning of Armenian Parallel**
Beginning	Hiro	weaving, formation, birth	hiṙ, hirel	rotation, spiral, to join, arrange, weave
Formation Curving	Kokore I	curving, rounding	kor	to bend, acquire curved shape, become round
Growth, Fullness	Hotu	swelling, growth, fertility	hord, huṙt‘i	abundant flow, fullness, fertility, abundance
Diminution, Decline	Kokore II	diminution, disappearance	korel, korč‘el	to diminish, be lost, disappear
End	Mutu	exhaustion, darkening, ending	mut‘, mug	darkness, absence of light, fading, darkening

As a result, we obtain a symmetrical semantic structure of the lunar cycle:

Hiro → Kokore I → Hotu → Kokore II → Mutu

beginning → formation → fullness → decline → end

Taking into account the **kore** ⟷ **kero** comparison proposed above, we suggest the following alternative model:

- **Hiro/Hilo** — beginning/threading/birth
- **Kero**/**Kekero* — formation/curving
- **Hotu/Hoku** — filling/maturation
- **Kore/Kokore** — decline/loss
- **Mutu/Muku** — ending/darkness

4. Conclusions

The system of Pre-Eastern Polynesian lunar night names may be viewed as a phase-based semantic whole, in which the names successively express birth, formation, fullness, decline, and ending, thus forming a complete linguistic-cultural model of lunar time.

Overall, the study confirms that the vocabulary of lunar calendars may serve as an important source for reconstructing ancient worldviews, systems of time reckoning, and possible linguistic-cultural connections.

The inclusion of Armenian in such comparative research opens new perspectives not only for Armenian studies, but also for broader comparative linguistic investigations, including the fields of historical-cultural astronomy and calendrical studies.

References

Acharyan, H. 1926. *Armenian Root Dictionary*. Yerevan: (in Arm.).

Aghayan, E. 1976. *Explanatory Dictionary of Modern Armenian*. Yerevan: Hayastan publ. house (in Arm.).

Alishan, Gh. 2021. *The Ancient Faith of the Armenians, or the Pagan Religions*. Yerevan: Edit Print publ. house (in Arm.).

Barthel, T.S. 1978. *The Eighth Land: The Polynesian Discovery and Settlement of Easter Island*. Honolulu: University of Hawaii Press.

Biggs, B. 1971. The Languages of Polynesia. *In: Linguistics in Oceania*. De Gruyter.

Blust, R. 2013. The Austronesian Languages. *Pages 203–219 of: The Austronesian Languages*.

Blust, R. 2019. The Austronesian Homeland and Dispersal. *Annual Review of Linguistics*, **5**, 417–434.

Buck, P. 1959. *The Vikings of the Pacific*. Chicago: University of Chicago Press.

Churchward, C.M. 1959. *Tongan Dictionary*.

DDAL. 2001. *Dialectal Dictionary of the Armenian Language*. Yerevan: National Academy of Sciences of Armenia (in Arm.).

EDMAL. 1974. *Explanatory Dictionary of the Modern Armenian Language*. Vol. 3. Yerevan: Academy of Sciences of the Armenian SSR (in Arm.).

Greenhill, S.J., & Clark, R. 2011. *POLLEX-Online: Polynesian Lexicon Project Online*.

Henry, T. 1928. *Ancient Tahiti*. Bernice P. Bishop Museum Bulletin, vol. 48. Honolulu: Bernice P. Bishop Museum.

Jahukyan, G. 2010. *Armenian Etymological Dictionary*. Yerevan: Asoghik publ. house (in Arm.).

Malkhasyants, St. 1944. *Armenian Explanatory Dictionary*. Yerevan: Haypethrat (in Arm.).

Métraux, A. 1940. *Ethnology of Easter Island*. Honolulu: Bernice P. Bishop Museum.

Pawley, A. 2003. Proto Polynesian Lexicon. *Pages 17–48 of: The Lexicon of Proto Oceanic*.

Pratt, G. 1911. *Samoan Dictionary*.

Pukui, M.K., & Elbert, S.H. 1986. *Hawaiian Dictionary*. Rev. edn. Honolulu: University of Hawaii Press.

Routledge, K. 1919. *The Mystery of Easter Island: The Story of an Expedition*. London: Hazell, Watson and Viney.

Stepanyan, L.G. The Denotations of the Concept of "Star" in Polynesian Languages and their Armenian Parallels. *Bazmavep*. in press.

Stepanyan, L.G. 2004a. The Armenian Highlands in Ancient Written Sources of the Far East and the Mythical Homeland of the Polynesians. *Pages 85–93 of: Proceedings of the First Scientific Conference on Armenology "The Armenian Highlands as the Cradle of Armenian and World Civilization" of the Institute of History of the RA NAS*.

Stepanyan, L.G. 2004b. The Armenian Highlands in Ancient Written Sources of the Near East and the Mythical Homeland of the Polynesians. *Pages 85–93 of: Proceedings of the First Scientific Conference on Armenology "The Armenian Highlands as the Cradle of Armenian and World Civilization" of the Institute of History of the National Academy of Sciences of the Republic of Armenia.*

Stepanyan, L.G. 2011. The Homeland of the Polynesians According to Toponyms (Pulotu/Polotu). *Bazmavep*, **1-2**, 308–328.

Stepanyan, L.G. 2015. *Armenian-Polynesian Linguistic and Cultural Commonalities.* Yerevan: Yason Publishing House. 380 pages.

Stepanyan, L.G. 2018. Comparative Comparison of Some Phonetic Features of Armenian and Polynesian Languages. *Echmiadzin*, **12**, 49–67.

Stepanyan, L.G. 2019. Rapanui-Armenian Biplanar (Morpho-Semantic) Coincidences as a Factual Basis for Excluding the Hypothesis of "Accidental Similarities". *Bazmavep*, **1-2**, 311–336.

Stepanyan, L.G. 2020. Reflections of Simple Voiceless Sounds of Polynesian Languages in Armenian. *Pages 128–146 of: Proceedings of the International Conference "Armenology in Mongolia".* V. Bryusov State University of Linguistics and Social Sciences, Yerevan.

Stepanyan, L.G. 2022. Refinements of the Structure of Polynesian Word Forms through Comparison with Armenian Parallels. *Echmiadzin*, **3**, 70–91.

Stepanyan, L.G. 2023. A Brief Comparative Analysis of the Positional Stress of the Armenian-Polynesian Word Parallels. *In: Proceedings of the International Conference "Armenian Studies in the Context of Languages and Cultures".*

Stepanyan, L.G. 2024. On the Proto-form of the Native Armenian Word Yerkin "Heaven" and its Armenian Parallels. *Communications of BAO*, **71(1)**, 153–157.

Stepanyan, L.G. 2025. Phonetic and Semantic Developments of the Native Armenian Word "Yerkin" in Polynesian Languages and Armenian. *Communications of BAO*, **72(1)**, 162–168.

Tregear, E. 1891. *The Maori-Polynesian Comparative Dictionary.* Wellington: Lyon & Blair.

Valério, M. 2024. The Rongorongo 'Lunar Calendar' of Rapa Nui (Easter Island) and the Type of Script. *In:* Ferrara, Silvia, Montecchi, Barbara, & Valério, Miguel (eds), *Writing from Invention to Decipherment.* Oxford University Press.

Valério, M., Tamburini F. Corazza M. 2025. Computational Analysis Reveals Historical Trajectory of East-Polynesian Lunar Calendars. *arXiv e-prints*, dec.

Williams, H.W. 1971. *A Dictionary of the Māori Language.* 7th edn. Wellington: GP Publications.